

**Title:**

Explicit and parameter-adaptive boundary control laws for parabolic partial differential equations

Author:

[Smyshlyaev, Andrey S.](#)

Acceptance Date:

01-01-2006

Degree:

Ph. D., [UC San Diego](#)

Permalink:

<http://escholarship.org/uc/item/7189m296>

Abstract:

The dissertation introduces a new constructive approach to the problem of boundary stabilization of linear parabolic partial differential equations (PDEs). The approach is based on an infinite-dimensional extension of the backstepping method. Using a Volterra integral transformation, the unstable plant is converted to an exponentially stable target system and the control gain is found as a solution of a certain well-posed hyperbolic PDE. In addition to stabilizing controllers, we also introduce inverse optimal controllers, which provide low control effort and robustness margins. For many physically motivated cases feedback laws are constructed explicitly and the closed-loop solutions are found in closed form. For the case when the measurements are available only at the boundary, we develop exponentially convergent observers that are dual to the state feedback controllers. These observers are then combined with the controllers to obtain the solution to the output feedback problem with actuator and sensor located on the same or the opposite boundaries. For the plants with constant unknown parameters we design the certainty equivalence adaptive controllers with two types of identifiers: passivity-based identifiers and swapping identifiers. For the plants with unknown spatially-varying parameters we design the adaptive scheme based on the Lyapunov method. The control gain is computed through an approximate solution of a linear PDE or through a limited number of recursive integrations. We show the robustness of the proposed scheme with respect to an error in the online gain computation. Finally, we consider a problem of output feedback stabilization of PDEs with unknown, spatially varying reaction, advection, and diffusion parameters. Both sensing and actuation are performed at the boundary. We construct a transformation of the original system into the PDE analog of "observer canonical form," with unknown parameters multiplying the measured output. Input and output filters are implemented so that a dynamic parametrization of the problem is converted into a static parametrization where a gradient estimation algorithm is used. We also solve the problem of the adaptive output tracking of a desired reference trajectory prescribed at the boundary



eScholarship
University of California

eScholarship provides open access, scholarly publishing services to the University of California and delivers a dynamic research platform to scholars worldwide.

UNIVERSITY OF CALIFORNIA, SAN DIEGO

Explicit and Parameter-Adaptive Boundary Control Laws
for Parabolic Partial Differential Equations

A dissertation submitted in partial satisfaction of the requirements for the degree
Doctor of Philosophy

in

Engineering Sciences (Mechanical Engineering)

by

Andrey S. Smyshlyaev

Committee in charge:

Professor Miroslav Krstić, Chair
Professor Thomas Bewley
Professor Robert Bitmead
Professor William Helton
Professor William McEneaney

2006

Copyright
Andrey S. Smyshlyaev, 2006
All rights reserved.

The dissertation of Andrey S. Smyshlyaev is approved,
and it is acceptable in quality and form for publication
on microfilm:

Chair

University of California, San Diego

2006

TABLE OF CONTENTS

Signature Page	iii
Table of Contents	iv
List of Figures	vii
List of Tables	ix
Acknowledgments	x
Vita, Publications, and Fields of Study	xii
Abstract	xiii
Chapter 1 Introduction	1
Chapter 2 State Feedback Controllers for a Class of Parabolic PDEs	5
1. Introduction	5
2. Problem Formulation.	7
3. PDE for the Kernel	8
4. Converting the PDE into an Integral Equation	10
5. Analysis of the Integral Equation by a Successive Approximation Series	14
6. Properties of the Closed Loop System	17
7. Inverse Optimal Stabilization	19
8. Reducing the Control Effort through Adaptation	23
9. Numerical Results	26
10. Conclusions	28
Chapter 3 Closed Form Controllers for Reaction-Advection-Diffusion Systems	30
1. Unstable Heat Equation	30
2. Heat Equation with Destabilizing Boundary Condition	36
3. Explicit Solution for a Family of Plants with Spatially Varying Reaction	39
4. Solid Propellant Rocket Model	42
5. Plant with Spatially Varying Diffusivity	43
6. Unstable Heat Equation with Non-Constant Thermal Conductivity .	46
7. Combining Previous Results	47
Chapter 4 Time-Varying Systems	50
1. PDE for Gain Kernel	50
2. Closed form controllers	51
3. Simulations	55

Chapter 5	Observers	57
1.	Introduction	57
2.	Problem Statement	59
3.	Observer Design for Anti-Collocated Setup	59
4.	Observer Design for Collocated Setup	63
Chapter 6	Output Feedback Controllers	67
1.	Anti-collocated setup	67
2.	Collocated setup	68
3.	Closed Form Compensators	69
Chapter 7	Certainty Equivalence Adaptive Controllers with Passive Identifiers	80
1.	Introduction	80
2.	Benchmark Plant	82
3.	3D Reaction-Advection-Diffusion Plant	88
4.	Proof of Theorem 7.4	91
5.	Simulations	99
Chapter 8	Certainty Equivalence Adaptive Controllers with Swapping Identifiers	102
1.	Benchmark Plant	102
2.	Reaction-Advection-Diffusion System	106
3.	Proof of Theorem 8.2	109
4.	Simulations	115
Chapter 9	Closed Form Output Feedback Adaptive Controllers	116
1.	Introduction	116
2.	Benchmark Plant with Unknown Parameter in the Domain	117
3.	Proof of Theorem 9.1	119
4.	Benchmark Plant with Unknown Parameter in the Boundary Condition	124
5.	Proof of Theorem 9.5	127
6.	Plant with Two Unknown Parameters	130
7.	Simulations	131
8.	Conclusions	132
Chapter 10	Adaptive Control for PDEs with Spatially Varying Coefficients .	134
1.	Introduction	134
2.	Problem Statement	135
3.	Non-Adaptive Control Design	136
4.	Robustness To Error In Gain Kernel	137
5.	Adaptive Design	147
6.	Proof of Theorem 10.4	151
7.	Design With Other Parameters	153
8.	Simulations	153

Chapter 11 Output Feedback Adaptive Control	158
1. Introduction	158
2. Problem Formulation	159
3. Transformation to Observer Canonical Form	160
4. Non-Adaptive Controller	161
5. Estimator	162
6. Update laws	165
7. Main result	167
8. Output Tracking	174
9. Reaction-Advection-Diffusion Systems	176
10. Simulations	177
Chapter 12 Future Work	179
Bibliography	181

LIST OF FIGURES

2.1	The comparison between LQR (solid) and inverse optimal (dashed) controllers: (a) L_2 -norm of the state; (b) the control effort; (c) the adaptive gain; (d) the state for inverse optimal controller.	28
3.1	Stabilizing gain kernel $k_1(y)$ for unstable heat equation (3.1.1)–(3.1.2) with $\lambda = 17$	33
3.2	Dependence of the gain kernel on the level of instability.	34
3.3	Amount of total gain as a function of λ	35
3.4	The comparison between stabilizing (solid) and inverse optimal (dashed) controllers: (a) L_2 -norm of the state; (b) the control effort; (c) the adaptive gain.	37
3.5	”One-peak” $\lambda_\sigma(x)$ for different values of σ and x_0	39
3.6	Gain kernel $k_1(y)$ for (6.3.34)–(6.3.35).	41
3.7	The function $\varepsilon(x)$ for different values of ε_0 , θ_0 , and x_0 . From left to right: peak value and flatness are arbitrary; extremum can be set to max or min; location of extremum is arbitrary; linear functions matched.	45
3.8	The function $\varepsilon(x)$ from (3.5.70) and the corresponding kernel $k(1, y)$ for different parameter values. Dotted line shows the kernel for $\varepsilon(x) \equiv 1$	47
3.9	The simulation results for the plant with spatially varying diffusivity. Top left: the diffusivity profile; top right: the gain kernel; bottom: the L_2 -norm of open loop (dashed) and closed loop (solid) response.	48
4.1	The function $\lambda(t)$ from (4.2.19) for $\lambda_0 = 10$, $\omega_0 = 5$, and $t_0 = 1$. . .	54
4.2	The function $\lambda(t)$ from (4.2.22) for $\lambda_0 = 5$, $a = 0.03$, and $b = 0.25$. .	54
4.3	The simulation results for (4.1.1)–(4.1.2) with controllers (4.2.17) (solid) and (4.2.27) (dashed). From left to right: $\lambda(t)$; L_2 -norm of the gain kernel; L_2 -norm of the state; the control effort.	55
6.1	Observer gain for the unstable heat equation.	71
6.2	Exponential convergence of the observer for the unstable heat equation.	71
6.3	Pole-zero map and Bode plot of the compensator for unstable heat equation.	72
6.4	Closed-loop response with a low-order compensator.	73
6.5	”One-peak” $\lambda_{\alpha\beta}(x)$ for $\alpha = 4$ and $\varepsilon = 1$	75
6.6	Observer gain for $\alpha = 4$ and $\varepsilon = 1$	76
6.7	Bode plot of $C(j\omega)$ for $g = 8$	78
7.1	The domain Ω for the plant (7.3.37).	89

7.2	The closed loop state for the plant (7.5.88) at different times.	99
7.3	The parameter estimates for the plant (7.5.88) with adaptive controller based on passive identifier.	100
8.1	The parameter estimates and the closed loop state for the plant (8.2.29)–(8.2.31) with adaptive controller based on swapping identifier (solid — $\hat{\varepsilon}$, dashed — \hat{b} , dash-dotted — $\hat{\lambda}$).	115
9.1	The state $u(x, t)$ with the adaptive output feedback controller (9.6.104).	132
9.2	The parameters \hat{g} (solid) and \hat{q} (dashed). The unknown parameters are set to $g = 4$ and $q = 2$	133
10.1	The final profile of the estimate $\hat{\lambda}(x, t)$ (dashed) versus true $\lambda(x)$ (solid).	154
10.2	The final profile of the estimate $\hat{b}(x, t)$ (dashed) versus true $b(x)$ (solid).	155
10.3	The parameter estimates $\hat{\lambda}(x, t)$ and $\hat{b}(x, t)$	156
10.4	The closed loop state $u(x, t)$	157
11.1	Left: The closed loop state $u(x, t)$. Right: The parameter estimates $\hat{\theta}_1(t)$ (solid) and $\hat{\theta}_2(t)$ (dashed).	177
11.2	Left: The control effort for the adaptive tracking. Right: Reference signal at the boundary (dashed) and actual evolution of the output (solid).	178

LIST OF TABLES

10.1	Minimum number of terms n required to satisfy the condition (10.4.51) for different $\bar{\lambda}$	147
------	--	-----

ACKNOWLEDGMENTS

I would like to express my highest gratitude to my advisor Professor Miroslav Krstić for his fantastic guidance, endless enthusiasm, and unconditional readiness to help.

I gratefully acknowledge the members of my committee for reading this manuscript and their valuable comments.

I thank my former and current fellow graduate students Kartik Ariyur, Lawrence Yuan, Eugenio Schuster, Rafael Vazquez, Nick Killingsworth, Marco Luethi, Antranik Siranosian, and Jennie Cochran for fruitful discussions and friendly environment in the lab.

I am especially indebted to my wife Olga, who has continually offered her love and support.

This dissertation includes the reprints of the following papers:

A. Smyshlyaev and M. Krstic, “Closed form boundary state feedbacks for a class of 1D partial integro-differential equations,” *IEEE Trans. on Automatic Control*, vol. 49, no. 12, pp. 2185-2202, 2004. (Chapters 2, 3)

A. Smyshlyaev and M. Krstic, “On control design for PDEs with space-dependent diffusivity or time-dependent reactivity,” *Automatica*, 41, pp. 1601-1608, 2005. (Chapters 3, 4)

A. Smyshlyaev and M. Krstic, “Backstepping observers for a class of parabolic PDEs,” *Systems and Control Letters*, vol.54, pp. 613-625, 2005. (Chapters 5, 6)

A. Smyshlyaev and M. Krstic, “Adaptive boundary control for unstable parabolic PDEs—Part II: Estimation-based designs,” accepted to *Automatica*, 2006. (Chapters 7, 8)

A. Smyshlyaev and M. Krstic, “Adaptive boundary control for unstable parabolic PDEs—Part III: Output feedback examples with swapping identifiers,” accepted to *Automatica*, 2006. (Chapter 9)

A. Smyshlyaev and M. Krstic, “Lyapunov adaptive boundary control for parabolic PDEs with spatially varying coefficients,” *Proceedings of 2006 American Control*

Conference, pp. 41-48. (Chapter 10)

A. Smyshlyaev and M. Krstic, “Output-Feedback Adaptive Control for Parabolic PDEs with Spatially Varying Coefficients,” *2006 Conference on Decision and Control*. (Chapter 11)

The dissertation author was the primary author and the co-author listed in these publications directed and supervised the research.

VITA

1999	B.S. in Applied Mathematics and Physics, Moscow Institute of Physics and Technology, Russia
2001	M.S. in Applied Mathematics and Physics, Moscow Institute of Physics and Technology, Russia
2001–2006	Research Assistant, Department of MAE University of California, San Diego
2006	Ph.D. in Engineering Sciences (Mechanical Engineering), University of California, San Diego

PUBLICATIONS

A. Smyshlyaev and M. Krstic, “Closed form boundary state feedbacks for a class of 1D partial integro-differential equations,” *IEEE Trans. on Automatic Control*, vol. 49, no. 12, pp. 2185-2202, 2004.

A. Smyshlyaev and M. Krstic, “Backstepping observers for a class of parabolic PDEs,” *Systems and Control Letters*, vol.54, pp. 613-625, 2005.

A. Smyshlyaev and M. Krstic, “On control design for PDEs with space-dependent diffusivity or time-dependent reactivity,” *Automatica*, 41, pp. 1601-1608, 2005.

A. Smyshlyaev and M. Krstic, “Adaptive boundary control for unstable parabolic PDEs-Part II: Estimation-based designs,” accepted to *Automatica*, 2006.

A. Smyshlyaev and M. Krstic, “Adaptive boundary control for unstable parabolic PDEs-Part III: Output feedback examples with swapping identifiers,” accepted to *Automatica*, 2006.

FIELDS OF STUDY

Major Field: Engineering

Studies in Control Theory.

Professors Miroslav Krstić, Robert Bitmead, and Robert Skelton

Studies in Fluid Mechanics.

Professors Juan Lasheras, Paul Linden, Stefan Llewellyn Smith

Studies in Numerical Methods.

Professors Tom Bewley, Costas Pozrikidis

ABSTRACT OF THE DISSERTATION

Explicit and Parameter-Adaptive Boundary Control Laws
for Parabolic Partial Differential Equations

by

Andrey S. Smyshlyaev

Doctor of Philosophy in Engineering Sciences (Mechanical Engineering)

University of California, San Diego, 2006

Professor Miroslav Krstić, Chair

The dissertation introduces a new constructive approach to the problem of boundary stabilization of linear parabolic partial differential equations (PDEs).

The approach is based on an infinite-dimensional extension of the backstepping method. Using a Volterra integral transformation, the unstable plant is converted to an exponentially stable target system and the control gain is found as a solution of a certain well-posed hyperbolic PDE. In addition to stabilizing controllers, we also introduce inverse optimal controllers, which provide low control effort and robustness margins. For many physically motivated cases feedback laws are constructed explicitly and the closed-loop solutions are found in closed form.

For the case when the measurements are available only at the boundary, we develop exponentially convergent observers that are dual to the state feedback controllers. These observers are then combined with the controllers to obtain the solution to the output feedback problem with actuator and sensor located on the same or the opposite boundaries.

For the plants with constant unknown parameters we design the certainty equivalence adaptive controllers with two types of identifiers: passivity-based identifiers and swapping identifiers. For the plants with unknown spatially-varying parameters we design the adaptive scheme based on the Lyapunov method. The

control gain is computed through an approximate solution of a linear PDE or through a limited number of recursive integrations. We show the robustness of the proposed scheme with respect to an error in the online gain computation.

Finally, we consider a problem of output feedback stabilization of PDEs with unknown, spatially varying reaction, advection, and diffusion parameters. Both sensing and actuation are performed at the boundary. We construct a transformation of the original system into the PDE analog of “observer canonical form,” with unknown parameters multiplying the measured output. Input and output filters are implemented so that a dynamic parametrization of the problem is converted into a static parametrization where a gradient estimation algorithm is used. We also solve the problem of the adaptive output tracking of a desired reference trajectory prescribed at the boundary.

Chapter 1

Introduction

Motivation

After about three decades of development, PDE control theory consists of a wealth of mathematically impressive results that solve stabilization and optimal control problems [66, 40, 41, 2, 46, 7, 20, 45, 52, 27, 51]. Two of the main driving principles in this development have been *generality* and *extending* the existing finite dimensional results. The latter objective has led to extending (at least) two of the basic control theoretic results to PDEs: pole placement and optimal/robust control. While these efforts have been successful, by following the extremely general finite dimensional path ($\dot{x} = Ax + Bu$, where A and B can be any matrices), they have diverted the attention from structure-specific opportunities that exist in PDEs.

Structure is particularly pronounced in *boundary control* problems for PDEs. Backstepping techniques for parabolic systems, focused on revealing and exploiting this structure, have been under development since about 1998 [3, 4, 11, 12, 10, 13], but have been limited to discretized formulations until a recent breakthrough by Liu [42].

This dissertation introduces continuum backstepping method as a structure-specific paradigm for parabolic PDEs. By recognizing the underlying structure of

the plant, this method results in a simpler (from a conceptual as well as numerical point of view) solution to boundary control problems than existing approaches. For many practically relevant problems, the control laws are even found in closed form.

The backstepping method also allows to solve many PDE control problems that have not been solved before, such as boundary control for PDEs with unknown parameters. While adaptive control of finite dimensional systems is a mature area that has produced methods for most LTI systems of interest, adaptive control techniques have been developed for only a few of the classes of PDEs for which non-adaptive controllers exist [44, 29, 9, 62, 48, 8, 24, 67, 26, 43, 32, 33, 31, 25]. We developed the first adaptive controllers for parabolic PDEs with unknown, spatially varying reaction, advection, and diffusion coefficients and only boundary sensing and actuation.

Contributions

1. **Boundary Controllers for a Class of Parabolic PDEs ([55], Chapters 2,3).** We design boundary controllers for a certain class of parabolic PDEs. The problem is formulated as a design of an integral operator whose kernel is required to satisfy a certain hyperbolic PDE. We establish this equation's well posedness and the properties of the control kernel. In addition to stabilizing controllers, we also introduced inverse optimal backstepping controllers, which provide low control effort and robustness margins. An adaptation mechanism is developed to reduce the conservativeness of the inverse optimal controller, and the performance bounds are derived. A numerical scheme for the kernel PDE is proposed which compares favorably with that associated with operator Riccati equations.
2. **Closed Form Controllers ([55],[57], Chapters 3, 4).** For a broad class of practically relevant parabolic PDEs that describe thermal/fluid and

chemically reacting problems we developed closed-form, ready-to-implement boundary controllers. The closed-loop solutions are also found in closed form.

3. **Boundary Observers for a Class of Parabolic PDEs ([56], Chapters 5, 6).** In applications, it is often impossible or undesirable to cover the entire domain of the problem with sensors. The realistic situation is when the measurements are available only at the boundary. We developed observers for a wide range of thermal/fluid problems with boundary sensing. These observers are dual to backstepping state feedback controllers developed in Chapter 2. By combining these observers with the backstepping controllers we obtained the solution to the output feedback problem with only scalar (point) measurement and actuation, with actuator and sensor located on the same or the opposite boundaries.
4. **Adaptive Control for PDEs using Passivity-based and Swapping Identifiers. ([58], Chapters 7, 8)** In applications that incorporate thermal-fluid or chemically reacting dynamics, physical parameters like reaction, diffusion, or advection coefficients are often unknown. For the plants with constant unknown parameters we design the certainty equivalence adaptive controllers with two types of identifiers: passivity-based identifiers and swapping identifiers. We prove a separation principle result for both types of the identifiers combined with backstepping controllers.
5. **Closed Form Output Feedback Adaptive Controllers for Two Benchmark PDEs ([59], Chapter 9)** We develop output feedback adaptive controllers for two benchmark parabolic PDEs motivated by a model of thermal instability in solid propellant rockets. Both benchmark plants are unstable, have infinite relative degree, and are controlled from the boundary. One plant has an unknown parameter in the PDE and the other in the boundary condition. In both cases the unknown parameter multiplies the measured output

of the system, which is obtained with a boundary sensor located on the “opposite side” of the domain from the actuator. We show how two benchmarks examples can be combined and illustrate the adaptive stabilization design by simulation.

6. Adaptive Controllers for Plants with Spatially Varying Coefficients.

([60], **Chapter 10**) We design the first adaptive controllers for the reaction-advection-diffusion plants with spatially-varying parameters that use only boundary actuation. The control gain is computed through an approximate solution of a linear PDE or through a limited number of recursive integrations. We show the robustness of the proposed scheme with respect to an error in the online gain computation. The results are illustrated with simulations.

7. Output Feedback Adaptive Control. ([61], **Chapter 11**) We consider

a problem of output feedback stabilization of distributed parameter systems with unknown reaction, advection, and diffusion parameters. Both sensing and actuation are performed at the boundary and the unknown parameters are allowed to be spatially varying. We construct a special transformation of the original system into the PDE analog of “observer canonical form,” with unknown parameters multiplying the measured output. Input and output filters are implemented so that a dynamic parametrization of the problem is converted into a static parametrization where a gradient estimation algorithm is used. The control gain is computed through the numerical solution of an integral equation. We also solve the problem of the adaptive output tracking of a desired reference trajectory prescribed at the boundary. We illustrate the result with simulations.

Chapter 2

State Feedback Controllers for a Class of Parabolic PDEs

2.1 Introduction

In this chapter we design continuum backstepping controllers for a class of parabolic PDEs that build upon the discretized formulations [3, 4, 11, 12, 10, 13] and a recent result by Liu [42].

The design requires the solution of a linear Klein-Gordon-type hyperbolic PDE on a triangular domain, an easier task than solving an operator Riccati equation or executing the procedure for pole placement. An important result of the proposed method from the practical point of view is that in addition to solving the stabilization problem, it also naturally leads to controllers that are inverse optimal, which has important practical consequences of guaranteeing stability margins. We also propose an adaptive control law to reduce the control effort and derive explicit bounds on the state and control.

In many cases the controllers can be found in closed form. We will consider these special cases in Chapter 3.

When the control gain can not be obtained in closed form, we suggest an effective computational scheme, based on the Ablowitz-Kruskal-Ladik method

[1], commonly applied to the Klein-Gordon PDE arising in quantum mechanics and the study of solitary waves. We make a numerical comparison of our design and the traditional LQR approach and show that the proposed approach requires much less computational effort while exhibiting comparable performance.

The prior work on stabilization of general parabolic equations includes, among others, the results of Triggiani [66] and Lasiecka and Triggiani [40] who developed a general framework for the structural assignment of eigenvalues in parabolic problems through the use of semigroup theory. Separating the open loop system into a finite dimensional unstable part and an infinite dimensional stable part, they apply feedback boundary control that stabilizes the unstable part while leaving the stable part stable. An LQR approach in Lasiecka and Triggiani [41] is also applicable to this problem. A unified treatment of both interior and boundary observations/control generalized to semilinear problems can be found in [2]. Nambu [46] developed auxiliary functional observers to stabilize diffusion equations using boundary observation and feedback. Stabilizability by boundary control in the optimal control setting is discussed by Bensoussan et al. [7]. For the general Pritchard–Salamon class of state–space systems a number of frequency–domain results has been established on stabilization during the last decade (see, e.g. [19] and [45] for a survey). The placement of finitely many eigenvalues was generalized to the case of moving infinitely many eigenvalues by Russel [52]. The stabilization problem can be also approached using the abstract theory of boundary control systems developed by Fattorini [27] that results in a dynamical feedback controller (see remarks in [20, Section 3.5]). Solvability and open-loop controllability of linear parabolic PDEs using integral operator transformations were considered by Colton [18] and Seidman [53]. Extensive surveys on the controllability and stabilizability theory of linear partial differential equations can be found in [51, 41].

2.2 Problem Formulation.

We consider the following class of linear parabolic partial integro-differential equations:

$$\begin{aligned} u_t(x, t) = & \varepsilon(x)u_{xx}(x, t) + b(x)u_x(x, t) + \lambda(x)u(x, t) \\ & + g(x)u(0, t) + \int_0^x f(x, y)u(y, t) dy \end{aligned} \quad (2.2.1)$$

for $x \in (0, 1)$, $t > 0$, with boundary conditions¹

$$u_x(0, t) = qu(0, t), \quad (2.2.2)$$

$$u(1, t) = U(t) \text{ or } u_x(1, t) = U(t), \quad (2.2.3)$$

where $U(t)$ is the control input and the coefficients are assumed to be

$$\begin{aligned} \varepsilon(x) &> 0 \text{ for all } x \in [0, 1], \quad \varepsilon \in C^2[0, 1], \quad q \in \mathbb{R}, \\ b &\in C^1[0, 1], \quad \lambda, g \in C[0, 1], \quad f \in C([0, 1] \times [0, 1]), \end{aligned} \quad (2.2.4)$$

The control objective is to stabilize the equilibrium $u(x, t) \equiv 0$.

The equation (2.2.8) is in fact a partial integro-differential equation, but for convenience we abuse the terminology and call it a PDE.

Before we start, let us introduce the following change of variables (the so-called Gauge transformation)

$$\bar{u}(\bar{x}) = \varepsilon^{-1/4}(x)u(x)e^{\int_0^x \frac{b(s)}{2\varepsilon(s)} ds} \quad (2.2.5)$$

$$\bar{x} = \int_0^x \frac{ds}{\sqrt{\varepsilon(s)}} \left(\int_0^1 \frac{ds}{\sqrt{\varepsilon(s)}} \right)^{-1}. \quad (2.2.6)$$

where there is an implicit coordinate change within the transformation (2.2.5) as the term on the left $\bar{u}(\bar{x})$ is a function of \bar{x} while the term on the right is a function

¹The case of Dirichlet boundary condition at the zero end can be handled by setting $q = +\infty$.

of x . One can show that the modified plant has the following parameters:

$$\begin{aligned}
\bar{\varepsilon} &= \left(\int_0^1 \frac{ds}{\sqrt{\varepsilon(s)}} \right)^{-2}, & \bar{b}(\bar{x}) &= 0 \\
\bar{\lambda}(\bar{x}) &= \lambda(x) + \frac{\varepsilon''(x)}{4} - \frac{b'(x)}{2} - \frac{3}{16} \frac{(\varepsilon'(x))^2}{\varepsilon(x)} + \frac{1}{2} \frac{(b(x)\varepsilon'(x))}{\varepsilon(x)} - \frac{1}{4} \frac{b^2(x)}{\varepsilon(x)} \\
\bar{q} &= q \sqrt{\frac{\varepsilon(0)}{\bar{\varepsilon}}} + \frac{b(0)}{2\sqrt{\bar{\varepsilon}\varepsilon(0)}} + \frac{\varepsilon'(0)}{4\sqrt{\bar{\varepsilon}\varepsilon(0)}} \\
\bar{g}(\bar{x}) &= g(x) \left(\frac{\varepsilon(0)}{\varepsilon(x)} \right)^{\frac{1}{4}} e^{\int_0^x \frac{b(s)}{2\varepsilon(s)} ds} \\
\bar{f}(\bar{x}, \bar{y}) &= f(x, y) \left(\frac{\varepsilon^3(y)}{\varepsilon(x)\bar{\varepsilon}^2} \right)^{\frac{1}{4}} e^{\int_0^x \frac{b(s)}{2\varepsilon(s)} ds} \tag{2.2.7}
\end{aligned}$$

We are now going to drop "bars" for convenience and write the plant as

$$u_t(x, t) = \varepsilon u_{xx}(x, t) + \lambda(x) u(x, t) + g(x) u(0, t) + \int_0^x f(x, y) u(y, t) dy \tag{2.2.8}$$

$$u_x(0, t) = qu(0, t), \tag{2.2.9}$$

$$u(1, t) = U(t) \text{ or } u_x(1, t) = U(t). \tag{2.2.10}$$

Thus, the effect of the transformation (2.2.5)–(2.2.6) is to eliminate $b(x)$ from the original problem (2.2.1) and make $\varepsilon(x)$ constant.

2.3 PDE for the Kernel

We look for a backstepping-like coordinate transformation

$$w(x, t) = u(x, t) - \int_0^x k(x, y) u(y, t) dy \tag{2.3.11}$$

that transforms system (2.2.8)–(2.2.10) into the system

$$w_t(x, t) = \varepsilon w_{xx}(x, t) - cw(x, t), \quad x \in (0, 1), \tag{2.3.12}$$

$$w_x(0, t) = qw(0, t), \tag{2.3.13}$$

$$w(1, t) = 0 \text{ or } w_x(1, t) = 0, \tag{2.3.14}$$

which is exponentially stable for $c \geq \varepsilon \bar{q}^2$ (respectively, $c \geq \varepsilon \bar{q}^2 + \varepsilon/2$) where $\bar{q} = \max\{0, -q\}$. The free parameter c can be used to set the desired rate of

stability. Once we find the transformation (2.3.11) (namely $k(x, y)$), the boundary condition (2.3.14) gives the controller in the form

$$u(1, t) = U(t) = \int_0^1 k_1(y)u(y, t) dy \quad (2.3.15)$$

for the Dirichlet actuation and

$$u_x(1, t) = U(t) = k_1(1)u(1, t) + \int_0^1 k_2(y)u(y, t) dy \quad (2.3.16)$$

for the Neumann actuation. Here we denoted

$$k_1(y) = k(1, y), \quad k_2(y) = k_x(1, y). \quad (2.3.17)$$

Differentiating (2.3.11) we get²:

$$\begin{aligned} w_{xx}(x, t) &= u_{xx}(x, t) - u(x) \frac{d}{dx} k(x, x) - k(x, x) u_x(x, t) - k_x(x, x) u(x) \\ &\quad - \int_0^x k_{xx}(x, y) u(y, t) dy. \end{aligned} \quad (2.3.18)$$

$$\begin{aligned} w_t(x, t) &= u_t(x, t) - \int_0^x k(x, y) \left\{ \varepsilon u_{yy}(y, t) + \lambda(y) u(y, t) + g(y) u(0, t) + \right. \\ &\quad \left. + \int_0^y f(y, \xi) u(\xi, t) d\xi \right\} dy \\ &= u_t(x, t) - \varepsilon k(x, x) u_x(x, t) + \varepsilon k(x, 0) u_x(0, t) + \varepsilon k_y(x, x) u(x, t) \\ &\quad - \varepsilon k_y(x, 0) u(0, t) - \varepsilon \int_0^x k_{yy}(x, y) u(y, t) dy \\ &\quad - \int_0^x k(x, y) \lambda(y) u(y, t) dy - u(0, t) \int_0^x k(x, y) g(y) dy \\ &\quad - \int_0^x u(y, t) \left(\int_y^x k(x, \xi) f(\xi, y) d\xi \right) dy. \end{aligned} \quad (2.3.19)$$

²We use the following notation: $k_x(x, x) = k_x(x, y)|_{y=x}$, $k_y(x, x) = k_y(x, y)|_{y=x}$, $\frac{d}{dx} k(x, x) = k_x(x, x) + k_y(x, x)$.

Substituting (2.3.19) and (2.3.18) into equations (2.3.12)–(2.3.13) and using (2.2.8)–(2.2.9) we obtain the following equation

$$\begin{aligned} & \int_0^x \{ \varepsilon k_{xx}(x, y) - \varepsilon k_{yy}(x, y) - (\lambda(y) + c)k(x, y) \} u(y, t) dy \\ & + \left\{ \lambda(x) + c + 2\varepsilon \frac{d}{dx} k(x, x) \right\} u(x, t) \\ & + \int_0^x f(x, y) u(y, t) dy - \int_0^x u(y, t) \int_y^x k(x, \xi) f(\xi, y) d\xi dy \\ & + \left\{ g(x) - \int_0^x k(x, y) g(y) dy - \varepsilon k_y(x, 0) + \varepsilon q k(x, 0) \right\} u(0, t) = 0. \end{aligned} \quad (2.3.20)$$

For this equation to be verified for all $u(x, t)$ the following PDE for $k(x, y)$ must be satisfied:

$$\varepsilon k_{xx}(x, y) - \varepsilon k_{yy}(x, y) = (\lambda(y) + c)k(x, y) - f(x, y) + \int_y^x k(x, \xi) f(\xi, y) d\xi \quad (2.3.21)$$

for $(x, y) \in \mathcal{T}$ with boundary conditions

$$\varepsilon k_y(x, 0) = \varepsilon q k(x, 0) + g(x) - \int_0^x k(x, y) g(y) dy, \quad (2.3.22)$$

$$k(x, x) = -\frac{1}{2\varepsilon} \int_0^x (\lambda(y) + c) dy. \quad (2.3.23)$$

Here we denote $\mathcal{T} = \{(x, y) : 0 < y < x < 1\}$. Note that one of the boundary conditions is on the characteristic (Goursat-type) and the other is non-local, i.e. contains an integral term. We will prove well posedness of (2.3.21)–(2.3.23) in the next two sections.³

2.4 Converting the PDE into an Integral Equation

We derive now an integral equation equivalent to the system (2.3.21)–(2.3.23). We introduce the standard change of variables [64]

$$\xi = x + y, \quad \eta = x - y, \quad (2.4.24)$$

³General books on PDEs (see, e.g., [64]) do establish well posedness of second-order hyperbolic PDEs, but not with integral terms and these boundary conditions.

and denote

$$G(\xi, \eta) = k(x, y) = k\left(\frac{\xi + \eta}{2}, \frac{\xi - \eta}{2}\right), \quad (2.4.25)$$

transforming problem (2.3.21)–(2.3.23) to the following PDE:

$$\begin{aligned} 4\varepsilon G_{\xi\eta}(\xi, \eta) = & a\left(\frac{\xi - \eta}{2}\right)G(\xi, \eta) - f\left(\frac{\xi + \eta}{2}, \frac{\xi - \eta}{2}\right) \\ & + \int_{(\xi - \eta)/2}^{(\xi + \eta)/2} G\left(\frac{\xi + \eta}{2} + \tau, \frac{\xi + \eta}{2} - \tau\right) f\left(\tau, \frac{\xi - \eta}{2}\right) d\tau \end{aligned} \quad (2.4.26)$$

for $(\xi, \eta) \in \mathcal{T}_1$ with boundary conditions

$$\varepsilon G_{\xi}(\xi, \xi) = \varepsilon G_{\eta}(\xi, \xi) + \varepsilon q G(\xi, \xi) + g(\xi) - \int_0^{\xi} G(\xi + \tau, \xi - \tau) g(\tau) d\tau, \quad (2.4.27)$$

$$G(\xi, 0) = -\frac{1}{4\varepsilon} \int_0^{\xi} a\left(\frac{\tau}{2}\right) d\tau. \quad (2.4.28)$$

Here we introduced $\mathcal{T}_1 = \{\xi, \eta : 0 < \xi < 2, 0 < \eta < \min(\xi, 2 - \xi)\}$ and $a(\tau) = \lambda(\tau) + c$.

Integrating (2.4.26) with respect to η from 0 to η and using (2.4.28) we obtain

$$\begin{aligned} G_{\xi}(\xi, \eta) = & -\frac{1}{4\varepsilon} a\left(\frac{\xi}{2}\right) + \frac{1}{4\varepsilon} \int_0^{\eta} a\left(\frac{\xi - s}{2}\right) G(\xi, s) ds - \frac{1}{4\varepsilon} \int_0^{\eta} f\left(\frac{\xi + \tau}{2}, \frac{\xi - \tau}{2}\right) d\tau \\ & + \frac{1}{4\varepsilon} \int_0^{\eta} \int_{\xi}^{\xi + \eta - s} G(\tau, s) f\left(\frac{\tau - s}{2}, \xi - \frac{\tau + s}{2}\right) d\tau ds. \end{aligned} \quad (2.4.29)$$

Integrating (2.4.29) with respect to ξ from η to ξ gives

$$\begin{aligned} G(\xi, \eta) = & G(\eta, \eta) - \frac{1}{4\varepsilon} \int_{\eta}^{\xi} a\left(\frac{\tau}{2}\right) d\tau - \frac{1}{4\varepsilon} \int_{\eta}^{\xi} \int_0^{\eta} f\left(\frac{s + \tau}{2}, \frac{s - \tau}{2}\right) d\tau ds \\ & + \frac{1}{4\varepsilon} \int_{\eta}^{\xi} \int_0^{\eta} a\left(\frac{\tau - s}{2}\right) G(\tau, s) ds d\tau \\ & + \frac{1}{4\varepsilon} \int_{\eta}^{\xi} \int_0^{\eta} \int_{\mu}^{\mu + \eta - s} G(\tau, s) f\left(\frac{\tau - s}{2}, \mu - \frac{\tau + s}{2}\right) d\tau ds d\mu. \end{aligned} \quad (2.4.30)$$

Now we want to find an equation for $G(\eta, \eta)$. From (2.4.27) we have

$$\begin{aligned} \frac{d}{d\xi} G(\xi, \xi) &= G_\xi(\xi, \xi) + G_\eta(\xi, \xi) \\ &= 2G_\xi(\xi, \xi) - qG(\xi, \xi) - \frac{1}{\varepsilon}g(\xi) + \frac{1}{\varepsilon} \int_0^\xi G(\xi + s, \xi - s)g(s) ds. \end{aligned} \quad (2.4.31)$$

Using (2.4.29) with $\eta = \xi$ we can write (2.4.31) in the form of differential equation for $G(\xi, \xi)$

$$\begin{aligned} \frac{d}{d\xi} G(\xi, \xi) + qG(\xi, \xi) &= -\frac{1}{2\varepsilon}a\left(\frac{\xi}{2}\right) + \frac{1}{2\varepsilon} \int_0^\xi a\left(\frac{\xi - s}{2}\right) G(\xi, s) ds \\ &\quad - \frac{1}{2\varepsilon} \int_0^\xi f\left(\frac{\xi + \tau}{2}, \frac{\xi - \tau}{2}\right) d\tau \\ &\quad + \frac{1}{2\varepsilon} \int_0^\xi \int_\xi^{2\xi - s} G(\tau, s) f\left(\frac{\tau - s}{2}, \xi - \frac{\tau + s}{2}\right) d\tau ds \\ &\quad - \frac{1}{\varepsilon}g(\xi) + \frac{1}{\varepsilon} \int_0^\xi G(\xi + s, \xi - s)g(s) ds. \end{aligned} \quad (2.4.32)$$

Integrating (2.4.32) using the variation of constants formula we obtain

$$\begin{aligned} G(\xi, \xi) &= -\frac{1}{2\varepsilon} \int_0^\xi e^{q(\tau - \xi)} \left[a\left(\frac{\tau}{2}\right) + 2g(\tau) \right] d\tau \\ &\quad - \frac{1}{2\varepsilon} \int_0^\xi e^{q(\tau - \xi)} \int_0^\tau f\left(\frac{\tau + s}{2}, \frac{\tau - s}{2}\right) ds d\tau \\ &\quad + \frac{1}{2\varepsilon} \int_0^\xi e^{q(\tau - \xi)} \int_0^\tau a\left(\frac{\tau - s}{2}\right) G(\tau, s) ds d\tau \\ &\quad + \frac{1}{\varepsilon} \int_0^\xi e^{q(\tau - \xi)} \int_0^\tau G(\tau + s, \tau - s)g(s) ds d\tau \\ &\quad + \frac{1}{2\varepsilon} \int_0^\xi e^{q(\mu - \xi)} \int_0^\mu \int_\mu^{2\mu - s} G(\tau, s) f\left(\frac{\tau - s}{2}, \mu - \frac{\tau + s}{2}\right) d\tau ds d\mu. \end{aligned} \quad (2.4.33)$$

Substituting equation (2.4.33) for $\xi = \eta$ into (2.4.30) we obtain an integral equation for G :

$$G(\xi, \eta) = G_0(\xi, \eta) + F[G](\xi, \eta), \quad (2.4.34)$$

where

$$\begin{aligned} G_0(\xi, \eta) = & -\frac{1}{4\varepsilon} \int_{\eta}^{\xi} a\left(\frac{\tau}{2}\right) d\tau - \frac{1}{2\varepsilon} \int_0^{\eta} e^{q(\tau-\eta)} \left[a\left(\frac{\tau}{2}\right) + 2g(\tau) \right] d\tau \\ & -\frac{1}{4\varepsilon} \int_{\eta}^{\xi} \int_0^{\eta} f\left(\frac{s+\tau}{2}, \frac{s-\tau}{2}\right) d\tau ds \\ & -\frac{1}{2\varepsilon} \int_0^{\eta} e^{q(\tau-\eta)} \int_0^{\tau} f\left(\frac{\tau+s}{2}, \frac{\tau-s}{2}\right) ds d\tau, \end{aligned} \quad (2.4.35)$$

$$\begin{aligned} F[G](\xi, \eta) = & \frac{1}{2\varepsilon} \int_0^{\eta} e^{q(\tau-\eta)} \int_0^{\tau} a\left(\frac{\tau-s}{2}\right) G(\tau, s) ds d\tau \\ & +\frac{1}{4\varepsilon} \int_{\eta}^{\xi} \int_0^{\eta} a\left(\frac{\tau-s}{2}\right) G(\tau, s) ds d\tau \\ & +\frac{1}{2\varepsilon} \int_0^{\eta} \int_s^{2\eta-s} e^{q(\frac{\tau+s}{2}-\eta)} g\left(\frac{\tau-s}{2}\right) G(\tau, s) d\tau ds \\ & +\frac{1}{2\varepsilon} \int_0^{\eta} e^{q(\mu-\eta)} \int_0^{\mu} \int_{\mu}^{2\mu-s} f\left(\frac{\tau-s}{2}, \mu - \frac{\tau+s}{2}\right) G(\tau, s) d\tau ds d\mu \\ & +\frac{1}{4\varepsilon} \int_{\eta}^{\xi} \int_0^{\eta} \int_{\mu}^{\mu+\eta-s} f\left(\frac{\tau-s}{2}, \mu - \frac{\tau+s}{2}\right) G(\tau, s) d\tau ds d\mu. \end{aligned} \quad (2.4.36)$$

We thus proved the following statement.

Lemma 2.1. *Any $G(\xi, \eta)$ satisfying (2.4.26)–(2.4.28) also satisfies integral equation (2.4.34).*

2.5 Analysis of the Integral Equation by a Successive Approximation Series

Using the result of the previous section we can now compute a uniform bound on the solutions by the method of successive approximations.⁴

With G_0 defined in (2.4.35), let

$$G_{n+1}(\xi, \eta) = F[G_n], \quad n = 0, 1, 2, \dots \quad (2.5.37)$$

and denote

$$\bar{\lambda} = \sup_{x \in [0,1]} |\lambda(x)|, \quad \bar{g} = \sup_{x \in [0,1]} |g(x)|, \quad \bar{f} = \sup_{(x,y) \in [0,1] \times [0,1]} |f(x,y)|. \quad (2.5.38)$$

First we estimate $G_n(\xi, \eta)$:

$$\begin{aligned} |G_0(\xi, \eta)| &\leq \frac{1}{4\varepsilon}(\bar{\lambda} + c)(\xi - \eta) + \frac{1}{2\varepsilon}(\bar{\lambda} + c + 2\bar{g})\eta + \frac{1}{4\varepsilon}\bar{f}\eta^2 + \frac{1}{4\varepsilon}\bar{f}(\xi - \eta)\eta \\ &\leq \frac{1}{\varepsilon}(\bar{\lambda} + c + \bar{f} + \bar{g})(1 + e^{-q}) \equiv M. \end{aligned} \quad (2.5.39)$$

Suppose that

$$|G_n(\xi, \eta)| \leq M^{n+1} \frac{(\xi + \eta)^n}{n!}. \quad (2.5.40)$$

⁴The results of this section can be also obtained using the argument that the operator F is compact and does not have (-1) as eigenvalue, which means that the operator on the right hand side of (2.4.34) is bounded invertible. However, we use the successive approximations approach because it can be used for finding an approximate solution to the kernel by symbolic calculation, because the expressions for successive terms are used to derive explicit controllers in Chapter 3, and because this approach yields a quantitative bound on the kernel (such a bound on the kernel of the inverse transformation is needed in the inverse optimal design in Section 2.7).

Then we have

$$\begin{aligned}
|G_{n+1}(\xi, \eta)| &\leq \frac{1}{4\varepsilon} M^{n+1} \frac{1}{n!} \left\{ (\bar{\lambda} + c) \int_{\eta}^{\xi} \int_0^{\eta} (\tau + s)^n ds d\tau \right. \\
&\quad + \frac{1}{2\varepsilon} \int_0^{\eta} e^{q(\mu-\eta)} \int_0^{\mu} \int_{\mu}^{2\mu-s} f\left(\frac{\tau-s}{2}, \mu - \frac{\tau+s}{2}\right) G(\tau, s) d\tau ds d\mu \\
&\quad + 2(\bar{\lambda} + c) \int_0^{\eta} e^{q(\tau-\eta)} \int_0^{\tau} (\tau + s)^n ds d\tau \\
&\quad + 2\bar{g} \int_0^{\eta} \int_s^{2\eta-s} e^{q(\frac{\tau+s}{2}-\eta)} (\tau + s)^n d\tau ds \\
&\quad + \bar{f} \int_{\eta}^{\xi} \int_0^{\eta} \int_{\mu}^{\mu+\eta-s} (\tau + s)^n d\tau ds d\mu \\
&\quad \left. + 2\bar{f} \int_0^{\eta} e^{q(\mu-\eta)} \int_0^{\mu} \int_{\mu}^{2\mu-s} (\tau + s)^n d\tau ds d\mu \right\} \\
&\leq \frac{1}{4\varepsilon} M^{n+1} \frac{1}{n!} \left\{ 2(\bar{\lambda} + c) \frac{(\xi + \eta)^{n+1}}{n+1} + 2(1 + e^{-q})(\bar{\lambda} + c) \frac{(\xi + \eta)^{n+1}}{n+1} \right. \\
&\quad \left. + 4(1 + e^{-q})\bar{g} \frac{(\xi + \eta)^{n+1}}{n+1} + 2\bar{f} \frac{(\xi + \eta)^{n+1}}{n+1} + 2(1 + e^{-q})\bar{f} \frac{(\xi + \eta)^{n+1}}{n+1} \right\} \\
&\leq M^{n+2} \frac{(\xi + \eta)^{n+1}}{(n+1)!} . \tag{2.5.41}
\end{aligned}$$

So, by induction (2.5.40) is proved. Note also that $G_n(\xi, \eta)$ is $C^2(\mathcal{T}_1)$ which follows from (2.4.35)–(2.4.36) with the assumption (2.2.4). Therefore the series

$$G(\xi, \eta) = \sum_{n=0}^{\infty} G_n(\xi, \eta) \tag{2.5.42}$$

converges absolutely and uniformly in \mathcal{T}_1 and its sum G is a twice continuously differentiable solution of equation (2.4.34) with a bound $|G(\xi, \eta)| \leq M \exp(M(\xi + \eta))$. The uniqueness of this solution can be proved by the following argument. Suppose $G'(\xi, \eta)$ and $G''(\xi, \eta)$ are two different solutions of (2.4.34). Then $\Delta G(\xi, \eta) =$

$G'(\xi, \eta) - G''(\xi, \eta)$ satisfies the homogeneous integral equation (2.4.36) in which G_n and G_{n+1} are changed to ΔG . Using the above result of boundedness we have $|\Delta G(\xi, \eta)| \leq 2Me^{2M}$. Using this inequality in the homogeneous integral equation and following the same estimates as in (2.5.41) we get that $\Delta G(\xi, \eta)$ satisfies for all n

$$|\Delta G(\xi, \eta)| \leq 2M^{n+1}e^{2M} \frac{(\xi + \eta)^n}{n!} \rightarrow 0 \text{ as } n \rightarrow \infty. \quad (2.5.43)$$

Thus $\Delta G \equiv 0$, which means that (2.5.42) is a unique solution to (2.4.34). By direct substitution we can check that it is also a unique (by Lemma 2.1) solution to PDE (2.4.26)–(2.4.28). Thus we proved the following result.

Theorem 2.2. *The equation (2.3.21) with boundary conditions (2.3.22)–(2.3.23) has a unique $C^2(\mathcal{T})$ solution. The bound on the solution is*

$$|k(x, y)| \leq Me^{2Mx} \quad (2.5.44)$$

where M is given by (2.5.39).

To prove stability we need to prove that the transformation (2.3.11) is invertible. The proof that for (2.3.11) an inverse transformation with bounded kernel exists can be found in [3], [42], and can be also inferred from [47, p. 254]. The other way to prove it is to directly find and analyze the PDE for the kernel of the inverse transformation. We take this route because we need the inverse kernel for further quantitative analysis. Let us denote the kernel of the inverse transformation by $l(x, y)$. The transformation itself has the form

$$u(x, t) = w(x, t) + \int_0^x l(x, y)w(y, t) dy. \quad (2.5.45)$$

Substituting (2.5.45) into equations (2.3.12)–(2.3.14) and using (2.2.8)–(2.2.10) we obtain the following PDE governing $l(x, y)$:

$$\varepsilon l_{xx}(x, y) - \varepsilon l_{yy}(x, y) = -(\lambda(x) + c)l(x, y) - f(x, y) - \int_y^x l(\tau, y)f(x, \tau) d\tau \quad (2.5.46)$$

for $(x, y) \in \mathcal{T}$ with boundary conditions

$$\varepsilon l_y(x, 0) = \varepsilon q l(x, 0) + g(x), \quad (2.5.47)$$

$$l(x, x) = -\frac{1}{2\varepsilon} \int_0^x (\lambda(y) + c) dy. \quad (2.5.48)$$

This hyperbolic PDE is a little bit simpler than the one for k (the boundary condition does not contain an integral term), but has a very similar structure. So we can apply the same approach of converting the PDE to an integral equation and using a method of successive approximations to show that the inverse kernel exists and has the same properties as we proved for the direct kernel.

Theorem 2.3. *The equation (2.5.46) with boundary conditions (2.5.47)–(2.5.48) has a unique $C^2(\mathcal{T})$ solution. The bound on the solution is*

$$|l(x, y)| \leq M e^{2Mx} \quad (2.5.49)$$

where M is given by (2.5.39).

2.6 Properties of the Closed Loop System

Theorems 2.2 and 2.3 establish the equivalence of norms of u and w in both L_2 and H_1 . From the properties of the damped heat equation (2.3.12)–(2.3.14) (discussed in some detail in [4] and [42]), exponential stability in both L_2 and H_1 follows. Furthermore, it can be proved (see, e.g. [3]) that if the kernels (2.3.17) are bounded then the system (2.2.8)–(2.2.9) with a boundary condition (2.3.15) or (2.3.16) is well posed. Thus, we get the following main result.

Theorem 2.4. *For any initial data $u_0 \in H_1(0, 1)$ compatible with the boundary conditions (2.2.9), (2.3.15), the system (2.2.8)–(2.2.9) with Dirichlet boundary control (2.3.15) has a unique classical solution $u \in C^{2,1}((0, 1) \times (0, \infty))$ and is exponentially stable at the origin, $u(x, t) \equiv 0$:*

$$\|u(t)\|_{H_1} \leq C e^{-(c-\varepsilon\bar{q}^2)t} \|u_0\|_{H_1}, \quad (2.6.50)$$

where C is a positive constant independent of u_0 .

For any initial data $u_0 \in H_1(0, 1)$ compatible with the boundary conditions (2.2.9), (2.3.16), the system (2.2.8)–(2.2.9) with Neumann boundary control (2.3.16) has a unique classical solution $u \in C^{2,1}((0, 1) \times (0, \infty))$ and is exponentially stable at the origin, $u(x, t) \equiv 0$:

$$\|u(t)\|_{H_1} \leq C e^{-(c-\varepsilon\bar{q}^2-1/2)t} \|u_0\|_{H_1}. \quad (2.6.51)$$

With the backstepping method employing a target system in the simple heat equation form, it becomes possible to write the solution of the closed loop system (2.2.8)–(2.2.9), (2.3.15) explicitly, in terms of the initial condition $u_0(x)$ and the kernels $k(x, y)$ and $l(x, y)$. We show how this is done for $q = +\infty$, since in this case the solution to the target system (2.3.12)–(2.3.14) can be written in the most compact way:

$$w(x, t) = 2 \sum_{n=1}^{\infty} e^{-(c+\varepsilon\pi^2 n^2)t} \sin(\sqrt{\varepsilon}\pi n x) \int_0^1 w_0(\xi) \sin(\sqrt{\varepsilon}\pi n \xi) d\xi. \quad (2.6.52)$$

The initial condition $w_0(x)$ can be calculated explicitly from $u_0(x)$ using the transformation (2.3.11):

$$w_0(x) = u_0(x) - \int_0^x k(x, y) u_0(y) dy. \quad (2.6.53)$$

Substituting (2.6.52) and (2.6.53) into the inverse transformation (2.5.45) and changing the order of integration we obtain the following result, which we specialize in a subsequent development for a subclass of PDEs.

Lemma 2.5. *For $q = +\infty$, the unique solution to the closed loop system (2.2.8)–(2.2.9), (2.3.15) is given by*

$$u(x, t) = \sum_{n=1}^{\infty} e^{-(c+\varepsilon\pi^2 n^2)t} \phi_n(x) \int_0^1 \psi_n(\xi) u_0(\xi) d\xi, \quad (2.6.54)$$

where

$$\phi_n(x) = 2 \left(\sin(\sqrt{\varepsilon}\pi n x) + \int_0^x l(x, y) \sin(\sqrt{\varepsilon}\pi n y) dy \right) \quad (2.6.55)$$

$$\psi_n(x) = \sin(\sqrt{\varepsilon}\pi n x) - \int_x^1 k(y, x) \sin(\sqrt{\varepsilon}\pi n y) dy. \quad (2.6.56)$$

One can directly see from (2.6.54) that the backstepping controller has moved the eigenvalues from their open-loop (unstable) locations into locations of the damped heat equation $-(c + \varepsilon\pi^2n^2)$. It is interesting to note, that although infinitely many eigenvalues cannot be arbitrarily assigned, our controller is able to assign all of them to the particular location $-(c + \varepsilon\pi^2n^2)$. The eigenfunctions of the closed loop system are assigned to $\phi_n(x)$.

Comparison with pole placement. The results of this section should be evaluated in comparison to the well-known results by Triggiani [66] which represent pole placement for PDEs. In [66] one first finds the unstable eigenvalues and the corresponding eigenvectors of the open-loop system. Suppose there are n of them. Then one solves the auxiliary elliptic problem and compute n integrals (which are L_2 inner products of the elliptic solution and the unstable modes). After that solves an n -dimensional matrix equation to find the desired kernel. In contrast, our method, for this 1D parabolic class, consists of successive integrations (symbolic or numerical) to obtain several terms of the series (2.5.42). Another option is to solve the kernel PDE (2.3.21)–(2.3.23) directly by an effective numerical procedure (see Section 2.9). Most importantly, as we shall show in Chapter 3, our method in many cases leads to closed-form controllers. Another issue is the familiar non-robustness of pole placement controllers. Even in the finite dimensional case it is known that backstepping is more robust than pole placement because it converts a system into a tri-diagonal Hessenberg form, rather than a companion form. Furthermore, as we show next, our controllers can be modified (without recalculating the gain kernel) to have robustness margins.

2.7 Inverse Optimal Stabilization

In this section we show how to solve an inverse optimal stabilization problem (pursued for finite-dimensional systems in [37]) for system (2.2.8)–(2.2.10). We design a controller that not only stabilizes the system (2.2.8)–(2.2.9) [as (2.3.15)

or (2.3.16) do] but also minimizes some meaningful cost functional. The stabilizing controllers designed in the previous sections do not possess this property.

For our main result, stated next, we remind the reader that⁵

$$w(1) = u(1) - \int_0^1 k_1(y)u(y) dy. \quad (2.7.57)$$

We point out that, in this section, w satisfies a heat equation (2.3.12)–(2.3.13) with a much more complicated boundary condition at $x = 1$; hence, w should be understood primarily as a coordinate transformation from u , or a short way of writing (2.3.11). The kernel PDE does not change, so the same $k(x, y)$ and $l(x, y)$ are used in this section as in the stabilization problem.

Theorem 2.6. *For any $c > \varepsilon(2\bar{q}^2 + 1)$ and $\beta \geq 2$ the control law*

$$u_x^*(1, t) = -\frac{\beta}{R} \left(u(1, t) - \int_0^1 k_1(y)u(y, t) dy \right) \quad (2.7.58)$$

stabilizes the system (2.2.8)–(2.2.9) in $L_2(0, 1)$ and minimizes the cost functional

$$J(u) = \int_0^\infty (Q(u) + R u_x(1, t)^2) dt \quad (2.7.59)$$

with

$$R = \left(|l(1, 1)| + \int_0^1 l_x(1, y)^2 dy + \bar{q} \right)^{-1} > 0 \quad (2.7.60)$$

and

$$\begin{aligned} Q(u) = & \frac{1}{R} \beta^2 w^2(1) + 2\beta \left\{ l(1, 1)w^2(1) + w(1) \int_0^1 l_x(1, y)w(y) dy \right. \\ & \left. + \bar{q}w^2(0) + \int_0^1 w_x^2 dx + \frac{c}{\varepsilon} \int_0^1 w^2 dx \right\}, \end{aligned} \quad (2.7.61)$$

where

$$Q(u) \geq \frac{1}{R} \beta(\beta - 2)w^2(1) + \frac{2\beta}{\varepsilon} [c - \varepsilon(2\bar{q}^2 + 1)] \int_0^1 w^2 dx + \beta \int_0^1 w_x^2 dx. \quad (2.7.62)$$

⁵Starting from this section, we drop t -dependence for clarity when it does not lead to a confusion, so that $w(1) \equiv w(1, t)$, etc.

Proof. Taking a Lyapunov function in the form

$$V = \frac{1}{2} \int_0^1 w^2(x, t) dx \quad (2.7.63)$$

we get

$$\begin{aligned} \dot{V} &= \varepsilon \int_0^1 w w_{xx} dx - c \int_0^1 w^2 dx \\ &= \varepsilon w(1) u_x(1) - \varepsilon w(1) \int_0^1 l_x(1, y) w(y) dy - \varepsilon l(1, 1) w^2(1) - \varepsilon \bar{q} w^2(0) \\ &\quad - \varepsilon \int_0^1 w_x^2 dx - c \int_0^1 w^2 dx. \end{aligned} \quad (2.7.64)$$

Using (2.7.64) we can write $Q(u)$ in the form

$$Q(u) = \frac{1}{R} \beta^2 w^2(1) + 2\beta \left(w(1) u_x(1) - \frac{1}{\varepsilon} \dot{V} \right). \quad (2.7.65)$$

Substituting now (2.7.65) into the cost functional (2.7.59) we obtain

$$\begin{aligned} J(u) &= \int_0^\infty \left[\frac{1}{R} \beta^2 w^2(1) + 2\beta \left(w(1) u_x(1) - \frac{1}{\varepsilon} \dot{V} \right) + R u_x(1)^2 \right] dt \\ &= \frac{2\beta}{\varepsilon} V(0) - \frac{2\beta}{\varepsilon} V(\infty) + R \int_0^\infty \left[u_x(1) + \frac{\beta}{R} w(1) \right]^2 dt \\ &= \frac{2\beta}{\varepsilon} V(0) - \frac{2\beta}{\varepsilon} V(\infty) + R \int_0^\infty [u_x(1) - u_x^*(1)]^2 dt. \end{aligned} \quad (2.7.66)$$

To complete the proof, we first show that Q is positive definite:

$$\begin{aligned} Q(u) &\geq \frac{1}{R} \beta(\beta - 2) w^2(1) + \frac{2\beta}{R} w^2(1) + 2\beta \int_0^1 w_x^2 dx + \frac{2\beta c}{\varepsilon} \int_0^1 w^2 dx \\ &\quad - 2\beta \left(|l(1, 1)| w^2(1) + \bar{q} w^2(0) + |w(1)| \int_0^1 |l_x(1, y) w(y)| dy \right). \end{aligned} \quad (2.7.67)$$

Using (2.7.60), the Cauchy-Schwartz inequality, and Agmon's inequality

$$\max_{x \in [0, 1]} w^2(x) \leq w^2(1) + 2 \sqrt{\int_0^1 w^2(x) dx} \sqrt{\int_0^1 w_x^2(x) dx}, \quad (2.7.68)$$

we get the following estimate:

$$\begin{aligned}
Q(u) &\geq \frac{1}{R}\beta(\beta-2)w^2(1) + \frac{2\beta}{R}w^2(1) \\
&\quad - 2\beta \left(|l(1,1)|w^2(1) + \bar{q}w^2(1) + 2\bar{q}^2 \int_0^1 w^2 dx + \frac{1}{2} \int_0^1 w_x^2 dx \right. \\
&\quad \left. + \int_0^1 w^2 dx + w^2(1) \int_0^1 l_x(1,y)^2 dy - \int_0^1 w_x^2 dx - \frac{c}{\varepsilon} \int_0^1 w^2 dx \right) \\
&\geq \frac{1}{R}\beta(\beta-2)w^2(1) + 2\beta w^2(1) \left(\frac{1}{R} - |l(1,1)| - \bar{q} - \int_0^1 l_x(1,y)^2 dy \right) \\
&\quad + \frac{2\beta}{\varepsilon}[c - \varepsilon(2\bar{q}^2 + 1)] \int_0^1 w^2 dx + \beta \int_0^1 w_x^2 dx \\
&\geq \frac{1}{R}\beta(\beta-2)w^2(1) + \frac{2\beta}{\varepsilon}[c - \varepsilon(2\bar{q}^2 + 1)] \int_0^1 w^2 dx + \beta \int_0^1 w_x^2 dx. \quad (2.7.69)
\end{aligned}$$

So, Q is a positive definite functional which makes (2.7.59) a reasonable cost which puts penalty both on the state and the control. From (2.7.65) we now have

$$\begin{aligned}
\dot{V} &= \frac{\beta\varepsilon}{2R}w^2(1) + \varepsilon w(1)u_x(1) - \frac{\varepsilon}{2\beta}Q \\
&\leq -[c - \varepsilon(2\bar{q}^2 + 1)] \int_0^1 w^2 dx - \frac{\varepsilon}{2} \int_0^1 w_x^2 dx, \quad (2.7.70)
\end{aligned}$$

which proves that controller $u_x^*(1)$ stabilizes the system (2.3.12)–(2.3.13) (and thus the original system (2.2.8)–(2.2.9)). Setting now $V(\infty) = 0$ in (2.7.66) completes the proof. \square

Meaning of inverse optimality. The inverse optimality result is of considerable significance but its meaning is not obvious. We explain it next. A prevalent method one would pursue for the class of systems considered in this paper is the design of an infinite dimensional linear quadratic regulator (LQR). This approach would result in stability and good performance but would require the solution of an infinite dimensional Riccati equation. On the other hand, the inverse optimality result for our 1D parabolic class, which is given explicitly and does not require the solution of a Riccati equation,⁶ may appear somewhat limited in that

⁶In fact, the Riccati equation is explicitly solved. The solution is $(Id - \mathcal{K})^*(Id - \mathcal{K})$, where Id is the identity operator, \mathcal{K} is the operator corresponding to the transformation $u(x) \mapsto \int_0^x k(x, \xi)u(\xi)d\xi$, and $*$ denotes the adjoint of the operator. The Riccati equation, whose solution this is, is difficult to write without extensive additional notation.

it does not solve the optimal control problem for an *arbitrary* cost functional, but, instead, solves it for a very specialized cost functional (2.7.59)–(2.7.61). However, this cost functional is shown to be positive definite and bounded from below by L_2 and H_1 norms, thus constraining both the (spatial) energy of the transients and the (spatial) peaks of the transients. We also remind the reader of the often overlooked infinite gain margin of inverse optimal controllers (not possessed by ordinary stabilizing controllers), which allows the gain to be of any size, provided it is above a minimal stabilizing value (note that β in Theorem 2.6 is an arbitrary number greater than 2). The other benefit of inverse optimality is the 60° phase margin (the ability to tolerate a certain class of passive but possibly large actuator unmodeled dynamics), which although not stated here, is provable.

Computational comparison between LQR and inverse optimal approach.

Instead of requiring the solution of an operator Riccati equation, the inverse optimal approach for our 1D parabolic class requires a solution of a *linear* hyperbolic PDE, an object conceptually less general than an operator Riccati equation (which is *quadratic*), and numerically easier to solve. The hyperbolic PDE (2.3.21)–(2.3.23) can be solved in several ways: in closed form (see Chapter 3) for a subclass of plants; by truncating the series (2.5.42), although it is hard to say a priori how many terms should be kept; and directly, using a technique from [1] (see Section 2.9). In Section 2.9 we show that the last approach results in more than an order of magnitude in savings of computational time over solving a Riccati equation (for comparable performance), showing the advantage of a structure specific approach.

2.8 Reducing the Control Effort through Adaptation

The controller gain in (2.7.58) contains R that is rather conservative. We show how the control effort can be reduced by using adaptation to start with a zero gain and raise it on line to a stabilizing value. The result is given by the

following theorem.

Theorem 2.7. *The controller*

$$u_x(1, t) = -\hat{\theta}w(1, t) = -\hat{\theta} \left(u(1, t) - \int_0^1 k_1(y)u(y, t) dy \right) \quad (2.8.71)$$

with an update law

$$\dot{\hat{\theta}} = \gamma w^2(1, t), \quad \hat{\theta}(0) = 0, \quad \gamma > 0 \quad (2.8.72)$$

applied to system (2.2.8)–(2.2.9) guarantees the following bounds for the state $u(x, t)$:

$$\sup_{t \geq 0} \int_0^1 u^2(x, t) dx \leq (1 + \bar{l})^2 \left\{ (1 + \bar{k})^2 \int_0^1 u^2(x, 0) dx + \frac{2\varepsilon}{\gamma R^2} \right\} \quad (2.8.73)$$

$$\int_0^\infty \int_0^1 u^2(x, t) dx dt \leq \frac{(1 + \bar{l})^2}{2[c - \varepsilon(2\bar{q}^2 + 1)]} \left\{ (1 + \bar{k})^2 \int_0^1 u^2(x, 0) dx + \frac{2\varepsilon}{\gamma R^2} \right\}, \quad (2.8.74)$$

and the following bound for control $u_x(1, t)$:

$$\int_0^\infty u_x^2(1, t) dt \leq \frac{2\gamma R}{\varepsilon^2} \left((1 + \bar{k})^2 \int_0^1 u^2(x, 0) dx + \frac{4\varepsilon}{\gamma R^2} \right)^2, \quad (2.8.75)$$

where $\bar{l} = \sup_{(x,y) \in \mathcal{T}} l(x, y)$ and $\bar{k} = \sup_{(x,y) \in \mathcal{T}} k(x, y)$.

Proof. Denote

$$\theta = \frac{\beta}{2R} = \frac{\beta}{2} \left(|l(1, 1)| + \int_0^1 l_x(1, y)^2 dy + \bar{q} \right), \quad \theta = \hat{\theta} + \tilde{\theta}. \quad (2.8.76)$$

Taking Lyapunov function

$$V_1 = \frac{1}{2} \int_0^1 w^2(x, t) dx + \frac{\varepsilon}{2\gamma} \tilde{\theta}^2 \quad (2.8.77)$$

and using (2.7.70) we get

$$\dot{V}_1 = \varepsilon w(1)(\hat{\theta}w(1) + u_x(1)) + \tilde{\theta} \left(\varepsilon w^2(1) - \frac{\varepsilon}{\gamma} \dot{\hat{\theta}} \right) - \frac{\varepsilon}{2\beta} Q. \quad (2.8.78)$$

Choosing the controller and the update law as in (2.8.71), (2.8.72), respectively, we obtain

$$\dot{V}_1 \leq -\frac{\varepsilon}{2R}(\beta - 2)w^2(1) - [c - \varepsilon(2\bar{q}^2 + 1)] \int_0^1 w^2 dx - \frac{\varepsilon}{2} \int_0^1 w_x^2 dx. \quad (2.8.79)$$

From (2.8.77) and (2.8.79) the following estimates easily follow

$$\sup_{t \geq 0} \int_0^1 w^2(x, t) dx \leq \int_0^1 w^2(x, 0) dx + \frac{\varepsilon}{\gamma} \tilde{\theta}^2(0), \quad (2.8.80)$$

$$\int_0^\infty \int_0^1 w^2(x, t) dx dt \leq \frac{1}{2[c - \varepsilon(2\bar{q}^2 + 1)]} \left(\int_0^1 w^2(x, 0) dx + \frac{\varepsilon}{\gamma} \tilde{\theta}^2(0) \right), \quad (2.8.81)$$

$$\begin{aligned} \int_0^\infty u_x^2(1, t) dt &\leq \int_0^\infty \hat{\theta}^2(t) w(1, t)^2 dt \leq 2(\theta^2 + \sup_{t \geq 0} \tilde{\theta}^2(t)) \int_0^\infty w(1, t)^2 dt \\ &\leq 2 \left(2\theta^2 + \frac{\gamma}{\varepsilon} \int_0^1 w(x, 0)^2 dx \right) \frac{R}{\varepsilon(\beta - 2)} \left(\int_0^1 w(x, 0)^2 dx + \frac{\varepsilon}{\gamma} \theta^2 \right) \\ &\leq \frac{\gamma R}{\varepsilon^2(\beta - 2)} \left(\int_0^1 w^2(x, 0) dx + \frac{\varepsilon \beta^2}{2\gamma R^2} \right)^2. \end{aligned} \quad (2.8.82)$$

Using (2.3.11) and (2.5.45) one can get the relationship between the norms of u and w

$$\|u\|^2 \leq (1 + \bar{l})^2 \|w\|^2, \quad \|w\|^2 \leq (1 + \bar{k})^2 \|u\|^2. \quad (2.8.83)$$

where $\bar{l} = \sup_{(x,y) \in \mathcal{T}} l(x, y)$, $\bar{k} = \sup_{(x,y) \in \mathcal{T}} k(x, y)$. Now (2.8.80)–(2.8.82) with (2.8.83) and $\beta = 2\sqrt{2}$ give estimates (2.8.73)–(2.8.75), respectively. \square

The adaptive controllers are not inverse optimal, but they perform better than stabilizing controllers and use less gain than non-adaptive inverse optimal ones. As the numerical simulations in Section 2.9 and Chapter 3 will show, actual savings of the control effort can be quite large: for the considered settings the adaptive controller uses several dozen times less gain than the non-adaptive one would.

Although the results of this and previous section are stated for Neumann boundary control, our approach is not restricted to it. One way to address the Dirichlet case is to use (2.8.71) to express $u(1, t)$:

$$u(1, t) = -\frac{1}{\hat{\theta}} u_x(1, t) + \int_0^1 k_1(y) u(y, t) dy. \quad (2.8.84)$$

with the dynamics of $\hat{\theta}$ given by (2.8.72). The only restriction is that $\hat{\theta}(0) > 0$. Of course, this controller puts a penalty on $u_x(1, t)$ instead of $u(1, t)$, so it can not

be called optimal as a Dirichlet controller. To get a true inverse optimal Dirichlet controller we write similarly to (2.8.71)–(2.8.72):

$$u(1, t) = -\hat{\theta}w_x(1, t), \quad \dot{\hat{\theta}} = \gamma w_x^2(1, t), \quad (2.8.85)$$

or, using the expression for $w_x(1, t)$,

$$w_x(1, t) = u_x(1, t) - k_1(1)u(1, t) - \int_0^1 k_2(y)u(y, t) dy, \quad (2.8.86)$$

the controller can be written as

$$u(1, t) = -\frac{\hat{\theta}}{1 + \hat{\theta} \int_0^1 (\lambda(y) + c) dy} \left(u_x(1, t) - \int_0^1 k_2(y)u(y, t) dy \right). \quad (2.8.87)$$

The initial value of the adaptive gain $\hat{\theta}(0)$ can be taken zero in meaningful stabilization problems where $\lambda(x) \geq 0$. Note the structural similarity of the controllers (2.8.84) and (2.8.87). Both employ an integral operator of u measured for all $x \in [0, 1)$ and a measurement of u_x at $x = 1$. The optimality of the controller (2.8.87) can be proved along the same lines as in the proof of Theorem 2.7.

2.9 Numerical Results

In this section we present the results of numerical simulations for the plant (2.2.8)–(2.2.9) with Dirichlet boundary control. The parameters of the system were taken to be $\varepsilon = 1$, $\lambda(x) = 14 - 16(x - 1/2)^2$, $q = 2$, and initial condition $u_0(x) = 1 + \sin(3\pi x/2)$. With these parameters the system has one unstable eigenvalue at 7.8.

Instead of calculating the series (2.5.42) we directly numerically solve the PDE (2.3.21)–(2.3.23). This PDE resembles the Klein-Gordon PDE [21] but it contains additional terms, evolves on a different domain and has more complicated boundary conditions. The scheme for this equation should be selected carefully since the term with $\lambda(x)$ can cause numerical instability. We suggest the following second order accuracy Ablowitz-Kruskal-Ladik [1] scheme which we modified to

suit the geometry and boundary conditions of the kernel PDE:

$$k_j^{i+1} = -k_j^{i-1} + k_{j+1}^i + k_{j-1}^i + a_j h^2 \frac{k_{j+1}^i + k_{j-1}^i}{2}, \quad (2.9.88)$$

$$k_{i+1}^{i+1} = k_i^i - \frac{h}{4}(a_i + a_{i+1}), \quad k_1^1 = 0, \quad (2.9.89)$$

$$k_1^{i+1} = -k_1^{i-1} + 2k_2^i \frac{1 + a_1 h^2/2}{1 + qh(1 + a_1 h^2/2)}. \quad (2.9.90)$$

Here $k_j^i = k((i-1)h, (j-1)h)$, $i = 2, \dots, N$, $j = 2, \dots, i-1$, $a_i = (\lambda((i-1)h) + c)/\varepsilon$, $h = 1/N$, N is the number of steps. The key feature of this scheme is the discretization of the $a(y)k(x, y)$ -term, averaging $k(x, y)$ in the y -direction.

The terms with $g(x)$ and $f(x, y)$ can also be incorporated into the scheme. We do not consider them here because proving stability of the modified numerical scheme in this case is beyond the scope of this paper.

A static LQR controller (with unity penalties on the state and control) was implemented using the most popular Galerkin approximation, although more advanced techniques exist [14]. We used the discretization with $N = 100$ steps. Computation of the gain kernel for the backstepping controller using the scheme (2.9.88)–(2.9.90) took as much as 20 times less time than for the LQR/Riccati kernel. This suggests that our method may be of even more interest in 2D and 3D problems where the cost of solving operator Riccati equation becomes nearly prohibitive [14]. Symbolic computation using the series (2.5.42) is also possible; four terms G_0, \dots, G_3 are sufficient for practical implementation giving relative error 0.6% with respect to the numerical solution.

The results of the simulations of the closed loop system are presented in Figure 2.1. The system was discretized using a BTCS finite difference method with 100 steps. We used the Dirichlet adaptive controller with $c = 0$, $\gamma = 1$, $\hat{\theta}(0) = 0.5$. Figure 2.1 (c) shows the evolution of the adaptive gain, its maximum value turns out to be about 50 times less than the conservative (constant) inverse optimal gain. The control effort and the L_2 norm of the closed loop state are shown in Figures 2.1 (a) and (b), respectively. We see that LQR controller shows just slightly better performance.

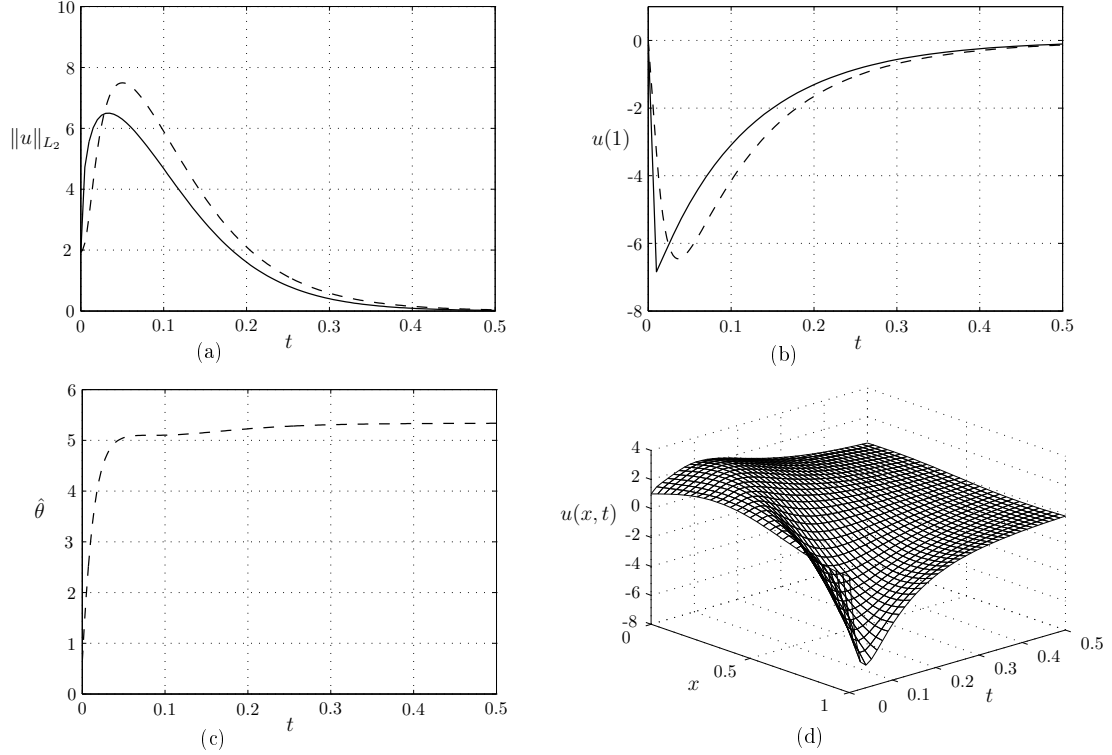


Figure 2.1: The comparison between LQR (solid) and inverse optimal (dashed) controllers: (a) L_2 -norm of the state; (b) the control effort; (c) the adaptive gain; (d) the state for inverse optimal controller.

2.10 Conclusions

The backstepping technique might be best appreciated by readers familiar with the historical developments of finite dimensional *nonlinear* control. The first systematic nonlinear control methods were the methods of optimal control, which require the ‘solution’ of Hamilton-Jacobi-Bellman nonlinear *PDEs*. The breakthrough in nonlinear control came with the differential geometric theory and feedback linearization, which recognized the structure of nonlinear control systems and exploited it using coordinate transformations and feedback cancellations. (Backstepping boundary control, incidentally, uses the same approach—a linear integral transformation plus boundary feedback.) In the same way that nonlinear *PDEs* (HJB) are more complex than what ODE control problems call for, operator Ric-

cati equations are more than what linear boundary control calls for in the 1D parabolic class in this chapter. In summary, backstepping, with its linear hyperbolic PDE for the gain kernel, is unique in not exceeding the complexity of the PDE control problem that it is solving.

This chapter is in part a reprint of the material as it appears in A. Smyshlyaev and M. Krstic, “Closed form boundary state feedbacks for a class of 1D partial integro-differential equations,” *IEEE Trans. on Automatic Control*, vol. 49, no. 12, pp. 2185-2202, 2004.

A. Smyshlyaev and M. Krstic, “On control design for PDEs with space-dependent diffusivity or time-dependent reactivity,” *Automatica*, 41, pp. 1601-1608, 2005.

The dissertation author was the primary author and the coauthor listed in this publication directed the research which forms the basis for this chapter.

Chapter 3

Closed Form Controllers for Reaction-Advection-Diffusion Systems

One of the striking features of our approach is that it leads to explicit feedback controllers for many physically relevant problems. In this chapter we present closed form solutions to six distinct problems and then show how to combine them for a rather general class of plants.

Apart from the obvious practical benefit of having a closed form control law, the explicit gain kernels allow us to find explicit solutions for the closed loop system, offering valuable insight into how control affects eigenvalues and eigenfunctions. Another possible usage is in testing numerical schemes, similar to the role analytical solutions to Burgers' equation play in computational fluid dynamics.

3.1 Unstable Heat Equation

Consider the system

$$u_t(x, t) = \varepsilon_0 u_{xx}(x, t) + \lambda_0 u(x, t), \quad x \in (0, 1), \quad (3.1.1)$$

$$u(0, t) = 0, \quad (3.1.2)$$

where ε_0 and λ_0 are constants. The open-loop system (3.1.1)–(3.1.2) (with $u(1, t) = 0$ or $u_x(1, t) = 0$) is unstable with arbitrarily many unstable eigenvalues (for large λ_0/ε_0). Although this constant coefficient problem may appear easy, the explicit boundary stabilization result in the case of arbitrary ε_0 , λ_0 is not available in the literature.

The backstepping methods for solving the boundary control problem for (3.1.1)–(3.1.2) have been considered in [13], [3], and [42]. In [13], the stabilizing controller was constructed in a closed form, but only for $\lambda_0 < 3\pi^2\varepsilon_0/4$ (i.e. for the case of one unstable eigenvalue). In [3], finite-dimensional backstepping was applied to the discretized version of the system (3.1.1)–(3.1.2) for arbitrary λ_0 and shown to be convergent in L_∞ . In [42], the kernel PDE was derived and shown to be well posed.

We will thoroughly explore this problem to illustrate all the results of Chapter 2.

The kernel PDE (2.3.21)–(2.3.23) takes the following form:

$$k_{xx}(x, y) - k_{yy}(x, y) = \lambda k(x, y) \quad (3.1.3)$$

$$k(x, 0) = 0, \quad (3.1.4)$$

$$k(x, x) = -\frac{\lambda x}{2}, \quad (3.1.5)$$

where we denote $\lambda = (\lambda_0 + c)/\varepsilon_0$. Let us solve this equation directly by the method of successive approximations. Integral equation (2.4.34) for G becomes

$$G(\xi, \eta) = -\frac{\lambda}{4}(\xi - \eta) + \frac{\lambda}{4} \int_{\eta}^{\xi} \int_0^{\eta} G(\tau, s) ds d\tau. \quad (3.1.6)$$

Now set

$$G_0(\xi, \eta) = -\frac{\lambda}{4}(\xi - \eta), \quad G_{n+1}(\xi, \eta) = \frac{\lambda}{4} \int_{\eta}^{\xi} \int_0^{\eta} G_n(\tau, s) ds d\tau. \quad (3.1.7)$$

Fortunately, we can find the general term G_n in closed form:

$$G_n(\xi, \eta) = -\frac{(\xi - \eta) \xi^n \eta^n}{(n!)^2(n+1)} \left(\frac{\lambda}{4}\right)^{n+1}. \quad (3.1.8)$$

Now we can calculate the series (2.5.42):

$$G(\xi, \eta) = \sum_{n=0}^{\infty} G_n(\xi, \eta) = -\frac{\lambda(\xi - \eta)}{2} \frac{I_1(\sqrt{\lambda\xi\eta})}{\sqrt{\lambda\xi\eta}}, \quad (3.1.9)$$

where I_1 is a modified Bessel function of order one. Writing (3.1.9) in terms of x, y gives the following solution for $k(x, y)$

$$k(x, y) = -\lambda y \frac{I_1\left(\sqrt{\lambda(x^2 - y^2)}\right)}{\sqrt{\lambda(x^2 - y^2)}}, \quad (3.1.10)$$

which gives the gain kernels

$$k_1(y) = k(1, y) = -\lambda y \frac{I_1\left(\sqrt{\lambda(1 - y^2)}\right)}{\sqrt{\lambda(1 - y^2)}}. \quad (3.1.11)$$

and

$$k_2(y) = k_x(1, y) = -\lambda y \frac{I_2\left(\sqrt{\lambda(1 - y^2)}\right)}{1 - y^2}. \quad (3.1.12)$$

A comparison of this result and the kernel obtained by finite-dimensional backstepping [3] is presented in Figure 3.1. Both kernels can be used to successfully stabilize the system. However, applying infinite-dimensional backstepping transformation to the plant (3.1.1)–(3.1.2) first and then dealing with the resulting kernel PDE leads to a *smooth kernel*, whereas the approach [3] of discretizing the plant (3.1.1)–(3.1.2) first and then applying finite-dimensional backstepping results in a discontinuous oscillating kernel (which is still stabilizing).

In Figure 3.2 the kernel $k_1(y)$ is plotted for several values of λ . We see that the maximum of the absolute value of the kernel moves to the left as λ grows. We can actually calculate the area under the curves in Figure 2 and estimate an amount of total gain effort required:

$$E = \int_0^1 |k_1(y)| dy = \lambda \int_0^1 y \frac{I_1\left(\sqrt{\lambda(1 - y^2)}\right)}{\sqrt{\lambda(1 - y^2)}} dy = \int_0^{\sqrt{\lambda}} I_1(z) dz = I_0\left(\sqrt{\lambda}\right) - 1. \quad (3.1.13)$$

In Figure 3.3 the dependence of total gain on the level of instability is shown. As $\lambda \rightarrow \infty$, E behaves as $E \sim e^{\sqrt{\lambda}}/(\sqrt{2\pi} \lambda^{1/4})$.

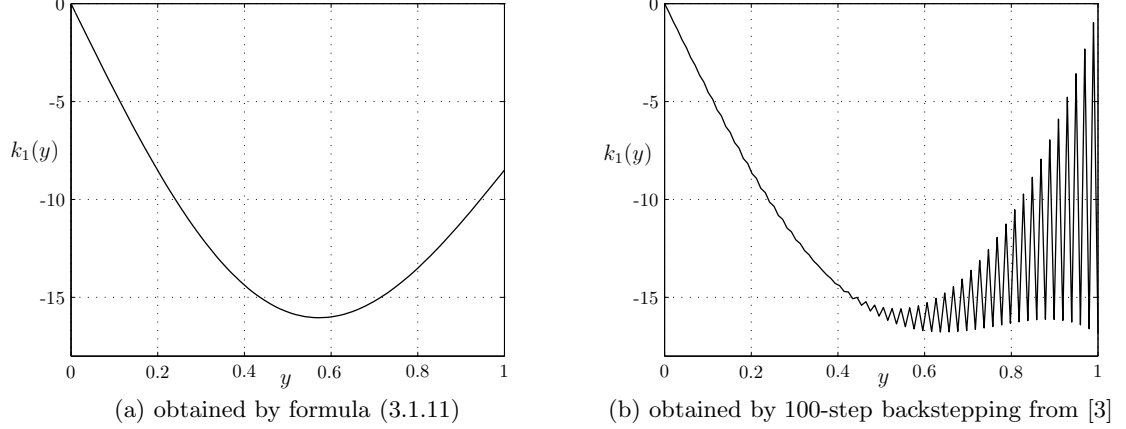


Figure 3.1: Stabilizing gain kernel $k_1(y)$ for unstable heat equation (3.1.1)–(3.1.2) with $\lambda = 17$.

With both $k(x, y)$ and $l(x, y)$ being explicit, we calculate $\phi_n(x)$ and $\psi_n(x)$ in (2.6.55)–(2.6.56) and get the following result.

Theorem 3.1. *The solution to the closed loop system (3.1.1)–(3.1.2), (2.3.15) with $k_1(y)$ given by (3.1.11) is*

$$\begin{aligned}
 u(x, t) = & 2 \sum_{n=1}^{\infty} e^{-(c+\varepsilon_0\pi^2 n^2)t} \frac{\sqrt{\varepsilon_0}\pi n}{\sqrt{\lambda_0 + \varepsilon_0\pi^2 n^2}} \sin \sqrt{\lambda_0 + \varepsilon_0\pi^2 n^2} x \\
 & \times \int_0^1 \left(\sin(\sqrt{\varepsilon_0}\pi n \xi) + \int_{\xi}^1 \xi \frac{I_1(\sqrt{\lambda(\tau^2 - \xi^2)})}{\sqrt{\lambda(\tau^2 - \xi^2)}} \sin(\sqrt{\varepsilon_0}\pi n \tau) d\tau \right) \\
 & \times u_0(\xi) d\xi. \tag{3.1.14}
 \end{aligned}$$

This result is proved using Lemma 2.5. In particular, the integral in (2.6.55) is solved explicitly with the help of [50]. It can also be shown [50] that $\frac{\sqrt{\varepsilon}\pi n}{\sqrt{\lambda + \varepsilon\pi^2 n^2}} \sin \sqrt{\lambda + \varepsilon\pi^2 n^2} x$ and $\sin(\sqrt{\varepsilon}\pi n \xi) + \int_{\xi}^1 \xi \frac{I_1(\sqrt{\lambda(\tau^2 - \xi^2)})}{\sqrt{\lambda(\tau^2 - \xi^2)}} \sin(\sqrt{\varepsilon}\pi n \tau) d\tau$ are orthonormal bases.

Now let us construct an inverse-optimal controller. First we need to find the kernel of the inverse transformation. Noticing that in our case $l(x, y) = -k(x, y)$ when λ is replaced by $-\lambda$, we immediately obtain

$$l(x, y) = -\lambda y \frac{J_1(\sqrt{\lambda(x^2 - y^2)})}{\sqrt{\lambda(x^2 - y^2)}} \tag{3.1.15}$$

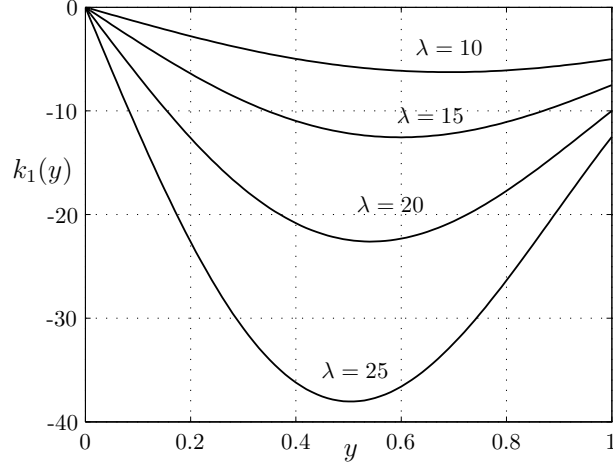


Figure 3.2: Dependence of the gain kernel on the level of instability.

where J_1 is the usual (non-modified) Bessel function of the first order. Since $l(x, y)$ is now available in closed form we can get more careful estimates than in Chapter 2:

$$\begin{aligned} \int_0^1 |l_x(1, y)| dy &= \int_0^1 \frac{\lambda y}{1-y^2} \left| J_2 \left(\sqrt{\lambda(1-y^2)} \right) \right| dy \\ &= \lambda \int_0^{\sqrt{\lambda}} \frac{|J_2(z)|}{z} dz \leq \lambda + 1. \end{aligned} \quad (3.1.16)$$

So, we obtain from (2.7.64)

$$\dot{V} \leq w(1) \left(u_x(1) + \frac{1}{2}(\lambda + 1)^2 w(1) + \frac{\lambda}{2} w(1) \right) - \frac{1}{2} \int_0^1 w_x^2 dx - c \int_0^1 w^2 dx. \quad (3.1.17)$$

Taking now

$$u_x(1, t) = -\beta \frac{(\lambda + 1)^2 + \lambda}{2} \left(u(1, t) + \int_0^1 \lambda y \frac{I_1(\sqrt{\lambda(1-y^2)})}{\sqrt{\lambda(1-y^2)}} u(y, t) dy \right), \quad \beta \geq 2 \quad (3.1.18)$$

we get the Neumann controller that solves an inverse optimal stabilization problem. The Dirichlet controller can be obtained using (2.8.87) and (3.1.12). Let us summarize the results in the following theorem.

Theorem 3.2. *The controller (2.3.15) with the kernel (3.1.11) stabilizes the unstable heat equation (3.1.1)–(3.1.2). The controller (3.1.18), while stabilizing (3.1.1)–*

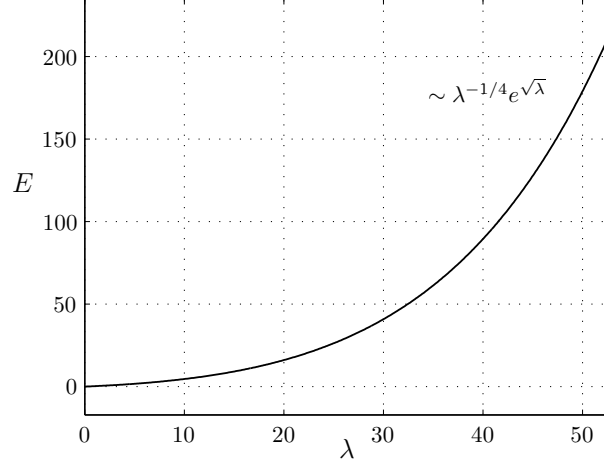


Figure 3.3: Amount of total gain as a function of λ .

(3.1.2), also minimizes the cost functional (2.7.59) with Q given by (2.7.61) and $R^{-1} = ((\lambda + 1)^2 + \lambda)/2$.

The penalty on the control in this case seems to become smaller as λ increases, but in fact only the ratio between $Q(u)$ and R matters, which can not be estimated in our design. This is another difference with the LQR approach: in LQR the penalties on the state and the control are constant and in our design these penalties are free to change. In both approaches the optimal value of the functional changes with λ and grows unbounded as $\lambda \rightarrow \infty$.

The comparison of the stabilizing and adaptive inverse optimal controller is presented in Figure 3.4. The system (3.1.1)–(3.1.2) was simulated with $\lambda_0 = 10$, $\varepsilon = 1$, $c = 0$, and the initial condition $u_0(x) = \sin(\pi x)$. The adaptation gain was taken as $\gamma = 2$. We can see that, compared to the stabilizing controller, the adaptive inverse optimal controller achieves better performance with less control effort. We can also estimate how much gain it actually saves compared to a non-adaptive controller. As (3.1.18) shows, the gain of the non-adaptive controller should be greater than or equal to $(\lambda + 1)^2 + \lambda = 131$, while the adaptive gain is less than or equal to 2.85 at all times [Figure 3.4 (c)]. So the adaptive controller used $131/2.85 = 46$ times less gain.

For the case of a homogeneous Neumann boundary condition at $x = 0$ for the equation (3.1.1) it is easy to repeat all the steps we have done for the Dirichlet case and get the following closed form solution for the kernel:

$$k(x, y) = -\lambda x \frac{I_1(\sqrt{\lambda(x^2 - y^2)})}{\sqrt{\lambda(x^2 - y^2)}}. \quad (3.1.19)$$

Note that the leading factor here is x , versus y in (3.1.10). The maximum of the absolute value of the kernel is reached at $x = 0$. This makes sense because the control has to react the most aggressively to perturbations that are the farthest from it. The total gain can be calculated to be [50]

$$E = \int_0^1 |k_1(y)| dy = \lambda \int_0^1 \frac{I_1(\sqrt{\lambda(1 - y^2)})}{\sqrt{\lambda(1 - y^2)}} dy = \cosh(\sqrt{\lambda}) - 1. \quad (3.1.20)$$

3.2 Heat Equation with Destabilizing Boundary Condition

We now consider a more complicated system

$$u_t(x, t) = \varepsilon_0 u_{xx}(x, t) + \lambda_0 u(x, t), \quad (3.2.21)$$

$$u_x(0, t) = qu(0, t), \quad (3.2.22)$$

where the boundary condition on the uncontrolled end is mixed and can cause instability for $q < 0$. This type of boundary condition appears for example in a solid propellant rocket model [10] and can also arise due to transformation (2.2.5). The results of the previous subsection apply when $q = 0$ or $q = +\infty$. We will use them here to get the solution for an arbitrary q .

The gain kernel PDE takes the following form:

$$k_{xx}(x, y) - k_{yy}(x, y) = \lambda k(x, y), \quad (3.2.23)$$

$$k_y(x, 0) = qk(x, 0), \quad (3.2.24)$$

$$k(x, x) = -\frac{\lambda x}{2}. \quad (3.2.25)$$

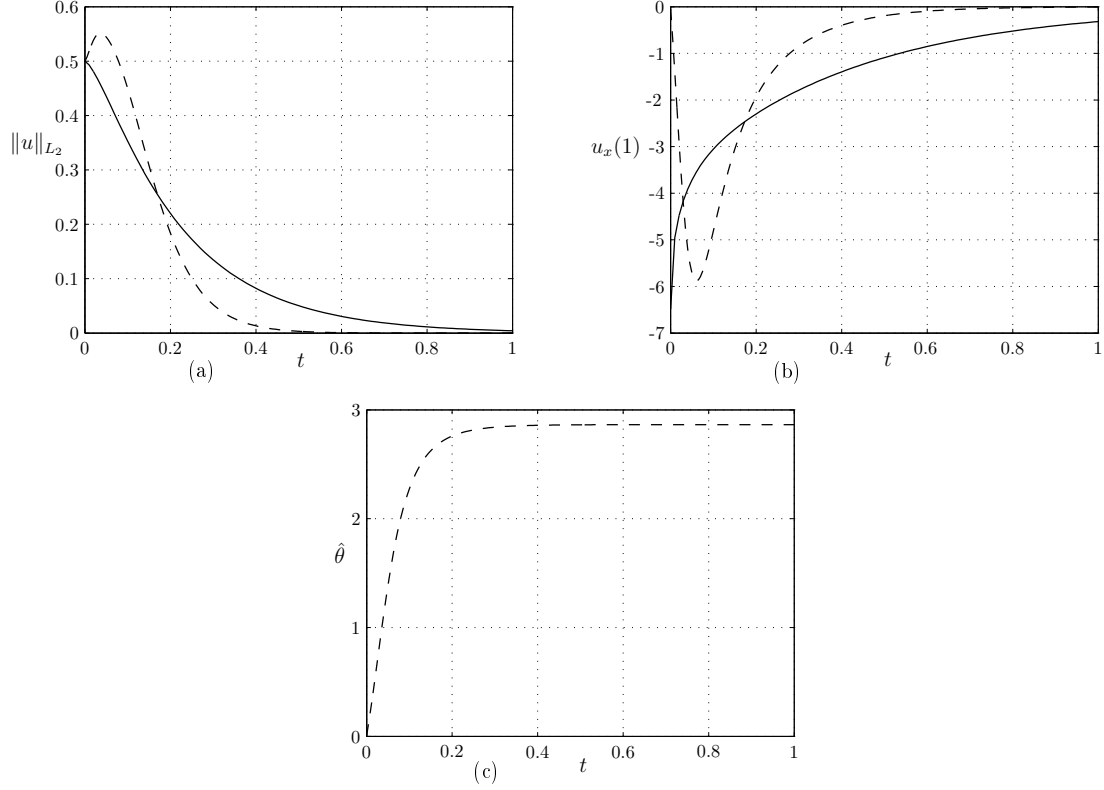


Figure 3.4: The comparison between stabilizing (solid) and inverse optimal (dashed) controllers: (a) L_2 -norm of the state; (b) the control effort; (c) the adaptive gain.

where $\lambda = (\lambda_0 + c)/\varepsilon_0$. We propose to search for a solution in the following form

$$k(x, y) = -\lambda x \frac{I_1(\sqrt{\lambda(x^2 - y^2)})}{\sqrt{\lambda(x^2 - y^2)}} + \int_0^{x-y} I_0(\sqrt{\lambda(x+y)(x-y-\tau)}) \rho(\tau) d\tau. \quad (3.2.26)$$

Here the first term is a solution to (3.2.23)–(3.2.25) with $q = 0$ which has been obtained in the previous subsection. The second term is just one of the solutions to (3.2.23), ρ being a function to be determined. We can see now that (3.2.26) is a solution to (3.2.23), (3.2.25) and we need only to choose $\rho(\tau)$ so that (3.2.24) is satisfied. Substituting (3.2.26) into (3.2.24) we obtain the following integral

equation for $\rho(x)$:

$$\rho(x) + \int_0^x \rho(\tau) \left(\frac{\lambda}{2} \tau \frac{I_1(\sqrt{\lambda x(x-\tau)})}{\sqrt{\lambda x(x-\tau)}} + q I_0(\sqrt{\lambda x(x-\tau)}) \right) d\tau = \sqrt{\lambda} q I_1(\sqrt{\lambda} x). \quad (3.2.27)$$

To solve this equation we apply the Laplace transform with respect to x to both sides of (3.2.27) and get:

$$\begin{aligned} \rho(s) + \int_0^\infty e^{-s\xi} \int_0^\xi \rho(\tau) \left(\frac{\lambda}{2} \tau \frac{I_1(\sqrt{\lambda \xi(\xi-\tau)})}{\sqrt{\lambda \xi(\xi-\tau)}} + q I_0(\sqrt{\lambda \xi(\xi-\tau)}) \right) d\tau d\xi \\ = q \frac{s - \sqrt{s^2 - \lambda}}{\sqrt{s^2 - \lambda}}. \end{aligned} \quad (3.2.28)$$

After changing the order of integration, calculating the inner integral, and introducing a new variable $s' = (s + \sqrt{s^2 - \lambda})/2$ we obtain:

$$\int_0^\infty \rho(\tau) e^{-s'\tau} d\tau = q \frac{s - \sqrt{s^2 - \lambda}}{q + \sqrt{s^2 - \lambda}}, \quad (3.2.29)$$

Now using the relation $s = s' + \lambda/(4s')$ we get

$$\rho(s') = \frac{2q\lambda}{(2s' + q)^2 - (\lambda + q^2)}. \quad (3.2.30)$$

Taking the inverse Laplace transform gives

$$\rho(x) = \frac{q\lambda}{\sqrt{\lambda + q^2}} e^{-qx/2} \sinh \frac{\sqrt{\lambda + q^2}}{2} x. \quad (3.2.31)$$

Substituting (3.2.31) into (3.2.26) we get the following expression for the gain kernel given in quadratures.

Theorem 3.3. *The solution to (3.2.23)–(3.2.25) is*

$$\begin{aligned} k(x, y) = & \frac{q\lambda}{\sqrt{\lambda + q^2}} \int_0^{x-y} e^{-q\tau/2} \sinh \left(\frac{\sqrt{\lambda + q^2}}{2} \tau \right) I_0(\sqrt{\lambda(x+y)(x-y-\tau)}) d\tau \\ & - \lambda x \frac{I_1(\sqrt{\lambda(x^2 - y^2)})}{\sqrt{\lambda(x^2 - y^2)}}. \end{aligned} \quad (3.2.32)$$

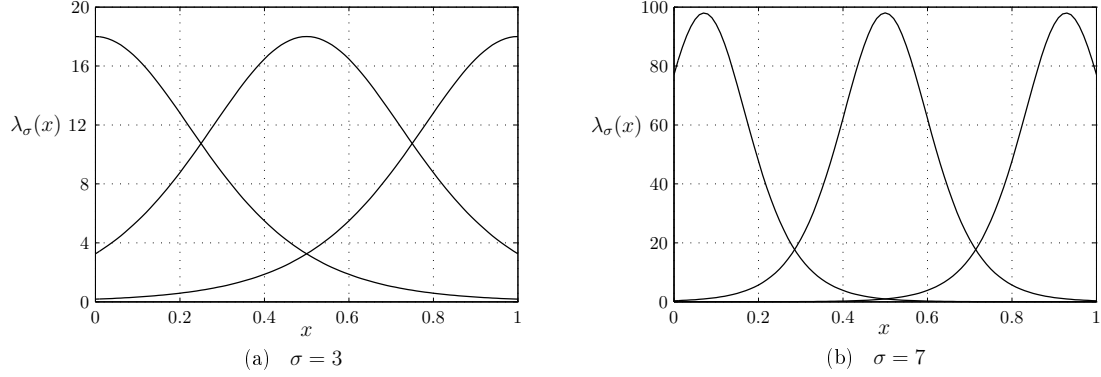


Figure 3.5: "One-peak" $\lambda_\sigma(x)$ for different values of σ and x_0 .

3.3 Explicit Solution for a Family of Plants with Spatially Varying Reaction

Consider the system

$$u_t(x, t) = u_{xx}(x, t) + \lambda_\sigma(x)u(x, t), \quad (3.3.33)$$

$$u(0, t) = 0, \quad (3.3.34)$$

where $\lambda_\sigma(x)$ is given by

$$\lambda_\sigma(x) = \frac{2\sigma^2}{\cosh^2(\sigma(x - x_0))}. \quad (3.3.35)$$

This $\lambda_\sigma(x)$ parametrizes a family of "one-peak" functions. The maximum of $\lambda_\sigma(x)$ is $2\epsilon\sigma^2$ and is achieved at $x = x_0$. The parameters σ and x_0 can be chosen to give the maximum an arbitrary value and location. Examples of $\lambda_\sigma(x)$ for different values of σ and x_0 are shown in Figure 3.5. The "sharpness" of the peak is not arbitrary and is given by $\lambda''_{\max} = -\lambda_{\max}^2/\epsilon$. Despite the strange-looking expression for $\lambda_\sigma(x)$, the system (6.3.34)–(6.3.35) can approximate very well the linearized model of a chemical tubular reactor (see [12] and references therein) which is open loop unstable.

Our result on stabilization of (6.3.34)–(6.3.35) is given by the following theorem.

Theorem 3.4. *The controller*

$$u(1, t) = - \int_0^1 \sigma e^{\sigma \tanh \sigma x_0 (1-y)} [\tanh \sigma x_0 - \tanh(\sigma(x_0 - y))] u(y, t) dy \quad (3.3.36)$$

stabilizes the system (6.3.34)–(6.3.35).

Proof. The kernel PDE for (6.3.34)–(6.3.35) is

$$k_{xx}(x, y) - k_{yy}(x, y) = \lambda_\sigma(y) k(x, y), \quad (3.3.37)$$

$$k(x, 0) = 0, \quad (3.3.38)$$

$$k(x, x) = -\frac{1}{2} \int_0^x \lambda_\sigma(\tau) d\tau. \quad (3.3.39)$$

Postulating $k(x, y) = X(x)Y(y)$, we have the following set of ODE's:

$$X''(x) = \mu X(x), \quad (3.3.40)$$

$$Y''(y) = Y(y)(\mu + 2X(y)Y'(y) + 2X'(y)Y(y)), \quad (3.3.41)$$

$$Y(0) = 0, \quad (3.3.42)$$

where μ is an arbitrary parameter. Let us choose $X(x) = e^{\sqrt{\mu}x}$ and substitute it into (3.3.41). We get

$$Y''(y) - 2e^{\sqrt{\mu}y}Y'(y)Y(y) - 2\sqrt{\mu}e^{\sqrt{\mu}y}Y^2(y) - \mu Y(y) = 0. \quad (3.3.43)$$

Changing variables $Y(y) = Z(y)e^{-\sqrt{\mu}y}$ we arrive at the following ODE:

$$Z''(y) - 2Z'(y)Z(y) - 2\sqrt{\mu}Z'(y) = 0 \quad (3.3.44)$$

$$Z(0) = 0, \quad (3.3.45)$$

$$Z'(0) = \mu - \sigma^2. \quad (3.3.46)$$

Here we introduced a new arbitrary parameter σ . The solution to the problem (3.3.44)–(3.3.46) is

$$Z(y) = -\sigma (\tanh(\sigma(y - x_0)) + \tanh \sigma x_0), \quad (3.3.47)$$

where $\tanh \sigma x_0 = \sqrt{\mu}/\sigma$.

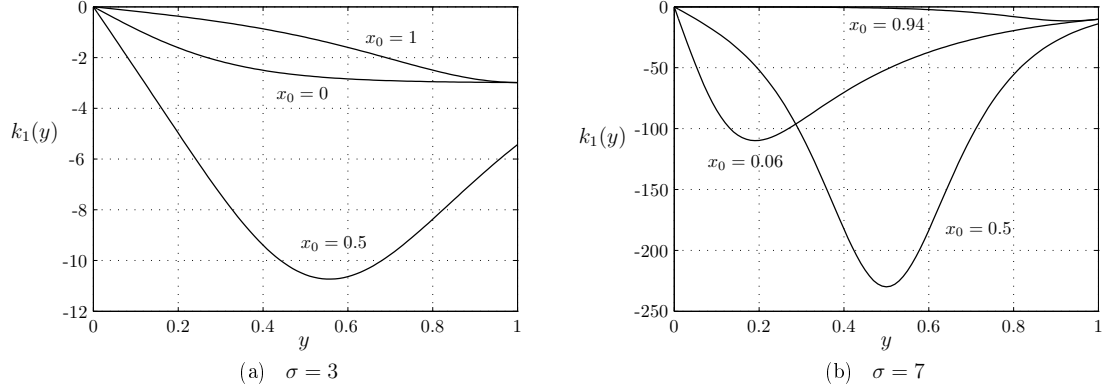


Figure 3.6: Gain kernel $k_1(y)$ for (6.3.34)–(6.3.35).

Now we can check that

$$\lambda_\sigma(x) = -2(X(x)Y(x))' = -2Z'(x) = \frac{2\sigma^2}{\cosh^2(\sigma(x - x_0))}, \quad (3.3.48)$$

which gives (3.3.35). Using (3.3.47) we obtain the kernel

$$k(x, y) = -\sigma e^{\sigma \tanh \sigma x_0 (x-y)} (\tanh \sigma x_0 - \tanh(\sigma(x_0 - y))). \quad (3.3.49)$$

Setting $x = 1$ in (3.3.49) concludes the proof. \square

In Figure 3.6 the stabilizing kernels corresponding to $\lambda_\sigma(x)$ from Figure 3.5 are shown. We can see that the control effort depends very much on the location of the peak of $\lambda_\sigma(x)$, which has an obvious explanation. When the peak is close to $x = 1$, the controller's influence is very high, when it is close to $x = 0$, the boundary condition (6.3.35) helps to stabilize, so the worst case is the peak somewhere in the middle of the domain.

One can show that the most general $\lambda(x)$ for which the controller can be found using the method of separation of variables is

$$\lambda(x) = 2(\alpha^2 - \beta^2) \frac{\alpha^2 h^2(x) + (\beta^2 - \gamma^2) \sinh^2(\alpha x)}{(\alpha \cosh(\alpha x) h(x) - \sinh(\alpha x) h'(x))^2}, \quad (3.3.50)$$

where α , β , and γ are arbitrary constants and

$$h(x) = \cosh(\beta x) + \frac{\gamma}{\beta} \sinh(\beta x). \quad (3.3.51)$$

The control gain kernel for the plant with this $\lambda(x)$ is given by

$$k(x, y) = -\frac{(\alpha^2 - \beta^2)h(y) \sinh(\beta x)}{\alpha \cosh(\alpha y)h(y) - \sinh(\alpha y)h'(y)}. \quad (3.3.52)$$

If the plant has the mixed boundary condition (2.2.9) instead of the Dirichlet one, then the formulae above should be modified by setting $\gamma = q$.

3.4 Solid Propellant Rocket Model

Consider the system

$$u_t(x, t) = u_{xx}(x, t) + g(x)u(0, t), \quad x \in (0, 1), \quad (3.4.53)$$

$$u_x(0, t) = 0. \quad (3.4.54)$$

The control gain PDE (2.3.21)–(2.3.23) takes the form

$$k_{xx}(x, y) - k_{yy}(x, y) = 0 \quad (3.4.55)$$

$$k_y(x, 0) = g(x) - \int_0^x k(x, y)g(y) dy, \quad (3.4.56)$$

$$k(x, x) = 0. \quad (3.4.57)$$

To solve this equation, let us first note that (3.4.55) has a general solution of the form

$$k(x, y) = \phi(x - y) + \psi(x + y). \quad (3.4.58)$$

From the boundary conditions (3.4.57) we get $\phi(0) + \psi(2x) = 0$. Without loss of generality we can set $\psi \equiv 0$ and $\phi(0) = 0$. Then $k(x, y) = \phi(x - y)$ and after substituting this expression into the boundary condition (3.4.56) we get

$$-\phi'(x) = g(x) - \int_0^x \phi(x - y)g(y) dy \quad (3.4.59)$$

Applying Laplace transform with respect to x we get

$$\begin{aligned} -s\phi(s) + \phi(0) &= g(s) - \phi(s)g(s) \\ \phi(s) &= \frac{g(s)}{g(s) - s}. \end{aligned} \quad (3.4.60)$$

We obtained the explicit solution for the gain kernel for any function $g(x)$.

Let us apply this result to a linearized model of unstable burning in solid propellant rockets which has $g(x) = g_0 e^{\alpha x}$ where g_0 and α are constants (for more details see [10] and references therein). The open-loop system with such $g(x)$ is unstable for any $g_0 > 2$, $\alpha \geq 0$. We have

$$g(s) = \frac{g_0}{s - \alpha}, \quad \phi(s) = \frac{g_0}{g_0 - s^2 + \alpha s} \quad (3.4.61)$$

and taking inverse Laplace transform we get

$$k(x, y) = -\frac{g_0}{g} e^{\frac{\alpha}{2}(x-y)} \sinh(g(x-y)), \quad g = \sqrt{g_0 + \frac{\alpha^2}{4}}. \quad (3.4.62)$$

We arrive at the following result:

Theorem 3.5. *The controller*

$$u(1, t) = - \int_0^1 \frac{g_0 e^{\frac{\alpha}{2}(1-y)}}{g} \sinh(g(1-y)) u(y, t) dy \quad (3.4.63)$$

exponentially stabilizes the zero solution of the system (3.4.53)–(3.4.54).

Again, the closed loop solutions can be obtained explicitly. For example, for $g(x) = g_0$ one can get:

$$\begin{aligned} u(x, t) = & 2 \sum_{n=0}^{\infty} e^{-\sigma_n^2 t} \frac{g (\cos(\sigma_n x) - 1) + \sigma_n^2 \cos(\sigma_n x)}{\sigma_n^2 + g} \\ & \times \int_0^1 u_0(\xi) \left\{ \cos(\sigma_n \xi) + (-1)^n \frac{\sqrt{g}}{\sigma_n} \sinh(\sqrt{g}(1 - \xi)) \right\} d\xi \end{aligned} \quad (3.4.64)$$

where $\sigma_n = \pi n + \frac{\pi}{2}$.

3.5 Plant with Spatially Varying Diffusivity

Consider the following plant:

$$u_t(x, t) = \varepsilon(x) u_{xx}(x, t) + \lambda u(x, t), \quad (3.5.65)$$

$$u(0, t) = 0. \quad (3.5.66)$$

Let us first apply the transformation (2.2.5). Then we get

$$\bar{u}_t(\bar{x}, t) = \bar{\varepsilon} u_{\bar{x}\bar{x}}(x, t) + \left(\lambda + \frac{1}{4} \varepsilon''(x) - \frac{3}{16} \frac{\varepsilon'^2(x)}{\varepsilon(x)} \right) \bar{u}(\bar{x}, t), \quad (3.5.67)$$

$$\bar{u}(0, t) = 0. \quad (3.5.68)$$

Suppose that the following condition is satisfied for some constant C :

$$\frac{1}{4} \varepsilon''(x) - \frac{3}{16} \frac{\varepsilon'^2(x)}{\varepsilon(x)} = C. \quad (3.5.69)$$

Then the plant has constant parameters and we can apply the results of the Section 3.1. There are two solutions to the nonlinear ODE (3.5.69). The first solution is

$$\varepsilon(x) = \varepsilon_0(x - x_0)^2, \quad (3.5.70)$$

where ε_0 and x_0 are arbitrary (not violating the condition $\varepsilon(x) > 0$ on $x \in [0, 1]$) constant parameters and $C = -\varepsilon_0/4$.

The other solution is three-parametric and thus is more interesting:

$$\varepsilon(x) = \varepsilon_0(1 + \theta_0(x - x_0)^2)^2, \quad (3.5.71)$$

where ε_0 , θ_0 , x_0 are arbitrary constants and $C = \varepsilon_0\theta_0$. This solution can give a very good approximation on $x \in [0, 1]$ to many functions, including (3.5.70). So, we will focus our attention on the solution (3.5.71).

The function (3.5.71) always has one maximum or one minimum (for the range of the parameters that do not violate the condition $\varepsilon(x) > 0$). The value and the location of the maximum (minimum) can be arbitrarily set by ε_0 and x_0 , correspondingly. The sign of θ_0 determines if it is a maximum or minimum and the value of θ_0 can set arbitrary “sharpness” of the extremum (Fig. 3.7a-c). By selecting the maximum (minimum) outside of the region $[0, 1]$ and changing the extremum value and sharpness we can almost perfectly match any linear function as well (Fig. 3.7d). Using (2.2.6), (3.1.10), (3.5.71) we get the following result:

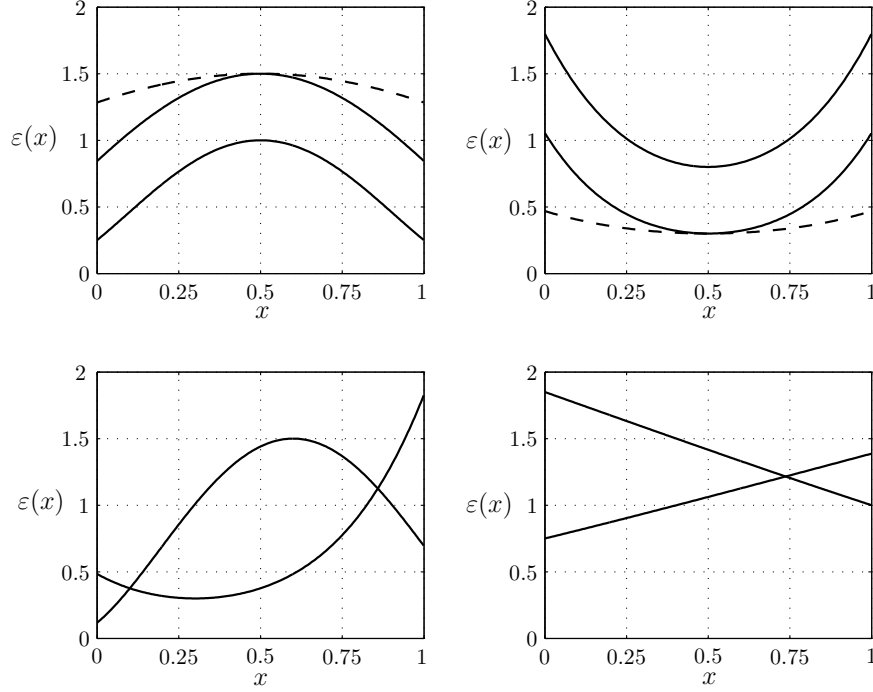


Figure 3.7: The function $\varepsilon(x)$ for different values of ε_0 , θ_0 , and x_0 . From left to right: peak value and flatness are arbitrary; extremum can be set to max or min; location of extremum is arbitrary; linear functions matched.

Theorem 3.6. *The controller (3.1.1) with*

$$k(x, y) = -\bar{y} \frac{\lambda + c}{\sqrt{\varepsilon(0)}} \frac{\varepsilon^{1/4}(x)}{\varepsilon^{3/4}(y)} \frac{I_1 \left(\sqrt{\frac{\lambda+c}{\varepsilon(0)}} (\bar{x}^2 - \bar{y}^2) \right)}{\sqrt{\frac{\lambda+c}{\varepsilon(0)}} (\bar{x}^2 - \bar{y}^2)} \quad (3.5.72)$$

where $\bar{x} = \varphi(x)$, $\bar{y} = \varphi(y)$,

$$\varphi(\xi) = \frac{1 + \theta_0 x_0^2}{\sqrt{\theta_0}} \left(\text{atan}(\sqrt{\theta_0}(\xi - x_0)) + \text{atan}(\sqrt{\theta_0}x_0) \right) \quad (3.5.73)$$

exponentially stabilizes the zero solution of the system (3.5.65)–(3.5.66) with $\varepsilon(x)$ given by (3.5.71).

Remark 3.7. If the boundary condition (3.5.66) is changed to $u_x(0, t) = 0$, the only change in the control gain (3.5.72) would be the leading factor \bar{x} instead of \bar{y} . For the mixed boundary condition $u_x(0, t) = qu(0, t)$ the closed form solution (far more complicated) is also possible and can be inferred from [55]. \square

3.6 Unstable Heat Equation with Non-Constant Thermal Conductivity

Many problems (e.g., heat conduction in non-homogeneous materials [16]) have a structure different from that of (3.5.65). The heat equation with space-dependent thermal conductivity is usually written in the following form:

$$u_t(x, t) = \frac{d}{dx} \left(\varepsilon(x) \frac{d}{dx} u(x, t) \right) + \lambda u(x, t), \quad (3.6.74)$$

$$u(0, t) = 0. \quad (3.6.75)$$

With a change of variables $u = \sqrt{\varepsilon(x)}v$ we have

$$v_t = \varepsilon(x)v_{xx} + \left(\lambda + \frac{\varepsilon'^2(x)}{4\varepsilon(x)} - \frac{\varepsilon''(x)}{2} \right) v, \quad (3.6.76)$$

$$v(0, t) = 0. \quad (3.6.77)$$

One can see now that if the expression in the brackets in (3.6.76) is constant, then we can apply the results of Section 3.1. It turns out that the solution (3.5.70) makes this expression constant. Using (2.2.6), (3.1.10), and (3.5.70) we get the following result.

Theorem 3.8. *The controller (3.1.1) with*

$$k(x, y) = -\bar{y} \frac{\lambda + c}{\sqrt{\varepsilon(0)}} \frac{\varepsilon^{3/4}(x)}{\varepsilon^{5/4}(y)} \frac{I_1 \left(\sqrt{\frac{\lambda+c}{\varepsilon(0)}} (\bar{x}^2 - \bar{y}^2) \right)}{\sqrt{\frac{\lambda+c}{\varepsilon(0)}} (\bar{x}^2 - \bar{y}^2)}, \quad (3.6.78)$$

where

$$\bar{x} = -x_0 \log(1 - x/x_0), \quad \bar{y} = -x_0 \log(1 - y/x_0) \quad (3.6.79)$$

exponentially stabilizes the zero solution of the system (3.6.74)–(3.6.75) with $\varepsilon(x)$ given by (3.5.70).

Note, that Remark 3.7 holds here as well. Since the minimum of the function (3.5.70) is always a zero, x_0 should be chosen outside of the region $[0, 1]$ to keep $\varepsilon(x) > 0$ for $x \in [0, 1]$. This means that $\varepsilon(x)$ given by (3.5.70) can

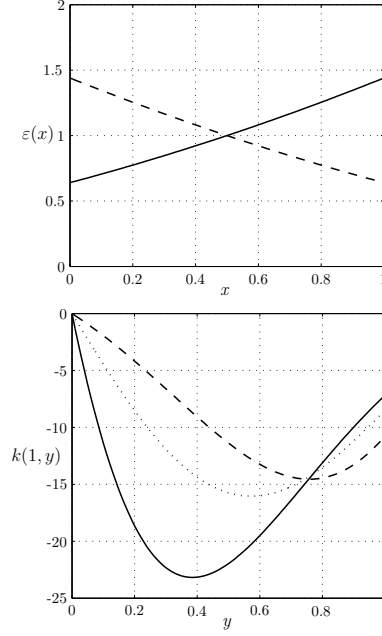


Figure 3.8: The function $\varepsilon(x)$ from (3.5.70) and the corresponding kernel $k(1, y)$ for different parameter values. Dotted line shows the kernel for $\varepsilon(x) \equiv 1$.

approximate linear functions on $[0, 1]$ very well. In Fig. 3.8 the function $\varepsilon(x)$ and the corresponding control gains are shown for different parameter values.

For $\varepsilon(x) = 1 + 0.4 \sin(6\pi x)$ the results of simulation are presented in Fig. 3.9. The controller was implemented on a coarse grid with only 6 points.

3.7 Combining Previous Results

The solutions presented in Sections 3.1–3.6 can be combined to obtain the explicit results for more complex systems. For example, consider the system

$$u_t(x, t) = \varepsilon u_{xx}(x, t) + (\lambda_\sigma(x) + \lambda_0) u(x, t), \quad (3.7.80)$$

$$u(0, t) = 0. \quad (3.7.81)$$

Denote by $k^\sigma(x, y)$ and $k^\lambda(x, y)$ the (closed form) control gains for the equations (6.3.34)–(6.3.35) and (3.1.1)–(3.1.2), respectively. The transformation

$$\bar{w}(x, t) = u(x, t) - \int_0^x k^\sigma(x, y) u(y, t) dy \quad (3.7.82)$$

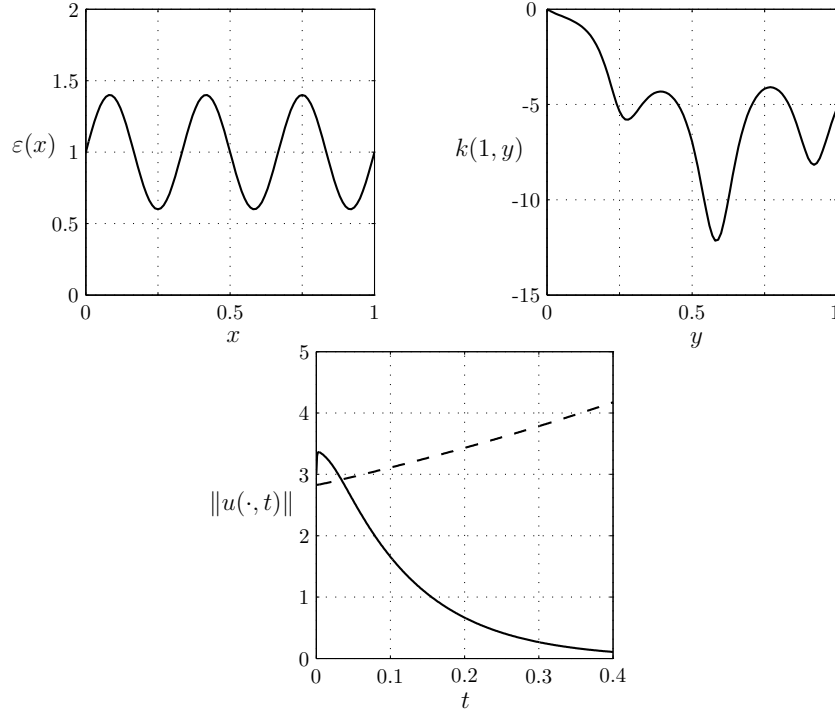


Figure 3.9: The simulation results for the plant with spatially varying diffusivity. Top left: the diffusivity profile; top right: the gain kernel; bottom: the L_2 -norm of open loop (dashed) and closed loop (solid) response.

maps (3.7.80)–(3.7.81) into the intermediate system

$$\bar{w}_t(x, t) = \varepsilon \bar{w}_{xx}(x, t) + \lambda_0 \bar{w}(x, t), \quad (3.7.83)$$

$$\bar{w}(0, t) = 0. \quad (3.7.84)$$

Now we apply to (3.7.83)–(3.7.84) the transformation

$$w(x, t) = \bar{w}(x, t) - \int_0^x k^\lambda(x, y) \bar{w}(y, t) dy \quad (3.7.85)$$

to map it into the system

$$w_t(x, t) = \varepsilon w_{xx}(x, t) - cw(x, t), \quad (3.7.86)$$

$$w(0, t) = 0, \quad (3.7.87)$$

$$w(1, t) = 0. \quad (3.7.88)$$

Using (3.7.85) and (3.7.82) we derive the transformation directly from $u(x, t)$ into $w(x, t)$:

$$\begin{aligned} w(x, t) &= u(x, t) - \int_0^x k^\sigma(x, y)u(y, t) dy \\ &\quad - \int_0^x k^\lambda(x, y) \left(u(y, t) - \int_0^y k^\sigma(y, \xi)u(\xi, t) d\xi \right) dy \\ &= u(x, t) - \int_0^x k^c(x, y)u(y, t) dy, \end{aligned} \quad (3.7.89)$$

where k^c stands for the combined kernel:

$$k^c(x, y) = k^\sigma(x, y) + k^\lambda(x, y) - \int_y^x k^\lambda(x, \xi)k^\sigma(\xi, y) d\xi. \quad (3.7.90)$$

For example, for $\lambda(x) = \lambda + 2\sigma^2/\cosh^2(\sigma x)$ one gets the closed-form solution

$$k^c(x, y) = -\lambda y \frac{I_1\left(\sqrt{\lambda(x^2 - y^2)}\right)}{\sqrt{\lambda(x^2 - y^2)}} - \sigma \tanh(\sigma y) I_0\left(\sqrt{\lambda(x^2 - y^2)}\right). \quad (3.7.91)$$

In the same fashion one can obtain explicit stabilizing controllers for even more complicated plants. For example, using the results of the present chapter, it can be done for the following 6-parameter family of plants

$$u_t(x, t) = \varepsilon u_{xx}(x, t) + bu_x(x, t) + \lambda_0 u(x, t) + g_0 e^{\alpha x} u(0, t), \quad (3.7.92)$$

$$u_x(0, t) = qu(0, t). \quad (3.7.93)$$

This chapter is in part a reprint of the material as it appears in

A. Smyshlyaev and M. Krstic, “Closed form boundary state feedbacks for a class of 1D partial integro-differential equations,” *IEEE Trans. on Automatic Control*, vol. 49, no. 12, pp. 2185-2202, 2004.

The dissertation author was the primary author and the coauthor listed in this publication directed the research which forms the basis for this chapter.

Chapter 4

Time-Varying Systems

In previous chapters we considered linear time-invariant systems. The approach can be further extended to the PDEs with time-varying coefficients.

4.1 PDE for Gain Kernel

Consider the following plant

$$u_t(x, t) = \varepsilon_0 u_{xx}(x, t) + \lambda(x, t)u(x, t), \quad (4.1.1)$$

$$u_x(0, t) = qu(0, t), \quad (4.1.2)$$

where λ is the continuous function of time.

The PDEs of the type (4.1.1)–(4.1.2) can arise for example in the trajectory tracking problems for nonlinear distributed parameter systems. Following our approach we search for the transformation

$$w(x, t) = u(x, t) - \int_0^x k(x, y, t)u(y, t) dy \quad (4.1.3)$$

that maps (4.1.1)–(4.1.2) into the exponentially stable target system. The difference with time-invariant case is that the transformation kernel now depends on the third variable—time. After substitution of (4.1.3) into (4.1.1)–(4.1.2), we get the following kernel PDE for $k = k(x, y, t)$:

$$k_t = \varepsilon_0(k_{xx} - k_{yy}) - (\lambda(y, t) + c)k \quad (4.1.4)$$

with boundary conditions

$$k_y(x, 0, t) = qk(x, 0, t), \quad (4.1.5)$$

$$k(x, x, t) = -\frac{1}{2\varepsilon_0} \int_0^x (\lambda(\xi, t) + c) d\xi. \quad (4.1.6)$$

The stabilization problem is now converted to the problem of solvability of (4.1.4)–(4.1.6). PDEs of this type have been studied by Colton [18] who proved that they are well-posed on a finite time interval. For the general $\lambda(x, t)$ PDE (4.1.4)–(4.1.6) needs to be solved numerically.

4.2 Closed form controllers

We present here explicit controllers that can stabilize the following plant with smooth $\lambda(t)$:

$$u_t(x, t) = \varepsilon_0 u_{xx}(x, t) + \lambda(t)u(x, t), \quad (4.2.7)$$

$$u(0, t) = 0. \quad (4.2.8)$$

For this system the kernel PDE (4.1.4)–(4.1.6) takes the following form:

$$k_t(x, y, t) = k_{xx}(x, y, t) - k_{yy}(x, y, t) - \lambda(t)k(x, y, t), \quad (4.2.9)$$

$$k(x, 0, t) = 0, \quad (4.2.10)$$

$$k(x, x, t) = -\frac{x}{2}\lambda(t). \quad (4.2.11)$$

Without loss of generality we have set $\varepsilon_0 = 1$, $c = 0$ here. Let us make the following change of variables:

$$k(x, y, t) = -\frac{y}{2}e^{-\int_0^t \lambda(\tau) d\tau} f(z, t), \quad z = \sqrt{x^2 - y^2}. \quad (4.2.12)$$

We get the following PDE in one spatial variable for the function $f(z, t)$:

$$f_t(z, t) = f_{zz}(z, t) + \frac{3}{z}f_z(z, t) \quad (4.2.13)$$

with boundary conditions

$$f_z(0, t) = 0, \quad (4.2.14)$$

$$f(0, t) = \lambda(t)e^{\int_0^t \lambda(\tau) d\tau} := F(t). \quad (4.2.15)$$

The $C_{z,t}^{2,1}$ solution to this problem is [54]

$$f(z, t) = \sum_{n=0}^{\infty} \frac{1}{n!(n+1)!} \left(\frac{z}{2}\right)^{2n} F^{(n)}(t). \quad (4.2.16)$$

This solution is rather explicit. Since $z \leq 1$ and squared factorial increases very fast with n , one can obtain very accurate approximations to $f(z, t)$ using just several terms of the sum.

It can be shown that the operator (4.1.3) from u to w , as functions of x , is bounded invertible in both $L_2(0, 1)$ and $H_1(0, 1)$, uniformly in time.

Theorem 4.1. *The controller*

$$\begin{aligned} u(1, t) = & - \int_0^1 \frac{y}{2} e^{-\int_0^t \lambda(\tau) d\tau} \times \\ & \times \left(\sum_{n=0}^{\infty} \frac{(1-y^2)^n F^{(n)}(t)}{4^n n!(n+1)!} \right) u(y, t) dy \end{aligned} \quad (4.2.17)$$

exponentially stabilizes the system (4.2.7)–(4.2.8).

Remark 4.2. If the boundary condition (4.2.8) is changed to $u_x(0, t) = 0$, the only difference in the controller (4.2.17) would be the leading factor $(1/2)$ instead of $(y/2)$. \square

There are two cases when it is easy to compute the series (4.2.16) in closed form: when $F(t)$ is a combination of exponentials (since it is easy to compute the n -th derivative of $F(t)$ in this case) or a polynomial (since the series is finite).

Let us consider two examples.

Example 4.3. Let $F(t)$ be

$$F(t) = e^{\lambda_0 t} \{ \lambda_0 \cosh \omega_0(t - t_0) + \sinh \omega_0(t - t_0) \}, \quad (4.2.18)$$

where λ_0 , ω_0 and t_0 are arbitrary constants. This $F(t)$ corresponds to the following $\lambda(t)$:

$$\lambda(t) = \lambda_0 + \omega_0 \tanh(\omega_0(t - t_0)) \quad (4.2.19)$$

This $\lambda(t)$ approximates a rapid change from a constant level $\lambda_0 - \omega_0$ to a constant level $\lambda_0 + \omega_0$ at a time $t = t_0$ (Fig. 4.1). Substituting (4.2.18) into (4.2.16) and computing the sum we get the following control gain:

$$\begin{aligned} k(x, y, t) = & -\frac{y}{2\sqrt{x^2 - y^2} \cosh(\omega_0(t - t_0))} \times \\ & \times \left\{ \sqrt{\lambda_0 + \omega_0} I_1 \left(\sqrt{(\lambda_0 + \omega_0)(x^2 - y^2)} \right) e^{-\omega_0(t - t_0)} \right. \\ & \left. + \sqrt{\lambda_0 - \omega_0} I_1 \left(\sqrt{(\lambda_0 - \omega_0)(x^2 - y^2)} \right) e^{\omega_0(t - t_0)} \right\}. \end{aligned} \quad (4.2.20)$$

Example 4.4. Let $F(t)$ be

$$F(t) = e^{\lambda_0 t} (\lambda_0((t + a)^2 + b^2) + 2(t + a)), \quad (4.2.21)$$

where λ_0 , a and $b \neq 0$ are arbitrary constants. This $F(t)$ corresponds to the following $\lambda(t)$:

$$\lambda(t) = \lambda_0 + \frac{2(t + a)}{(t + a)^2 + b^2}. \quad (4.2.22)$$

This $\lambda(t)$ can approximate some "one-peak" functions (Fig. 4.2). Substituting (4.2.21) into (4.2.16) and computing the sum we get the following control gain:

$$\begin{aligned} k(x, y, t) = & -\lambda_0 y \frac{I_1(\sqrt{\lambda_0} z)}{\sqrt{\lambda_0} z} - y \frac{t + a}{(t + a)^2 + b^2} I_0(\sqrt{\lambda_0} z) \\ & - \frac{y}{4\sqrt{\lambda_0}} \frac{z I_1(\sqrt{\lambda_0} z)}{(t + a)^2 + b^2}, \quad z = \sqrt{x^2 - y^2}, \end{aligned} \quad (4.2.23)$$

where I_0 and I_1 are modified Bessel functions.

We should mention that there is a simpler solution to the problem of stabilization of (4.2.7)–(4.2.8) which is obtained by converting it by a change of variables

$$u(x, t) = v(x, t) e^{\int_0^t \lambda(\tau) d\tau}. \quad (4.2.24)$$

into a PDE with constant coefficients

$$v_t(x, t) = \varepsilon_0 v_{xx}(x, t), \quad (4.2.25)$$

$$v(0, t) = 0. \quad (4.2.26)$$

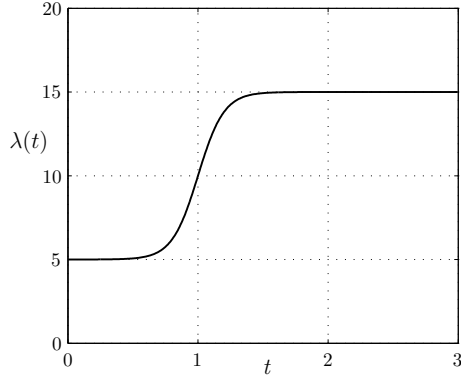


Figure 4.1: The function $\lambda(t)$ from (4.2.19) for $\lambda_0 = 10$, $\omega_0 = 5$, and $t_0 = 1$.

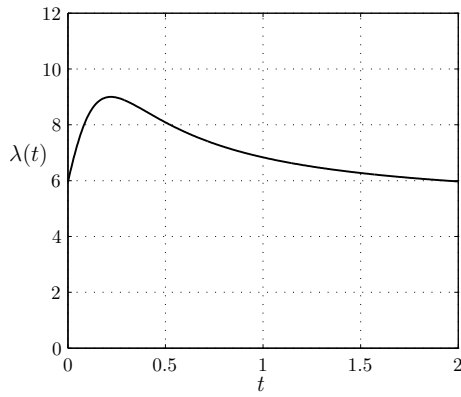


Figure 4.2: The function $\lambda(t)$ from (4.2.22) for $\lambda_0 = 5$, $a = 0.03$, and $b = 0.25$.

This problem can be now stabilized using the results of [55] (or Chapter 3) with the controller

$$u(1, t) = - \int_0^1 \frac{c}{\varepsilon_0} y \frac{I_1 \left(\sqrt{\frac{c}{\varepsilon_0} (1 - y^2)} \right)}{\sqrt{\frac{c}{\varepsilon_0} (1 - y^2)}} u(y, t) dy. \quad (4.2.27)$$

The decay rate of the closed-loop v -system is equal to the decay rate of the target system, i.e., $e^{-(c+\varepsilon_0\pi^2)t}$. So the closed-loop stability of u -system is guaranteed by satisfying the condition [35, p.226]

$$c > \limsup_{t \rightarrow \infty} \lambda(t) - \varepsilon_0 \pi^2, \quad (4.2.28)$$

or $c > -\varepsilon_0 \pi^2$ if $\lambda \in L_1(0, \infty) \cup L_2(0, \infty)$.

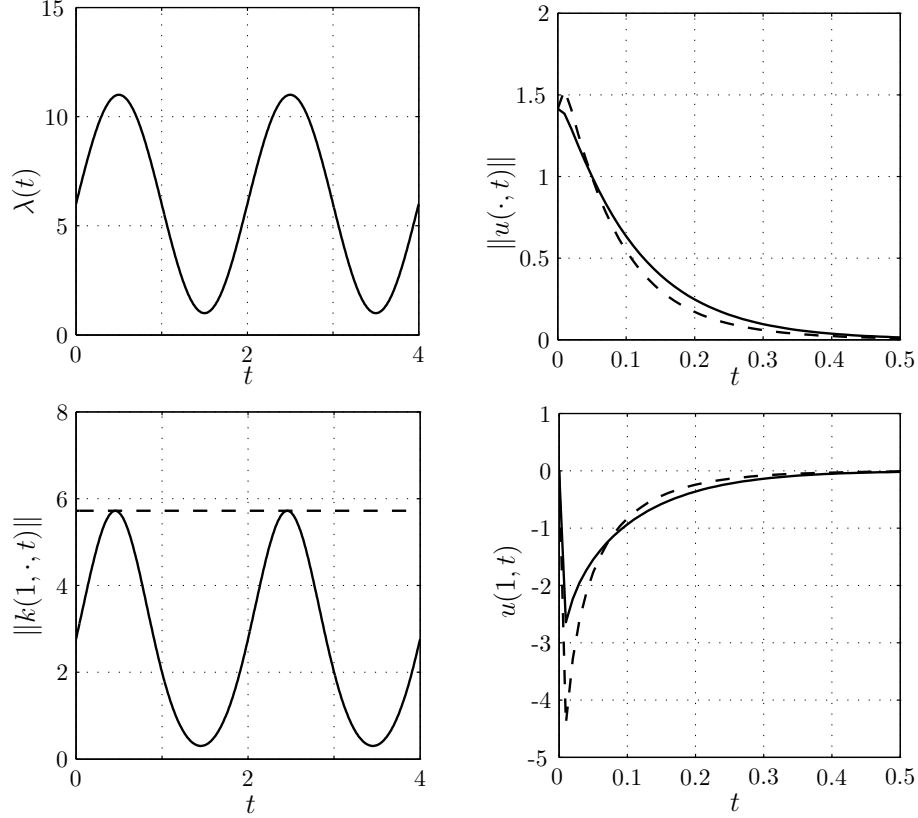


Figure 4.3: The simulation results for (4.1.1)–(4.1.2) with controllers (4.2.17) (solid) and (4.2.27) (dashed). From left to right: $\lambda(t)$; L_2 -norm of the gain kernel; L_2 -norm of the state; the control effort.

Although the controller (4.2.27) stabilizes (4.2.7)–(4.2.8) for any $\lambda(t)$, it is most suitable for the cases when minimum and maximum values of $\lambda(t)$ are close, for example when it is a constant plus sinusoid with small amplitude. When $\lambda(t)$ has significant drops and rises, this method will use unnecessarily large initial control effort (Example 1) or result in poor initial performance (Example 2) (see next section). For such cases the design (4.2.17) is advantageous.

4.3 Simulations

We presented several closed form boundary controllers for stabilization of parabolic PDEs with time-varying parameters. When the plant coefficients cannot

be accurately approximated by families of functions for which explicit solutions can be found, the kernel PDE (4.1.4)–(4.1.6) should be solved numerically. For the case of $\lambda(t) = 6 + 5\sin(\pi t)$ the results are shown in Fig. 4.3. We can see the advantage of the controller (4.2.17) over (4.2.27) for this type of $\lambda(t)$ — lower control effort in the initial transient.

This chapter is in part a reprint of the material as it appears in A. Smyshlyaev and M. Krstic, “On control design for PDEs with space-dependent diffusivity or time-dependent reactivity,” *Automatica*, 41, pp. 1601-1608, 2005. The dissertation author was the primary author and the coauthor listed in this publication directed the research which forms the basis for this chapter.

Chapter 5

Observers

5.1 Introduction

In this chapter we propose backstepping based infinite dimensional observers for a class of linear parabolic partial integro-differential equations with sensing restricted to the boundary.

To solve this problem we draw inspiration from a recent paper of Krener and Kang [34] in which a finite dimensional backstepping observer is proposed for nonlinear ODEs. They discover and exploit a triangular structure dual to that for the backstepping controller design [36]. The complexities present due to nonlinearities in finite dimension make the Krener-Kang observer non-global. This limitation is not an issue in our problem, as the class of parabolic PDEs we consider is linear. Our observers, due to the infinite dimension, take a form in which they are almost unrecognizable as Krener-Kang observers, however their structure is exactly that of Krener and Kang, where duality with backstepping control is exploited.

Our observer design for linear parabolic PDEs involves a linear Volterra transformation of the observer error system into a heat equation, with the aid of output injection. The transformation kernel satisfies a linear hyperbolic (Klein-Gordon type) PDE dual to the PDE studied for the state-feedback problem by

Liu [42]. While observers are of interest on their own merit as state estimators/forecasters, putting them together with our earlier boundary stabilizers yields output feedback compensators for a class of parabolic PDEs.

Past efforts in linear observer design for PDEs include the infinite dimensional Luenberger approach [20], [41]. A unified treatment of both interior and boundary observations/control generalized to semilinear problems can be found in [2]. Fuji [28] and Nambu [46] developed auxiliary functional observers to stabilize diffusion equations using boundary observation and feedback. For the general Pritchard–Salamon class of state–space systems a number of frequency–domain results has been established on stabilization during the last decade (see, e.g. [19] and [45] for surveys). Christofides [17] developed nonlinear output-feedback controllers for parabolic PDE systems for which the eigenspectrum can be separated into a finite-dimensional slow part and an infinite-dimensional stable fast part.

While our method is certainly not the first solution to the problems of boundary observer design or output-feedback boundary control, it has several distinguishing features. First of all, it takes advantage of the structure of the system, resulting in a problem of solving a linear hyperbolic PDE for the gain kernel, an object much easier, both conceptually and computationally, than operator Riccati equations arising in LQG approaches to boundary control. Second, the problem is solved essentially by calculus making a design procedure clear and constructive and the analysis easy in contrast to standard abstract approaches (semigroups, etc.). Last but not least, for a number of physically relevant problems we are able to find the observer/controller kernels in closed form, i.e., as explicit functions of the spatial variable. This, in turn, allows to even find closed-loop solutions explicitly.

5.2 Problem Statement

We consider the following class of parabolic PDEs:

$$\begin{aligned} u_t(x, t) = & \varepsilon(x)u_{xx}(x, t) + b(x)u_x(x, t) + \lambda(x)u(x, t) \\ & + g(x)u(0, t) + \int_0^x f(x, y)u(y, t) dy, \end{aligned} \quad (5.2.1)$$

for $x \in (0, 1)$, $t > 0$, with boundary conditions

$$u_x(0, t) = qu(0, t), \quad (5.2.2)$$

$$u(1, t) = U(t) \quad \text{or} \quad u_x(1, t) = U(t), \quad (5.2.3)$$

As has been shown in Chapter 2, without loss of generality we can set $\varepsilon(x) = \text{const}$, $b(x) \equiv 0$. The PDE (5.2.1)–(5.2.2) is actuated at $x = 1$ (using either Dirichlet or Neumann actuation) by a boundary input $U(t)$ that can be any function of time or a feedback law.

The problem is to design an exponentially convergent observer for the plant with only boundary measurements available. The observer design depends on the type (Dirichlet/Neumann) and the location of measurement and actuation. We consider two setups: the anti-collocated setup, when sensor and actuator are placed at the opposite ends, and the collocated case, when sensor and actuator are placed at the same end. There is no much technical difference between the cases of Dirichlet and Neumann actuation, so we pick one (Neumann) for anti-collocated case and the other (Dirichlet) for collocated case.

5.3 Observer Design for Anti-Collocated Setup

Suppose the only available measurement of our system is at $x = 0$, the opposite end to actuation. We propose the following observer for the system (5.2.1)–

(5.2.3) with Dirichlet actuation :

$$\begin{aligned}\hat{u}_t(x, t) &= \varepsilon \hat{u}_{xx}(x, t) + \lambda(x) \hat{u}(x, t) + g(x) u(0, t) + \int_0^x f(x, y) \hat{u}(y, t) dy \\ &\quad + p_1(x)[u(0, t) - \hat{u}(0, t)],\end{aligned}\tag{5.3.4}$$

$$\hat{u}_x(0, t) = qu(0, t) + p_{10}[u(0, t) - \hat{u}(0, t)],\tag{5.3.5}$$

$$\hat{u}(1, t) = U(t).\tag{5.3.6}$$

Here $p_1(x)$ and p_{10} are output injection functions (p_{10} is a constant) *to be designed*. Note that we introduce output injection not only in the equation (5.3.4) but also at the boundary where measurement is available. We also implicitly use the additional output injection here in a form $q(u(0, t) - \hat{u}(0, t))$ that cancels the dependency on q in the error dynamics.

The observer (5.3.4)–(5.3.6) is in the standard form of "copy of the system plus injection of the output estimation error," i.e., it mimics the finite dimensional case where observers of the form $\dot{\hat{x}} = A\hat{x} + Bu + L(y - C\hat{x})$ are used for plants $\dot{x} = Ax + Bu$, $y = Cx$. This standard form allows us to pursue duality between the observer and the controller design — to find the observer gain function using the solution to the stabilization problem we found in Chapter 2, similar to the way duality is used to find the gains of a Luenberger observer based on the pole placement control algorithm, or to the way duality is used to construct a Kalman filter based on the LQR design.

The observer error $\tilde{u}(x, t) = u(x, t) - \hat{u}(x, t)$ satisfies the following PDE:

$$\tilde{u}_t(x, t) = \varepsilon \tilde{u}_{xx}(x, t) + \lambda(x) \tilde{u}(x, t) + \int_0^x f(x, y) \tilde{u}(y, t) dy - p_1(x) \tilde{u}(0, t)\tag{5.3.7}$$

$$\tilde{u}_x(0, t) = -p_{10} \tilde{u}(0, t),\tag{5.3.8}$$

$$\tilde{u}(1, t) = 0.\tag{5.3.9}$$

Observer gains $p_1(x)$ and p_{10} should be now chosen to stabilize the system (5.3.7)–(5.3.9). We solve the problem of stabilization of (5.3.7)–(5.3.9) by the same integral transformation approach as the (state feedback) boundary *control* problem in

Chapter 2. We look for a backstepping-like coordinate transformation

$$\tilde{u}(x, t) = \tilde{w}(x, t) - \int_0^x p(x, y) \tilde{w}(y, t) dy \quad (5.3.10)$$

that transforms system (5.3.7)–(5.3.9) into the exponentially stable (for $\tilde{c} \geq 0$) system

$$\tilde{w}_t(x, t) = \varepsilon \tilde{w}_{xx}(x, t) - \tilde{c} \tilde{w}(x, t), \quad x \in (0, 1), \quad (5.3.11)$$

$$\tilde{w}_x(0, t) = 0, \quad (5.3.12)$$

$$\tilde{w}(1, t) = 0. \quad (5.3.13)$$

The free parameter \tilde{c} can be used to set the desired observer convergence speed. It is in general different from the analogous coefficient c in control design since one usually wants the estimator to be faster than the state feedback closed-loop dynamics.

By substituting (5.3.10) into (5.3.7)–(5.3.9) we obtain a set of conditions on the kernel $p(x, y)$ in the form of the hyperbolic PDE

$$\varepsilon p_{yy}(x, y) - \varepsilon p_{xx}(x, y) = (\lambda(x) + c)p(x, y) - f(x, y) + \int_y^x p(\xi, y) f(x, \xi) d\xi \quad (5.3.14)$$

for $(x, y) \in \mathcal{T} = \{x, y : 0 < y < x < 1\}$, with the boundary conditions

$$\frac{d}{dx} p(x, x) = \frac{1}{2\varepsilon} (\lambda(x) + c), \quad (5.3.15)$$

$$p(1, y) = 0. \quad (5.3.16)$$

that yield

$$\begin{aligned} \tilde{w}_t(x, t) &= \varepsilon \tilde{w}_{xx}(x, t) - \tilde{c} \tilde{w}(x, t) - \varepsilon p(x, 0) \tilde{w}_x(0, t) \\ &\quad + (\varepsilon p_y(x, 0) - p_1(x)) \tilde{w}(0, t), \end{aligned} \quad (5.3.17)$$

$$\tilde{w}_x(0, t) = (p(0, 0) - p_{10}) \tilde{w}(0, t), \quad (5.3.18)$$

$$\tilde{w}(1, t) = 0. \quad (5.3.19)$$

Comparing this with (5.3.11)–(5.3.13), it follows that the observer gains should be chosen as

$$p_1(x) = \varepsilon p_y(x, 0), \quad p_{10} = p(0, 0). \quad (5.3.20)$$

The problem is first to prove that PDE (5.3.14)–(5.3.16) is well-posed. Once the solution $p(x, y)$ to the problem (5.3.14)–(5.3.16) is found, the observer gains can be obtained from (5.3.20).

Let us make a change of variables

$$\begin{aligned}\check{x} &= 1 - y, & \check{y} &= 1 - x, & \check{\lambda}(\check{y}) &= \lambda(x), & \check{f}(\check{x}, \check{y}) &= f(x, y), \\ \check{p}(\check{x}, \check{y}) &= p(x, y).\end{aligned}\tag{5.3.21}$$

In these new variables the problem (5.3.14)–(5.3.16) becomes

$$\varepsilon \check{p}_{\check{x}\check{x}}(\check{x}, \check{y}) - \varepsilon \check{p}_{\check{y}\check{y}}(\check{x}, \check{y}) = (\check{\lambda}(\check{y}) + \tilde{c})\check{p}(\check{x}, \check{y}) - \check{f}(\check{x}, \check{y}) + \int_{\check{y}}^{\check{x}} \check{p}(\check{x}, \xi) \check{f}(\xi, \check{y}) d\xi \tag{5.3.22}$$

$$\check{p}(\check{x}, 0) = 0, \tag{5.3.23}$$

$$\check{p}(\check{x}, \check{x}) = -\frac{1}{2\varepsilon} \int_0^{\check{x}} (\check{\lambda}(\xi) + \tilde{c}) d\xi. \tag{5.3.24}$$

This PDE is in class (2.3.21)–(2.3.23) (with $q = \infty$, $g(x) = 0$, c replaced by \tilde{c} , λ replaced by $\check{\lambda}$, and f replaced by \check{f}). Hence, using Theorem 2.3 we obtain the following result.

Theorem 5.1. *The equation (5.3.14) with boundary conditions (5.3.15)–(5.3.16) has a unique $C^2(\mathcal{T})$ solution. The kernel $r(x, y)$ of the inverse transformation*

$$\tilde{w}(x, t) = \tilde{u}(x, t) + \int_0^x r(x, y) \tilde{u}(y, t) dy \tag{5.3.25}$$

is also a unique $C^2(\mathcal{T})$ function.

The fact that the observer gain in transposed and switched variables satisfies the same class of PDEs as control gain is reminiscent of the duality property of state-feedback and observer design problems for linear finite-dimensional systems. The difference between the equations for observer and control gains is due to the fact that the observer error system does not contain terms with $g(x)$ and q because $u(0, t)$ is measured.

The observer gains in the new coordinates are given by

$$p_1(x) = -\varepsilon \check{p}_{\check{x}}(1, 1 - x), \quad p_{10} = \check{p}(1, 1). \tag{5.3.26}$$

The exponential stability of the target system (5.3.11)–(5.3.13) and invertibility of the transformation (5.3.10) (established in Theorem 2.3) imply the exponential stability of (5.3.7)–(5.3.9) both in L_2 and H_1 (see [4] and [42] for details and references). The result is formulated in the following theorem.

Theorem 5.2. *Let $p(x, y)$ be the solution of the system (5.3.14)–(5.3.16). Then for any $\tilde{u}_0(x) \in L_2(0, 1)$ the system (5.3.7)–(5.3.9) with $p_1(x)$ and p_{10} given by (5.3.20) has a unique classical solution $\tilde{u}(x, t) \in C^{2,1}((0, 1) \times (0, \infty))$. Additionally, the origin $\tilde{u}(x, t) \equiv 0$ is exponentially stable in the $L_2(0, 1)$ and $H_1(0, 1)$ norms.*

This result can be readily extended to the Neumann type of actuation as well. All the computational issues related to solving (5.3.14)–(5.3.16) numerically (for cases when closed form solutions can be obtained see Chapter 3) are addressed in Chapter 2.

5.4 Observer Design for Collocated Setup

Suppose now that the only available measurement is at the same end with actuation ($x = 1$). We will concentrate on the case with $u(1, t)$ measured and $u_x(1, t)$ actuated which is the usual setting for thermal/chemical problems (temperature/concentration is available and the gradients are used for actuation). It is quite straightforward to adapt the design to the opposite setting which usually occurs in fluid problems (shear stress is measured and velocity is a control variable).

We solve this problem with a restriction on the class (5.2.1)–(5.2.2) by setting $f(x, y) \equiv 0$, $g(x) \equiv 0$. This restriction is necessary because the observer problem in the collocated case is "upper-triangular," thus the "lower-triangular" terms with $g(x)$ and $f(x, y)$ are not allowed.

Consider the following observer:

$$\hat{u}_t(x, t) = \varepsilon \hat{u}_{xx}(x, t) + \lambda(x) \hat{u}(x, t) + p_1(x)[u(1, t) - \hat{u}(1, t)], \quad (5.4.27)$$

$$\hat{u}_x(0, t) = q \hat{u}(0, t), \quad (5.4.28)$$

$$\hat{u}_x(1, t) = -p_{10}[u(1, t) - \hat{u}(1, t)] + U(t). \quad (5.4.29)$$

Here $p_1(x)$ and p_{10} are output injection functions *to be designed*. The difference with the anti-collocated case (apart from injecting $u(1, t)$ instead of $u(0, t)$) is that the gain p_{10} is introduced in the other boundary condition.

The observer error $\tilde{u}(x)$ satisfies the equation

$$\tilde{u}_t(x, t) = \varepsilon \tilde{u}_{xx}(x, t) + \lambda(x) \tilde{u}(x, t) - p_1(x) \tilde{u}(1, t), \quad (5.4.30)$$

$$\tilde{u}_x(0, t) = q \tilde{u}(0, t), \quad (5.4.31)$$

$$\tilde{u}_x(1, t) = p_{10} \tilde{u}(1, t). \quad (5.4.32)$$

We are looking for the transformation:

$$\tilde{u}(x, t) = \tilde{w}(x, t) - \int_x^1 p(x, y) \tilde{w}(y, t) dy \quad (5.4.33)$$

that transforms (5.4.30)–(5.4.32) into the exponentially stable (for $\tilde{c} \geq \varepsilon/2 + \max\{0, -\varepsilon q|q|\}$) target system

$$\tilde{w}_t(x, t) = \varepsilon \tilde{w}_{xx}(x, t) - \tilde{c} \tilde{w}(x, t), \quad x \in (0, 1), \quad (5.4.34)$$

$$\tilde{w}_x(0, t) = q \tilde{w}(0, t), \quad (5.4.35)$$

$$\tilde{w}_x(1, t) = 0. \quad (5.4.36)$$

Note, that the transformation (5.4.33) is in upper-triangular form. By substituting (5.4.33) into (5.4.30)–(5.4.32) we get the set of conditions on the kernel $p(x, y)$ in the form of hyperbolic PDE

$$\varepsilon p_{yy}(x, y) - \varepsilon p_{xx}(x, y) = (\lambda(x) + \tilde{c}) p(x, y), \quad (5.4.37)$$

with the boundary conditions

$$p_x(0, y) = qp(0, y), \quad (5.4.38)$$

$$p(x, x) = -\frac{1}{2\varepsilon} \int_0^x (\lambda(\xi) + \tilde{c}) d\xi. \quad (5.4.39)$$

that yield

$$\begin{aligned}\tilde{w}_t(x, t) &= \varepsilon \tilde{w}_{xx}(x, t) - \tilde{c} \tilde{w}(x, t) + \varepsilon p(x, 1) \tilde{w}_x(1, t) \\ &\quad - (\varepsilon p_y(x, 1) + p_1(x)) \tilde{w}(1, t),\end{aligned}\tag{5.4.40}$$

$$\tilde{w}_x(0, t) = q \tilde{w}(0, t),\tag{5.4.41}$$

$$\tilde{w}_x(1, t) = (p_{10} - p(1, 1)) \tilde{w}(1, t).\tag{5.4.42}$$

Comparing this with (5.4.34)–(5.4.36), it follows that the observer gains should be chosen as

$$p_1(x) = -\varepsilon p_y(x, 1), \quad p_{10} = p(1, 1).\tag{5.4.43}$$

Once the solution $p(x, y)$ to the problem (5.4.37)–(5.4.39) is found, the observer gains can be obtained from (5.4.43). Similar to the anti-collocated case we introduce new variables

$$\check{x} = y, \quad \check{y} = x, \quad \check{p}(\check{x}, \check{y}) = p(x, y),\tag{5.4.44}$$

in which (5.4.37)–(5.4.39) becomes

$$\varepsilon \check{p}_{\check{x}\check{x}}(\check{x}, \check{y}) - \varepsilon \check{p}_{\check{y}\check{y}}(\check{x}, \check{y}) = (\lambda(\check{y}) + \tilde{c}) \check{p}(\check{x}, \check{y}), \quad (\check{x}, \check{y}) \in \mathcal{T}\tag{5.4.45}$$

$$\check{p}_{\check{y}}(\check{x}, 0) = q \check{p}(\check{x}, 0),\tag{5.4.46}$$

$$\check{p}(\check{x}, \check{x}) = -\frac{1}{2\varepsilon} \int_0^{\check{x}} (\lambda(\xi) + \tilde{c}) d\xi,\tag{5.4.47}$$

This is exactly the same PDE as (2.3.21)–(2.3.23) for $k(\check{x}, \check{y})$ (with c replaced by \tilde{c}) and therefore the existence and uniqueness of the solution of (5.4.37)–(5.4.39) and invertibility of the transformation (5.4.33) immediately follow. The duality between the observer and control design is even more evident here than in the anti-collocated case: the kernel of the observer transformation (5.4.33) is equal to the kernel of the control transformation (2.3.11) with switched variables, $p(x, y) = k(y, x)$ (for the same rate of convergence, i.e., $\tilde{c} = c$). The observer gains in the new coordinates are given by

$$p_1(x) = -\varepsilon \tilde{p}_x(1, x), \quad p_{10} = \tilde{p}(1, 1).\tag{5.4.48}$$

For $\tilde{c} = c$ these gains are equal (up to a constant factor $-\varepsilon$) to the control gains.

A kernel well posedness result similar to Theorem 2.2 holds here. By similar argument to one for the anti-collocated case we obtain the following result.

Theorem 5.3. *Let $p(x, y)$ be the solution of the system (5.4.37)–(5.4.39). Then for any $\tilde{u}_0(x) \in L_2(0, 1)$ the system (5.4.30)–(5.4.32) with $p_1(x)$ and p_{10} given by (5.4.43) has a unique classical solution $\tilde{u}(x, t) \in C^{2,1}((0, 1) \times (0, \infty))$. Additionally, the origin $\tilde{u}(x, t) \equiv 0$ is exponentially stable in the $L_2(0, 1)$ and $H_1(0, 1)$ norms.*

This chapter is in part a reprint of the material as it appears in

A. Smyshlyaev and M. Krstic, “Backstepping observers for a class of parabolic PDEs,” *Systems and Control Letters*, vol.54, pp. 613-625, 2005.

The dissertation author was the primary author and the coauthor listed in this publication directed the research which forms the basis for this chapter.

Chapter 6

Output Feedback Controllers

The exponentially convergent observers developed in previous chapter are independent of the control input and can be used with any controller. In this section we combine these observers with their natural dual controllers — backstepping controllers — to solve the output-feedback problem fully by backstepping.

6.1 Anti-collocated setup

Theorem 6.1. *Let $k_1(x)$ be the solution of (2.3.17), (2.3.21)–(2.3.23), $p_1(x)$, p_{10} be the solutions of (5.3.14)–(5.3.16), (5.3.20) and let the assumptions (2.2.4), $\tilde{c} \geq 0$, and $c \geq \max\{0, -\varepsilon q|q|\}$ hold. Then for any $u_0, \hat{u}_0 \in L_2(0, 1)$ the system consisting of the plant (2.2.8)–(2.2.9), the controller*

$$u(1, t) = \int_0^1 k_1(y) \hat{u}(y, t) dy, \quad (6.1.1)$$

and the observer

$$\begin{aligned} \hat{u}_t(x, t) &= \varepsilon \hat{u}_{xx}(x, t) + \lambda(x) \hat{u}(x, t) + g(x) u(0, t) \\ &\quad + \int_0^x f(x, y) \hat{u}(y, t) dy + p_1(x)[u(0, t) - \hat{u}(0, t)], \end{aligned} \quad (6.1.2)$$

$$\hat{u}_x(0, t) = qu(0, t) + p_{10}[u(0, t) - \hat{u}(0, t)], \quad (6.1.3)$$

$$\hat{u}(1, t) = \int_0^1 k_1(y) \hat{u}(y, t) dy, \quad (6.1.4)$$

has a unique classical solution $u(x, t)$, $\hat{u}(x, t) \in C^{2,1}((0, 1) \times (0, \infty))$ and is exponentially stable at the origin, $u(x, t) \equiv 0$, $\hat{u}(x, t) \equiv 0$, in the $L_2(0, 1)$ and $H_1(0, 1)$ norms.

Proof. The coordinate transformation

$$\hat{w}(x, t) = \hat{u}(x, t) - \int_0^x k(x, y) \hat{u}(y, t) dy \quad (6.1.5)$$

maps (6.1.2)–(6.1.4) into the system

$$\begin{aligned} \hat{w}_t(x, t) &= \varepsilon \hat{w}_{xx}(x, t) - c \hat{w}(x, t) \\ &\quad + \left\{ p_1(x) + g(x) - \int_0^x k(x, y) (p_1(y) + g(y)) dy \right\} \tilde{w}(0, t), \end{aligned} \quad (6.1.6)$$

$$\hat{w}_x(0, t) = q \hat{w}(0, t) + (p_{10} + q) \tilde{w}(0, t), \quad (6.1.7)$$

$$\hat{w}(1, t) = 0. \quad (6.1.8)$$

The \tilde{w} -system (5.3.11)–(5.3.13) and the homogeneous part of the \hat{w} -system (6.1.6)–(6.1.8) (without $\tilde{w}(0, t)$, where $\tilde{w}(0, t)$ is driving the \hat{w} -system (6.1.6)–(6.1.7) through a C^1 function of x) are exponentially stable heat equations. The interconnection of the two heat equations (\hat{w} , \tilde{w}) is a cascade, and therefore the combined (\hat{w} , \tilde{w}) system is exponentially stable in L^2 and H^1 . Hence, the system (\hat{u} , \tilde{u}) is also exponentially stable since it is related to (\hat{w} , \tilde{w}) by the invertible coordinate transformation (5.3.10), (6.1.5). This directly implies the closed-loop stability of (u, \hat{u}) . \square

6.2 Collocated setup

Theorem 6.2. *Let $k_1(x)$, $k_2(x)$ be the solutions of (2.3.17), (2.3.21)–(2.3.23), $p_1(x)$, p_{10} be the solutions of (5.4.37)–(5.4.39), (5.4.43) and let the assumptions (2.2.4) and \tilde{c} , $c \geq \varepsilon/2 + \max\{0, -\varepsilon q|q|\}$ hold. Then for any u_0 , $\hat{u}_0 \in L_2(0, 1)$ the system consisting of the plant (2.2.8)–(2.2.9) ($g(x) \equiv 0$, $f(x, y) \equiv 0$), the controller*

$$u_x(1, t) = k_1(1)u(1, t) + \int_0^1 k_2(y)\hat{u}(y, t) dy, \quad (6.2.9)$$

and the observer

$$\hat{u}_t(x, t) = \varepsilon \hat{u}_{xx}(x, t) + \lambda(x) \hat{u}(x, t) + p_1(x)[u(1, t) - \hat{u}(1, t)], \quad (6.2.10)$$

$$\hat{u}_x(0, t) = q \hat{u}(0, t), \quad (6.2.11)$$

$$\hat{u}_x(1, t) = k_1(1)u(1, t) + \int_0^1 k_2(y) \hat{u}(y, t) dy, \quad (6.2.12)$$

has a unique classical solution $u(x, t)$, $\hat{u}(x, t) \in C^{2,1}((0, 1) \times (0, \infty))$ and is exponentially stable at the origin, $u(x, t) \equiv 0$, $\hat{u}(x, t) \equiv 0$, in the $L_2(0, 1)$ and $H_1(0, 1)$ norms.

Proof. Very similar to the proof of Theorem 6.1. \square

6.3 Closed Form Compensators

In this section we present several cases for which our approach gives explicit observers and output feedbacks¹.

6.3.1 Unstable heat equation

Observer design. Consider the unstable heat equation with boundary actuation and sensing:²

$$u_t = \varepsilon u_{xx} + \lambda_0 u, \quad (6.3.13)$$

$$u_x(0) = 0, \quad (6.3.14)$$

$$u(1) = U(t). \quad (6.3.15)$$

The open-loop system (6.3.13)–(6.3.14) (with $U = 0$) is unstable with arbitrarily many unstable eigenvalues.

Let us consider the anti-collocated setup. The equation (5.3.22)–(5.3.24)

¹For the sake of notational simplicity we set $\tilde{c} = c$ in this section.

²Throughout this section we drop (x, t) -dependence for clarity wherever it is possible, so $u(0, t) = u(0)$, $u(x, t) = u$, etc.

for the observer gain takes the form

$$\check{p}_{\check{x}\check{x}}(\check{x}, \check{y}) - \check{p}_{\check{y}\check{y}}(\check{x}, \check{y}) = \lambda \check{p}(\check{x}, \check{y}) \quad (6.3.16)$$

$$\check{p}(\check{x}, 0) = 0, \quad (6.3.17)$$

$$\check{p}(\check{x}, \check{x}) = -\lambda \frac{\check{x}}{2}, \quad (6.3.18)$$

where $\lambda = (\lambda_0 + c)/\varepsilon$. The solution to (6.3.16)–(6.3.18) is (see Chapter 3)

$$\check{p}(\check{x}, \check{y}) = -\lambda \check{y} \frac{I_1(\sqrt{\lambda(\check{x}^2 - \check{y}^2)})}{\sqrt{\lambda(\check{x}^2 - \check{y}^2)}}. \quad (6.3.19)$$

I_1 is the modified Bessel function of the first order. Using (5.3.26) we obtain the observer gains

$$p_1(x) = \varepsilon \frac{\lambda(1-x)}{x(2-x)} I_2\left(\sqrt{\lambda x(2-x)}\right), \quad p_{10} = -\lambda/2. \quad (6.3.20)$$

In Fig. 6.1 the observer gain $p_1(x)$ is shown for different values of the parameter λ . The exponential convergence of the observer for $\lambda = 5$ is illustrated in Fig. 6.2. We can see that observer converges to the plant even though the plant is unstable.

Output feedback compensator. We can now write the explicit solution to the output-feedback problem. The gain kernel for the state-feedback problem has been found in Chapter 3 by solving (2.3.21)–(2.3.23) analytically:

$$k(x, y) = -\lambda x \frac{I_1(\sqrt{\lambda(x^2 - y^2)})}{\sqrt{\lambda(x^2 - y^2)}}. \quad (6.3.21)$$

Using (6.3.21), (6.3.20), and Theorem 6.1 we get the following result.

Theorem 6.3. *The controller*

$$u(1) = - \int_0^1 \lambda \frac{I_1(\sqrt{\lambda(1-y^2)})}{\sqrt{\lambda(1-y^2)}} \hat{u}(y) dy \quad (6.3.22)$$

with the observer

$$\hat{u}_t = \varepsilon \hat{u}_{xx} + \lambda_0 \hat{u} + \varepsilon \frac{\lambda(1-x)}{x(2-x)} I_2\left(\sqrt{\lambda x(2-x)}\right) [u(0) - \hat{u}(0)], \quad (6.3.23)$$

$$\hat{u}_x(0) = -\frac{\lambda}{2} [u(0) - \hat{u}(0)], \quad (6.3.24)$$

$$\hat{u}(1) = - \int_0^1 \lambda \frac{I_1(\sqrt{\lambda(1-y^2)})}{\sqrt{\lambda(1-y^2)}} \hat{u}(y) dy, \quad (6.3.25)$$

stabilizes the zero solution of the system (6.3.13)–(6.3.14).

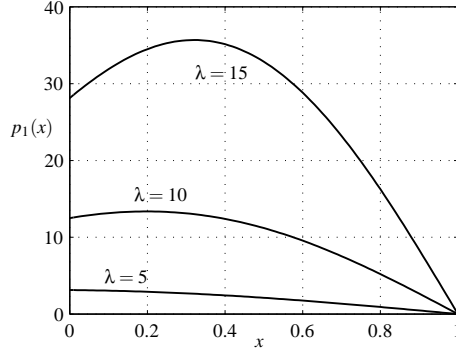


Figure 6.1: Observer gain for the unstable heat equation.

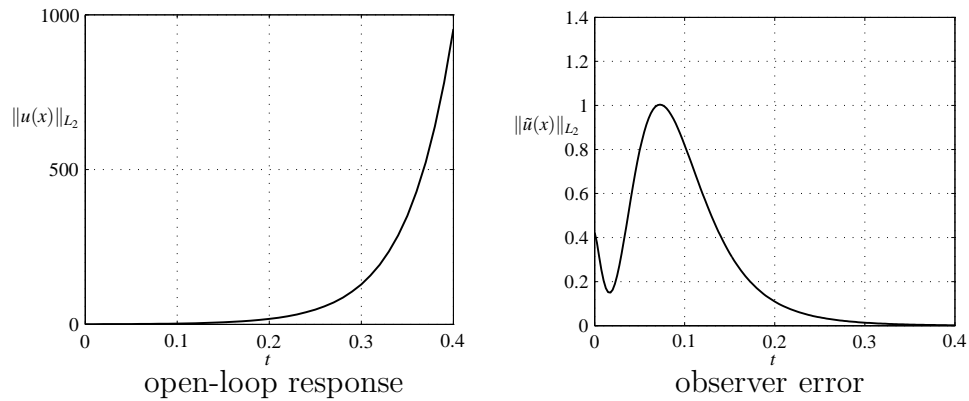


Figure 6.2: Exponential convergence of the observer for the unstable heat equation.

The above result can be easily extended for Neumann type of actuation.

The closed-loop system has been simulated with $\varepsilon = 1$, $\lambda_0 = 10$, $c = 5$, $u(x, 0) = 2e^{-2x} \sin(\pi x)$. With this choice of parameters the open-loop system has two unstable eigenvalues. The plant and the observer are discretized using a finite difference method. Since designs exist where, in principle, the order of the observer can be as low as the number of unstable eigenvalues, we design the low order compensator by taking a coarse 6-point grid (keeping the fine discretization of the plant, 100 points in our case, for simulation). In Fig. 6.3, the pole-zero map and Bode plots of the low order compensator are shown. The reduced order compensator is able to stabilize the system (Fig. 6.4).

Closed-loop solution. With every part of our design being explicit we can even write the closed loop solution of the system (6.3.13)–(6.3.14) together

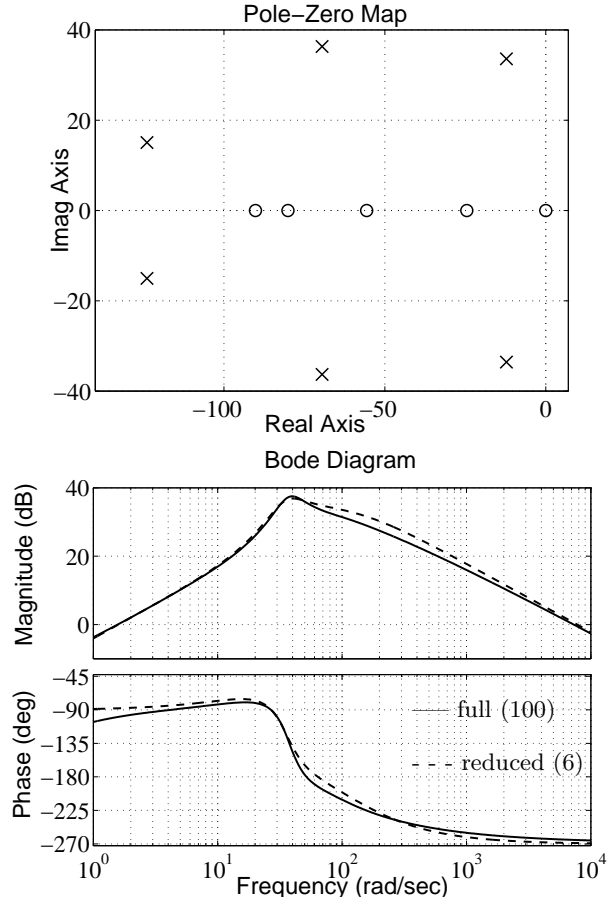


Figure 6.3: Pole-zero map and Bode plot of the compensator for unstable heat equation.

with compensator (6.3.22)–(6.3.25) explicitly, in terms of the initial conditions $u_0(x)$, $\hat{u}_0(x)$.

Theorem 6.4. *The solution to the closed loop system (6.3.13)–(6.3.14), (6.3.22)–(6.3.25) is*

$$\begin{aligned}
 u(x, t) = & 2 \sum_{n=0}^{\infty} e^{-(c+\mu_n^2)t} \cos \sqrt{\lambda + \mu_n^2} x \left\{ \int_0^1 \psi_n(\xi) u_0(\xi) d\xi \right. \\
 & \left. + \mu_n (-1)^n \left(C_n t + \sum_{m \neq n}^{\infty} C_m \frac{1 - e^{(\mu_n^2 - \mu_m^2)t}}{\mu_n^2 - \mu_m^2} \right) \right\}, \quad (6.3.26)
 \end{aligned}$$

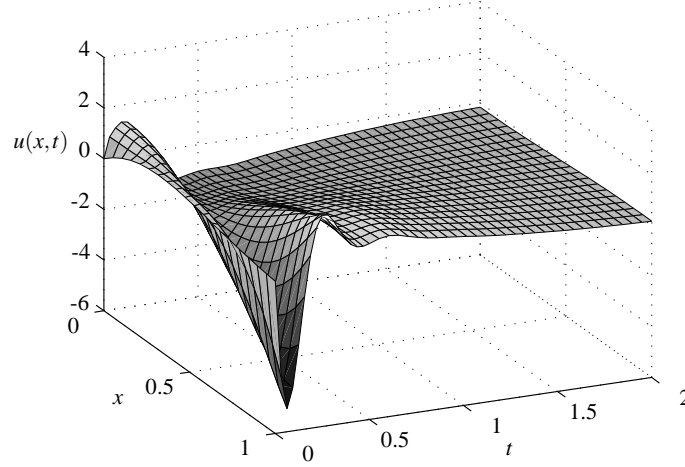


Figure 6.4: Closed-loop response with a low-order compensator.

where $\mu_n = \pi(n + 1/2)$,

$$C_n = 2 \left(\int_0^1 \lambda \frac{I_1(\sqrt{\lambda\xi(2-\xi)})}{\sqrt{\lambda\xi(2-\xi)}} \psi'_n(\xi) d\xi \right) \times \left(\int_0^1 \frac{\sin \sqrt{\lambda + \mu_n^2}(1-\xi)}{\sqrt{\lambda + \mu_n^2}} (u_0(\xi) - \hat{u}_0(\xi)) d\xi \right), \quad (6.3.27)$$

$$\psi_n(x) = \cos(\mu_n x) + \int_0^x \lambda \xi \frac{I_1(\sqrt{\lambda(x^2 - \xi^2)})}{\sqrt{\lambda(x^2 - \xi^2)}} \cos(\mu_n \xi) d\xi. \quad (6.3.28)$$

Proof. We set $\varepsilon = 1$ for simplicity. We start by solving the damped heat equation (5.3.11)–(5.3.13):

$$\tilde{w}(x, t) = 2 \sum_{n=0}^{\infty} e^{-(c+\mu_n^2)t} \cos(\mu_n x) \int_0^1 \tilde{w}_0(\xi) \cos(\mu_n \xi) d\xi, \quad \mu_n = \pi \left(n + \frac{1}{2} \right). \quad (6.3.29)$$

The initial condition \tilde{w}_0 can be calculated explicitly from \tilde{u}_0 via (5.3.25). Substituting the result into (5.3.10), changing the order of integration, and calculating some of the integrals we obtain

$$\begin{aligned} \tilde{u}(x, t) &= 2 \sum_{n=0}^{\infty} e^{-(c+\mu_n^2)t} \frac{\mu_n}{\lambda + \mu_n^2} \sin \sqrt{\lambda + \mu_n^2}(1-x) \\ &\times \int_0^1 \left(\sin \mu_n \xi + \int_{\xi}^1 \lambda \xi \frac{I_1(\sqrt{y^2 - \xi^2})}{\sqrt{y^2 - \xi^2}} \sin \mu_n y dy \right) \tilde{u}_0(1-\xi) d\xi \end{aligned} \quad (6.3.30)$$

Now we solve the controller target system

$$w_t(x, t) = w_{xx}(x, t) - cw(x, t), \quad (6.3.31)$$

$$w_x(0, t) = 0, \quad w(1, t) = - \int_0^1 k(1, y) \tilde{u}(y) dy \equiv d(t), \quad (6.3.32)$$

where the boundary condition $w(1, t)$ appears due to output-feedback instead of state-feedback:

$$\begin{aligned} w(x, t) = & 2 \sum_{n=0}^{\infty} e^{-(c+\mu_n^2)t} \cos(\mu_n x) \\ & \times \left(\int_0^1 w_0(\xi) \cos(\mu_n \xi) d\xi + (-1)^n \mu_n \int_0^t e^{(c+\mu_n^2)\tau} d(\tau) d\tau \right) \end{aligned} \quad (6.3.33)$$

The initial condition w_0 can be calculated explicitly from u_0 via (2.3.11). Substituting (6.3.33) into the inverse transformation (2.5.45) and calculating the integrals we obtain (6.3.26)–(6.3.28). \square

6.3.2 Chemical tubular reactor

Another case in which we can find the explicit gains is the heat equation with a non-constant coefficient:

$$u_t(x, t) = \varepsilon u_{xx}(x, t) + \lambda_{\alpha\beta}(x)u(x, t), \quad x \in (0, 1), \quad (6.3.34)$$

$$u(0, t) = 0, \quad (6.3.35)$$

where

$$\lambda_{\alpha\beta}(x) = \frac{2\varepsilon\alpha^2}{\cosh^2(\alpha x - \beta)}. \quad (6.3.36)$$

The coefficient $\lambda_{\alpha\beta}(x)$ parameterizes a family of "one-peak" functions. The free parameters α and β are chosen so that the maximum of $\lambda_{\alpha\beta}(x)$ is $2\alpha^2$ and is achieved at $x = \beta/\alpha$. Examples of $\lambda_{\alpha\beta}(x)$ for different values of α and β are shown in Fig. 6.5. Equations of the form (6.3.34)–(6.3.35) often describe the heat/mass transfer systems with heat generation or volumetric chemical reactions, for example chemical tubular reactor (see [12] and references therein). The open-loop system (6.3.34)–(6.3.35) (with $u(1) = 0$) is unstable for all three cases shown in Fig. 6.5.

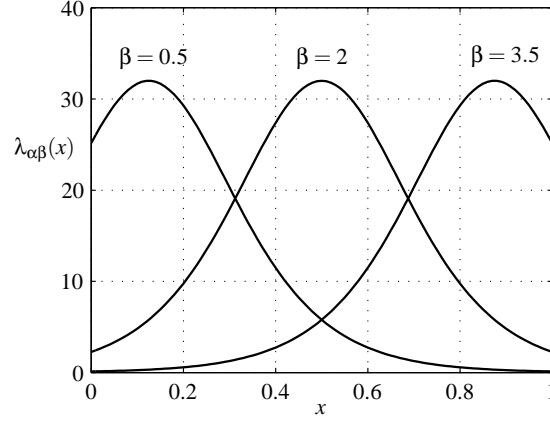


Figure 6.5: "One-peak" $\lambda_{\alpha\beta}(x)$ for $\alpha = 4$ and $\varepsilon = 1$.

Since the plant is in the diagonal form (there are no terms with $g(x)$ and $f(x, y)$), we choose to collocate the sensor and the actuator at $x = 1$. Following our approach we easily get the following result.

Theorem 6.5. *The controller*

$$u_x(1, t) = -\alpha(\tanh \beta - \tanh(\beta - \alpha))u(1) + \int_0^1 k_2(y)\hat{u}(y, t) dy, \quad (6.3.37)$$

with the observer

$$\hat{u}_t(x, t) = \varepsilon \hat{u}_{xx}(x, t) + \lambda_{\alpha\beta}(x) \hat{u}(x, t) + p_1(x)[u(1) - \hat{u}(1)] \quad (6.3.38)$$

$$\hat{u}(0, t) = 0, \quad (6.3.39)$$

$$\hat{u}_x(1, t) = -\alpha(\tanh \beta - \tanh(\beta - \alpha))\hat{u}(1) + \int_0^1 k_2(y)\hat{u}(y, t) dy, \quad (6.3.40)$$

where

$$k_2(x) = p_1(x) = \varepsilon \alpha^2 \tanh(\beta) e^{(1-x)\alpha \tanh \beta} (\tanh \beta - \tanh(\beta - \alpha x)), \quad (6.3.41)$$

stabilizes the zero solution of the system (6.3.34)–(6.3.35).

Proof. The stabilizing kernel $k_2(x)$ for (6.3.34)–(6.3.35) was obtained in Chapter 3. Using (5.4.48) we get the observer gain (6.3.41). The stability of the closed-loop system is ensured by Theorem 6.2. \square

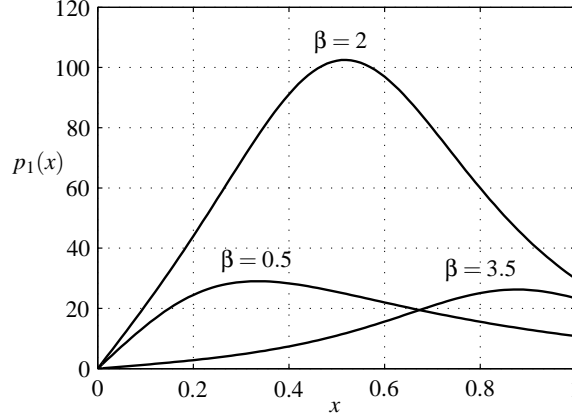


Figure 6.6: Observer gain for $\alpha = 4$ and $\varepsilon = 1$.

In Fig. 6.6 the observer gains corresponding to $\lambda_{\alpha\beta}(x)$ from Fig. 6.5 are shown.

6.3.3 Combining solutions

In Sections 6.3.1 and 6.3.2 we considered two interesting examples of solving an output-feedback problem explicitly, in a closed form. One can actually combine these two solutions to get a solution for a heat equation with $\lambda(x) = \lambda_0 + \lambda_{\alpha\beta}(x)$. It can be done in two steps. First, transform the error system into the target system (5.4.34)–(5.4.36) with $c = -\lambda_0$. It will give a PDE for $p(x, y)$ with $\lambda(x) = \lambda_{\alpha\beta}(x)$ whose solution we know. The target system will not be stable, but it will have constant coefficients. Second, stabilize this target system with $p_1(x)$ corresponding to a constant λ_0 . The resulting gain will be expressed in quadratures in terms of gains for λ_0 and $\lambda_{\alpha\beta}(x)$. Denote by $p^{\alpha\beta}(x, y)$ and $p^\lambda(x, y)$ the observer gains for the heat equation with $\lambda(x) = \lambda_{\alpha\beta}(x)$ and $\lambda(x) = \lambda_0$ ($a = (\lambda_0 + c)/\varepsilon$), respectively. Then following the procedure described above we obtain the observer gain for the heat equation with $\lambda(x) = \lambda_0 + \lambda_{\alpha\beta}(x)$:

$$p_1(x) = p_1^\lambda(x) + p_1^{\alpha\beta}(x) + \varepsilon p_{10}^\lambda p^{\alpha\beta}(x, 1) - \int_x^1 p^{\alpha\beta}(x, \xi) p_1^\lambda(\xi) d\xi, \quad (6.3.42)$$

$$p_{10} = p_{10}^\lambda + p_{10}^{\alpha\beta}. \quad (6.3.43)$$

For example for $\beta = 0$ one can get the closed-form solution

$$p_1(x) = \frac{\varepsilon\lambda}{1-x^2} I_2 \left(\sqrt{\lambda(1-x^2)} \right) + \varepsilon\lambda\alpha \tanh(\alpha x) \frac{I_1(\sqrt{\lambda(1-x^2)})}{\sqrt{\lambda(1-x^2)}}. \quad (6.3.44)$$

The control gain kernel can be obtained from (6.3.42)–(6.3.43) using (5.4.48). Thus, we can obtain the explicit solution to an output-feedback problem for a heat equation with nonconstant coefficients and arbitrary level of instability.

6.3.4 Frequency domain compensator

The solutions obtained in previous sections can be used to get explicit compensator transfer functions (treating $u(0, t)$ or $u(1, t)$ as an input and $u(1, t)$ or $u_x(1, t)$ as an output). We illustrate this point with the following system inspired by a solid propellant rocket model [10]

$$u_t(x, t) = u_{xx}(x, t) + gu(0, t), \quad (6.3.45)$$

$$u_x(0, t) = 0. \quad (6.3.46)$$

$$u(1, t) = U(t). \quad (6.3.47)$$

The observer

$$\hat{u}_t(x, t) = \hat{u}_{xx}(x, t) + gu(0, t), \quad (6.3.48)$$

$$\hat{u}_x(0, t) = 0, \quad (6.3.49)$$

$$\hat{u}(1, t) = U(t) \quad (6.3.50)$$

with direct injection of the reaction term $gu(0, t)$ is exponentially convergent. The stabilizing controller, whose state-feedback version was found in Chapter 3, is

$$u(1, t) = U(t) = -\sqrt{g} \int_0^1 \sinh(\sqrt{g}(1-y)) \hat{u}(y, t) dy. \quad (6.3.51)$$

We want to find a transfer function from the input $u(0, t)$ to the output $u(1, t)$, i.e., $u(1, s) = -C(s)u(0, s)$. Taking the Laplace transform of (6.3.48)–(6.3.50), setting the initial condition to zero, $\hat{u}(x, 0) = 0$, we have (for simplicity of notation

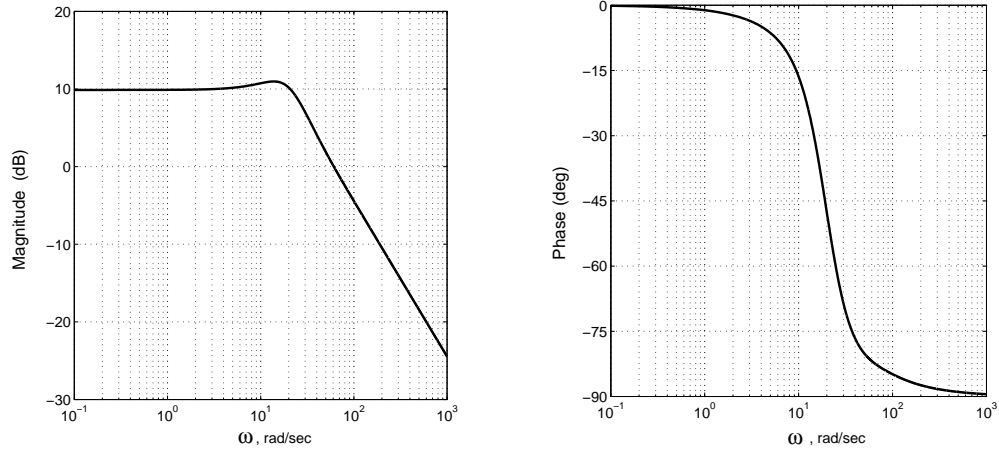


Figure 6.7: Bode plot of $C(j\omega)$ for $g = 8$.

we denote by $\hat{u}(x, s)$ and $u(0, s)$ the Laplace transforms of $\hat{u}(x, t)$ and $u(0, t)$, respectively):

$$s\hat{u}(x, s) = \hat{u}_{xx}(x, s) + gu(0, s), \quad (6.3.52)$$

$$\hat{u}_x(0, s) = 0, \quad (6.3.53)$$

$$\hat{u}(1, s) = -\sqrt{g} \int_0^1 \sinh(\sqrt{g}(1-y))\hat{u}(y, s) dy. \quad (6.3.54)$$

The equation (6.3.52) with boundary conditions (6.3.53)–(6.3.54) is a second order ODE with respect to x (we regard s as a parameter). The solution of (6.3.52) satisfying (6.3.53) is:

$$\hat{u}(x, s) = \hat{u}(0, s) \cosh(\sqrt{s}x) + \frac{g}{s}(1 - \cosh(\sqrt{s}x))u(0, s) \quad (6.3.55)$$

Using boundary condition (6.3.54) we obtain $\hat{u}(0, s)$:

$$\hat{u}(0, s) = \frac{\cosh(\sqrt{s}) - \cosh(\sqrt{g})}{s \cosh(\sqrt{s}) - g \cosh(\sqrt{g})} gu(0, s) \quad (6.3.56)$$

Substituting now (6.3.56) into (6.3.55) with $x = 1$ we obtain the following result:

Theorem 6.6. *The transfer function of the system (6.3.48)–(6.3.51) with $u(0, t)$ as an input and $u(1, t)$ as an output is*

$$C(s) = \frac{g}{s} \left(-1 + \frac{(s - g) \cosh(\sqrt{s}) \cosh(\sqrt{g})}{s \cosh(\sqrt{s}) - g \cosh(\sqrt{g})} \right) \quad (6.3.57)$$

The validation of application of the above procedure for linear parabolic PDEs (which proves that $C(s)$ is indeed a transfer function) can be found in [20, Chapter 4]. Note that $s = 0$ is not a pole:

$$C(0) = \frac{g}{2} + \frac{1}{\cosh(\sqrt{g})} - 1. \quad (6.3.58)$$

The transfer function (6.3.57) has infinitely many poles, all of them are real and negative. The Bode plots of $C(s)$ for $g = 8$ are presented in Fig. 6.7. It is evident from the Bode plots that $C(s)$ can be approximated by a second order, relative degree one transfer function. For example, a pretty good estimate would be

$$C(s) \approx 60 \frac{s + 17}{s^2 + 25s + 320}. \quad (6.3.59)$$

The relative degree one nature of the compensator is the result of employing a full order (rather than a reduced order) observer.

This chapter is in part a reprint of the material as it appears in A. Smyshlyaev and M. Krstic, “Backstepping observers for a class of parabolic PDEs,” *Systems and Control Letters*, vol.54, pp. 613-625, 2005.

The dissertation author was the primary author and the coauthor listed in this publication directed the research which forms the basis for this chapter.

Chapter 7

Certainty Equivalence Adaptive Controllers with Passive Identifiers

7.1 Introduction

We study the boundary control problem for a class of unstable 3D reaction-advection-diffusion PDEs with *unknown coefficients*. No solution presently exists for this problem (even in 1D) due to the absence of parametrized families of controllers for such systems. We make explicit controllers introduced in Chapter 3 adaptive by designing parameter identifiers and substituting the parameter estimates they generate into the control law. Adaptive controllers designed in this way are referred to as “certainty equivalence.” Stability of such controllers is a highly non-trivial question because the parameter estimates make the adaptive controller nonlinear even when the PDE plant is linear. In this paper we prove the “separation principle”—the global stability of such a nonlinear closed-loop PDE system.

The parameter identifiers for use in the certainty equivalence approach to adaptive control can be split into two classes: passivity-based identifiers and

swapping identifiers [36]. In this chapter we design the controllers based on passive identifiers. The “passive,” a.k.a. the “observer-based” approach has so far been the prevalent identification technique in existing results on adaptive control for PDEs [8, 9, 29, 48, 62]. This approach is appealing due to its simplicity—it employs an observer in the form of a copy of the plant, plus a stabilizing error term—however, it has so far not been used in boundary control problems.

In the class of reaction-advection-diffusion PDEs for which we design identifiers, all three classes of coefficients are allowed to be unknown—the reaction coefficients, advection coefficients, and diffusion coefficients. We prove that both the passive and swapping identifiers are stable with all the coefficients unknown and present our simulations in the case where they are all unknown. However, a fundamental obstacle exists in the estimation-based designs which makes closed-loop stability very hard to prove when the *diffusion coefficient* (the coefficient multiplying the second spatial derivatives) is unknown. The reason for this is that for closed-loop stability (with unknown diffusion) one seems to need a Sobolev bound on the “estimation error” which is one order higher than what stability analysis for the identifiers provides. Thus, we state closed-loop stability for known diffusion, though we illustrate it in simulations for unknown diffusion.

Early works on adaptive control of infinite-dimensional systems were for plants stabilizable by non-identifier based high gain feedback [44], under a relative degree one assumption. State-feedback model reference adaptive control (MRAC) was extended to PDEs in [29, 9, 62, 48, 8] but not for the case of boundary control. Efforts in [24, 67] made use of positive realness assumptions where relative degree one is implicit, except in some examples where this restriction is cleverly overcome. Stochastic adaptive LQR with least-squares parameter estimation and state feedback was pursued in [26]. Adaptive control of nonlinear PDEs was studied in [43, 32, 33]. Adaptive controllers for nonlinear systems on lattices were designed in [31]. An experimentally validated adaptive boundary controller for a flexible beam was presented in [25].

Throughout the Chapters 7–11 we assume well posedness of the closed-loop systems in the interest of space and due to the parabolic character of these systems which ensures their benign behavior, as supported by numerical results that we show for each adaptive design. An example on how one derives the Sobolev estimates of higher order (H_4), the key step in a proof of well posedness, is given in [38].

Notation. The spatial $L_2(0, 1)$ norm is denoted by $\| \cdot \|$. The temporal norms are denoted by \mathcal{L}_∞ , \mathcal{L}_1 , and \mathcal{L}_2 for $t \geq 0$. We denote by l_1 a generic function in \mathcal{L}_1 . The symbols $I_1(\cdot)$, $J_1(\cdot)$ denote the corresponding Bessel functions.

7.2 Benchmark Plant

In this section we consider a simple plant to illustrate the main ideas of our approach in a tutorial way without the extensive notation that is needed in higher dimension like 2D and 3D and with more than one physical parameter.

Consider a one-dimensional unstable heat equation

$$u_t(x, t) = u_{xx}(x, t) + \lambda u(x, t) \quad (7.2.1)$$

$$u(0, t) = 0 \quad (7.2.2)$$

$$u(1, t) = U(t), \quad (7.2.3)$$

with one unknown parameter λ . Our objective is to regulate the state of this system to zero from the boundary with Dirichlet actuation $U(t)$. For $U(t) = 0$ this system can have an arbitrarily large number of unstable eigenvalues.

For the case of known λ , the following control method has been proposed

in [55]: use a transformation¹

$$w(x) = u(x) - \int_0^x k(x, \xi) u(\xi) d\xi \quad (7.2.4)$$

$$k(x, \xi) = -\lambda \xi \frac{I_1 \left(\sqrt{\lambda(x^2 - \xi^2)} \right)}{\sqrt{\lambda(x^2 - \xi^2)}} \quad (7.2.5)$$

to map (7.2.1)–(7.2.2) into an exponentially stable system

$$w_t = w_{xx} \quad (7.2.6)$$

$$w(0) = w(1) = 0. \quad (7.2.7)$$

The stabilizing control law is then given by

$$u(1) = - \int_0^1 \lambda \xi \frac{I_1 \left(\sqrt{\lambda(1 - \xi^2)} \right)}{\sqrt{\lambda(1 - \xi^2)}} u(\xi) d\xi. \quad (7.2.8)$$

By certainty equivalence principle, the controller in case of unknown λ will be given by (7.2.8) with λ replaced by its estimate $\hat{\lambda}$:

$$u(1) = - \int_0^1 \hat{\lambda} \xi \frac{I_1 \left(\sqrt{\hat{\lambda}(1 - \xi^2)} \right)}{\sqrt{\hat{\lambda}(1 - \xi^2)}} u(\xi) d\xi. \quad (7.2.9)$$

Consider the following system

$$\hat{u}_t = \hat{u}_{xx} + \hat{\lambda} u + \gamma^2 (u - \hat{u}) \int_0^1 u^2(x) dx \quad (7.2.10)$$

$$\hat{u}(0) = 0 \quad (7.2.11)$$

$$\hat{u}(1) = u(1). \quad (7.2.12)$$

Such systems are often called "observers" because they incorporate a copy of the plant though they are not used for state estimation. This identifier employs a copy of the PDE plant and an additional nonlinear term. The term "passive identifier" comes from the fact that an operator from the parameter estimation error $\tilde{\lambda} = \lambda - \hat{\lambda}$ to the inner product of u with $u - \hat{u}$ is strictly passive. The

¹To reduce notational burden we suppress time dependence everywhere and x -dependence where it does not lead to a confusion.

additional nonlinear term in (7.2.10) acts as nonlinear damping whose task is to ensure square integrability of $\dot{\tilde{\lambda}}$ (i.e., in our notation, $\dot{\tilde{\lambda}} \in \mathcal{L}_2$). This slows down the adaptation and serves as an alternative to update law normalization needed to achieve certainty equivalence.

Consider the error signal $e = u - \hat{u}$ which satisfies the following PDE

$$e_t = e_{xx} + \tilde{\lambda}u - \gamma^2 e \|u\|^2 \quad (7.2.13)$$

$$e(0) = 0 \quad (7.2.14)$$

$$e(1) = 0. \quad (7.2.15)$$

With a Lyapunov function

$$V = \frac{1}{2} \int_0^1 e^2(x) dx + \frac{\tilde{\lambda}^2}{2\gamma} \quad (7.2.16)$$

we get

$$\dot{V} = -\|e_x\|^2 - \gamma^2 \|e\|^2 \|u\|^2 + \tilde{\lambda} \int_0^1 e(x)u(x) dx - \frac{\tilde{\lambda}\dot{\tilde{\lambda}}}{\gamma}. \quad (7.2.17)$$

Choosing the update law

$$\dot{\tilde{\lambda}} = \gamma \int_0^1 (u(x) - \hat{u}(x))u(x) dx, \quad (7.2.18)$$

we obtain

$$\dot{V} \leq -\|e_x\|^2 - \gamma^2 \|e\|^2 \|u\|^2, \quad (7.2.19)$$

which implies $V(t) \leq V(0)$ and from the definition of V we get that $\tilde{\lambda}$ and $\|e\|$ are bounded. Integrating (7.2.19) with respect to time from zero to infinity we get the properties $\|e_x\|, \|e\|\|u\| \in \mathcal{L}_2$. From the update law (7.2.18) we get $|\dot{\tilde{\lambda}}| \leq \gamma\|e\|\|u\|$ and so $\dot{\tilde{\lambda}} \in \mathcal{L}_2$.

For the case of unknown λ the transformation (7.2.4) is modified as follows:

$$\hat{w}(x) = \hat{u}(x) - \int_0^x \hat{k}(x, \xi) \hat{u}(\xi) d\xi \quad (7.2.20)$$

$$\hat{k}(x, \xi) = -\hat{\lambda}\xi \frac{I_1\left(\sqrt{\hat{\lambda}(x^2 - \xi^2)}\right)}{\sqrt{\hat{\lambda}(x^2 - \xi^2)}}. \quad (7.2.21)$$

It maps (7.2.10)–(7.2.12) into the following target system (see Lemma 7.5 from Section 7.4)

$$\hat{w}_t = \hat{w}_{xx} + \dot{\hat{\lambda}} \int_0^x \frac{\xi}{2} \hat{w}(\xi) d\xi + (\hat{\lambda} + \gamma^2 \|u\|^2) e_1 \quad (7.2.22)$$

$$\hat{w}(0) = \hat{w}(1) = 0, \quad (7.2.23)$$

where

$$e_1 = e - \int_0^x \hat{k}(x, \xi) e(\xi) d\xi. \quad (7.2.24)$$

We observe that, in comparison to the non-adaptive target system (7.2.6)–(7.2.7), two additional terms appear in (7.2.22)–(7.2.23), both going to zero in some sense, since the identifier guarantees $\|e\|, \dot{\hat{\lambda}} \in \mathcal{L}_2$. The proof of boundedness of all the signals based on the joint analysis of e and \hat{w} systems is shown next.

Before we proceed, let us state two useful results.

Lemma 7.1 (Lemma 3.1 in [43]). *Suppose that the function $f(t)$ defined on $[0, \infty)$ satisfies the following conditions:*

- (i) $f(t) \geq 0$ for all $t \in [0, \infty)$,
- (ii) $f(t)$ is differentiable on $[0, \infty)$ and there exists a constant M such that

$$f'(t) \leq M, \quad \forall t \geq 0, \quad (7.2.25)$$

- (iii) $\int_0^\infty f(t) dt < \infty$.

Then we have

$$\lim_{t \rightarrow \infty} f(t) = 0. \quad (7.2.26)$$

Lemma 7.2 (Lemma B.6 in [36]). *Let v , l_1 , and l_2 be real-valued functions defined on R_+ , and let c be a positive constant. If l_1 and l_2 are nonnegative and in \mathcal{L}_1 and satisfy the differential inequality*

$$\dot{v} \leq -cv + l_1(t)v + l_2(t), \quad v(0) \geq 0 \quad (7.2.27)$$

then $v \in \mathcal{L}_\infty \cap \mathcal{L}_1$.

Let us denote a bound on $\hat{\lambda}$ by λ_0 . The function $\hat{k}(x, \xi)$ is bounded and twice continuously differentiable with respect to x and ξ , therefore there exist constants M_1, M_2, M_3 such that

$$\|e_1\| \leq M_1 \|e\| \quad (7.2.28)$$

$$\|u\| \leq \|\hat{u}\| + \|e\| \leq M_2 \|\hat{w}\| + \|e\| \quad (7.2.29)$$

$$\|u_x\| \leq \|\hat{u}_x\| + \|e_x\| \leq M_3 \|\hat{w}_x\| + \|e_x\|. \quad (7.2.30)$$

To prove boundedness of all the signals, we estimate

$$\begin{aligned} \frac{1}{2} \frac{d}{dt} \|\hat{w}\|^2 &= - \int_0^1 \hat{w}_x^2 dx + \dot{\hat{\lambda}} \int_0^1 \hat{w}(x) \int_0^x \frac{\xi}{2} \hat{w}(\xi) d\xi dx \\ &\quad + (\hat{\lambda} + \gamma^2 \|u\|^2) \int_0^1 e_1 \hat{w} dx \\ &\leq -\|\hat{w}_x\|^2 + \frac{|\dot{\hat{\lambda}}|}{2} \|\hat{w}\|^2 + M_1 \lambda_0 \|\hat{w}\| \|e\| \\ &\quad + \gamma^2 M_1 \|u\| (M_2 \|\hat{w}\| + \|e\|) \|\hat{w}\| \|e\| \\ &\leq -\frac{1}{4} \|\hat{w}\|^2 + \frac{1}{16} \|\hat{w}\|^2 + |\dot{\hat{\lambda}}|^2 \|\hat{w}\|^2 + \frac{1}{16} \|\hat{w}\|^2 \\ &\quad + 4M_1^2 \lambda_0^2 \|e\|^2 + \frac{1}{16} \|\hat{w}\|^2 \\ &\quad + 8\gamma^4 M_1^2 M_2^2 \|u\|^2 \|e\|^2 \|\hat{w}\|^2 + \frac{\|e\|^2}{16M_2^2} \\ &\leq -\frac{1}{16} \|\hat{w}\|^2 + \left(4M_1^2 \lambda_0^2 + \frac{1}{16M_2^2} \right) \|e\|^2 \\ &\quad + \left(|\dot{\hat{\lambda}}|^2 + 8\gamma^4 M_1^2 M_2^2 \|u\|^2 \|e\|^2 \right) \|\hat{w}\|^2 \\ &\leq -\frac{1}{16} \|\hat{w}\|^2 + l_1 \|\hat{w}\|^2 + l_1, \end{aligned} \quad (7.2.31)$$

where l_1 denotes a generic function in \mathcal{L}_1 . The last inequality follows from the properties $\dot{\hat{\lambda}}, \|u\| \|e\|, \|e\| \in \mathcal{L}_2$. Using Lemma 7.2 we get $\|\hat{w}\| \in \mathcal{L}_\infty \cap \mathcal{L}_2$. From (7.2.29) we get $\|u\|, \|\hat{u}\| \in \mathcal{L}_\infty \cap \mathcal{L}_2$, and (7.2.18) implies that $\dot{\hat{\lambda}}$ is bounded.

In order to get pointwise in x boundedness we show the boundedness of

$\|\hat{w}_x\|$ and $\|e_x\|$:

$$\begin{aligned}
\frac{1}{2} \frac{d}{dt} \int_0^1 \hat{w}_x^2 dx &= \int_0^1 \hat{w}_x \hat{w}_{xt} dx = - \int_0^1 \hat{w}_{xx} \hat{w}_t dx \\
&= - \int_0^1 \hat{w}_{xx}^2 dx - \frac{\dot{\lambda}}{2} \int_0^1 \hat{w}_{xx} \int_0^x \xi w(\xi) d\xi dx \\
&\quad - (\hat{\lambda} + \gamma^2 \|u\|^2) \int_0^1 e_1 \hat{w}_{xx} dx \\
&\leq -\frac{1}{8} \|\hat{w}_x\|^2 + \frac{|\dot{\lambda}|^2 \|\hat{w}\|^2}{4} + (\lambda_0 + \gamma^2 \|u\|^2)^2 M_1 \|e\|^2
\end{aligned} \tag{7.2.32}$$

$$\begin{aligned}
\frac{1}{2} \frac{d}{dt} \int_0^1 e_x^2 dx &= - \int_0^1 e_{xx} e_t dx \\
&\leq -\|e_{xx}\|^2 + |\tilde{\lambda}| \|e_{xx}\| \|u\| - \gamma^2 \|e_x\|^2 \|u\|^2 \\
&\leq -\frac{1}{8} \|e_x\|^2 + \frac{1}{2} |\tilde{\lambda}|^2 \|u\|^2.
\end{aligned} \tag{7.2.33}$$

Since the right hand sides of (7.2.32) and (7.2.33) are square integrable, using Lemma 7.2 we get $\|\hat{w}_x\|, \|e_x\| \in \mathcal{L}_\infty \cap \mathcal{L}_2$. Using (7.2.30) we get $\|u_x\|, \|\hat{u}_x\| \in \mathcal{L}_\infty \cap \mathcal{L}_2$. From Agmon's inequality

$$\max_{x \in [0,1]} |u(x, t)|^2 \leq 2 \|u\| \|u_x\| \tag{7.2.34}$$

we get the boundedness of u and \hat{u} for all $x \in [0, 1]$.

To show the regulation of u to zero, we note that

$$\frac{1}{2} \frac{d}{dt} \|e\|^2 < \infty, \quad \frac{1}{2} \frac{d}{dt} \|\hat{w}\|^2 < \infty, \tag{7.2.35}$$

and using Lemma 7.1 (which is an alternative to Barbalat's lemma) we get $\|\hat{w}\| \rightarrow 0$, $\|e\| \rightarrow 0$ as $t \rightarrow \infty$. From (7.2.29) it follows that $\|\hat{u}\| \rightarrow 0$ and $\|u\| \rightarrow 0$. Using Agmon's inequality and the fact that $\|u_x\|$ is bounded, we get the regulation of u to zero for all $x \in [0, 1]$:

$$\lim_{t \rightarrow \infty} \max_{x \in [0,1]} |u(x, t)| \leq \lim_{t \rightarrow \infty} (2 \|u\| \|u_x\|)^{1/2} = 0. \tag{7.2.36}$$

7.3 3D Reaction-Advection-Diffusion Plant

We present now a passivity-based design for a plant in a three-dimensional setting:

$$u_t = \varepsilon(u_{xx} + u_{yy} + u_{zz}) + b_1 u_x + b_2 u_y + b_3 u_z + \lambda u \quad (7.3.37)$$

for $(x, y, z) \in \Omega$, where the domain Ω is a cylinder with top and bottom of arbitrary shape Γ (Fig. 7.1). This configuration of the domain Ω is essential because it allows us to view the problem as many 1D problems with $0 \leq x \leq 1$ and fixed y, z . We assume Dirichlet boundary conditions on the boundary $\partial\Omega$,

$$u = 0, \quad (x, y, z) \in \partial\Omega \setminus \{x = 1\}, \quad (7.3.38)$$

except at the top of the cylinder $x = 1$ where the actuation is applied,

$$u(1, y, z) = U(t, y, z), \quad (y, z) \in \Gamma. \quad (7.3.39)$$

The parameters $\varepsilon > 0$, b_1 , b_2 , b_3 , λ are assumed to be unknown.

For the notational convenience let us use the following notation later in this section:

$$\begin{aligned} \Delta u &= u_{xx} + u_{yy} + u_{zz}, \quad \nabla u = (u_x, u_y, u_z)^T \\ \mathbf{b} &= (b_1, b_2, b_3)^T \\ \|u\|^2 &\triangleq \int_{\Gamma} \int_0^1 \int_0^1 u^2(x, y, z) dx dy dz \triangleq \int_{\Omega} u^2 d\Omega \\ \|\nabla u\|^2 &\triangleq \int_{\Omega} \nabla u \cdot \nabla u d\Omega. \end{aligned} \quad (7.3.40)$$

We will employ the following “observer”

$$\begin{aligned} \hat{u}_t &= \hat{\varepsilon} \Delta \hat{u} + \hat{\mathbf{b}} \cdot \nabla \hat{u} + \hat{\lambda} u + \gamma^2 (u - \hat{u}) \|\nabla u\|^2, \\ &\quad (x, y, z) \in \Omega \end{aligned} \quad (7.3.41)$$

$$\hat{u} = 0, \quad (x, y, z) \in \partial\Omega \setminus \{x = 1\} \quad (7.3.42)$$

$$\hat{u} = u, \quad x = 1, (y, z) \in \Gamma. \quad (7.3.43)$$

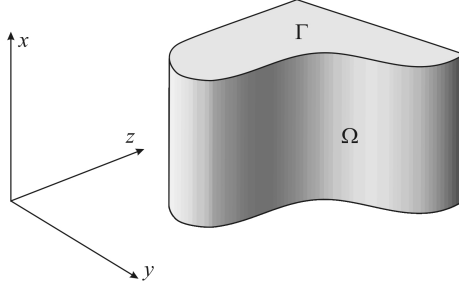


Figure 7.1: The domain Ω for the plant (7.3.37).

There are two main differences compared to 1D case with one parameter in Section 7.2. First, since the diffusion coefficient ε is unknown we must use projection to ensure $\hat{\varepsilon} > \underline{\varepsilon} > 0$. We define the projection operator as

$$\text{Proj}_{\underline{\varepsilon}}\{\tau\} = \begin{cases} 0 & , \hat{\varepsilon} = \underline{\varepsilon} \text{ and } \tau < 0 \\ \tau & , \text{ else } . \end{cases} \quad (7.3.44)$$

Although this operator is discontinuous it is possible to introduce a small boundary layer instead of a hard switch which will avoid dealing with Filippov solutions and noise due to frequent switching of the update law (see [38] for more details). However, we use (7.3.44) here for notational clarity. Note that $\hat{\varepsilon}$ does not require the projection from above and all other parameters do not require projection at all.

Second, we can see in (7.3.41) that while the diffusion and advection coefficients multiply the operators of \hat{u} , the reaction coefficient multiplies u in the observer. This is necessary in order to eliminate any λ -dependence in the error system so that it is stable.

The error signal $e = u - \hat{u}$ satisfies the following PDE:

$$\begin{aligned} e_t &= \hat{\varepsilon} \Delta e + \hat{\mathbf{b}} \cdot \nabla e + \tilde{\varepsilon} \Delta u + \tilde{\mathbf{b}} \cdot \nabla u + \tilde{\lambda} u \\ &\quad - \gamma^2 e \|\nabla u\|^2, \quad (x, y, z) \in \Omega \end{aligned} \quad (7.3.45)$$

$$e = 0, \quad (x, y, z) \in \partial\Omega. \quad (7.3.46)$$

Using a Lyapunov function

$$V = \frac{1}{2} \int_{\Omega} e^2 d\Omega + \frac{\tilde{\varepsilon}^2}{2\gamma_1} + \frac{|\tilde{\mathbf{b}}|^2}{2\gamma_2} + \frac{\tilde{\lambda}^2}{2\gamma_3} \quad (7.3.47)$$

we get

$$\begin{aligned} \dot{V} &= -\hat{\varepsilon} \|\nabla e\|^2 - \gamma^2 \|e\|^2 \|\nabla u\|^2 \\ &\quad + \tilde{\varepsilon} \int_{\Omega} e \Delta u d\Omega + \int_{\Omega} e (\tilde{\mathbf{b}} \cdot \nabla u) d\Omega \\ &\quad + \tilde{\lambda} \int_{\Omega} e u d\Omega - \frac{1}{\gamma_0} \tilde{\varepsilon} \dot{\tilde{\varepsilon}} - \frac{1}{\gamma_1} \tilde{\mathbf{b}} \cdot \dot{\tilde{\mathbf{b}}} - \frac{1}{\gamma_2} \tilde{\lambda} \dot{\tilde{\lambda}}. \end{aligned} \quad (7.3.48)$$

With update laws

$$\dot{\tilde{\varepsilon}} = -\gamma_0 \text{Proj}_{\tilde{\varepsilon}} \left\{ \int_{\Omega} \nabla u \cdot \nabla (u - \hat{u}) d\Omega \right\} \quad (7.3.49)$$

$$\dot{\tilde{\mathbf{b}}} = \gamma_1 \int_{\Omega} (u - \hat{u}) \nabla u d\Omega \quad (7.3.50)$$

$$\dot{\tilde{\lambda}} = \gamma_2 \int_{\Omega} (u - \hat{u}) u d\Omega, \quad (7.3.51)$$

where $\gamma_0, \gamma_1, \gamma_2 > 0$ we get

$$\dot{V} \leq -\underline{\varepsilon} \|\nabla e\|^2 - \gamma^2 \|e\|^2 \|\nabla u\|^2, \quad (7.3.52)$$

which implies $V(t) \leq V(0)$ so that $\tilde{\varepsilon}$, $|\tilde{\mathbf{b}}|$, $\tilde{\lambda}$, $\|e\|$ are bounded. Integrating (7.3.52) with respect to time from zero to infinity we get square integrability of $\|\nabla e\|$, $\|e\| \|\nabla u\|$, which, together with the update laws (7.3.49)–(7.3.51), gives square integrability of $|\dot{\tilde{\mathbf{b}}}|$ and $\dot{\tilde{\lambda}}$.

Lemma 7.3. *The identifier (7.3.41)–(7.3.43) with update laws (7.3.50)–(7.3.51) guarantees the following properties:*

$$\|\nabla e\|, \|e\| \|\nabla u\| \in \mathcal{L}_2, \quad \|e\| \in \mathcal{L}_{\infty} \cap \mathcal{L}_2, \quad (7.3.53)$$

$$\tilde{\varepsilon}, \tilde{b}_1, \tilde{b}_2, \tilde{b}_3, \tilde{\lambda} \in \mathcal{L}_{\infty}, \quad \dot{\tilde{b}}_1, \dot{\tilde{b}}_2, \dot{\tilde{b}}_3, \dot{\tilde{\lambda}} \in \mathcal{L}_2. \quad (7.3.54)$$

We employ the following controller

$$\begin{aligned}
u(1, y, z) = & - \int_0^1 \frac{\hat{\lambda} + c}{\hat{\varepsilon}} \xi e^{-\frac{\hat{b}_1(1-\xi)}{2\hat{\varepsilon}}} \\
& \times \frac{I_1 \left(\sqrt{\frac{\hat{\lambda}+c}{\hat{\varepsilon}}(1-\xi^2)} \right)}{\sqrt{\frac{\hat{\lambda}+c}{\hat{\varepsilon}}(1-\xi^2)}} \hat{u}(\xi, y, z) d\xi
\end{aligned} \tag{7.3.55}$$

with $c \geq 0$, which is a straightforward generalization of the one proposed in [55] for the case of known parameters.

Starting with the result on stability of the identifier, we now turn to proving closed-loop stability. Unfortunately, it is very hard to prove the result in the case of unknown ε . This is because, while the identifier guarantees the properties (7.3.53) for $\|e\|$ and $\|\nabla e\|$, it does not provide any estimates for $\|\Delta e\|$ which are required in the case of unknown ε . Therefore for the closed-loop result we assume that ε is known and set $\hat{\varepsilon} = \varepsilon$ everywhere. The update law (7.3.49) nevertheless achieves closed-loop stability for unknown ε in simulations, as shown in Section 7.5.

Theorem 7.4. *Consider the plant (7.3.37), (7.3.38) with the controller (7.3.55). If the closed loop system that consists of (7.3.37), (7.3.38), (7.3.55), identifier (7.3.41)–(7.3.43), and update laws (7.3.50), (7.3.51) has a classical solution $(\hat{\mathbf{b}}, \hat{\lambda}, u, \hat{u})$, then for any $\hat{\mathbf{b}}(0), \hat{\lambda}(0)$ and any initial conditions $u_0, \hat{u}_0 \in L_2(\Omega)$, the signals $\hat{\mathbf{b}}, \hat{\lambda}, u, \hat{u}$ are bounded and u is regulated to zero for all $(x, y, z) \in \Omega$:*

$$\lim_{t \rightarrow \infty} \max_{(x, y, z) \in \Omega} |u(x, y, z, t)| = 0. \tag{7.3.56}$$

7.4 Proof of Theorem 7.4

We will use Poincare and Agmon's inequalities (see, e.g., [63]):

$$\|u\| \leq d_1(\Gamma) \|\nabla u\| \tag{7.4.57}$$

$$\max_{(x, y, z) \in \Omega} |u| \leq d_2(\Gamma) \|u\|_{H_1}^{1/2} \|u\|_{H_2}^{1/2}. \tag{7.4.58}$$

Here d_1 and d_2 are constants that depend only on Γ . The main difficulty in proving the result in 3D case compared to 1D case is that we need to show H_2 (instead of H_1) boundedness and H_1 (instead of L_2) regulation in order to have pointwise boundedness and regulation.

7.4.1 Target system

We use the following transformation

$$\hat{w}(x, y, z) = \hat{u}(x, y, z) - \int_0^x \hat{k}(x, \xi) \hat{u}(\xi, y, z) d\xi \quad (7.4.59)$$

$$\hat{k}(x, \xi) = -\frac{\hat{\lambda} + c}{\varepsilon} \xi e^{-\frac{\hat{b}_1(x-\xi)}{2\varepsilon}} \frac{I_1\left(\sqrt{\frac{\hat{\lambda}+c}{\varepsilon}}(x^2 - \xi^2)\right)}{\sqrt{\frac{\hat{\lambda}+c}{\varepsilon}}(x^2 - \xi^2)}, \quad (7.4.60)$$

which is a generalized version of the transformation presented in [55] for the case of known parameters.

Lemma 7.5. *The transformation (7.4.59)–(7.4.60) maps (7.3.41)–(7.3.43) into the target system*

$$\begin{aligned} \hat{w}_t &= \varepsilon \Delta \hat{w} + \hat{\mathbf{b}} \cdot \nabla \hat{w} - c \hat{w} + \dot{\hat{b}}_1 \Phi_1[\hat{w}] + \dot{\hat{\lambda}} \Phi_2[\hat{w}] \\ &\quad + (\hat{\lambda} + \gamma^2 \|\nabla u\|^2) e_1, \end{aligned} \quad (7.4.61)$$

$$\hat{w} = 0, \quad (x, y, z) \in \partial\Omega. \quad (7.4.62)$$

where

$$\Phi_i[\hat{w}] = \int_0^x \varphi_i(x, \xi) \hat{w}(\xi, y, z) d\xi \quad (7.4.63)$$

$$e_1 = e - \int_0^x \hat{k}(x, \xi) e(\xi, y, z) d\xi. \quad (7.4.64)$$

and

$$\begin{aligned} \varphi_1(x, \xi) &= \frac{x - \xi}{2\varepsilon} \hat{k}(x, \xi) + \frac{1}{2\varepsilon} \int_\xi^x (x - \sigma) \hat{k}(x, \sigma) \hat{l}(\sigma, \xi) d\sigma \\ \varphi_2(x, \xi) &= \frac{\xi}{2\varepsilon} e^{-\frac{\hat{b}_1}{2\varepsilon}(x-\xi)}. \end{aligned} \quad (7.4.65)$$

Proof. Substituting (7.4.59) into (7.3.41) we get

$$\begin{aligned}\hat{w}_t &= \varepsilon \Delta \hat{w} + \hat{\mathbf{b}} \cdot \nabla \hat{w} - c \hat{w} + (\hat{\lambda} + \gamma^2 \|\nabla u\|^2) e_1 \\ &\quad - \int_0^x \left(\hat{b}_1 \hat{k}_{\hat{b}_1}(x, \xi) + \hat{\lambda} \hat{k}_{\hat{\lambda}}(x, \xi) \right) \hat{u}(\xi, y, z) d\xi\end{aligned}\quad (7.4.66)$$

To replace \hat{u} with \hat{w} we use an inverse transformation

$$\hat{u} = \hat{w} + \int_0^x \hat{l}(x, \xi) \hat{w}(\xi, y, z) d\xi \quad (7.4.67)$$

$$\hat{l}(x, \xi) = -\frac{\hat{\lambda} + c}{\varepsilon} \xi e^{-\frac{\hat{b}_1(x-\xi)}{2\varepsilon}} \frac{J_1\left(\sqrt{\frac{\hat{\lambda}+c}{\varepsilon}(x^2-\xi^2)}\right)}{\sqrt{\frac{\hat{\lambda}+c}{\varepsilon}(x^2-\xi^2)}}. \quad (7.4.68)$$

We have

$$\begin{aligned}&\int_0^x \hat{k}_{\hat{\lambda}}(x, \xi) \hat{u}(\xi, y, z) d\xi = \\ &\int_0^x \left(\hat{k}_{\hat{\lambda}}(x, \xi) + \int_{\xi}^x \hat{k}_{\hat{\lambda}}(x, \sigma) \hat{l}(\sigma, \xi) d\sigma \right) \hat{w}(\xi, y, z) d\xi,\end{aligned}\quad (7.4.69)$$

and similarly for \hat{b}_1 . Computing the inner integrals with the help of [50] we get (7.4.61)–(7.4.65). \square

We should mention that while the target system (7.4.61)–(7.4.62) is complicated, only the proof is affected by this complexity and not the design (which is simple).

7.4.2 Boundedness

Let us denote the bounds on $|\hat{\mathbf{b}}|$, $\hat{\lambda}$ by b_0 , λ_0 . Since \hat{k} and \hat{l} and their derivatives with respect to parameters are bounded functions, we have the estimates

$$\|e_1\| \leq M_1 \|e\|, \quad \|\nabla u\| \leq M_2 \|\nabla \hat{w}\| + \|\nabla e\|, \quad (7.4.70)$$

where M_1 , M_2 are some constants. The functions φ_1 , φ_2 are also bounded, let us denote these bounds by $\bar{\varphi}_1$, $\bar{\varphi}_2$.

First we show the boundedness of the L_2 -norm, starting with

$$\begin{aligned}
\frac{1}{2} \frac{d}{dt} \|\hat{w}\|^2 &= -\varepsilon \|\nabla \hat{w}\|^2 - c \|\hat{w}\|^2 \\
&\quad + \dot{\hat{b}}_1 \int_{\Omega} \hat{w} \Phi_1 d\Omega + \dot{\hat{\lambda}} \int_{\Omega} \hat{w} \Phi_2 d\Omega \\
&\quad + (\hat{\lambda} + \gamma^2 \|\nabla u\|^2) \int_{\Omega} e_1 \hat{w} d\Omega.
\end{aligned} \tag{7.4.71}$$

Using the estimate

$$\begin{aligned}
\dot{\hat{b}}_1 \int_{\Omega} \hat{w} \Phi_1 d\Omega &\leq |\dot{\hat{b}}_1| \bar{\varphi}_1 \|\hat{w}\|^2 \\
&\leq \frac{\varepsilon}{8d_1^2} \|\hat{w}\|^2 + \frac{2}{\varepsilon} d_1^2 |\dot{\hat{b}}_1|^2 \bar{\varphi}_1^2 \|\hat{w}\|^2 \\
&\leq \frac{\varepsilon}{8} \|\nabla \hat{w}\|^2 + l_1 \|\hat{w}\|^2,
\end{aligned} \tag{7.4.72}$$

and similarly for the term with $\dot{\hat{\lambda}}$, we get

$$\begin{aligned}
\frac{1}{2} \frac{d}{dt} \|\hat{w}\|^2 &\leq -\frac{3\varepsilon}{4} \|\nabla \hat{w}\|^2 + l_1 \|\hat{w}\|^2 + M_1 \lambda_0 \|\hat{w}\| \|e\| \\
&\quad + \gamma^2 M_1 \|\nabla u\| (M_2 \|\nabla \hat{w}\| + \|\nabla e\|) \|\hat{w}\| \|e\| \\
&\leq -\frac{3\varepsilon}{4} \|\nabla \hat{w}\|^2 + l_1 \|\hat{w}\|^2 + \frac{d_1^2}{\varepsilon} M_1^2 \lambda_0^2 \|e\|^2 \\
&\quad + \frac{\varepsilon}{4d_1^2} \|\hat{w}\|^2 + \frac{\varepsilon}{4} \|\nabla \hat{w}\|^2 + \frac{\varepsilon}{4M_2^2} \|\nabla e\|^2 \\
&\quad + \frac{2}{\varepsilon} \gamma^4 M_1^2 M_2^2 \|\nabla u\|^2 \|e\|^2 \|\hat{w}\|^2 \\
&\leq -\frac{\varepsilon}{4} \|\nabla \hat{w}\|^2 + l_1 \|\hat{w}\|^2 + l_1.
\end{aligned} \tag{7.4.73}$$

Using Lemma 7.2 we get $\|\hat{w}\| \in \mathcal{L}_{\infty} \cap \mathcal{L}_2$. Integrating (7.4.73) with respect to time from zero to infinity we also get $\|\nabla \hat{w}\| \in \mathcal{L}_2$ and therefore $\|\nabla \hat{u}\|, \|\nabla u\| \in \mathcal{L}_2$.

Now let us show H_1 boundedness. In this case it is enough to consider e

and \hat{w} systems separately. First,

$$\begin{aligned}
\frac{1}{2} \frac{d}{dt} \|\nabla e\|^2 &= \int_{\Omega} \nabla e_t \nabla e \, d\Omega = - \int_{\Omega} e_t \Delta e \, d\Omega \\
&\leq -\varepsilon \|\Delta e\|^2 + b_0 \|\Delta e\| \|\nabla e\| + |\tilde{\mathbf{b}}| \|\Delta e\| \|\nabla u\| \\
&\quad + |\tilde{\lambda}| \|\Delta e\| \|u\| - \gamma^2 \|\nabla e\|^2 \|\nabla u\|^2 \\
&\leq -\varepsilon \|\Delta e\|^2 + \frac{\varepsilon}{4} \|\Delta e\|^2 + \frac{b_0^2}{\varepsilon} \|\nabla e\|^2 + \frac{\varepsilon}{4} \|\Delta e\|^2 \\
&\quad + \frac{|\tilde{\mathbf{b}}|^2}{\varepsilon} \|\nabla u\|^2 + \frac{\varepsilon}{4} \|\Delta e\|^2 + \frac{|\tilde{\lambda}|^2}{\varepsilon} \|u\|^2 \\
&\leq -\frac{\varepsilon}{4} \|\Delta e\|^2 + l_1.
\end{aligned} \tag{7.4.74}$$

Using Lemma 7.2 we get $\|\nabla e\| \in \mathcal{L}_{\infty} \cap \mathcal{L}_2$. Second,

$$\begin{aligned}
\frac{1}{2} \frac{d}{dt} \|\nabla \hat{w}\|^2 &= - \int_{\Omega} \hat{w}_t \Delta \hat{w} \, d\Omega \\
&= -\varepsilon \|\Delta \hat{w}\|^2 - c \|\nabla \hat{w}\|^2 - \int_{\Omega} \Delta \hat{w} (\hat{\mathbf{b}} \cdot \nabla \hat{w}) \, d\Omega \\
&\quad - \dot{b}_1 \int_{\Omega} \Delta \hat{w} \Phi_1 \, d\Omega - \dot{\lambda} \int_{\Omega} \Delta \hat{w} \Phi_2 \, d\Omega \\
&\quad + (\hat{\lambda} + \gamma^2 \|\nabla u\|^2) \int_{\Omega} e \Delta \hat{w} \, d\Omega.
\end{aligned} \tag{7.4.75}$$

Using the estimates

$$\begin{aligned}
\int_{\Omega} \Delta \hat{w} (\hat{\mathbf{b}} \cdot \nabla \hat{w}) \, d\Omega &\leq b_0 \|\Delta \hat{w}\| \|\nabla \hat{w}\| \\
&\leq \frac{\varepsilon}{8} \|\Delta \hat{w}\|^2 + \frac{2b_0^2}{\varepsilon} \|\nabla \hat{w}\|^2 \\
&\leq \frac{\varepsilon}{8} \|\Delta \hat{w}\|^2 + l_1, \\
\dot{b}_1 \int_{\Omega} \Delta \hat{w} \Phi_1 \, d\Omega &\leq \frac{\varepsilon}{8} \|\Delta \hat{w}\|^2 + l_1 \|\hat{w}\|^2,
\end{aligned} \tag{7.4.76}$$

and similarly for the term with $\dot{\hat{\lambda}}$, we get

$$\begin{aligned}
\frac{1}{2} \frac{d}{dt} \|\nabla \hat{w}\|^2 &\leq -\frac{5\varepsilon}{8} \|\Delta \hat{w}\|^2 + l_1 \|\hat{w}\|^2 + l_1 \\
&\quad + \gamma^2 M_1 M_2 \|\nabla u\| \|\nabla \hat{w}\| \|\Delta \hat{w}\| \|e\| \\
&\quad + \gamma^2 M_1 \|\nabla u\| \|\nabla e\| \|\Delta \hat{w}\| \|e\| \\
&\quad + M_1 \lambda_0 \|\Delta \hat{w}\| \|e\| \\
&\leq -\frac{5\varepsilon}{8} \|\Delta \hat{w}\|^2 + l_1 + \frac{\varepsilon \|\Delta \hat{w}\|^2}{4} + \frac{2M_1^2 \lambda_0^2 \|e\|^2}{\varepsilon} \\
&\quad + \frac{2}{\varepsilon} \gamma^4 M_1^2 M_2^2 \|\nabla u\|^2 \|e\|^2 \|\nabla \hat{w}\|^2 \\
&\quad + \frac{2}{\varepsilon} \gamma^4 M_1^2 \|\nabla u\|^2 \|\nabla e\|^2 \|e\|^2 + \frac{\varepsilon}{8} \|\Delta \hat{w}\|^2 \\
&\leq -\frac{\varepsilon}{4} \|\Delta \hat{w}\|^2 + l_1 \|\nabla \hat{w}\|^2 + l_1. \tag{7.4.77}
\end{aligned}$$

Using Lemma 7.2 we get $\|\nabla \hat{w}\| \in \mathcal{L}_\infty \cap \mathcal{L}_2$ and therefore $\|\nabla \hat{u}\|, \|\nabla u\| \in \mathcal{L}_\infty \cap \mathcal{L}_2$. Integrating (7.4.74), (7.4.77) we also get $\|\Delta e\|, \|\Delta \hat{w}\| \in \mathcal{L}_2$ and therefore $\|\Delta \hat{u}\|, \|\Delta u\| \in \mathcal{L}_2$.

Note that from the above properties and (7.4.74)–(7.4.77) it follows that $(d/dt)\|\nabla e\|^2$ and $(d/dt)\|\nabla \hat{w}\|^2$ are bounded. By Lemma 7.1 we get $\|\nabla e\|, \|\nabla \hat{w}\| \rightarrow 0$ and therefore $\|\nabla \hat{u}\|, \|\nabla u\| \rightarrow 0$ as $t \rightarrow \infty$.

In order to prove pointwise boundedness in 3D we need to show that the H_2 norms of the signals are bounded. It is more convenient to prove the boundedness of $\|\hat{w}_t\|$ and $\|e_t\|$ first and then use the equations (7.4.61), (7.3.45) to bound the H_2 norms. We start with

$$\begin{aligned}
\frac{1}{2} \frac{d}{dt} \|e_t\|^2 &= \int_{\Omega} e_t e_{tt} d\Omega \\
&\leq -\varepsilon \|\nabla e_t\|^2 + |\dot{\mathbf{b}}| \|e_t\| \|\nabla e\| \\
&\quad + |\dot{\mathbf{b}}| \|e_t\| \|\nabla u\| + |\tilde{\mathbf{b}}| \|\nabla e_t\| \|u_t\| \\
&\quad + |\dot{\hat{\lambda}}| \|e_t\| \|u\| + |\tilde{\hat{\lambda}}| \|e_t\| \|u_t\| \\
&\quad + \gamma^2 \|e\| \|e_t\| \left| \frac{d}{dt} \|\nabla u\|^2 \right|. \tag{7.4.78}
\end{aligned}$$

We first note that

$$\|u_t\|^2 \leq 2(\varepsilon^2 \|\Delta u\|^2 + |\mathbf{b}|^2 \|\nabla u\|^2 + \lambda^2 \|u\|^2) \leq l_1 \quad (7.4.79)$$

and

$$\begin{aligned} \|e\| \|e_t\| \left| \frac{d}{dt} \|\nabla u\|^2 \right| &\leq 2 \|e\| \|e_t\| \left| \frac{d}{dt} (M_2^2 \|\nabla \hat{w}\|^2 + \|\nabla e\|^2) \right| \\ &\leq 2 \|e\| \|e_t\| (M_2^2 \|\nabla \hat{w}\| \|\nabla \hat{w}_t\| + \|\nabla e\| \|\nabla e_t\|) \\ &\leq l_1 + \frac{\varepsilon}{8} \|\nabla e_t\|^2 + c_1 \|\nabla \hat{w}_t\|^2, \end{aligned} \quad (7.4.80)$$

where c_1 is an arbitrary constant. We have

$$\begin{aligned} \frac{1}{2} \frac{d}{dt} \|e_t\|^2 &\leq -\varepsilon \|\nabla e_t\|^2 + |\dot{\mathbf{b}}|^2 \|e_t\|^2 + \frac{1}{2} (\|\nabla e\|^2 + \|\nabla u\|^2) \\ &\quad + \frac{4}{\varepsilon} \|u_t\|^2 (|\tilde{\mathbf{b}}|^2 + d_1^2 |\tilde{\lambda}|^2) + \frac{\varepsilon}{8} \|\nabla e_t\|^2 \\ &\quad + \frac{\varepsilon}{8d_1^2} \|e_t\|^2 + \frac{1}{2} |\dot{\lambda}|^2 \|e_t\|^2 + \frac{1}{2} \|u\|^2 \\ &\quad + l_1 + \frac{\varepsilon}{4} \|\nabla e_t\|^2 + c_1 \|\nabla \hat{w}_t\|^2 \\ &\leq -\frac{\varepsilon}{2} \|\nabla e_t\|^2 + l_1 \|e_t\|^2 + c_1 \|\nabla \hat{w}_t\|^2 + l_1. \end{aligned} \quad (7.4.81)$$

Now we estimate the time derivative of $\|\hat{w}_t\|^2$.

$$\begin{aligned} \frac{1}{2} \frac{d}{dt} \|\hat{w}_t\|^2 &= \int_{\Omega} \hat{w}_t \hat{w}_{tt} d\Omega \\ &\leq -\varepsilon \|\nabla \hat{w}_t\|^2 + |\dot{\mathbf{b}}| \|\hat{w}_t\| \|\nabla \hat{w}\| - c \|\hat{w}_t\|^2 \\ &\quad + |\ddot{b}_1| \bar{\varphi}_1 \|\hat{w}_t\| \|\hat{w}\| + |\dot{b}_1| \|\hat{w}_t \dot{\Phi}_1\| \\ &\quad + |\ddot{\lambda}| \bar{\varphi}_2 \|\hat{w}_t\| \|\hat{w}\| + |\dot{\lambda}| \|\hat{w}_t \dot{\Phi}_2\| \\ &\quad + (\lambda_0 + \gamma^2 \|\nabla u\|^2) \|e_{1t}\| \|\hat{w}_t\| \\ &\quad + \left(|\dot{\lambda}| + \gamma^2 \left| \frac{d}{dt} \|\nabla u\|^2 \right| \right) \|e\| M_1 \|\hat{w}_t\|. \end{aligned} \quad (7.4.82)$$

Using the estimates

$$\begin{aligned}
\|\hat{w}_t \dot{\Phi}_1\|^2 &\leq \bar{\varphi}_1^2 \|\hat{w}_t\|^2 + M_3 \|\hat{w}_t\|^2 \|\hat{w}\|^2, \\
\|\hat{w}_t \dot{\Phi}_2\|^2 &\leq \bar{\varphi}_2^2 \|\hat{w}_t\|^2 + M_4 \|\hat{w}_t\|^2 \|\hat{w}\|^2, \\
|\ddot{b}_1|^2 &\leq 2\gamma_1^2 \|e_t\|^2 \|\nabla u\|^2 + 2\gamma_1^2 \|e\|^2 \|\nabla u_t\|^2 \\
&\leq l_1 \|e_t\|^2 + M_5 (\|\nabla \hat{w}_t\|^2 + \|\nabla e_t\|^2), \\
|\ddot{\lambda}|^2 &\leq 2\gamma_2^2 \|e_t\|^2 \|u\|^2 + 2\gamma_2^2 \|e\|^2 \|u_t\|^2 \\
&\leq l_1 \|e_t\|^2 + l_1, \\
\|e_{1t}\|^2 &\leq 2M_1^2 \|e_t\|^2 + M_6 \|e\|^2,
\end{aligned} \tag{7.4.83}$$

we get

$$\begin{aligned}
\frac{1}{2} \frac{d}{dt} \|\hat{w}_t\|^2 &\leq -\varepsilon \|\nabla \hat{w}_t\|^2 + \frac{1}{2} |\dot{\mathbf{b}}|^2 \|\hat{w}_t\|^2 + \frac{1}{2} \|\nabla \hat{w}\|^2 \\
&\quad + l_1 \|e_t\|^2 + c_2 (\|\nabla \hat{w}_t\|^2 + \|\nabla e_t\|^2) \\
&\quad + \frac{M_5 \bar{\varphi}_1^2}{4c_2} \|\hat{w}\|^2 \|\hat{w}_t\|^2 + \frac{2}{\varepsilon} d_1^2 \bar{\varphi}_1^2 |\dot{b}_1|^2 \\
&\quad + \frac{\varepsilon}{8d_1^2} \|\hat{w}_t\|^2 + l_1 \|\hat{w}_t\|^2 + l_1 \|e_t\|^2 + l_1 \\
&\quad + l_1 \|\hat{w}_t\|^2 + \frac{2}{\varepsilon} d_1^2 \bar{\varphi}_2^2 |\dot{\lambda}|^2 + \frac{\varepsilon}{8d_1^2} \|\hat{w}_t\|^2 \\
&\quad + l_1 \|\hat{w}_t\|^2 + \frac{4\lambda_0^2 M_1^2 d_1^2}{\varepsilon} \|e_t\|^2 + \frac{\varepsilon}{8d_1^2} \|\hat{w}_t\|^2 \\
&\quad + l_1 \|e_t\|^2 + l_1 \|\hat{w}_t\|^2 + \frac{\varepsilon}{8} \|\nabla \hat{w}_t\|^2 + c_3 \|\nabla e_t\|^2 \\
&\quad + l_1 \|\hat{w}_t\|^2 + l_1 \\
&\leq -\left(\frac{\varepsilon}{4} - c_2\right) \|\nabla \hat{w}_t\|^2 + (c_2 + c_3) \|\nabla e_t\|^2 + l_1 \\
&\quad + \frac{4\lambda_0^2 M_1^2 d_1^2}{\varepsilon} \|e_t\|^2 + l_1 \|\hat{w}_t\|^2 + l_1 \|e_t\|^2.
\end{aligned} \tag{7.4.84}$$

Combining (7.4.84) and (7.4.81) with a weighting constant A we get

$$\begin{aligned}
\frac{A}{2} \frac{d}{dt} \|e_t\|^2 + \frac{1}{2} \frac{d}{dt} \|\hat{w}_t\|^2 &\leq -\left(\frac{\varepsilon}{4} - c_2 - c_1 A\right) \|\nabla \hat{w}_t\|^2 \\
&\quad - \left(\frac{\varepsilon}{2} A - \frac{4\lambda_0^2 M_1^2 d_1^4}{\varepsilon} - c_2 - c_3\right) \|\nabla e_t\|^2 \\
&\quad + l_1 \|\hat{w}_t\|^2 + \|e_t\|^2 + l_1
\end{aligned} \tag{7.4.85}$$

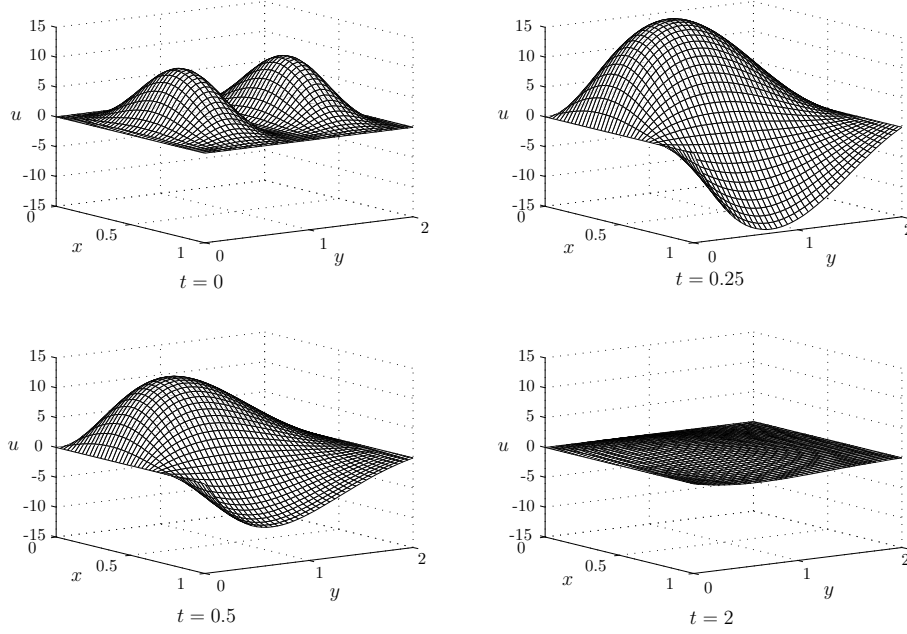


Figure 7.2: The closed loop state for the plant (7.5.88) at different times.

Choosing $A = 1 + 8\lambda_0^2 M_1^2 d_1^4 \varepsilon^{-2}$, $c_1 = \varepsilon/(16A)$, $c_2 = c_3 = \varepsilon/8$, we get

$$\begin{aligned} \frac{A}{2} \frac{d}{dt} \|e_t\|^2 + \frac{1}{2} \frac{d}{dt} \|\hat{w}_t\|^2 &\leq -\frac{\varepsilon}{16} \|\nabla \hat{w}_t\|^2 - \frac{\varepsilon}{4} \|\nabla e_t\|^2 \\ &\quad + l_1 \|\hat{w}_t\|^2 + \|e_t\|^2 + l_1. \end{aligned} \quad (7.4.86)$$

By Lemma 7.2 $\|\hat{w}_t\|, \|e_t\| \in \mathcal{L}_\infty \cap \mathcal{L}_2$ and therefore $\|\hat{u}_t\|, \|u_t\| \in \mathcal{L}_\infty \cap \mathcal{L}_2$. From (7.3.41) and (7.3.37) we get $\|\Delta \hat{u}\|, \|\Delta u\| \in \mathcal{L}_\infty \cap \mathcal{L}_2$. Using now Agmon's inequality (7.4.58) we get the regulation result:

$$\lim_{t \rightarrow \infty} \max_{(x,y,z) \in \Omega} |u(x, y, z, t)| \leq d_2 \lim_{t \rightarrow \infty} \|u\|_{H_1}^{1/2} \|u\|_{H_2}^{1/2} = 0. \quad (7.4.87)$$

7.5 Simulations

For the demonstration of our design we consider a 2D plant with four unknown parameters ε , b_1 , b_2 , and λ :

$$u_t = \varepsilon(u_{xx} + u_{yy}) + b_1 u_x + b_2 u_y + \lambda u \quad (7.5.88)$$

on the rectangle $0 \leq x \leq 1$, $0 \leq y \leq L$ with actuation applied on the side with $x = 1$ and Dirichlet boundary conditions on the other three sides. The adaptive

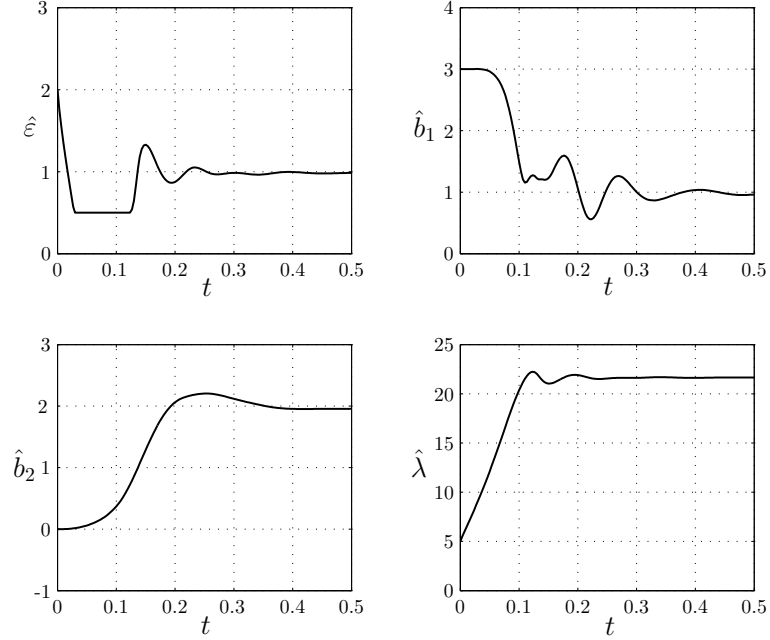


Figure 7.3: The parameter estimates for the plant (7.5.88) with adaptive controller based on passive identifier.

laws (7.3.49)–(7.3.51) are modified in a straightforward way from the 3D to the 2D setting. We set the simulation parameters to $\varepsilon = 1$, $b_1 = 1$, $b_2 = 2$, $\lambda = 22$, $L = 2$. With this choice the plant has two unstable eigenvalues at 8.4 and 1. Initial estimates are set to $\hat{\varepsilon}(0) = 2$, $\hat{b}_1(0) = 3$, $\hat{b}_2(0) = 0$, $\hat{\lambda}(0) = 5$ and the bound on $\hat{\varepsilon}$ from below is $\underline{\varepsilon} = 0.5$. The initial conditions for the plant and the observer are $u(x, y, 0) = 10 \sin^2(\pi x) \sin^2(\pi y)$ and $\hat{u}(x, y, 0) \equiv 0$. The results of the simulation are presented in Fig. 7.2 (several snapshots of the state) and Fig. 7.3 (estimates of the unknown parameters). One can see that projection keeps $\hat{\varepsilon} \geq \underline{\varepsilon} = 0.5$. All estimates come close to the true values at approximately $t = 0.5$ and after that the controller stabilizes the system.

This chapter is in part a reprint of the material as it appears in A. Smyshlyaev and M. Krstic, “Adaptive boundary control for unstable parabolic PDEs-Part II: Estimation-based designs,” accepted to *Automatica*, 2006.

The dissertation author was the primary author and the coauthor listed in this

publication directed the research which forms the basis for this chapter.

Chapter 8

Certainty Equivalence Adaptive Controllers with Swapping Identifiers

The swapping approach (often called simply the “gradient” method) is the most commonly used identification method in finite-dimensional adaptive control. In this chapter we report its first use in adaptive control for PDEs. Filters of the “regressor” and of the measured part of the plant are implemented to convert a dynamic parametrization of the problem (a parametrization that involves temporal derivatives) into a static one where standard gradient and least squares estimation techniques can be used. This method has a higher dynamic order than the passivity-based method because it uses “one-filter-per-unknown parameter” instead of just one filter. On the other hand the passivity-based approach does not allow standard gradient or least squares estimation.

8.1 Benchmark Plant

In this section we consider a simple plant to illustrate the main ideas of our approach in a tutorial way without the extensive notation that is needed in

higher dimension like 2D and 3D and with more than one physical parameter.

Consider a one-dimensional unstable heat equation

$$u_t(x, t) = u_{xx}(x, t) + \lambda u(x, t) \quad (8.1.1)$$

$$u(0, t) = 0 \quad (8.1.2)$$

$$u(1, t) = U(t), \quad (8.1.3)$$

with one unknown parameter λ . Our objective is to regulate the state of this system to zero from the boundary with Dirichlet actuation $U(t)$. For $U(t) = 0$ this system can have an arbitrarily large number of unstable eigenvalues.

The certainty equivalence controller is the same as in the previous chapter:

$$u(1) = - \int_0^1 \hat{\lambda} \xi \frac{I_1 \left(\sqrt{\hat{\lambda}(1 - \xi^2)} \right)}{\sqrt{\hat{\lambda}(1 - \xi^2)}} u(\xi) d\xi. \quad (8.1.4)$$

We employ two filters: the state filter

$$v_t = v_{xx} + u \quad (8.1.5)$$

$$v(0) = v(1) = 0 \quad (8.1.6)$$

and the input filter

$$\eta_t = \eta_{xx} \quad (8.1.7)$$

$$\eta(0) = 0 \quad (8.1.8)$$

$$\eta(1) = u(1). \quad (8.1.9)$$

The “estimation” error

$$e = u - \lambda v - \eta \quad (8.1.10)$$

is then exponentially stable:

$$e_t = e_{xx} \quad (8.1.11)$$

$$e(0) = 0 \quad (8.1.12)$$

$$e(1) = 0. \quad (8.1.13)$$

Using the static relationship (8.1.10) as a parametric model, we implement a “prediction error” as

$$\hat{e} = u - \hat{\lambda}v - \eta, \quad \hat{e} = e + \tilde{\lambda}v. \quad (8.1.14)$$

We choose the gradient update law with normalization

$$\dot{\hat{\lambda}} = \gamma \frac{\int_0^1 \hat{e}(x)v(x) dx}{1 + \|v\|^2}. \quad (8.1.15)$$

With a Lyapunov function

$$V = \frac{1}{2} \int_0^1 e^2 dx + \frac{1}{8\gamma} \tilde{\lambda}^2 \quad (8.1.16)$$

we get

$$\begin{aligned} \dot{V} &\leq - \int_0^1 e_x^2 dx - \frac{\int_0^1 \hat{e}^2(x) dx}{4(1 + \|v\|^2)} + \frac{\int_0^1 \hat{e}(x)e(x) dx}{4(1 + \|v\|^2)} \\ &\leq -\|e_x\|^2 - \frac{\|\hat{e}\|^2}{4(1 + \|v\|^2)} + \frac{\|e_x\| \|\hat{e}\|}{2\sqrt{1 + \|v\|^2}} \\ &\leq -\frac{1}{2}\|e_x\|^2 - \frac{1}{8} \frac{\|\hat{e}\|^2}{1 + \|v\|^2}. \end{aligned} \quad (8.1.17)$$

This gives the following properties

$$\frac{\|\hat{e}\|}{\sqrt{1 + \|v\|^2}} \in \mathcal{L}_2 \cap \mathcal{L}_\infty, \quad \tilde{\lambda} \in \mathcal{L}_\infty, \quad \dot{\hat{\lambda}} \in \mathcal{L}_2 \cap \mathcal{L}_\infty. \quad (8.1.18)$$

In contrast with the passive identifier, the normalization in the swapping identifier is employed in the update law. This makes $\dot{\hat{\lambda}}$ not only square integrable but also bounded.

We modify the transformation (7.2.4) in the following way for the case of unknown λ :

$$\hat{w}(x) = \hat{\lambda}v(x) + \eta(x) - \int_0^x \hat{k}(x, \xi)(\hat{\lambda}v(\xi) + \eta(\xi)) d\xi \quad (8.1.19)$$

with the same $\hat{k}(x, \xi)$ as in (7.2.20). Using (8.1.5)–(8.1.9) and the inverse transformation

$$\hat{\lambda}v(x) + \eta(x) = \hat{w}(x) + \int_0^x \hat{l}(x, \xi)\hat{w}(\xi) d\xi \quad (8.1.20)$$

$$\hat{l}(x, \xi) = -\hat{\lambda}\xi \frac{J_1 \left(\sqrt{\hat{\lambda}(x^2 - \xi^2)} \right)}{\sqrt{\hat{\lambda}(x^2 - \xi^2)}} \quad (8.1.21)$$

one can get the following PDE for \hat{w} :

$$\begin{aligned}\hat{w}_t &= \hat{w}_{xx} + \hat{\lambda} \left(\hat{e}(x) - \int_0^x \hat{k}(x, \xi) \hat{e}(\xi) d\xi \right) + \dot{\hat{\lambda}} v(x) \\ &\quad + \dot{\hat{\lambda}} \int_0^x \left(\frac{\xi}{2} \hat{w}(\xi) - \hat{k}(x, \xi) v(\xi) \right) d\xi\end{aligned}\tag{8.1.22}$$

$$\hat{w}(0) = \hat{w}(1) = 0.\tag{8.1.23}$$

In order to prove boundedness of all signals we rewrite the filter (8.1.5)–(8.1.6) as follows

$$v_t = v_{xx} + \hat{e} + \hat{w} + \int_0^x \hat{l}(x, \xi) \hat{w}(\xi) d\xi\tag{8.1.24}$$

$$v(0) = v(1) = 0.\tag{8.1.25}$$

We have now two interconnected systems for v and \hat{w} , (8.1.22)–(8.1.25), which are driven by the signals $\dot{\hat{\lambda}}$, $\hat{\lambda}$, and \hat{e} with properties (8.1.18). Note that the situation here is more complicated than in the passive design where we had to analyze only the \hat{w} -system (7.2.22)–(7.2.23). While the signal v feeds into \hat{w} -system (8.1.22)–(8.1.23) through a “convergent-to-zero” signal $\dot{\hat{\lambda}}$, the signal \hat{w} feeds into the v -system (8.1.24)–(8.1.25) through a bounded but possibly large gain \hat{l} . Therefore to prove the boundedness of $\|\hat{w}\|$ and $\|v\|$ we use a weighted Lyapunov function

$$W = A\|\hat{w}\|^2 + \|v\|^2,\tag{8.1.26}$$

where A is a large enough constant (for more details on how A is selected, see the more general case in Section 8.3.2). One can show then that

$$\dot{W} \leq -\frac{1}{4A}W + l_1W,\tag{8.1.27}$$

and with the help of Lemma 7.2 we get the boundedness of $\|\hat{w}\|$ and $\|v\|$. Using this result it can be shown that

$$\frac{d}{dt} (\|\hat{w}_x\|^2 + \|v_x\|^2) \leq -\|\hat{w}_{xx}\|^2 - \|v_{xx}\|^2 + l_1,\tag{8.1.28}$$

which proves that $\|\hat{w}_x\|$ and $\|v_x\|$ are bounded. From Agmon’s inequality we get that \hat{w} and v are bounded pointwise in x . Using Lemma 7.1 we get $\|\hat{w}\| \rightarrow 0$,

$\|v\| \rightarrow 0$ as $t \rightarrow \infty$. From (8.1.20) and (8.1.10) we get the pointwise boundedness of η and u and $\|u\| \rightarrow 0$. Finally, the pointwise regulation of u to zero follows from Agmon's inequality.

8.2 Reaction-Advection-Diffusion System

Let us consider now a swapping-based approach for the plant

$$u_t = \varepsilon u_{xx} + bu_x + \lambda u \quad (8.2.29)$$

$$u(0) = 0 \quad (8.2.30)$$

$$u(1) = U(t) \quad (8.2.31)$$

with three unknown parameters ε , b , λ . We restrict our attention to the 1D case here. The result can be readily extended to the 3D plant (7.3.37) in a similar fashion as in Section 7.3 for passive identifiers.

We need to employ four (the number of uncertain parameters plus one) filters. Let us first write the “estimation error” in the form

$$e = u - \varepsilon\psi - bp - \lambda v - \eta, \quad (8.2.32)$$

where v , p , ψ are filters for u , u_x , and u_{xx} , respectively,

$$v_t = \hat{\varepsilon}v_{xx} + \hat{b}v_x + u \quad (8.2.33)$$

$$v(0) = v(1) = 0, \quad (8.2.34)$$

$$p_t = \hat{\varepsilon}p_{xx} + \hat{b}p_x + u_x \quad (8.2.35)$$

$$p(0) = p(1) = 0, \quad (8.2.36)$$

$$\psi_t = \hat{\varepsilon}\psi_{xx} + \hat{b}\psi_x + u_{xx} \quad (8.2.37)$$

$$\psi(0) = \psi(1) = 0, \quad (8.2.38)$$

and η is the following filter:

$$\eta_t = \hat{\varepsilon}\eta_{xx} + \hat{b}\eta_x - \hat{b}u_x - \hat{\varepsilon}u_{xx} \quad (8.2.39)$$

$$\eta(0) = 0 \quad (8.2.40)$$

$$\eta(1) = u(1). \quad (8.2.41)$$

Note that in the case of known ε or b , the filter η is modified by dropping the corresponding terms $\hat{\varepsilon}u_{xx}$ or $\hat{b}u_x$ in (8.2.39), so that there is no need to measure u_{xx} or u_x .

With the filters (8.2.33)–(8.2.41) the estimation error (8.2.32) satisfies the following exponentially stable equation

$$e_t = \hat{\varepsilon}e_{xx} + \hat{b}e_x \quad (8.2.42)$$

$$e(0) = e(1) = 0 \quad (8.2.43)$$

We implement a "prediction error" as

$$\hat{e} = u - \hat{\varepsilon}\psi - \hat{b}p - \hat{\lambda}v - \eta, \quad (8.2.44)$$

which is related to the estimation error by

$$\hat{e} = e + \tilde{\varepsilon}\psi + \tilde{b}p + \tilde{\lambda}v. \quad (8.2.45)$$

One important difference with respect to the benchmark plant (8.1.1)–(8.1.3) is that the diffusion coefficient ε is now unknown and we must use projection to ensure $\hat{\varepsilon} > \underline{\varepsilon} > 0$ to keep parabolic character of the systems involved in the adaptive scheme. The projection operator is defined in (7.3.44).

We choose gradient update laws with normalization

$$\dot{\hat{\varepsilon}} = \gamma_1 \text{Proj}_{\underline{\varepsilon}} \left\{ \frac{\int_0^1 \hat{e}(x)\psi(x) dx}{1 + \|\psi\|^2 + \|p\|^2 + \|v\|^2} \right\} \quad (8.2.46)$$

$$\dot{\hat{b}} = \gamma_2 \frac{\int_0^1 \hat{e}(x)p(x) dx}{1 + \|\psi\|^2 + \|p\|^2 + \|v\|^2} \quad (8.2.47)$$

$$\dot{\hat{\lambda}} = \gamma_3 \frac{\int_0^1 \hat{e}(x)v(x) dx}{1 + \|\psi\|^2 + \|p\|^2 + \|v\|^2}, \quad (8.2.48)$$

where $\gamma_1, \gamma_2, \gamma_3 > 0$.

Lemma 8.1. *The update laws (8.2.46)–(8.2.48) guarantee the following properties*

$$\tilde{\varepsilon}, \tilde{b}, \tilde{\lambda} \in \mathcal{L}_\infty, \quad \dot{\tilde{\varepsilon}}, \dot{\tilde{b}}, \dot{\tilde{\lambda}} \in \mathcal{L}_2 \cap \mathcal{L}_\infty \quad (8.2.49)$$

$$\frac{\|\hat{e}\|}{\sqrt{1 + \|\psi\|^2 + \|p\|^2 + \|v\|^2}} \in \mathcal{L}_2 \cap \mathcal{L}_\infty. \quad (8.2.50)$$

Proof. With a Lyapunov function

$$V = \frac{1}{2} \int_0^1 e^2 dx + \frac{1}{8\gamma_1} \tilde{\varepsilon}^2 + \frac{1}{8\gamma_2} \tilde{b}^2 + \frac{1}{8\gamma_3} \tilde{\lambda}^2 \quad (8.2.51)$$

we get

$$\begin{aligned} \dot{V} &\leq - \int_0^1 e_x^2 dx - \frac{\int_0^1 \hat{e}(\tilde{\varepsilon}\psi + \tilde{b}p + \tilde{\lambda}v) dx}{4(1 + \|\psi\|^2 + \|p\|^2 + \|v\|^2)} \\ &\leq - \|e_x\|^2 - \frac{\int_0^1 \hat{e}^2(x) dx + \int_0^1 \hat{e}(x)e(x) dx}{4(1 + \|\psi\|^2 + \|p\|^2 + \|v\|^2)} \\ &\leq - \|e_x\|^2 - \frac{\|\hat{e}\|^2}{4(1 + \|\psi\|^2 + \|p\|^2 + \|v\|^2)} \\ &\quad + \frac{\|e_x\| \|\hat{e}\|}{2\sqrt{1 + \|\psi\|^2 + \|p\|^2 + \|v\|^2}} \\ &\leq - \frac{1}{2} \|e_x\|^2 - \frac{1}{8} \frac{\|\hat{e}\|^2}{1 + \|\psi\|^2 + \|p\|^2 + \|v\|^2} \end{aligned} \quad (8.2.52)$$

This gives

$$\frac{\|\hat{e}\|}{\sqrt{1 + \|\psi\|^2 + \|p\|^2 + \|v\|^2}} \in \mathcal{L}_2 \quad (8.2.53)$$

and the boundedness of $\tilde{\varepsilon}, \tilde{b}, \tilde{\lambda}$. From (8.2.45) we get

$$\frac{\|\hat{e}\|}{\sqrt{1 + \|\psi\|^2 + \|p\|^2 + \|v\|^2}} \in \mathcal{L}_\infty \quad (8.2.54)$$

and from the update laws (8.2.46)–(8.2.48) the boundedness and square integrability of $\dot{\tilde{\varepsilon}}, \dot{\tilde{b}},$ and $\dot{\tilde{\lambda}}$ follows. \square

We use the controller

$$\begin{aligned} u(1) &= - \int_0^1 \frac{\hat{\lambda} + c}{\hat{\varepsilon}} \xi e^{-\frac{\hat{b}(1-\xi)}{2\hat{\varepsilon}}} \frac{I_1 \left(\sqrt{\frac{\hat{\lambda}+c}{\hat{\varepsilon}}} (1 - \xi^2) \right)}{\sqrt{\frac{\hat{\lambda}+c}{\hat{\varepsilon}}} (1 - \xi^2)} \\ &\quad \times (\hat{\varepsilon}\psi(\xi) + \hat{b}p(\xi) + \hat{\lambda}v(\xi) + \eta(\xi)) d\xi \end{aligned} \quad (8.2.55)$$

with $c \geq 0$. The properties of the closed loop system with this control law will be established in the next section.

As in the case of passivity-based design, it is very hard to prove the closed-loop stability of the swapping-based scheme in the case of unknown ε . The reason for this is that while we have the properties (8.2.50) for $\|\hat{e}\|$, we cannot obtain any a-priori estimates for $\|\hat{e}_x\|$ which are needed in the proof for a plant with unknown ε . However, the update law (8.2.46) is successful in simulations, as shown in Section 8.4.

In the next section we are going to prove the following result for a plant with known ε .

Theorem 8.2. *Consider the plant (8.2.29), (8.2.30) with the controller (8.2.55). If the closed loop system that consists of (8.2.29)–(8.2.30), (8.2.55), the filters (8.2.33)–(8.2.35), (8.2.41) and update laws (8.2.47)–(8.2.48) has a classical solution $(\hat{b}, \hat{\lambda}, v, p, \eta, u)$, then for any $\hat{b}(0), \hat{\lambda}(0)$ and any initial conditions $v_0, p_0, \eta_0, u_0 \in L_2(0, 1)$, the signals $\hat{b}, \hat{\lambda}, v, p, \eta, u$ are bounded and u is regulated to zero for all $x \in [0, 1]$:*

$$\lim_{t \rightarrow \infty} \max_{x \in [0, 1]} |u(x, t)| = 0. \quad (8.2.56)$$

8.3 Proof of Theorem 8.2

8.3.1 Target system

We use the following transformation

$$\begin{aligned} \hat{w} &= \hat{b}p + \hat{\lambda}v + \eta \\ &\quad - \int_0^x \hat{k}(x, \xi) (\hat{b}p(\xi) + \hat{\lambda}v(\xi) + \eta(\xi)) d\xi, \end{aligned} \quad (8.3.57)$$

where $\hat{k}(x, \xi)$ differs from (7.4.60) only in \hat{b}_1 being replaced by \hat{b} :

$$\hat{k}(x, \xi) = -\frac{\hat{\lambda} + c}{\varepsilon} \xi e^{-\frac{\hat{b}(x-\xi)}{2\varepsilon}} \frac{I_1 \left(\sqrt{\frac{\hat{\lambda}+c}{\varepsilon}} (x^2 - \xi^2) \right)}{\sqrt{\frac{\hat{\lambda}+c}{\varepsilon}} (x^2 - \xi^2)}. \quad (8.3.58)$$

The inverse transformation is defined as

$$\hat{b}p + \hat{\lambda}v + \eta = \hat{w} + \int_0^x \hat{l}(x, \xi) \hat{w}(\xi) d\xi, \quad (8.3.59)$$

where the kernel $\hat{l}(x, \xi)$ is given by

$$\hat{l}(x, \xi) = -\frac{\hat{\lambda} + c}{\varepsilon} \xi e^{-\frac{\hat{b}(x-\xi)}{2\varepsilon}} \frac{J_1 \left(\sqrt{\frac{\hat{\lambda}+c}{\varepsilon}} (x^2 - \xi^2) \right)}{\sqrt{\frac{\hat{\lambda}+c}{\varepsilon}} (x^2 - \xi^2)}. \quad (8.3.60)$$

Lemma 8.3. *The transformation (8.3.57)–(8.3.58) produces the following target system*

$$\begin{aligned} \hat{w}_t &= \varepsilon \hat{w}_{xx} + \hat{b} \hat{w}_x - c \hat{w} + K[\dot{\hat{b}}p + \dot{\hat{\lambda}}v] \\ &\quad + \hat{\lambda} K[\hat{e}] + \int_0^x (\dot{\hat{b}}\varphi_1 + \dot{\hat{\lambda}}\varphi_2) \hat{w}(\xi) d\xi \end{aligned} \quad (8.3.61)$$

$$\hat{w}(0) = \hat{w}(1) = 0, \quad (8.3.62)$$

where

$$K[v] = v(x) - \int_0^x \hat{k}(x, \xi) v(\xi) d\xi \quad (8.3.63)$$

and

$$\begin{aligned} \varphi_1(x, \xi) &= \frac{x - \xi}{2\hat{e}} \hat{k}(x, \xi) + \frac{1}{2\varepsilon} \int_\xi^x (x - \sigma) \hat{k}(x, \sigma) \hat{l}(\sigma, \xi) d\sigma \\ \varphi_2(x, \xi) &= \frac{\xi}{2\hat{e}} e^{-\frac{\hat{b}}{2\varepsilon}(x-\xi)}. \end{aligned} \quad (8.3.64)$$

Proof. Substituting (8.3.57) into (8.2.29) we get

$$\begin{aligned} \hat{w}_t &= \varepsilon \hat{w}_{xx} + \hat{b} \hat{w}_x - c \hat{w} + K[\dot{\hat{b}}p + \dot{\hat{\lambda}}v] + \hat{\lambda} K[\hat{e}] \\ &\quad - \int_0^x (\dot{\hat{b}} \hat{k}_{\hat{b}}(x, \xi) + \dot{\hat{\lambda}} \hat{k}_{\hat{\lambda}}(x, \xi)) (\hat{b}p + \hat{\lambda}v + \eta) d\xi. \end{aligned} \quad (8.3.65)$$

Using the inverse transformation (8.3.59) we replace $(\hat{b}p + \hat{\lambda}v + \eta)$ in (8.3.65) by \hat{w} . Changing the order of the integration and computing the inner integral we get (8.3.61). \square

We point out that, similarly to the case of the passive identifier design, the target system (8.3.61)–(8.3.62) is complex while the design itself is simple.

8.3.2 Boundedness

Let us use (8.2.44) and (8.3.59) to write the state u in filters (8.2.33)–(8.2.36) as

$$u = \hat{e} + \hat{w} + \int_0^x \hat{l}(x, \xi) \hat{w}(\xi) d\xi. \quad (8.3.66)$$

We have now three interconnected systems for \hat{w} , v , and p with external driving signals \hat{e} , $\dot{\hat{b}}$, $\dot{\hat{\lambda}}$ which go to zero in some sense due to the identifier properties (8.2.49)–(8.2.50).

The identifier properties imply that \hat{k} and \hat{l} are bounded and thus φ_1 , φ_2 are bounded. We denote these bounds by $\bar{\varphi}_1$, $\bar{\varphi}_2$. The bounds on \hat{b} , $\hat{\lambda}$ are denoted by b_0 , λ_0 , respectively.

We have the following estimates

$$\int_0^1 \hat{w}(x) \int_0^x \varphi_i(x, \xi) \hat{w}(\xi) d\xi dx \leq \bar{\varphi}_i \|\hat{w}\|^2, \quad (8.3.67)$$

$$\int_0^1 \hat{w}(x) K[\hat{e}] dx \leq M_1 \|\hat{w}\| \|\hat{e}\| \quad (8.3.68)$$

$$\|u\| \leq \|\hat{e}\| + M_2 \|\hat{w}\|, \quad (8.3.69)$$

where M_1 and M_2 are some constants that depend on the bounds b_0 and λ_0 .

We are now going to perform an L_2 Lyapunov analysis of the (\hat{w}, v, p) system. We start with

$$\begin{aligned} \frac{1}{2} \frac{d}{dt} \|\hat{w}\|^2 &\leq -\varepsilon \|\hat{w}_x\|^2 + \lambda_0 M_1 \|\hat{w}\| \|\hat{e}\| \\ &\quad + M_1 \|\hat{w}\| \left(|\dot{\hat{b}}| \|p\| + |\dot{\hat{\lambda}}| \|v\| \right) \\ &\quad + \left(|\dot{\hat{b}}| \bar{\varphi}_1 + |\dot{\hat{\lambda}}| \bar{\varphi}_2 \right) \|\hat{w}\|^2 \\ &\leq -\varepsilon \|\hat{w}_x\|^2 + \frac{\varepsilon}{16} \|\hat{w}\|^2 + \frac{4\lambda_0^2 M_1^2}{\varepsilon} \|\hat{e}\|^2 \\ &\quad + c_1 (\|p\|^2 + \|v\|^2) \\ &\quad + \frac{M_1^2}{4c_1} \left(|\dot{\hat{b}}|^2 + |\dot{\hat{\lambda}}|^2 \right) \|\hat{w}\|^2 + \frac{\varepsilon}{16} \|\hat{w}\|^2 \\ &\quad + \frac{8}{\varepsilon} \left(|\dot{\hat{b}}|^2 \bar{\varphi}_1^2 + |\dot{\hat{\lambda}}|^2 \bar{\varphi}_2^2 \right) \|\hat{w}\|^2. \end{aligned} \quad (8.3.70)$$

Here by c_1 we denoted an arbitrary constant that will be defined later. Note that in the estimates we do not use the gain $c \geq 0$ to help stabilize the system.

Using properties (8.2.50) we have

$$\|\hat{e}\|^2 \leq l_1 \|p\|^2 + l_1 \|v\|^2 + l_1 \quad (8.3.71)$$

so (8.3.70) can be written as

$$\begin{aligned} \frac{1}{2} \frac{d}{dt} \|\hat{w}\|^2 &\leq -\frac{\varepsilon}{2} \|\hat{w}_x\|^2 + c_1 (\|p\|^2 + \|v\|^2) \\ &\quad + l_1 (\|\hat{w}\|^2 + \|p\|^2 + \|v\|^2) + l_1. \end{aligned} \quad (8.3.72)$$

We do a Lyapunov analysis for the filter v now:

$$\frac{1}{2} \frac{d}{dt} \|v\|^2 \leq -\varepsilon \|v_x\|^2 + \int_0^1 v u \, dx \quad (8.3.73)$$

Using (8.3.66) we have the estimate

$$\begin{aligned} \int_0^1 v u \, dx &\leq M_2 \|v\| \|\hat{w}\| + \|v\| \|\hat{e}\| \\ &\leq \frac{\varepsilon}{16} \|v\|^2 + \frac{4M_2^2}{\varepsilon} \|\hat{w}\|^2 + \frac{\varepsilon}{16} \|v\|^2 \\ &\quad + l_1 \|p\|^2 + l_1 \|v\|^2 + l_1 \end{aligned} \quad (8.3.74)$$

With this estimate (8.3.73) becomes

$$\begin{aligned} \frac{1}{2} \frac{d}{dt} \|v\|^2 &\leq -\frac{\varepsilon}{2} \|v_x\|^2 + \frac{4M_2^2}{\varepsilon} \|\hat{w}\|^2 \\ &\quad + l_1 \|p\|^2 + l_1 \|v\|^2 + l_1. \end{aligned} \quad (8.3.75)$$

The last system to analyze is the filter p :

$$\begin{aligned} \frac{1}{2} \frac{d}{dt} \|p\|^2 &\leq -\varepsilon \|p_x\|^2 + \int_0^1 p u_x \, dx \\ &\leq -\varepsilon \|p_x\|^2 + M_2 \|p_x\| \|\hat{w}\| + \|p_x\| \|\hat{e}\| \\ &\leq -\varepsilon \|p_x\|^2 + \frac{\varepsilon}{2} \|p_x\|^2 + \frac{M_2^2}{\varepsilon} \|\hat{w}\|^2 + \frac{1}{\varepsilon} \|\hat{e}\|^2 \\ &\leq -\frac{\varepsilon}{2} \|p_x\|^2 + \frac{M_2^2}{\varepsilon} \|\hat{w}\|^2 \\ &\quad + l_1 \|p\|^2 + l_1 \|v\|^2 + l_1. \end{aligned} \quad (8.3.76)$$

With a composite Lyapunov function

$$V = \frac{A}{2}\|\hat{w}\|^2 + \frac{1}{2}\|v\|^2 + \frac{1}{2}\|p\|^2, \quad (8.3.77)$$

where A is a constant yet to be defined, we get

$$\begin{aligned} \dot{V} \leq & -\left(\frac{\varepsilon}{2}A - \frac{20M_2^2}{\varepsilon}\right)\|\hat{w}_x\|^2 \\ & -\left(\frac{\varepsilon}{2} - 4c_1A\right)(\|v_x\|^2 + \|p_x\|^2) + l_1V. \end{aligned} \quad (8.3.78)$$

Choosing $A = 1 + 40M_2^2\varepsilon^{-2}$ and $c_1 = \varepsilon/(16A)$ we get

$$\dot{V} \leq -\frac{\varepsilon}{4A}V + l_1V. \quad (8.3.79)$$

Using Lemma 7.2 we get $V \in \mathcal{L}_\infty \cap \mathcal{L}_1$. Note that V depends on A , which depends on M_2 , which depends on b_0 and λ_0 , which in turn depend on the initial conditions of the system. However, $A \geq 1$, which implies that $\|\hat{w}\|^2, \|v\|^2, \|p\|^2 \leq 2V$, and hence $\|\hat{w}\|, \|v\|, \|p\| \in \mathcal{L}_\infty \cap \mathcal{L}_2$. Integrating (8.3.78) we also get $\|\hat{w}_x\|, \|v_x\|, \|p_x\| \in \mathcal{L}_2$.

We proceed now to H_1 analysis (it is needed to establish pointwise boundedness). We start with

$$\begin{aligned} \frac{1}{2}\frac{d}{dt}\|\hat{w}_x\|^2 &= \int_0^1 \hat{w}_x \hat{w}_{xt} dx = -\int_0^1 \hat{w}_{xx} \hat{w} dx \\ &\leq -\varepsilon\|\hat{w}_{xx}\|^2 + b_0\|\hat{w}_x\|\|\hat{w}_{xx}\| \\ &\quad + \lambda_0 M_1\|\hat{w}_{xx}\|\|\hat{e}\| \\ &\quad + M_1\|\hat{w}_{xx}\|\left(|\dot{b}|\|p\| + |\dot{\lambda}|\|v\|\right) \\ &\quad + \left(|\dot{b}|\bar{\varphi}_1 + |\dot{\lambda}|\bar{\varphi}_2\right)\|\hat{w}_{xx}\|\|\hat{w}\| \\ &\leq -\varepsilon\|\hat{w}_{xx}\|^2 + \frac{\varepsilon}{8}\|\hat{w}_{xx}\|^2 + \frac{2b_0^2}{\varepsilon}\|\hat{w}_x\|^2 \\ &\quad + \frac{\varepsilon}{8}\|\hat{w}_{xx}\|^2 + \frac{2\lambda_0^2 M_1^2}{\varepsilon}\|\hat{e}\|^2 \\ &\quad + \frac{\varepsilon}{8}\|\hat{w}_{xx}\|^2 + \frac{4M_1^2}{\varepsilon}\left(|\dot{b}|^2\|p\|^2 + |\dot{\lambda}|^2\|v\|^2\right) \\ &\quad + \frac{\varepsilon}{8}\|\hat{w}_{xx}\|^2 + \frac{4}{\varepsilon}\left(|\dot{b}|^2\bar{\varphi}_1^2 + |\dot{\lambda}|^2\bar{\varphi}_2^2\right)\|\hat{w}\|^2 \\ &\leq -\frac{\varepsilon}{2}\|\hat{w}_{xx}\|^2 + l_1 \end{aligned} \quad (8.3.80)$$

By Lemma 7.2 we get $\|\hat{w}_x\| \in \mathcal{L}_\infty \cap \mathcal{L}_2$. For the filter v we have

$$\begin{aligned} \frac{1}{2} \frac{d}{dt} \|v_x\|^2 &\leq -\varepsilon \|v_{xx}\|^2 + b_0 \|v_x\| \|v_{xx}\| + \|v_{xx}\| \|u\| \\ &\leq -\varepsilon \|v_{xx}\|^2 + \frac{\varepsilon}{2} \|v_{xx}\|^2 + \frac{b_0^2}{\varepsilon} \|v_x\|^2 + \frac{1}{\varepsilon} \|u\|^2 \\ &\leq -\frac{\varepsilon}{2} \|v_{xx}\|^2 + l_1. \end{aligned} \quad (8.3.81)$$

By Lemma 7.2 we get $\|v_x\| \in \mathcal{L}_\infty \cap \mathcal{L}_2$. For the filter p we have

$$\begin{aligned} \frac{1}{2} \frac{d}{dt} \|p_x\|^2 &\leq -\varepsilon \|p_{xx}\|^2 + b_0 \|p_x\| \|p_{xx}\| + \|p_{xx}\| \|u_x\| \\ &\leq -\frac{\varepsilon}{2} \|p_{xx}\|^2 + \frac{b_0^2}{\varepsilon} \|p_x\|^2 + \frac{1}{\varepsilon} \|u_x\|^2. \end{aligned} \quad (8.3.82)$$

Since

$$\begin{aligned} \|u_x\|^2 &\leq 2\|\hat{e}_x\|^2 + 2M_3\|\hat{w}_x\|^2 \\ &\leq 4\|e_x\|^2 + 4|\tilde{b}|^2\|p_x\|^2 + 4|\tilde{\lambda}|^2\|v_x\|^2 \leq l_1, \end{aligned} \quad (8.3.83)$$

we get

$$\frac{1}{2} \frac{d}{dt} \|p_x\|^2 \leq -\frac{\varepsilon}{2} \|p_{xx}\|^2 + l_1, \quad (8.3.84)$$

and by Lemma 7.2 $\|p_x\| \in \mathcal{L}_\infty \cap \mathcal{L}_2$.

By Agmon's inequality we get the pointwise boundedness of signals \hat{w} , v , and p . From (8.3.59) we get the boundedness of η . Since $u = e + bp + \lambda v + \eta$, the state u is also bounded.

In order to prove regulation we notice from (8.3.79) that

$$|\dot{V}| \leq \frac{\varepsilon}{4A} |V| + l_1 V < \infty, \quad (8.3.85)$$

where we used the fact that l_1 is a bounded function in this case. By Lemma 7.1 we get $V \rightarrow 0$ and thus \hat{w} , v , $p \rightarrow 0$. From (8.3.59) we get $\eta \rightarrow 0$ and therefore (8.2.32) implies $u \rightarrow 0$ as $t \rightarrow \infty$. Using the boundedness of $\|u_x\|$ by Agmon's inequality we get

$$\lim_{t \rightarrow \infty} \max_{x \in [0,1]} |u(x,t)| \leq \lim_{t \rightarrow \infty} 2\|u\|^{1/2} \|u_x\|^{1/2} = 0. \quad (8.3.86)$$

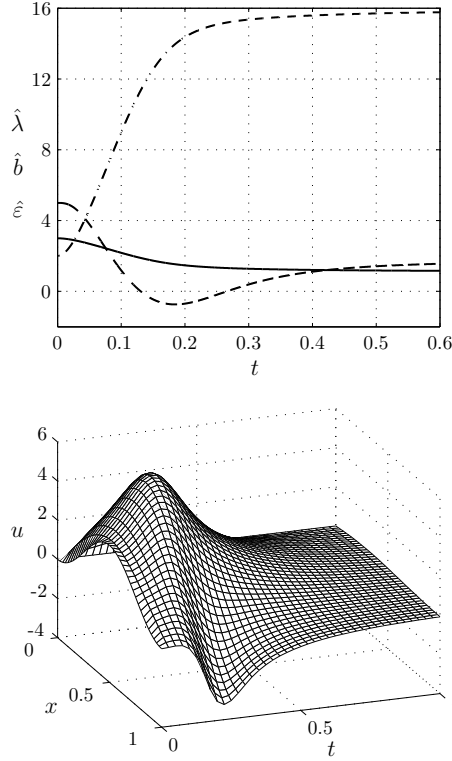


Figure 8.1: The parameter estimates and the closed loop state for the plant (8.2.29)–(8.2.31) with adaptive controller based on swapping identifier (solid — $\hat{\varepsilon}$, dashed — \hat{b} , dash-dotted — $\hat{\lambda}$).

8.4 Simulations

We demonstrate the design on a 1D plant (8.2.29)–(8.2.31) with parameters $\varepsilon = 1$, $b = 2$, $\lambda = 15$. The plant has one unstable eigenvalue at 4.1. Initial estimates are set to $\hat{\varepsilon}(0) = 3$, $\hat{b}(0) = 5$, $\hat{\lambda}(0) = 2$. The results of the simulation are presented in Fig. 8.1. Even though only the identifier properties (and not the closed-loop stabilization result) were proved in the case of an unknown diffusion coefficient, the adaptive controller successfully stabilizes the system. As expected for an adaptive regulation problem, the parameter estimates converge close to, but not exactly to the true parameter values.

Chapter 9

Closed Form Output Feedback Adaptive Controllers

9.1 Introduction

In a previous chapter we introduced a novel approach to *adaptive* control of PDEs where a parametrized family of boundary controllers can be combined with “swapping gradient” identifiers to yield global stability of the resulting non-linear PDE system. Only the *state*-feedback problem was considered before. For a different, narrower, class of systems, the *output*-feedback problem is solvable by this method, which is illustrated on two benchmark examples in this paper.

We consider two parametrically uncertain, *unstable* parabolic PDE plants controlled from the *boundary*. While these benchmark plants are simple in appearance, there does not exist an adaptive control design in the literature that is applicable to them due to the fact that they have infinite relative degree. Infinite relative degree arises in applications where actuators and sensors are on the “opposite sides” of the PDE domains. The two benchmark problems in this paper are motivated by a model of thermal instability in solid propellant rockets [10]. Our control laws are adaptive versions of the explicit boundary control laws developed in Chapter 3. Our adaptive observers are infinite dimensional extensions of

Kreisselmeier observers [36]. Our identifiers are designed using the swapping approach [36], prevalent in adaptive control of finite dimensional systems of relative degree higher than one. These identifiers remove the need for parameter projection and low adaptation gain present in Lyapunov output-feedback designs in [38].

Although for the sake of clarity we consider two separate benchmark problems, it is possible to design an adaptive controller for a combined problem (Section 9.6). Another reason for a separate consideration is a slightly weaker result for the benchmark plant with the unknown parameter in the boundary condition, due to an inherent difficulty observed in [8, 43].

9.2 Benchmark Plant with Unknown Parameter in the Domain

Consider the following plant

$$u_t(x, t) = u_{xx}(x, t) + gu(0, t), \quad (9.2.1)$$

$$u_x(0, t) = 0, \quad (9.2.2)$$

$$u(1, t) = U(t), \quad (9.2.3)$$

where $U(t)$ is a control signal. This system is inspired by a model of thermal instability in solid propellant rockets [10]. For $U(t) = 0$ this system is unstable if and only if $g > 2$. The plant can be written in the frequency domain as a transfer function from input $u(1)$ to output $u(0)$:

$$u(0, s) = \frac{s}{(s - g) \cosh \sqrt{s + g}} u(1, s). \quad (9.2.4)$$

We can see that it has no zeros (at $s = 0$ the transfer function is $2/(2 - g)$) and has infinitely many poles, one of which is unstable and approximately equal to g as $g \rightarrow +\infty$. So this is an infinite relative degree system.

The following transformation has been proposed in Chapter 3 for the case of known g :

$$w(x, t) = u(x, t) + \int_0^x \sqrt{g} \sinh \sqrt{g}(x - \xi) u(\xi, t) d\xi, \quad (9.2.5)$$

which maps (9.2.1)–(9.2.2) into an exponentially stable system

$$w_t(x, t) = w_{xx}(x, t), \quad (9.2.6)$$

$$w_x(0, t) = 0, \quad (9.2.7)$$

$$w(1, t) = 0. \quad (9.2.8)$$

A stabilizing control law is given by (9.2.5) evaluated at $x = 1$:

$$u(1, t) = - \int_0^1 \sqrt{g} \sinh \sqrt{g}(1 - \xi) u(\xi, t) d\xi. \quad (9.2.9)$$

Suppose now that we want to stabilize this system when g is unknown.

Our main result for this problem is summarized in the following theorem.

Theorem 9.1. *Consider the system (9.2.1)–(9.2.2) with the control*

$$u(1, t) = \int_0^1 k(1, \xi, \hat{g})(\hat{g}v(\xi, t) + \eta(\xi, t)) d\xi, \quad (9.2.10)$$

$$k(x, \xi, \hat{g}) = \begin{cases} -\sqrt{\hat{g}} \sinh \sqrt{\hat{g}}(x - \xi), & \hat{g} \geq 0, \\ \sqrt{-\hat{g}} \sin \sqrt{-\hat{g}}(x - \xi), & \hat{g} < 0, \end{cases} \quad (9.2.11)$$

where an update law for \hat{g} is

$$\dot{\hat{g}} = \gamma \frac{(u(0, t) - \hat{g}v(0, t) - \eta(0, t))v(0, t)}{1 + v^2(0, t)}, \quad (9.2.12)$$

and the filters $v(x, t)$, $\eta(x, t)$ are defined as

$$v_t(x, t) = v_{xx}(x, t) + u(0, t), \quad (9.2.13)$$

$$v_x(0, t) = 0, \quad (9.2.14)$$

$$v(1, t) = 0, \quad (9.2.15)$$

$$\eta_t(x, t) = \eta_{xx}(x, t), \quad (9.2.16)$$

$$\eta_x(0, t) = 0, \quad (9.2.17)$$

$$\eta(1, t) = u(1, t). \quad (9.2.18)$$

If the closed loop system (9.2.1)–(9.2.2), (9.2.10)–(9.2.18) has a classical solution (u, \hat{g}, v, η) , then for any $\hat{g}(0)$ and any initial conditions $u_0, v_0, \eta_0 \in L_2(0, 1)$, the signals \hat{g}, u, v, η are bounded and u is regulated to zero for all $x \in [0, 1]$:

$$\lim_{t \rightarrow \infty} \max_{x \in [0, 1]} |u(x, t)| = 0. \quad (9.2.19)$$

□

Although it may not be immediately obvious from (9.2.11), the control law (9.2.10)–(9.2.11) is a smooth function of \hat{g} . Note that a-priori knowledge of a bound on \hat{g} is not required in the swapping scheme (9.2.10)–(9.2.18) (as opposed to Lyapunov adaptive design in [38]).

9.3 Proof of Theorem 9.1

9.3.1 Target system

Introducing the error $e = u - gv - \eta$ we get an exponentially stable system

$$e_t(x, t) = e_{xx}(x, t), \quad (9.3.20)$$

$$e_x(0, t) = 0, \quad (9.3.21)$$

$$e(1, t) = 0. \quad (9.3.22)$$

The estimate $\hat{e} = u - \hat{g}v - \eta$ satisfies the following PDE

$$\hat{e}_t(x, t) = \hat{e}_{xx}(x, t) + \tilde{g}u(0, t) - \dot{\hat{g}}v(x, t), \quad (9.3.23)$$

$$\hat{e}_x(0, t) = 0, \quad (9.3.24)$$

$$\hat{e}(1, t) = 0. \quad (9.3.25)$$

The signal \hat{e} can be expressed through e as $\hat{e} = e + \tilde{g}v$.

The transformation

$$\begin{aligned} \hat{w}(x, t) &= \hat{g}v(x, t) + \eta(x, t) \\ &\quad - \int_0^x k(x, \xi, \hat{g})(\hat{g}v(\xi, t) + \eta(\xi, t)) d\xi \end{aligned} \quad (9.3.26)$$

with $k(x, \xi, \hat{g})$ given by (9.2.11) maps (9.2.13)–(9.2.18) into the following system

(Lemma 9.3):

$$\begin{aligned} \hat{w}_t(x, t) &= \hat{w}_{xx}(x, t) + \beta(x)\hat{e}(0, t) + \dot{\hat{g}}v \\ &\quad + \dot{\hat{g}} \int_0^x \alpha(x - \xi) (\hat{g}v(\xi, t) + \hat{w}(\xi, t)) d\xi, \end{aligned} \quad (9.3.27)$$

$$\hat{w}_x(0, t) = 0, \quad (9.3.28)$$

$$\hat{w}(1, t) = 0, \quad (9.3.29)$$

where

$$\alpha(x) = -\frac{1}{\hat{g}}k(x, 0, \hat{g}), \quad (9.3.30)$$

$$\beta(x) = k_\xi(x, 0, \hat{g}) = \begin{cases} \hat{g} \cosh \sqrt{\hat{g}}x, & \hat{g} \geq 0, \\ \hat{g} \cos \sqrt{-\hat{g}}x, & \hat{g} < 0, \end{cases} \quad (9.3.31)$$

9.3.2 Adaptive law

We take the following equation as a parametric model

$$e(0, t) = u(0, t) - gv(0, t) - \eta(0, t). \quad (9.3.32)$$

The estimation error is

$$\hat{e}(0, t) = u(0, t) - \hat{g}v(0, t) - \eta(0, t). \quad (9.3.33)$$

We use the gradient update law

$$\dot{\hat{g}} = \gamma \frac{\hat{e}(0, t)v(0, t)}{1 + v^2(0, t)}. \quad (9.3.34)$$

Lemma 9.2. *The adaptive law (9.3.34) guarantees the following properties:*

$$\frac{\hat{e}(0, t)}{\sqrt{1 + v^2(0, t)}} \in \mathcal{L}_2 \cap \mathcal{L}_\infty, \quad \tilde{g} \in \mathcal{L}_\infty, \quad \dot{\hat{g}} \in \mathcal{L}_2 \cap \mathcal{L}_\infty. \quad (9.3.35)$$

Proof. Using a Lyapunov function

$$V = \frac{1}{2} \int_0^1 e^2 dx + \frac{1}{2\gamma} \tilde{g}^2 \quad (9.3.36)$$

we get

$$\begin{aligned}
\dot{V} &= - \int_0^1 e_x^2 dx - \frac{\tilde{g}\hat{e}(0)v(0)}{1+v^2(0)} \\
&\leq - \int_0^1 e_x^2 dx - \frac{\hat{e}^2(0)}{1+v^2(0)} + \frac{e(0)\hat{e}(0)}{1+v^2(0)} \\
&\leq - \|e_x\|^2 - \frac{\hat{e}^2(0)}{1+v^2(0)} + \frac{\|e_x\||\hat{e}(0)|}{\sqrt{1+v^2(0)}} \\
&\leq - \frac{1}{2}\|e_x\|^2 - \frac{1}{2} \frac{\hat{e}^2(0)}{1+v^2(0)}
\end{aligned} \tag{9.3.37}$$

This gives the following properties

$$\frac{\hat{e}(0,t)}{\sqrt{1+v^2(0,t)}} \in \mathcal{L}_2, \quad \tilde{g} \in \mathcal{L}_\infty. \tag{9.3.38}$$

Since

$$\frac{\hat{e}(0,t)}{\sqrt{1+v^2(0,t)}} = \frac{e(0,t)}{\sqrt{1+v^2(0,t)}} + \tilde{g} \frac{v(0,t)}{\sqrt{1+v^2(0,t)}}, \tag{9.3.39}$$

$$\dot{\hat{g}} = \gamma \frac{\hat{e}(0,t)}{\sqrt{1+v^2(0,t)}} \frac{v(0,t)}{\sqrt{1+v^2(0,t)}}, \tag{9.3.40}$$

we get (9.3.35). \square

The explicit bound on \hat{g} in terms of initial conditions of all the signals can be obtained from (9.3.37):

$$\begin{aligned}
\hat{g}^2(t) &\leq 2g^2 + 2 \left(\tilde{g}(0)^2 + \gamma \int_0^1 e^2(x,0) dx \right) \\
&\leq 2g^2 + 2(g - \hat{g}(0))^2 \\
&\quad + 2\gamma \int_0^1 (u(x,0) - gv(x,0) - \eta(x,0))^2 dx.
\end{aligned} \tag{9.3.41}$$

We denote the bound on \hat{g} by g_0 . The above properties imply that functions α and β are bounded, let us denote these bounds by α_0 and β_0 .

9.3.3 Boundedness

The filter v can be rewritten in the following way

$$v_t(x,t) = v_{xx}(x,t) + \hat{w}(0,t) + \hat{e}(0,t), \tag{9.3.42}$$

$$v_x(0,t) = 0, \tag{9.3.43}$$

$$v(1,t) = 0. \tag{9.3.44}$$

We have two interconnected systems \hat{w} , v driven by a signal $\hat{e}(0, t)$ with properties (9.3.35). Consider a Lyapunov function

$$V_v = \frac{1}{2} \int_0^1 v^2(x) dx + \frac{1}{2} \int_0^1 v_x^2(x) dx. \quad (9.3.45)$$

We include the H_1 norm in the Lyapunov function because the signal $\hat{e}(0)$ is normalized by $1 + v^2(0)$ and $v^2(0)$ can only be bounded by $\|v_x\|^2$. Using Young's, Poincare's, and Agmon's inequalities we have¹

$$\begin{aligned} \dot{V}_v &= - \int_0^1 v_x^2 dx + (\hat{w}(0) + \hat{e}(0)) \int_0^1 v dx \\ &\quad - \int_0^1 v_{xx}^2 dx - (\hat{w}(0) + \hat{e}(0)) \int_0^1 v_{xx} dx \\ &\leq -\|v_x\|^2 + \frac{1}{8}\|v\|^2 + 4 \frac{\hat{e}^2(0)}{1 + v^2(0)} (1 + \|v_x\|^2) \\ &\quad + 4\|\hat{w}_x\|^2 - \|v_{xx}\|^2 + \frac{1}{2}\|v_{xx}\|^2 + \|\hat{w}_x\|^2 \\ &\quad + \frac{\hat{e}^2(0)}{1 + v^2(0)} (1 + \|v_x\|^2) \\ &\leq -\frac{1}{2}\|v_x\|^2 - \frac{1}{2}\|v_{xx}\|^2 + 5\|\hat{w}_x\|^2 + l_1\|v_x\|^2 + l_1, \end{aligned} \quad (9.3.46)$$

where l_1 is a generic function of time in $\mathcal{L}_1 \cap \mathcal{L}_\infty$. Using the following Lyapunov function for the \hat{w} -system,

$$V_{\hat{w}} = \frac{1}{2} \int_0^1 \hat{w}^2(x) dx \quad (9.3.47)$$

we get

$$\begin{aligned} \dot{V}_{\hat{w}} &= - \int_0^1 \hat{w}_x^2 dx + \hat{e}(0) \int_0^1 \beta \hat{w} dx + \dot{\hat{g}} \int_0^1 \hat{w} v dx \\ &\quad + \dot{\hat{g}} \int_0^1 \hat{w}(x) \int_0^x \alpha(x-y) (\hat{g} v(y) + \hat{w}(y)) dy dx \\ &\leq -\|\hat{w}_x\|^2 + \frac{c_1}{2} \|\hat{w}\|^2 + \frac{\beta_0^2}{2c_1} \frac{\hat{e}^2(0)}{1 + v^2(0)} (1 + \|v_x\|^2) \\ &\quad + \frac{|\dot{\hat{g}}|^2 (1 + \alpha_0 g_0)^2}{2c_1} \|v\|^2 + c_1 \|\hat{w}\|^2 + \frac{|\dot{\hat{g}}|^2 \alpha_0^2}{2c_1} \|\hat{w}\|^2 \\ &\leq -(1 - 6c_1) \|\hat{w}_x\|^2 + l_1 \|\hat{w}\|^2 + l_1 \|v_x\|^2 + l_1. \end{aligned} \quad (9.3.48)$$

¹We drop the dependence on time in the proofs to reduce notational burden.

Choosing $c_1 = 1/24$ and using a Lyapunov function $V = V_{\hat{w}} + (1/20)V_v$, we get

$$\begin{aligned}\dot{V} &\leq -\frac{1}{2}\|\hat{w}_x\|^2 - \frac{1}{40}\|v_x\|^2 - \frac{1}{40}\|v_{xx}\|^2 \\ &\quad + l_1\|\hat{w}\|^2 + l_1\|v_x\|^2 + l_1 \\ &\leq -\frac{1}{4}V + l_1V + l_1\end{aligned}\tag{9.3.49}$$

and by Lemma 9.4 we obtain $\|\hat{w}\|, \|v\|, \|v_x\| \in \mathcal{L}_2 \cap \mathcal{L}_\infty$. Using these properties we get

$$\begin{aligned}\frac{1}{2}\frac{d}{dt}\|\hat{w}_x\|^2 &\leq -\|\hat{w}_{xx}\|^2 + \beta_0|\hat{e}(0)|\|\hat{w}_{xx}\| \\ &\quad + |\dot{\hat{g}}|\|\hat{w}_{xx}\|((1 + \alpha_0 g_0)\|v\| + \alpha_0\|\hat{w}\|) \\ &\leq -\frac{1}{8}\|\hat{w}_x\|^2 + l_1,\end{aligned}\tag{9.3.50}$$

so that $\|\hat{w}_x\| \in \mathcal{L}_2 \cap \mathcal{L}_\infty$.

9.3.4 Regulation

Using the fact that $\|v_x\|, \|\hat{w}_x\|$ are bounded we get

$$\left|\frac{d}{dt}(\|v\|^2 + \|\hat{w}\|^2)\right| \leq l_1\|\hat{w}_x\|^2 + l_1\|v_x\|^2 + l_1 < \infty.\tag{9.3.51}$$

By Barbalat's lemma $\|\hat{w}\| \rightarrow 0, \|v\| \rightarrow 0$. From (9.3.54) we have $\|\eta\| \rightarrow 0$ and $\|\eta_x\|$ is bounded. Since $u = e + qv + \eta$, we get $\|u\| \rightarrow 0$ and $\|u_x\|$ is bounded. Finally, using Agmon's inequality we get

$$\lim_{t \rightarrow \infty} \max_{x \in [0,1]} |u(x, t)| \leq \lim_{t \rightarrow \infty} (2\|u\|\|u_x\|)^{1/2} = 0.\tag{9.3.52}$$

Lemma 9.3. *The transformation (9.3.26) maps the system (9.2.1)–(9.2.2), (9.2.10) into (9.3.27)–(9.3.29). The transformation (9.5.84) maps the system (9.4.57)–(9.4.58), (9.4.72) into (9.5.85)–(9.5.87).*

Proof. It is easy to check that boundary conditions (9.3.28) and (9.3.29) are satisfied. Substituting (9.3.26) into (9.2.1) we get

$$\begin{aligned}\hat{w}_t &= \hat{w}_{xx} + \dot{\hat{g}}v - \dot{\hat{g}} \int_0^x \{(k_{\hat{g}}(x, \xi, \hat{g})\hat{g} + k(x, \xi, \hat{g}))v(\xi) \\ &\quad + k_{\hat{g}}(x, \xi, \hat{g})\eta(\xi)\} d\xi + k_{\xi}(x, 0, \hat{g})\hat{e}(0).\end{aligned}\tag{9.3.53}$$

To express the signal η in terms of v and \hat{w} we use the inverse transformation to (9.3.26):

$$\hat{g}v(x, t) + \eta(x, t) = \hat{w}(x, t) - \hat{g} \int_0^x (x - \xi) \hat{w}(\xi, t) d\xi. \quad (9.3.54)$$

Changing the order of integration and taking the necessary derivatives of $k(x, \xi, \hat{g})$ we come to (9.3.27)–(9.3.29).

The second part of the lemma is proved in the same way. It is easy to check that (9.5.84) satisfies the boundary conditions (9.5.86) and (9.5.87). Substituting (9.5.84) into (9.4.57) we get (9.3.53) but with \hat{g} changed to \hat{q} everywhere. To express the signal η in terms of v and \hat{w} we use the inverse transformation of (9.5.84):

$$\hat{q}v(x, t) + \eta(x, t) = \hat{w}(x, t) - \hat{q} \int_0^x \hat{w}(\xi, t) d\xi. \quad (9.3.55)$$

Changing the order of integration and taking necessary derivatives of $k(x, \xi, \hat{q})$ we come to (9.5.85)–(9.5.87). \square

Lemma 9.4 (Lemma B.6 in [36]). *Let v , l_1 , and l_2 be real-valued functions defined on R_+ , and let c be a positive constant. If l_1 and l_2 are nonnegative and in \mathcal{L}_1 and satisfy the differential inequality*

$$\dot{v} \leq -cv + l_1(t)v + l_2(t), \quad v(0) \geq 0 \quad (9.3.56)$$

then $v \in \mathcal{L}_\infty \cap \mathcal{L}_1$.

9.4 Benchmark Plant with Unknown Parameter in the Boundary Condition

Consider the following plant

$$u_t(x, t) = u_{xx}(x, t), \quad (9.4.57)$$

$$u_x(0, t) = -qu(0, t), \quad (9.4.58)$$

$$u(1, t) = U(t), \quad (9.4.59)$$

where $U(t)$ is the control signal. This is an example of a system with a parametric uncertainty in the boundary condition, a hard-to-stabilize case even with full state feedback with in-domain actuation [8]. With $U(1) = 0$ this PDE is unstable if and only if $q > 1$. The plant can be written in the frequency domain as a transfer function from input $u(1)$ to output $u(0)$:

$$u(0, s) = \frac{\sqrt{s}}{\sqrt{s} \cosh \sqrt{s} - q \sinh \sqrt{s}} u(1, s). \quad (9.4.60)$$

Since this transfer function has infinitely many poles and no zeros (at $s = 0$ the transfer function is $1/(1 - q)$), this is an infinite relative degree system. One of the poles is unstable and is approximately equal to q^2 as $q \rightarrow +\infty$.

For the case of known q the transformation

$$w(x, t) = u(x, t) - \int_0^x k(x, \xi) u(\xi, t) d\xi \quad (9.4.61)$$

was used in [55] to map (9.4.57)–(9.4.58) into the target system

$$w_t(x, t) = w_{xx}(x, t) - cw(x, t), \quad (9.4.62)$$

$$w_x(0, t) = -qw(0, t), \quad (9.4.63)$$

$$w(1, t) = 0, \quad (9.4.64)$$

which is exponentially stable for $c \geq \max\{q|q|, 0\}$. However, this stability condition cannot be used when q is unknown. Instead, let us use (9.4.61) to map (9.4.57)–(9.4.58) into a different target system,

$$w_t(x, t) = w_{xx}(x, t), \quad (9.4.65)$$

$$w_x(0, t) = 0, \quad (9.4.66)$$

$$w(1, t) = 0. \quad (9.4.67)$$

It can be shown that the kernel $k(x, \xi)$ must satisfy the following conditions:

$$k_{xx} - k_{\xi\xi} = 0, \quad (9.4.68)$$

$$k_\xi(x, 0) = -qk(x, 0), \quad (9.4.69)$$

$$k(x, x) = -q. \quad (9.4.70)$$

The solution to this PDE is

$$k(x, \xi) = -qe^{q(x-\xi)}. \quad (9.4.71)$$

Suppose now that we want to stabilize the plant (9.4.57)–(9.4.59) when q is unknown. We have the following result.

Theorem 9.5. *Consider the system (9.4.57)–(9.4.58) with the control*

$$u(1, t) = -\int_0^1 \hat{q}e^{\hat{q}(1-\xi)}(\hat{q}v(\xi, t) + \eta(\xi, t)) d\xi, \quad (9.4.72)$$

where the update law for \hat{q} is

$$\dot{\hat{q}} = \gamma \frac{(u(0, t) - \hat{q}v(0, t) - \eta(0, t))v(0, t)}{1 + v^2(0, t)}, \quad (9.4.73)$$

and the filters $v(x, t)$, $\eta(x, t)$ are defined as

$$v_t(x, t) = v_{xx}(x, t), \quad (9.4.74)$$

$$v_x(0, t) = -u(0, t), \quad (9.4.75)$$

$$v(1, t) = 0, \quad (9.4.76)$$

$$\eta_t(x, t) = \eta_{xx}(x, t), \quad (9.4.77)$$

$$\eta_x(0, t) = 0, \quad (9.4.78)$$

$$\eta(1, t) = u(1, t). \quad (9.4.79)$$

If the closed loop system (9.4.57)–(9.4.58), (9.4.72)–(9.4.79) has a classical solution (u, \hat{q}, v, η) , then for any $\hat{q}(0)$ and any initial conditions $u_0, v_0, \eta_0 \in L_2(0, 1)$, the signals $\hat{q}(t)$, $\|u\|$, $\|v\|$, $\|\eta\|$ are bounded and $\|u\|$ is regulated to zero:

$$\lim_{t \rightarrow \infty} \|u\| = 0. \quad (9.4.80)$$

In addition, $u(x, t)$ is square integrable in t for all $x \in [0, 1]$.

Although the plants considered in Sections 9.2 (g -system) and 9.4 (q -system) look quite similar, the adaptive stabilization problem for the latter is substantially harder due to uncertainty in the boundary condition. The proof becomes harder and the end result is a little weaker — L_2 boundedness and regulation instead of pointwise boundedness and regulation.

9.5 Proof of Theorem 9.5

9.5.1 Target system

Introducing the error $e = u - qv - \eta$ we get an exponentially stable system

$$e_t(x, t) = e_{xx}(x, t), \quad (9.5.81)$$

$$e_x(0, t) = 0, \quad (9.5.82)$$

$$e(1, t) = 0. \quad (9.5.83)$$

The transformation

$$\begin{aligned} \hat{w}(x, t) &= \hat{q}v(x, t) + \eta(x, t) \\ &+ \int_0^x \hat{q}e^{\hat{q}(x-\xi)}(\hat{q}v(\xi, t) + \eta(\xi, t)) d\xi \end{aligned} \quad (9.5.84)$$

maps (9.4.57)–(9.4.58), (9.4.72) into the following system (Lemma 9.3):

$$\begin{aligned} \hat{w}_t(x, t) &= \hat{w}_{xx}(x, t) + \hat{q}^2 e^{\hat{q}x} \hat{e}(0, t) + \dot{\hat{q}}v \\ &+ \dot{\hat{q}} \int_0^x e^{\hat{q}(x-\xi)}(\hat{q}v(\xi, t) + \hat{w}(\xi, t)) d\xi, \end{aligned} \quad (9.5.85)$$

$$\hat{w}_x(0, t) = -\hat{q}\hat{e}(0, t), \quad (9.5.86)$$

$$\hat{w}(1, t) = 0. \quad (9.5.87)$$

9.5.2 Adaptive law properties

This step is almost the same as in Section 9.3 for the g -system. We take the following equation as a parametric model

$$e(0, t) = u(0, t) - qv(0, t) - \eta(0, t). \quad (9.5.88)$$

The estimation error is

$$\hat{e}(0, t) = u(0, t) - \hat{q}v(0, t) - \eta(0, t). \quad (9.5.89)$$

Using the gradient update law

$$\dot{\hat{q}} = \gamma \frac{\hat{e}(0, t)v(0, t)}{1 + v^2(0, t)} \quad (9.5.90)$$

we get the following properties (as in Lemma 9.2)

$$\frac{\hat{e}(0, t)}{\sqrt{1 + v^2(0, t)}} \in \mathcal{L}_2 \cap \mathcal{L}_\infty, \quad \tilde{q} \in \mathcal{L}_\infty, \quad \dot{\hat{q}} \in \mathcal{L}_2 \cap \mathcal{L}_\infty. \quad (9.5.91)$$

We denote the bound on \hat{q} by q_0 .

9.5.3 Boundedness

First we rewrite v -filter as

$$v_t(x, t) = v_{xx}(x, t), \quad (9.5.92)$$

$$v_x(0, t) = -\hat{w}(0, t) - \hat{e}(0, t), \quad (9.5.93)$$

$$v(1, t) = 0, \quad (9.5.94)$$

We have two interconnected systems for \hat{w} and v driven by the signal $\hat{e}(0, t)$ with properties (9.5.91). Consider a Lyapunov function

$$V = \frac{1}{2} \int_0^1 \hat{w}^2(x) dx + \frac{1}{2} \int_0^1 v^2(x) dx. \quad (9.5.95)$$

We have

$$\begin{aligned} \dot{V} &= -\hat{w}(0)\hat{w}_x(0) - \int_0^1 \hat{w}_x^2 dx + \dot{\hat{q}} \int_0^1 \hat{w}(x)v(x) dx \\ &\quad + \dot{\hat{q}} \int_0^1 \hat{w}(x) \int_0^x e^{\hat{q}(x-\xi)} (\hat{q}v(\xi) + \hat{w}(\xi)) d\xi dx \\ &\quad + \hat{e}(0) \int_0^1 \hat{q}^2 e^{\hat{q}x} \hat{w}(x) dx - v(0)v_x(0) - \int_0^1 v_x^2 dx \\ &\leq -\|\hat{w}_x\|^2 + |\hat{e}(0)|(q_0|\hat{w}(0)| + q_0^2 e^{q_0} \|\hat{w}\|) + c_1 \|\hat{w}\|^2 \\ &\quad + \frac{(1 + q_0 e^{q_0})^2 |\dot{\hat{q}}|^2}{2c_1} \|v\|^2 + \frac{e^{2q_0} |\dot{\hat{q}}|^2}{2c_1} \|\hat{w}\|^2 \\ &\quad - \|v_x\|^2 + \frac{1}{2} \|v_x\|^2 + \frac{1}{2} \|\hat{w}_x\|^2 + |v(0)| |\hat{e}(0)|. \end{aligned} \quad (9.5.96)$$

Estimates of particular terms:

$$\begin{aligned}
q_0|\hat{e}(0)||\hat{w}(0)| &\leq q_0|\hat{w}(0)|\frac{\hat{e}(0)}{\sqrt{1+v^2(0)}}(1+|v(0)|) \\
&\leq c_2\|\hat{w}_x\|^2 + \frac{q_0^2}{4c_2}\frac{\hat{e}^2(0)}{1+v^2(0)} \\
&\quad + 2q_0\sqrt{\|\hat{w}\|\|\hat{w}_x\|\|v\|\|v_x\|}\frac{|\hat{e}(0)|}{\sqrt{1+v^2(0)}} \\
&\leq c_2\|\hat{w}_x\|^2 + l_1 \\
&\quad + \frac{q_0|\hat{e}(0)|}{\sqrt{1+v^2(0)}}(\|\hat{w}\|\|\hat{w}_x\| + \|v\|\|v_x\|) \\
&\leq c_2\|\hat{w}_x\|^2 + l_1 + c_3\|\hat{w}_x\|^2 + c_4\|v_x\|^2 \\
&\quad + q_0^2\frac{\hat{e}^2(0)}{1+v^2(0)}\left(\frac{\|v\|^2}{4c_3} + \frac{\|\hat{w}\|^2}{4c_4}\right) \\
&\leq c_2\|\hat{w}_x\|^2 + c_3\|\hat{w}_x\|^2 + c_4\|v_x\|^2 \\
&\quad + l_1\|v\|^2 + l_1\|\hat{w}\|^2 + l_1,
\end{aligned} \tag{9.5.97}$$

$$\begin{aligned}
q_0^2e^{q_0}|\hat{e}(0)||\hat{w}| &\leq q_0^2e^{q_0}\|\hat{w}\|\frac{\hat{e}(0)}{\sqrt{1+v^2(0)}}(1+|v(0)|) \\
&\leq c_5\|\hat{w}\|^2 + \frac{q_0^4e^{2q_0}}{4c_5}\frac{\hat{e}^2(0)}{1+v^2(0)} + c_6\|v_x\|^2 \\
&\quad + \frac{q_0^4e^{2q_0}}{4c_6}\frac{\hat{e}^2(0)}{1+v^2(0)}\|\hat{w}\|^2 \\
&\leq c_5\|\hat{w}\|^2 + c_6\|v_x\|^2 + l_1\|\hat{w}\|^2 + l_1,
\end{aligned} \tag{9.5.98}$$

$$\begin{aligned}
|v(0)||\hat{e}(0)| &\leq \frac{|v(0)||\hat{e}(0)|}{1+v^2(0)}(1+2\|v\|\|v_x\|) \\
&\leq \frac{c_7}{2}\|v_x\|^2 + \frac{1}{2c_7}\frac{\hat{e}^2(0)}{1+v^2(0)} + \frac{c_7}{2}\|v_x\|^2 \\
&\quad + \frac{2}{c_7}\left(\frac{|v(0)||\hat{e}(0)|}{1+v^2(0)}\right)^2\|v\|^2 \\
&\leq c_7\|v_x\|^2 + l_1\|v\|^2 + l_1.
\end{aligned} \tag{9.5.99}$$

In the last inequality we used the fact that \dot{q}^2 is an l_1 function. We have

$$\begin{aligned}
\dot{V} &\leq -\left(\frac{1}{2} - 4c_1 - c_2 - c_3 - 4c_5\right)\|\hat{w}_x\|^2 + l_1\|\hat{w}\|^2 \\
&\quad -\left(\frac{1}{2} - c_4 - c_6 - c_7\right)\|v_x\|^2 + l_1\|v\|^2 + l_1.
\end{aligned} \tag{9.5.100}$$

Choosing $4c_1 = c_2 = c_3 = 4c_5 = 1/16$, $c_4 = c_6 = c_7 = 1/12$, we get

$$\dot{V} \leq -\frac{1}{8}V + l_1V + l_1 \quad (9.5.101)$$

and by Lemma 9.4 we obtain $\|\hat{w}\|, \|v\| \in \mathcal{L}_2 \cap \mathcal{L}_\infty$.

9.5.4 Regulation

It is easy to see from (9.5.101) that \dot{V} is bounded from above. By using an alternative to Barbalat's lemma [43, Lemma 3.1] we get $V \rightarrow 0$, that is $\|\hat{w}\| \rightarrow 0$, $\|v\| \rightarrow 0$. From (9.3.55) we have $\|\eta\| \rightarrow 0$. Since $u = e + qv + \eta$, we get $\|u\| \rightarrow 0$.

By integrating (9.5.100) we get $\|\hat{w}_x\|, \|v_x\| \in \mathcal{L}_2$, and from (9.3.55) $\|\eta_x\| \in \mathcal{L}_2$ and therefore $\|u_x\| \in \mathcal{L}_2$. Square integrability in time of $u(x, t)$ for all $x \in [0, 1]$ follows from Agmon's inequality.

9.6 Plant with Two Unknown Parameters

For the sake of clarity and due to different adaptive regulation properties that can be achieved, we considered two benchmark problems separately. It is also possible to design an output feedback adaptive controller for the combined system

$$u_t(x, t) = u_{xx}(x, t) + gu(0, t), \quad (9.6.102)$$

$$u_x(0, t) = -qu(0, t), \quad (9.6.103)$$

This system is unstable if and only if $2q + g > 2$. The non-adaptive control law can be designed based on the controllers for separate problems by using the method described in [55, Sec. VIII-E]. We state here the stabilization result without a proof.

Theorem 9.6. *Consider the plant (9.6.102)–(9.6.103) with the controller*

$$u(1) = \int_0^1 \frac{r_1^2 e^{r_1(1-x)} - r_2^2 e^{r_2(1-x)}}{2\sqrt{\hat{g} + \hat{q}^2/4}} (\hat{g}v + \hat{q}p + \eta) dx, \quad (9.6.104)$$

where the update laws for \hat{g} and \hat{q} are

$$\dot{\hat{g}} = \gamma_1 \frac{\hat{e}(0)v(0,t)}{1 + v^2(0,t) + p^2(0,t)}, \quad (9.6.105)$$

$$\dot{\hat{q}} = \gamma_2 \frac{\hat{e}(0)p(0,t)}{1 + v^2(0,t) + p^2(0,t)}, \quad (9.6.106)$$

the input filter is

$$\eta_t = \eta_{xx} \quad (9.6.107)$$

$$\eta_x(0) = 0 \quad (9.6.108)$$

$$\eta(1) = u(1) \quad (9.6.109)$$

and the output filters are

$$\begin{aligned} v_t &= v_{xx} + u(0) & p_t &= p_{xx} \\ v_x(0) &= 0 & p_x(0) &= -u(0) \\ v(1) &= 0 & p(1) &= 0 \end{aligned} \quad (9.6.110)$$

with $\hat{e}(0) = u(0) - \hat{g}v(0) - \hat{q}p(0) - \eta(0)$ and

$$r_{1,2} = \frac{\hat{q}}{2} \mp \sqrt{\hat{g} + \frac{\hat{q}^2}{4}}. \quad (9.6.111)$$

If the closed loop system (9.6.102)–(9.6.111) has a classical solution $(u, \hat{g}, \hat{q}, v, p, \eta)$, then for any $\hat{g}(0), \hat{q}(0)$ and any initial conditions $u_0, v_0, p_0, \eta_0 \in L_2(0,1)$, the signals $\hat{g}(t), \hat{q}(t), \|u\|, \|v\|, \|p\|, \|\eta\|$ are bounded and $\|u\|$ is regulated to zero:

$$\lim_{t \rightarrow \infty} \|u\| = 0. \quad (9.6.112)$$

In addition, $u(x,t)$ is square integrable in t for all $x \in [0,1]$.

Remark 9.7. If the expression $\hat{g} + \hat{q}^2/4$ becomes negative, $r_{1,2}$ become complex. However, the control gain in (9.6.104) remains real and well defined.

9.7 Simulations

We present now the results of closed-loop simulations for the system (9.6.102)–(9.6.103). The plant parameters are set to $g = 4$ and $q = 2$, with

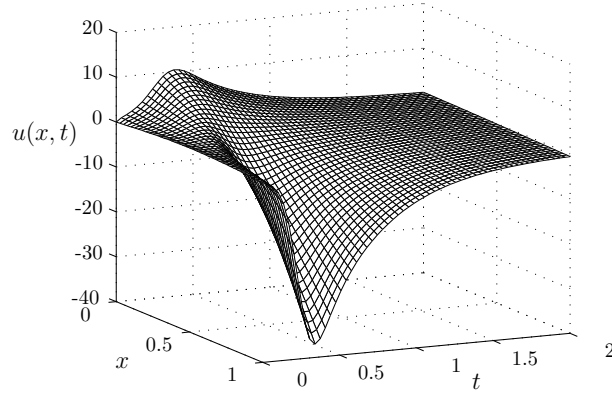


Figure 9.1: The state $u(x, t)$ with the adaptive output feedback controller (9.6.104).

these values the unstable eigenvalue ≈ 10 . For the update laws we take $\hat{g}(0) = 3$, $\hat{q}(0) = 1$, and $\gamma_1 = \gamma_2 = 15$. The results are shown in Fig. 9.1-9.2. We can see that although the instability occurs at the $x = 0$ boundary, the system is successfully regulated to zero by the control from the opposite boundary.

9.8 Conclusions

In general, swapping-based adaptive schemes [58] have a considerably higher dynamic order than Lyapunov-based schemes [38]. However, for the systems studied in this chapter we have been able to use the same set of Kreisselmeier filters for both designing an observer and for achieving a static parametrization from which a gradient update law is derived. Thus, the dynamic order for the output feedback designs in the present paper and in [38] is the same. The advantage of the swapping update laws in the present paper is that they are considerably simpler, whereas the advantage of the Lyapunov update laws in [38] is that they are derived from a complete Lyapunov function that incorporates the plant, the filters, and the update law, providing a tighter control over transient performance.

This chapter is in part a reprint of the material as it appears in A. Smyshlyaev and M. Krstic, “Adaptive boundary control for unstable parabolic PDEs-Part III: Output feedback examples with swapping identifiers,” accepted to

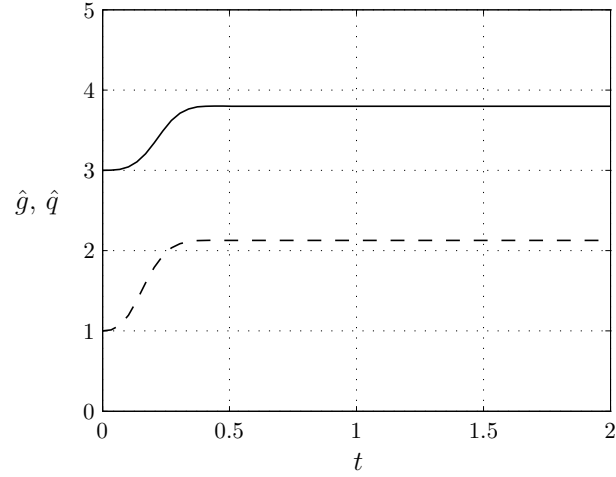


Figure 9.2: The parameters \hat{g} (solid) and \hat{q} (dashed). The unknown parameters are set to $g = 4$ and $q = 2$.

Automatica, 2006.

The dissertation author was the primary author and the coauthor listed in this publication directed the research which forms the basis for this chapter.

Chapter 10

Adaptive Control for PDEs with Spatially Varying Coefficients

10.1 Introduction

With only a scalar control input, infinite dimensional state, and infinite dimensional (functional) parametric uncertainties, unstable reaction-advection-diffusion PDEs with unknown spatially varying coefficients represent a formidable challenge. Previous approaches have dealt only with problems with domain-wide actuation [8, 9, 29, 48, 62] or with constant parameters [38, 58, 59]. In this chapter we solve this problem with only boundary actuation and spatially varying parameters.

To solve the problem we introduce several new concepts. We exploit the fact that our backstepping approach for parabolic PDEs requires only the solution of a linear hyperbolic PDE [55], rather than a nonlinear problem like a Riccati equation. While in principle even our linear problem would be numerically intractable online because the linear hyperbolic PDE would have to be solved at each time step (for each new value of the parameter estimate vector), we first prove that our non-adaptive backstepping approach is robust to approximations in solving the hyperbolic design PDE. This result, given for the general case of

spatially varying reaction, advection, and diffusion coefficients, constitutes the first half of our paper. The next novel idea we introduce is an adaptive control design that involves a careful reparametrization of the problem which results in a design with estimation of only the actual physical parameters. The parameter update laws are chosen based on a stability analysis involving a single Lyapunov function and, since the unknown parameters are functions (of space), the update laws are governed by PDEs. We prove global stability of the closed loop system and pointwise-in-space boundedness and regulation of the state. We end the paper with simulations that demonstrate the stabilizing ability of our adaptive controllers under wide spatial variations of the unknown parameters, with only boundary actuation, and, perhaps most importantly, without persistency of excitation. The latter implies that stabilization is achieved even in cases where it is impossible to perfectly identify the unknown parameters.

10.2 Problem Statement

We consider the plant

$$u_t(x, t) = \varepsilon(x)u_{xx}(x, t) + b(x)u_x(x, t) + \lambda(x)u(x, t) \quad (10.2.1)$$

$$u(0, t) = 0 \quad (10.2.2)$$

for $x \in [0, 1]$ with $u(1)$ or $u_x(1)$ used for actuation. The parameters $\varepsilon(x)$, $b(x)$, $\lambda(x)$ are unknown and we assume that $\varepsilon(x)$ is positive for all $x \in [0, 1]$ and $\lambda \in C[0, 1]$, $b \in C^1[0, 1]$, $\varepsilon \in C^2[0, 1]$.

The plant (10.2.1)–(10.2.2) encompasses a variety of reaction-advection-diffusion problems arising from the fluid, thermal and chemical systems. The dynamics of (10.2.1)–(10.2.2) are unstable due to the presence of the reaction term $\lambda(x)$. The objective is to stabilize the zero equilibrium of this system using the boundary input at $x = 1$. Previously, this problem has been solved using the backstepping approach for *known* parameters [56] and *unknown* but *constant* parameters [38, 58, 59].

The boundary condition at $x = 0$ is not restricted to be Dirichlet—it can be Neumann or mixed, the design can be extended to these cases in a straightforward way.

We will focus on Dirichlet actuation at $x = 1$. All the results can be easily extended to the case of Neumann actuation [55].

We focus our attention on the case of unknown $\lambda(x)$, while allowing $\varepsilon(x)$ and $b(x)$ to be known. This is done for three reasons. First, reaction term is the only source of instability in the equation (10.2.1) and thus is the most important term to handle. Second, the tools we introduce here for unknown $\lambda(x)$ and known $\varepsilon(x)$ and $b(x)$ will enable a designer who has understood them to develop a design where all of the coefficients are unknown, however, with considerable additional effort in analytical calculation and notation, which is the reason we do not pursue the problem in full generality here. We do however present the design and simulations for unknown $b(x)$. Third, the main issue that arises with unknown $b(x)$ and $\varepsilon(x)$ is related to the use of parameter projection, for example, to prevent the estimate of $\varepsilon(x)$ from becoming zero at some values of x , which would result in the controller gains becoming infinite. This is a standard issue in adaptive control [30, 36] and, while it requires technical care, it is not a conceptual issue but a "fix". Pursuing this issue would make it dominate our presentation and blur the concept we are trying to introduce, so we refrain from pursuing it and focus on unknown $\lambda(x)$.

10.3 Non-Adaptive Control Design

Before we proceed with the adaptive design, we first briefly present the control design for the case when the parameters of the plant (10.2.1) are known. Note that we cannot use the simplifying transformation (2.2.5) since the parameters are unknown. We use the transformation

$$w(x) = u(x) - \int_0^x k(x, y)u(y) dy, \quad (10.3.3)$$

to map (10.2.1)–(10.2.2) into the exponentially stable target system

$$w_t = \varepsilon(x)w_{xx} + b(x)w_x - cw, \quad (10.3.4)$$

$$w(0) = w(1) = 0. \quad (10.3.5)$$

Here c is an arbitrary nonnegative constant that allows the designer to change the desired decay rate of the closed loop system. The stabilizing controller is then implemented as

$$u(1) = \int_0^1 k(1, y)u(y) dy. \quad (10.3.6)$$

One can show that the kernel $k(x, y)$ of the transformation (10.3.3) must satisfy the following PDE

$$\begin{aligned} \varepsilon(x)k_{xx}(x, y) - (\varepsilon(y)k(x, y))_{yy} = \\ (\lambda(y) + c)k(x, y) - b(x)k_x(x, y) - (b(y)k(x, y))_y \end{aligned} \quad (10.3.7)$$

with boundary conditions

$$k(x, 0) = 0 \quad (10.3.8)$$

$$k(x, x) = -\frac{1}{2\sqrt{\varepsilon(x)}} \int_0^x \frac{\lambda(y) + c}{\sqrt{\varepsilon(y)}} dy \quad (10.3.9)$$

This PDE has been shown to be well posed in [56].

We are now going to address an important issue: robustness of the closed loop system with respect to the error in the kernel $k(x, y)$. We will carry out the analysis in the non-adaptive setting so that the complexity of the adaptive design does not obscure the picture.

10.4 Robustness To Error In Gain Kernel

When the coefficients ε , b , and λ are constant, the PDE (10.3.7)–(10.3.9) can be solved in closed form and thus the explicitly parametrized controllers can be obtained. This remarkable fact was exploited in [38] and [55] to design explicit adaptive schemes which avoid numerical computation of the gain at each time step.

In case of spatially varying ε , b , and λ the equation (10.3.7)–(10.3.9) has to be solved numerically. Therefore the need for the robustness analysis arises to ensure that the error in the kernel does not ruin the closed loop stability of the adaptive scheme. The exact question to ask can be formulated as follows: how small should the difference between the approximate and exact solutions of (10.3.7)–(10.3.9) be to guarantee that the target system (10.3.4)–(10.3.5) is exponentially stable?

The PDE (10.3.7)–(10.3.9) can be numerically solved in several ways. One way is to use a finite-difference scheme [55]. Another approach is to represent the solution of the kernel PDE as a successive approximation series. We will follow the second approach here, mainly because it is better suited for analysis.

Let us use the following recursive formula to approximate k ($k^n \rightarrow k$ as $n \rightarrow \infty$):

$$k^n(x, y) = \frac{\varepsilon^{\frac{1}{4}}(x)}{\varepsilon^{\frac{3}{4}}(y)} e^{-\int_y^x \frac{b(s)}{2\varepsilon(s)} ds} m^n(\xi, \eta), \quad (10.4.10)$$

where

$$m^0(\xi, \eta) = -\frac{1}{4} \int_{\eta}^{\xi} \lambda_a(\sigma, 0) d\sigma, \quad (10.4.11)$$

$$m^i(\xi, \eta) = m^0(\xi, \eta) + \frac{1}{4} \int_{\eta}^{\xi} \int_0^{\eta} \lambda_a(\sigma, s) m^{i-1}(\sigma, s) ds d\sigma \quad (10.4.12)$$

for $i = 1, 2, \dots, n$, the variables ξ and η are defined as

$$\begin{aligned} \xi &= \varphi(x) + \varphi(y), \quad \eta = \varphi(x) - \varphi(y), \\ \varphi(\zeta) &= \int_0^{\zeta} \frac{1}{\sqrt{\varepsilon(s)}} ds, \end{aligned} \quad (10.4.13)$$

and

$$\begin{aligned}
\lambda_a(\xi, \eta) = & \lambda(y) + c + \frac{1}{4} \left(\frac{b^2(x)}{\varepsilon(x)} - \frac{b^2(y)}{\varepsilon(y)} \right) \\
& - \frac{1}{2} \left(\frac{b(x)\varepsilon'(x)}{\varepsilon(x)} - \frac{b(y)\varepsilon'(y)}{\varepsilon(y)} \right) \\
& + \frac{3}{16} \left(\frac{\varepsilon'^2(x)}{\varepsilon(x)} - \frac{\varepsilon'^2(y)}{\varepsilon(y)} \right) \\
& - \frac{1}{4} (\varepsilon''(x) - \varepsilon''(y) - 2b'(x) + 2b'(y)). \tag{10.4.14}
\end{aligned}$$

Theorem 10.1. *There exists n^* such that for any initial data $u_0 \in L_2(0, 1)$ (respectively, $H_1(0, 1)$) the system (10.2.1)–(10.2.2) with the controller*

$$u(1, t) = \int_0^1 k^n(1, y) u(y, t) dy \tag{10.4.15}$$

where $n \geq n^$ and k^n is determined by (10.4.10)–(10.4.14), is exponentially stable at the origin $u \equiv 0$ in $L_2(0, 1)$ (resp. $H_1(0, 1)$) norms.*

10.4.1 Proof of Theorem 10.1

Let us make the following change of variables in (10.3.7)–(10.3.9):

$$k(x, y) = \frac{\varepsilon^{\frac{1}{4}}(x)}{\varepsilon^{\frac{3}{4}}(y)} e^{-\int_y^x \frac{b(s)}{2\varepsilon(s)} ds} m(\xi, \eta), \tag{10.4.16}$$

where ξ and η are given by (10.4.13). It can be shown that the function m then satisfies the following PDE:

$$4m_{\xi\eta}(\xi, \eta) = \lambda_a(\xi, \eta)m(\xi, \eta) \tag{10.4.17}$$

$$m(\xi, \xi) = 0 \tag{10.4.18}$$

$$m(\xi, 0) = -\frac{1}{4} \int_0^\xi \lambda_a(\sigma, 0) d\sigma, \tag{10.4.19}$$

We can see in (10.4.17) that the transformation (10.4.16) removes all the coefficients in front of derivatives in (10.3.7) by “augmenting” λ to λ_a . By integrating (10.4.17) twice we obtain an integral equation for m , the solution to which can be represented by successive approximations series (10.4.11)–(10.4.12).

With an approximate transformation

$$w(x) = u(x) - \int_0^x k^n(x, y)u(y) dy \quad (10.4.20)$$

we get the following target system

$$w_t = \varepsilon(x)w_{xx} + b(x)w_x - cw + \int_0^x \delta k^n(x, y)u(y) dy \quad (10.4.21)$$

$$w(0) = w(1) = 0. \quad (10.4.22)$$

where $\delta k^n(x, y)$ is the error due to approximation

$$\begin{aligned} \delta k^n(x, y) &= \varepsilon(x)k_{xx}^n - (\varepsilon(y)k^n)_{yy} - (\lambda(y) + c)k^n \\ &\quad + b(x)k_x^n + (b(y)k^n)_y. \end{aligned} \quad (10.4.23)$$

When $n \rightarrow \infty$, we have $k^n \rightarrow k$ and so $\delta k^n \rightarrow 0$. Note that the integral term in (10.4.21) contains u instead of w . To express u in terms of w we use the inverse transformation

$$u(x) = w(x) + \int_0^x l^n(x, y)w(y) dy. \quad (10.4.24)$$

The kernel of the inverse transformation l^n is related to k^n by the following equation:

$$l^n(x, y) = k^n(x, y) + \int_y^x k^n(x, \sigma)l^n(\sigma, y) d\sigma. \quad (10.4.25)$$

This relationship is easily obtained if we substitute (10.4.20) into (10.4.24), change the order of integration, and match the terms.

It is clear now that in order to determine when the system (10.4.21)–(10.4.22) is stable, we need to estimate δk^n , k^n , and l^n .

Lemma 10.2. *The following bounds hold:*

$$|\delta k^n(x, y)| \leq \alpha_n y(x^2 - y^2)^n \quad (10.4.26)$$

$$|k^n(x, y)| \leq yK, \quad (10.4.27)$$

$$|l^n(x, y)| \leq yL_n, \quad (10.4.28)$$

where $B = \max\{|\underline{b}|, |\bar{b}|\}$, \underline{b} , \bar{b} , $\underline{\varepsilon}$, $\bar{\varepsilon}$, $\bar{\lambda}_a$ denote the upper and lower bounds on b , ε , and $|\lambda_a|$, respectively, α_n , β , and L_n are defined as

$$\alpha_n = \frac{2e^{\frac{B}{2\underline{\varepsilon}}}\bar{\lambda}_a(\bar{\varepsilon}/\underline{\varepsilon})^{1/4}}{n!(n+1)!} \left(\frac{\bar{\lambda}_a}{4\underline{\varepsilon}}\right)^{n+1} \quad (10.4.29)$$

$$K = \frac{\bar{\varepsilon}^{1/4}}{\underline{\varepsilon}^{3/4}} e^{\frac{B}{2\underline{\varepsilon}}} \sqrt{\bar{\lambda}_a} I_1 \left(\sqrt{\bar{\lambda}_a/\underline{\varepsilon}} \right) \quad (10.4.30)$$

$$L_n = K + \alpha_n \frac{4\underline{\varepsilon} e^{\frac{K-2B}{4\underline{\varepsilon}}}}{\bar{\lambda}_a K^2} \quad (10.4.31)$$

and I_1 is a modified Bessel function of order one.

Proof. **Bound on δk^n**

If we substitute (10.4.10)–(10.4.14) into (10.4.23), after a long calculation one can show that

$$\begin{aligned} \delta k^n(x, y) &= \lambda_a(\varphi(x) + \varphi(y), \varphi(x) - \varphi(y)) \\ &\quad \times [k^{n-1}(x, y) - k^n(x, y)]. \end{aligned} \quad (10.4.32)$$

Using (10.4.11)–(10.4.12), it can be shown by induction that the following bound holds:

$$|m^n(\xi, \eta) - m^{n-1}(\xi, \eta)| \leq \frac{(\xi - \eta)\xi^n \eta^n}{n!(n+1)!} \left(\frac{\bar{\lambda}_a}{4}\right)^{n+1} \quad (10.4.33)$$

From (10.4.32), (10.4.10), and (10.4.33) we get

$$\begin{aligned} |\delta k^n(x, y)| &\leq \frac{\varepsilon^{\frac{1}{4}}(x)}{\varepsilon^{\frac{3}{4}}(y)} e^{-\int_y^x \frac{b(s)}{2\varepsilon(s)} ds} \varphi(y) \\ &\quad \times \frac{(\varphi^2(x) - \varphi^2(y))^n}{n!(n+1)!} \left(\frac{\bar{\lambda}_a}{4}\right)^{n+1} \end{aligned} \quad (10.4.34)$$

Noting that $\varphi(y) \leq y/\sqrt{\underline{\varepsilon}}$, we get (10.4.26).

Bound on k^n

Using the fact that $k^{-1} = m^{-1} = 0$ and (10.4.10), (10.4.33) we get the following estimate:

$$\begin{aligned} |k^n(x, y)| &\leq \sum_{i=0}^n |k^i(x, y) - k^{i-1}(x, y)| \\ &\leq y \sum_{i=0}^n \frac{2e^{\frac{B}{2\bar{\varepsilon}}}(\bar{\varepsilon}/\underline{\varepsilon})^{1/4}}{i!(i+1)!} \left(\frac{\bar{\lambda}_a}{4\underline{\varepsilon}}\right)^{i+1} \leq yK, \end{aligned} \quad (10.4.35)$$

where K , given by (10.4.30), is a sum of the series (10.4.35) when $n \rightarrow \infty$.

Note that (10.4.26) and (10.4.27) are tight bounds, since they become equalities when the parameters ε , b , λ are constant.

Conservative bound on l^n

Using (10.4.35) and the relation (10.4.25) between l^n and k^n , we get:

$$\begin{aligned} |l^n(x, y)| &\leq |k^n(x, y)| + \int_y^x |k^n(x, \sigma)| |l^n(\sigma, y)| d\sigma \\ &\leq Ky + K \int_y^x \sigma |l^n(\sigma, y)| d\sigma. \end{aligned} \quad (10.4.36)$$

Using Gronwall lemma we get the following bound:

$$|l^n(x, y)| \leq yK e^{\frac{K}{2}(x^2 - y^2)} \leq yK e^{\frac{K}{2}}, \quad (10.4.37)$$

where K is given by (10.4.30). Unfortunately, this bound very conservative (roughly, it is an exponential of an exponential of $\sqrt{\bar{\lambda}_a}$). One would prefer to have a less conservative bound to get a good practical estimate for the number of terms needed when computing the control gain using (10.4.10)–(10.4.14). Therefore we need to improve on the bound (10.4.37).

Sharp bound on l^n

Let us denote

$$\begin{aligned} \delta l^n &= \varepsilon(x) l_{xx}^n - (\varepsilon(y) l^n)_{yy} + (\lambda(x) + c) l^n \\ &\quad + b(x) l_x^n + (b(y) l^n)_y. \end{aligned} \quad (10.4.38)$$

The reason for considering the expression (10.4.38) is that its right hand side matches the PDE for the exact kernel of the inverse transformation [56] when $n \rightarrow \infty$, so that $\delta l^n \rightarrow 0$.

If we apply the inverse transformation (10.4.24) to the target system (10.4.21)–(10.4.22) and require the result to be identical to the original plant, we get the following relationship between δl^n and δk^n :

$$\begin{aligned} \delta l^n - \int_y^x \delta l^n(x, \xi) k^n(\xi, y) d\xi = \\ \delta k^n + \int_y^x l^n(x, \xi) \delta k^n(\xi, y) d\xi. \end{aligned} \quad (10.4.39)$$

Using the definitions (10.4.20) and (10.4.24) we can rewrite (10.4.39) in the following form

$$\begin{aligned} \delta l^n(x, y) = & \delta k^n(x, y) + \int_y^x \delta l^n(x, \xi) k^n(\xi, y) d\xi \\ & - \int_y^x k^n(x, \xi) \int_y^\xi \delta l^n(\xi, s) k^n(s, y) ds d\xi \\ & + \int_y^x k^n(x, \xi) \delta l^n(\xi, y) d\xi. \end{aligned} \quad (10.4.40)$$

This is an integral equation for δl^n with the kernels that do not depend on l^n . Using the bounds (10.4.26) and (10.4.35) we get the following inequality:

$$\begin{aligned} |\delta l^n(x, y)| \leq & \alpha_n y(x^2 - y^2) \\ & + K \int_y^x (y |\delta l^n(x, \xi)| + \xi |\delta l^n(\xi, y)|) d\xi \\ & + K^2 \int_y^x \int_y^\xi \xi y |\delta l^n(\xi, s)| ds d\xi. \end{aligned} \quad (10.4.41)$$

The sharpest bound for a solution of an integral inequality is given by a solution of the corresponding integral equation. We get the following estimate:

$$|\delta l^n(x, y)| \leq \frac{\alpha_n y}{\sqrt{2}K} \left(e^{\frac{K(\sqrt{2}-1)}{2}(x^2-y^2)} - 1 \right). \quad (10.4.42)$$

Since the PDEs (10.4.23) and (10.4.38) (without the errors δk^n and δl^n) differ only in the sign of the term without derivatives, we expect that the bound

on l^n should be equal to the bound (10.4.35) on k^n plus some additional term due to δl^n . Applying to (10.4.38) the same technique that we used to obtain (10.4.35) and using the bound (10.4.42) we get the following estimate:

$$|l^n(x, y)| \leq y \left(K + \alpha_n \frac{4\underline{\varepsilon} e^{\frac{K-2B}{4\underline{\varepsilon}}}}{\bar{\lambda}_a K^2} \right). \quad (10.4.43)$$

We can see that this bound is much better than the bound (10.4.37) since it approaches yK when n grows ($\alpha_n \rightarrow 0$) and not the exponential of K as (10.4.37) does.

□

Let us use the Lyapunov function candidate

$$V = \frac{1}{2} \int_0^1 \rho(x) w^2(x) dx, \quad (10.4.44)$$

where $\rho(x)$ will be chosen later. The reason for using weighting is that with standard L_2 norm as a Lyapunov function one cannot prove stability of the target system (10.4.21)–(10.4.22) without enforcing an additional condition on c . We have

$$\begin{aligned} \dot{V} &= \int_0^1 \rho(x) (\varepsilon(x) w w_{xx} + b(x) w w_x - c w^2) dx \\ &\quad + \int_0^1 \rho(x) w(x) \int_0^x \delta k^n(x, y) u(y) dy dx \\ &= - \int_0^1 \rho(x) \varepsilon(x) w_x^2 dx - cV \\ &\quad + \int_0^1 w w_x \left(\rho(x) b(x) - \frac{d(\rho(x) \varepsilon(x))}{dx} \right) dx \\ &\quad + \int_0^1 \rho(x) w(x) \int_0^x \delta k^n(x, y) u(y) dy dx. \end{aligned} \quad (10.4.45)$$

Let us choose

$$\rho(x) = \frac{1}{\varepsilon(x)} e^{\int_0^x \frac{b(s)}{\varepsilon(s)} ds}. \quad (10.4.46)$$

With this choice the integral with cross term $w w_x$ in (10.4.45) disappears and we get:

$$\begin{aligned} \dot{V} &= - \int_0^1 \rho(x) \varepsilon(x) w_x^2 dx - cV \\ &\quad + \int_0^1 \rho(x) w(x) \int_0^x \delta k^n(x, y) u(y) dy dx. \end{aligned} \quad (10.4.47)$$

The following lemma provides the estimate for the last term in (10.4.47).

Lemma 10.3. *There exists n^* such that for any $n \geq n^*$*

$$\int_0^1 \rho(x) w(x) \int_0^x \delta k^n(x, y) u(y) dy dx \leq \frac{\varepsilon}{2} \|w_x\|^2. \quad (10.4.48)$$

Proof. Using (10.4.24), after the change of the order of integration we get

$$\begin{aligned} &\int_0^1 \rho(x) w(x) \int_0^x \delta k^n(x, y) u(y) dy dx \leq \\ &+ \int_0^1 \rho(x) w(x) \int_0^x w(y) \int_y^x \delta k^n(x, \sigma) l^n(\sigma, y) d\sigma dy \\ &\int_0^1 \rho(x) w(x) \int_0^x \delta k^n(x, y) w(y) dx dy \\ &\leq \int_0^1 \rho(x) |w(x)| \int_0^x \alpha_n y L_n \frac{(x^2 - y^2)^{n+1}}{2(n+1)} |w(y)| dy dx \\ &+ \int_0^1 \rho(x) |w(x)| \int_0^x \alpha_n y (x^2 - y^2)^n |w(y)| dy dx. \end{aligned} \quad (10.4.49)$$

Let us estimate the following integral:

$$\begin{aligned} &\int_0^1 |w(x)| \int_0^x y (x^2 - y^2)^n |w(y)| dy dx \\ &\leq \|w\| \left(\int_0^1 \left(\int_0^x y (x^2 - y^2)^n |w(y)| dy \right)^2 dx \right)^{\frac{1}{2}} \\ &\leq \|w\| \left(\int_0^1 \frac{x^{2n+2}}{2(n+1)} \int_0^x \frac{(x^2 - y^2)^{n+1}}{n+1} w w_y dy dx \right)^{\frac{1}{2}} \\ &\leq \frac{2}{n+1} \|w_x\| \left(\int_0^1 \frac{1}{2} |w(x)| |w_x(x)| \frac{1}{4n+5} dx \right)^{\frac{1}{2}} \\ &\leq \frac{1}{(n+1)^{3/2}} \|w_x\|^2. \end{aligned} \quad (10.4.50)$$

Here we have used Cauchy-Schwartz and Poincare inequalities several times. Substituting the estimate (10.4.50) into (10.4.49), we get (10.4.48) if the following condition is satisfied:

$$\bar{\rho}\alpha_n \left(\frac{1}{(n+1)^{3/2}} + \frac{L_n}{2(n+1)(n+2)^{3/2}} \right) \leq \frac{\varepsilon}{2}, \quad (10.4.51)$$

where $\bar{\rho} = \underline{\varepsilon}^{-1} e^{2B/\underline{\varepsilon}}$ is the upper bound on $\rho(x)$. Since $\alpha_n \rightarrow 0$ as $n \rightarrow \infty$ and L_n is uniformly bounded, it is clear that there exist n^* such that (10.4.51) holds for all $n > n^*$. \square

Substituting (10.4.48) into (10.4.47) and using Poincare inequality we get

$$\dot{V} \leq -\frac{\varepsilon}{8} e^{-\frac{2B}{\varepsilon}} V - cV, \quad (10.4.52)$$

so that the zero equilibrium of the w -system is exponentially stable in L_2 -norm. It is straightforward to show with $\|w_x\|$ as a Lyapunov function that the condition (10.4.51) ensures H_1 stability as well. Therefore, u -system is also exponentially stable at the origin in L_2 and H_1 norms (since the inverse transformation (10.4.24) has a bounded kernel).

10.4.2 Practical issues

If one tries to use the condition (10.4.51) to calculate n^* , the result will be a rather conservative estimate. The reason is that although the bounds α_n and L_n are tight, they provide a good estimate on δk^n and l^n for different parameter ranges. While the bound on δk^n is good when $\lambda_a \geq 0$, the bound on l^n is good when $\lambda_a \leq 0$ and vice versa. Let us assume $\lambda_a \geq 0$ (which is normally the case if the plant is unstable), then it follows from (10.4.10)–(10.4.12) that k^n is negative and large. Thus, one can expect the kernel of the inverse transformation l^n to be “small”, not of the size of k^n as (10.4.43) suggests. We give the following “rule of thumb” bound on l^n in this case:

$$|l^n(x, y)| \leq y \frac{\bar{\lambda}_a}{2\underline{\varepsilon}}. \quad (10.4.53)$$

Table 10.1: Minimum number of terms n required to satisfy the condition (10.4.51) for different $\bar{\lambda}$.

$\bar{\lambda}_a/\underline{\varepsilon}$	10	20	40	60
n^* , with a conservative bound (10.4.37)	6	16	64	204
n^* , with a tight bound (10.4.43)	4	7	25	74
n^* , with a “rule of thumb” bound (10.4.53)	4	6	8	10

The motivation behind this bound is simple: since k^n in (10.4.25) is negative, one can assume that l^n will not grow beyond the “initial condition” $k^n(y, y)$ which is bounded by $\bar{\lambda}_a y/(2\underline{\varepsilon})$. It is not possible to prove the estimate (10.4.53), but numerical computations seem to confirm that it holds.

To illustrate how the minimum number of terms n^* required to satisfy (10.4.51) depends on the parameters of the plant and on the selection of L_n , we computed the value of n^* for different values of $\bar{\lambda}_a/\underline{\varepsilon}$ (we set $b(x) \equiv 0$ for this computation since b -term does not contribute to instability and thus n^* is not affected much) and using the different bounds on l^n (10.4.37), (10.4.43), and (10.4.53). The results are presented in Table 10.1. We can see that the bound (10.4.43) results in a much better estimate of n^* than the bound (10.4.37). It is also clear that in practice only several terms are sufficient.

One can use the “rule of thumb” estimate for l^n (10.4.53) and Stirling approximation $\ln n! \approx n \ln n - n$ to obtain the following approximation from (10.4.51)

$$n \geq \frac{e}{2} \sqrt{\frac{\bar{\lambda}_a}{\underline{\varepsilon}}} - 1. \quad (10.4.54)$$

This is a very good practical estimate of the number of terms needed for the implementation of the controller (10.4.10)–(10.4.14).

We are now ready to start with the adaptive control schemes.

10.5 Adaptive Design

Consider the plant (10.2.1)–(10.2.2) with known $\varepsilon(x)$, $b(x)$ and unknown $\lambda(x)$. Given the non-adaptive control scheme (10.3.6)–(10.3.9), the most natural

approach (the so-called indirect method) is to use the estimate $\hat{\lambda}(x)$ in (10.3.6)–(10.3.9) instead of $\lambda(x)$. The PDE for the control gain estimate \hat{k} becomes:

$$\begin{aligned} \varepsilon(x)\hat{k}_{xx} - (\varepsilon(y)\hat{k})_{yy} &= (\hat{\lambda}(y) + c)\hat{k} - b(x)\hat{k}_x \\ &\quad - (b(y)\hat{k})_y \end{aligned} \quad (10.5.55)$$

$$\hat{k}(x, 0) = 0 \quad (10.5.56)$$

$$\hat{k}(x, x) = -\frac{1}{2\sqrt{\varepsilon(x)}} \int_0^x \frac{\hat{\lambda}(y) + c}{\sqrt{\varepsilon(y)}} dy, \quad (10.5.57)$$

As we already pointed out in the previous section, one can follow two different approaches to obtain the solution to (10.5.55)–(10.5.57): use a finite-difference scheme or the successive approximation series. We leave the designer the choice to pick the more suitable method, however, we only prove the closed-loop stability result for the latter approach.

The recursive scheme (10.4.10)–(10.4.14) is modified as follows:

$$\hat{k}^n(x, y) = \frac{\varepsilon^{\frac{1}{4}}(x)}{\varepsilon^{\frac{3}{4}}(y)} e^{-\int_y^x \frac{b(s)}{2\varepsilon(s)} ds} \hat{m}^n(\xi, \eta) \quad (10.5.58)$$

where \hat{m}^n is obtained by

$$\hat{m}^0(\xi, \eta) = -\frac{1}{4} \int_0^x \hat{\lambda}_a(\sigma, 0) d\sigma \quad (10.5.59)$$

$$\begin{aligned} \hat{m}^i(\xi, \eta) &= \hat{m}^0(\xi, \eta) \\ &\quad + \frac{1}{4} \int_\eta^\xi \int_0^\eta \hat{\lambda}_a(\sigma, s) \hat{m}^{i-1}(\sigma, s) ds d\sigma \end{aligned} \quad (10.5.60)$$

for $i = 1, 2, \dots, n$.

$$\begin{aligned} \hat{\lambda}_a(\xi, \eta) &= \hat{\lambda}(y) + c + \frac{1}{4} \left(\frac{b^2(x)}{\varepsilon(x)} - \frac{b^2(y)}{\varepsilon(y)} \right) \\ &\quad - \frac{1}{2} \left(\frac{b(x)\varepsilon'(x)}{\varepsilon(x)} - \frac{b(y)\varepsilon'(y)}{\varepsilon(y)} \right) \\ &\quad + \frac{3}{16} \left(\frac{\varepsilon'^2(x)}{\varepsilon(x)} - \frac{\varepsilon'^2(y)}{\varepsilon(y)} \right) \\ &\quad - \frac{1}{4} (\varepsilon''(x) - \varepsilon''(y) - 2b'(x) + 2b'(y)). \end{aligned} \quad (10.5.61)$$

The variables x and y in (10.5.59) and (10.5.61) are expressed through ξ and η as $x = \varphi^{-1}((\xi + \eta)/2)$ and $y = \varphi^{-1}((\xi - \eta)/2)$. Note that all the variables with a “hat” depend on time although we do not explicitly indicate that.

Let us apply the transformation

$$w(x) = u(x) - \int_0^x \hat{k}^n(x, y)u(y) dy \quad (10.5.62)$$

to the plant (10.2.1)–(10.2.2). We get the following target system

$$\begin{aligned} w_t = & \varepsilon(x)w_{xx} + b(x)w_x - cw - \int_0^x \hat{k}_t^n(x, y)u(y) dy \\ & + \int_0^x \delta \hat{k}^n(x, y)u(y) dy + \tilde{\lambda}(x)u(x) \\ & - \int_0^x \tilde{\lambda}(y)\hat{k}^n(x, y)u(y) dy \end{aligned} \quad (10.5.63)$$

where u is related to w through the inverse transformation

$$u(x) = w(x) + \int_0^x \hat{l}^n(x, y)w(y) dy, \quad (10.5.64)$$

and $\tilde{\lambda} = \lambda - \hat{\lambda}$.

Using the idea of [38] to use a logarithm in the Lyapunov function we consider

$$V = \frac{1}{2} \log(1 + \|w\|_\rho^2) + \frac{1}{2\gamma} \|\tilde{\lambda}\|^2, \quad (10.5.65)$$

where $\|w\|_\rho$ is weighted L_2 norm of w :

$$\|w\|_\rho^2 = \int_0^1 \rho(x)w^2(x) dx. \quad (10.5.66)$$

and $\rho(x)$ is defined by (10.4.46).

Based on the Lyapunov function (10.5.65) we choose the following update law:

$$\begin{aligned} \hat{\lambda}_t(x, t) = & \gamma \frac{\rho(x)w(x)u(x)}{1 + \|w\|_\rho^2} \\ & - \gamma \frac{u(x) \int_x^1 \hat{k}^n(y, x)\rho(y)w(y) dy}{1 + \|w\|_\rho^2}, \end{aligned} \quad (10.5.67)$$

where γ is a positive constant.

Two main limitations of the Lyapunov approach are the need for the parameter projection and the restriction on the size of the adaptation gain (the reasons for these limitations will be clear from the proof of the closed-loop stability in Section 10.6). Projection means that the parameters should be kept within a-priori bounds: $\hat{\lambda} \in [\underline{\lambda}, \bar{\lambda}]$ for all x . The allowed size of the adaptation gain γ is inversely proportional to the size of the parameter set, so the a-priori bounds should not be too conservative. Although we do not explicitly write it in the update law (10.5.67), the following projection operator is used there:

$$\text{Proj}_{[\underline{\lambda}, \bar{\lambda}]} \{\tau\} = \begin{cases} 0, & \hat{\lambda} = \underline{\lambda} \text{ and } \tau < 0 \\ 0, & \hat{\lambda} = \bar{\lambda} \text{ and } \tau > 0 \\ \tau, & \text{else .} \end{cases} \quad (10.5.68)$$

Here τ denotes the nominal update law (10.5.67). Although this operator is discontinuous it is possible to introduce a small boundary layer instead of a hard switch which will avoid dealing with Filippov solutions and noise due to possible switching of the update law (see [38] for more details). However, we use (10.5.68) here for notational clarity.

Theorem 10.4. *Suppose that the closed loop system which consists of the plant (10.2.1)–(10.2.2), update law (10.5.67), and the controller*

$$u(1) = \int_0^1 \hat{k}^n(1, y) u(y) dy \quad (10.5.69)$$

has a well defined solution $(u, \hat{\lambda})$. Then, there exist n^ and γ^* such that, for all $n \geq n^*$ and $\gamma \in (0, \gamma^*)$, for any initial condition $u_0 \in H_1([0, 1])$ and any initial estimate $\hat{\lambda}_0 \in C^2[0, 1]$, the solutions $u(x, t)$, $\hat{\lambda}(x, t)$ are uniformly bounded and $\lim_{t \rightarrow \infty} u(x, t) = 0$ for all $x \in [0, 1]$.*

10.6 Proof of Theorem 10.4

It can be shown using (10.5.67) that

$$\begin{aligned} \dot{V} = & \frac{1}{1 + \|w\|_\rho^2} \left\{ - \int_0^1 \rho(x) \varepsilon(x) w_x^2 dx \right. \\ & - \int_0^1 \rho(x) w(x) \int_0^x \delta \hat{k}^n(x, y) u(y) dy dx \\ & \left. + \int_0^1 \rho(x) w(x) \int_0^x \hat{k}_t^n(x, y) u(y) dy dx \right\}. \end{aligned} \quad (10.6.70)$$

The second term here is due to approximation of the control kernel \hat{k} by (10.5.58)–(10.5.61) and the third term is due to the fact that \hat{k}^n is time-varying.

Next, by Lemma 10.3 there exists n^* such that for any $n \geq n^*$, the following holds:

$$\int_0^1 \rho(x) w(x) \int_0^x \delta \hat{k}^n(x, y) u(y) dy dx \leq \frac{\varepsilon}{2} \|w_x\|^2 \quad (10.6.71)$$

To estimate the last term in (10.6.70), let us first note that \hat{k}^n and \hat{l}^n are bounded, which follows from (10.5.58)–(10.5.61) and the fact that $\hat{\lambda}$ is bounded by projection bounds. Let us denote these bounds by K and L , respectively. From (10.5.58)–(10.5.61) one can show that

$$|\hat{k}_t^n(x, y)| \leq M \max_{x,t} |\hat{\lambda}_t(x)|, \quad (10.6.72)$$

where

$$M = \frac{\bar{\varepsilon}^{1/4} e^{B/2\bar{\varepsilon}}}{2\bar{\varepsilon}^{3/4}} I_0 \left(\sqrt{\bar{\lambda}_a / \bar{\varepsilon}} \right), \quad (10.6.73)$$

and I_0 denotes the modified Bessel function of order zero. To see how this bound is obtained, note from (10.5.58)–(10.5.59) that \hat{k}_t^0 is bounded by the maximum of $\hat{\lambda}_t$. Then from (10.5.60) we get that \hat{k}^1 is bounded by the maximums of \hat{k}_t^0 and $\hat{\lambda}_t$ and therefore is bounded by the maximum of $\hat{\lambda}_t$. By induction we obtain series of bounds which can then be summed up to get (10.6.73).

From the update law (10.5.67) we get

$$\max_{x,t} |\hat{\lambda}_t| \leq \gamma e^{B/\bar{\varepsilon}} (1 + L) (1 + K). \quad (10.6.74)$$

Using (10.6.72) and (10.6.74) we obtain

$$\begin{aligned} & \int_0^1 \rho(x)w(x) \int_0^x \hat{k}_t^n(x, y)u(y) dy dx \\ & \leq 2\gamma e^{B/\varepsilon} M(1+L)(1+K) \|w_x\|^2. \end{aligned} \quad (10.6.75)$$

Substituting the bounds (10.6.71) and (10.6.75) into (10.6.70), we get

$$\dot{V} \leq -\frac{\varepsilon(1-\gamma/\gamma^*)}{4(1+\|w\|_\rho^2)} \int_0^1 w_x^2 dx, \quad (10.6.76)$$

where

$$\gamma^* = \frac{\varepsilon}{8} e^{-B/\varepsilon} (M(1+L)(1+K))^{-1} \quad (10.6.77)$$

Therefore, $\|w\|$ is bounded and $\|w_x\|^2$ is integrable over infinite time for $\gamma < \gamma^*$.

Let us now prove the boundedness of $\|w_x\|^2$. We start with

$$\begin{aligned} \frac{1}{2} \frac{d}{dt} \|w_x\|^2 & \leq - \int_0^1 w_{xx} w_t dx \\ & \leq - \int_0^1 \varepsilon w_{xx}^2 dx - \int_0^1 b w_x w_{xx} dx - c \|w_x\|^2 \\ & \quad + \int_0^1 w_{xx}(x) \int_0^x \delta \hat{k}^n(x, y) u(y) dy \\ & \quad - \int_0^1 w_{xx}(x) \int_0^x \hat{k}_t^n(x, y) u(y) dy. \end{aligned} \quad (10.6.78)$$

Using the bounds (10.6.71)–(10.6.74) we get

$$\begin{aligned} \frac{1}{2} \frac{d}{dt} \|w_x\|^2 & \leq -\varepsilon \|w_{xx}\|^2 + B \|w_x\| \|w_{xx}\| \\ & \quad + \frac{\varepsilon}{2} \|w_{xx}\| \|w\| + \frac{\varepsilon}{4} \frac{\gamma}{\gamma^*} \|w_{xx}\| \|w\| - c \|w_x\|^2 \\ & \leq -\varepsilon \|w_{xx}\|^2 + \frac{\varepsilon}{4} \|w_{xx}\|^2 - c \|w_x\|^2 \\ & \quad + B \|w_x\|^2 + \frac{\varepsilon}{2} \|w_{xx}\|^2 \\ & \quad + \frac{\varepsilon}{8} \|w\|^2 + \frac{\varepsilon}{4} \|w_{xx}\|^2 + \frac{\varepsilon}{16} \|w\|^2 \\ & \leq \left(\frac{3\varepsilon}{4} + \frac{1}{\varepsilon} B^2 - c \right) \|w_x\|^2 \end{aligned} \quad (10.6.79)$$

Since $\|w_x\|^2$ is integrable over infinite time, by integrating (10.6.79) we get that $\|w_x\|$ is bounded. By Agmon inequality, $w(x, t)$ is uniformly bounded for all $t \geq 0$ and for all $x \in [0, 1]$.

In order to show regulation, let us estimate

$$\begin{aligned}
\left| \frac{1}{2} \frac{d}{dt} \|w\|^2 \right| &\leq \bar{\varepsilon} \|w_x\|^2 + B \|w\| \|w_x\| + c \|w\|^2 \\
&\quad + \frac{\bar{\varepsilon}}{4} \frac{\gamma}{\gamma^*} \|w_x\|^2 + \frac{\bar{\varepsilon}}{2} \|w_x\|^2 \\
&\quad + \gamma \bar{\lambda} e^{B/\bar{\varepsilon}} (1+L)(1+K). \tag{10.6.80}
\end{aligned}$$

The right hand side of this inequality is bounded, so $|\frac{d}{dt} \|w\|^2|$ is bounded. Recalling that $\|w\|^2$ is bounded and integrable over infinite time, by Barbalat's lemma we get $\|w(t)\| \rightarrow 0$ as $t \rightarrow \infty$. Using Agmon inequality we get $w(x, t) \rightarrow 0$ for all $x \in [0, 1]$ as $t \rightarrow \infty$.

The boundedness and regulation results for $u(x, t)$ follow from those for $w(x, t)$ due to the boundedness of the kernel \hat{l}^n of the transformation (10.5.64).

10.7 Design With Other Parameters

When the parameters $\varepsilon(x)$ and $b(x)$ are unknown, the methodology presented in this paper can still be used to design the adaptive scheme. Since the control gain depends on the derivatives of these parameters, it turns out that one needs to estimate $b'(x)$, $\varepsilon'(x)$, $\varepsilon''(x)$ separately in order to avoid measurement of u_x or u_{xx} . For example, the estimates $\hat{b}(x)$ and $\hat{b}_1(x)$ of $b(x)$ and $b'(x)$ respectively are updated as follows:

$$\begin{aligned}
\hat{b}_t(x, t) &= \gamma \frac{w(x) \int_0^x \hat{k}_x^n(x, \xi) u(\xi) d\xi}{1 + \|w\|^2} \\
&\quad + \gamma \frac{u(x) \int_x^1 \hat{k}_y^n(\xi, x) w(\xi) d\xi}{1 + \|w\|^2} \tag{10.7.81}
\end{aligned}$$

$$\hat{b}_{1t}(x, t) = -\gamma \frac{u(x) \int_x^1 \hat{k}^n(y, x) w(y) dy}{1 + \|w\|^2} \tag{10.7.82}$$

10.8 Simulations

We now present the simulation results for the plant (10.2.1)–(10.2.2) with unknown $b(x)$ and $\lambda(x)$.

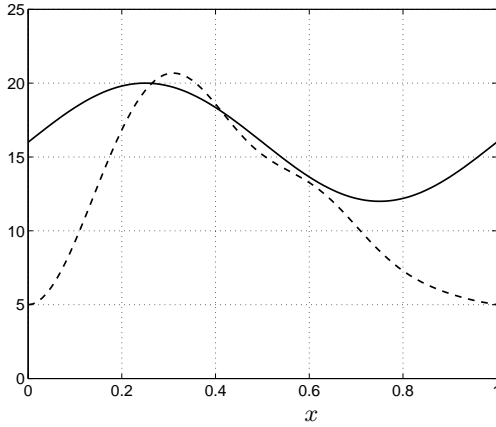


Figure 10.1: The final profile of the estimate $\hat{\lambda}(x, t)$ (dashed) versus true $\lambda(x)$ (solid).

As pointed out in [55], solving the PDE for the control gain is easy from the numerical point of view, an order of magnitude faster than solving Riccati equations. Computing the series (10.5.58)–(10.5.61) at each time step with sufficient accuracy takes just seconds (for the entire simulation) on a basic laptop computer, which makes the scheme implementable in real time.

We set $\lambda(x) = 16 + 4\sin(2\pi x)$ and $b(x) = 1 + 5x$ so that the plant is unstable and the initial estimates are $\hat{\lambda}(x, 0) \equiv 5$, $\hat{b}(x, 0) \equiv 0$. The evolution of the parameter estimates $\hat{\lambda}(x, t)$ and $\hat{b}(x, t)$ is shown in Figure 10.3. In Figures 10.1 and 10.2 the final profiles of $\hat{\lambda}(x, t)$ and $\hat{b}(x, t)$ are shown in comparison with the true $\lambda(x)$ and $b(x)$. As expected, $\hat{\lambda}(x, t)$ and $\hat{b}(x, t)$ do not converge to the true functions (because the system is not persistently excited). In Figure 10.4 the evolution of the state of the closed loop system is shown. One can see that the plant is successfully stabilized.

This chapter is in part a reprint of the material as it appears in A. Smyshlyaev and M. Krstic, “Lyapunov adaptive boundary control for parabolic PDEs with spatially varying coefficients,” *Proceedings of 2006 American Control Conference*, pp. 41-48.

The dissertation author was the primary author and the coauthor listed in this

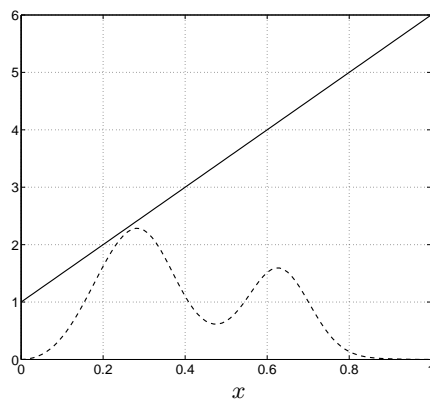


Figure 10.2: The final profile of the estimate $\hat{b}(x, t)$ (dashed) versus true $b(x)$ (solid).

publication directed the research which forms the basis for this chapter.

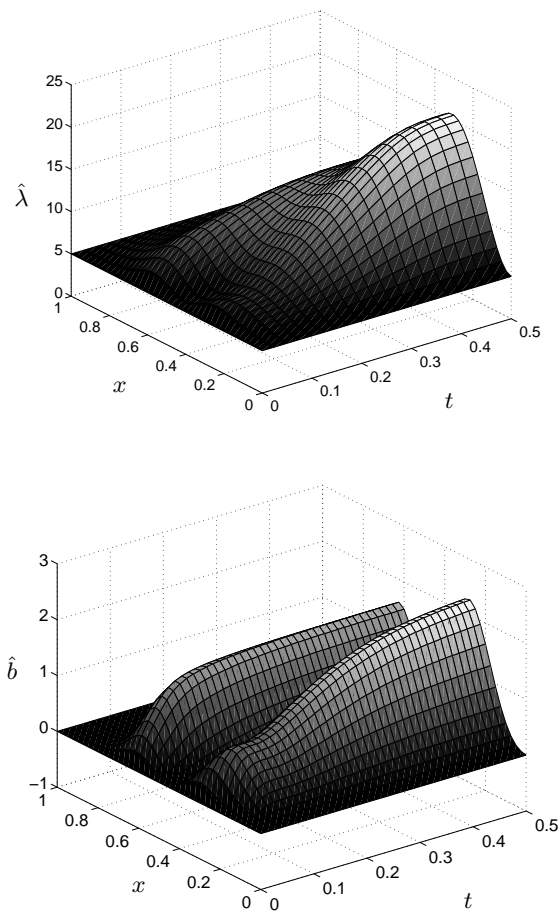


Figure 10.3: The parameter estimates $\hat{\lambda}(x, t)$ and $\hat{b}(x, t)$.

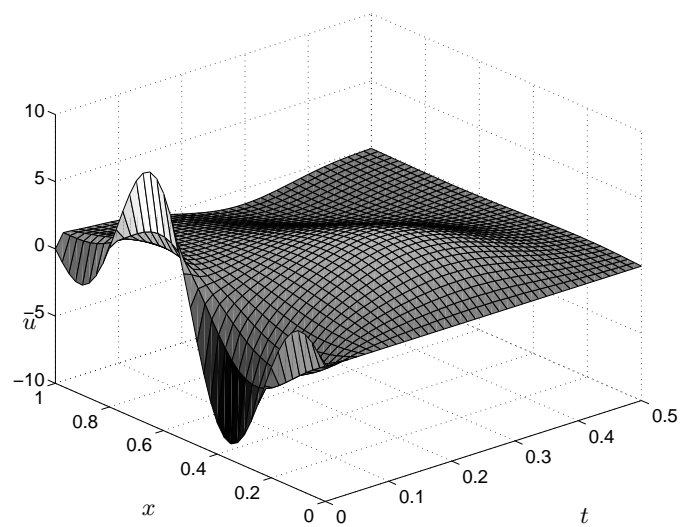


Figure 10.4: The closed loop state $u(x, t)$.

Chapter 11

Output Feedback Adaptive Control

11.1 Introduction

The existing results in adaptive control for parabolic PDEs [8, 9, 29, 48, 62, 58] all rely on full state measurement. For the first time, we consider a problem of *output* feedback stabilization of reaction-advection-diffusion systems with uncertain parameters. While this problem is novel even for the constant parameter case, we go further and design the adaptive scheme for spatially-varying unknown parameters.

We assume that both sensing and actuation are performed at the opposite *boundaries* of the PDE domain. Thus, the plant has infinite relative degree, infinite-dimensional state, infinite-dimensional (functional) parametric uncertainties, and only scalar input and output.

In Chapter 9 we solved an output-feedback problem for a particular benchmark plant with two constant parameters multiplying the output. In this chapter we introduce the transformation of a general parabolic system into a PDE analog of the observer canonical form. In this form the (spatially varying) uncertain parameters multiply the output rather than the state, and it is therefore a

generalization of the system considered in Chapter 9.

We use the adaptive observers that are infinite dimensional extensions of Kreisselmeier observers [36]. The identifiers are designed using the swapping approach [36], the usual method in adaptive control of finite dimensional systems of relative degree higher than one. Typically the swapping method requires one filter per unknown parameter and since we have functional parameters, infinitely many filters are needed. However, with a special algebraic representation of the filters we reduce their number down to only two.

Our control laws are adaptive versions of the boundary control laws developed in Chapter 2. We derive a special integro-differential equation in one variable for the control gain instead of a PDE given in Chapter 2.

Throughout the paper we assume well posedness of the closed loop systems and focus our efforts on the control design and a proof of stability of the adaptive scheme.

11.2 Problem Formulation

We consider the following plant

$$u_t(x, t) = u_{xx}(x, t) + \lambda(x)u(x, t) \quad (11.2.1)$$

for $0 < x < 1$ with boundary conditions

$$u_x(0, t) = 0 \quad (11.2.2)$$

$$u(1, t) = U(t) \text{ or } u_x(1, t) = U(t), \quad (11.2.3)$$

where $\lambda(x)$ is an *unknown* continuous function and $U(t)$ is the input. We assume that only $u(0, t)$ is available for measurement. The dynamics of the plant are unstable for large enough $\lambda(x)$. The objective is to regulate the state of the plant to zero using the boundary input and measurement.

We will focus on Dirichlet actuation here. All the results can be easily extended to Neumann actuation.

More general systems can be handled as outlined in Section 11.9.

11.3 Transformation to Observer Canonical Form

The key step in our design is the transformation of the original plant (11.2.1)–(11.2.2) into a system in which unknown parameters multiply the measured output. This can be achieved with the help of the backstepping transformation very similar (but not the same) to the one used in [56] for observer design.

Consider the transformation¹

$$v(x) = u(x) - \int_0^x p(x, y)u(y) dy \quad (11.3.4)$$

where $p(x, y)$ is a solution of the PDE

$$p_{xx}(x, y) - p_{yy}(x, y) = \lambda(y)p(x, y) \quad (11.3.5)$$

$$p(1, y) = 0 \quad (11.3.6)$$

$$p(x, x) = \frac{1}{2} \int_x^1 \lambda(s) ds. \quad (11.3.7)$$

One can show² that this transformation maps the system (11.2.1)–(11.2.2) into

$$v_t = v_{xx} + \theta(x)v(0) \quad (11.3.8)$$

$$v_x(0) = \theta_1 v(0) \quad (11.3.9)$$

$$v(1) = u(1) \quad (11.3.10)$$

where

$$\theta(x) = -p_y(x, 0) \quad (11.3.11)$$

$$\theta_1 = -p(0, 0) \quad (11.3.12)$$

are the new unknown parameters.

¹From now on, we will suppress the time dependence whenever possible.

²Due to the lack of space we omit this straightforward calculation.

The system (11.3.8)–(11.3.10) is the PDE analog of observer canonical form. Note from (11.3.4) that $v(0) = u(0)$ and therefore $v(0)$ is measured. The transformation (11.3.4) is invertible so that stability of v implies stability of u . Therefore it is enough to design the stabilizing controller for v -system and then use the condition $u(1) = v(1)$ (which follows from (11.3.6)) to obtain the controller for the original system. We are going to directly estimate the new unknown parameters $\theta(x)$ and θ_1 instead of estimating $\lambda(x)$. Thus, we do not need to solve the PDE (11.3.5)–(11.3.7) for the control scheme implementation.

11.4 Non-Adaptive Controller

First let us design the controller for the case of known $\lambda(x)$ (and therefore known $\theta(x)$ and θ_1).

It has been shown in Chapter 2 that backstepping transformation

$$w(x) = v(x) - \int_0^x k(x, y)v(y) dy \quad (11.4.13)$$

with $k(x, y)$ given as a solution of the PDE

$$k_{xx} - k_{yy} = 0 \quad (11.4.14)$$

$$k_y(x, 0) = \theta_1 k(x, 0) + \theta(x) - \int_0^x k(x, y)\theta(y) dy \quad (11.4.15)$$

$$k(x, x) = \theta_1 \quad (11.4.16)$$

maps the v -system into the exponentially stable target system

$$w_t = w_{xx} \quad (11.4.17)$$

$$w_x(0) = 0 \quad (11.4.18)$$

$$w(1) = 0. \quad (11.4.19)$$

The controller is obtained by setting $x = 1$ in (11.4.13):

$$v(1) = \int_0^1 k(1, y)v(y) dy. \quad (11.4.20)$$

One can simplify the PDE (11.4.14)–(11.4.16) by setting $k(x, y) = \kappa(x - y)$, which is a solution of (11.4.14). The function $\kappa(x)$ then has to satisfy the ordinary integro-differential equation

$$\kappa'(x) = -\theta_1 \kappa(x) - \theta(x) + \int_0^x \kappa(x - y) \theta(y) dy \quad (11.4.21)$$

$$\kappa(0) = \theta_1. \quad (11.4.22)$$

It is considerably easier to solve this equation in one variable than the original PDE.

We can write it as the following integral equation:

$$\begin{aligned} \kappa(x) = & \theta_1 - \int_0^x \theta(y) dy \\ & - \int_0^x \left[\theta_1 - \int_0^{x-y} \theta(s) ds \right] \kappa(y) dy \end{aligned} \quad (11.4.23)$$

Remark 11.1. Note that it is in fact possible to find the control gain explicitly for any *known* $\theta(x)$ and θ_1 by applying Laplace transform in x to (11.4.21) to get

$$\kappa(s) = \frac{\theta(s) - \theta_1}{\theta(s) - s - \theta_1}. \quad (11.4.24)$$

However, this formula is not very helpful in the adaptive setting when the parameter estimates are known only numerically and it is easier to solve (11.4.21)–(11.4.22) directly instead of computing direct and inverse Laplace transforms.

11.5 Estimator

The unknown parameters θ and $\theta(x)$ enter the boundary condition and the domain of the v -system. Therefore we will need the following output filters:

$$\phi_t = \phi_{xx} \quad (11.5.25)$$

$$\phi_x(0) = u(0) \quad (11.5.26)$$

$$\phi(1) = 0 \quad (11.5.27)$$

and

$$\Phi_t = \Phi_{xx} + \delta(x - \xi)u(0) \quad (11.5.28)$$

$$\Phi_x(0) = 0 \quad (11.5.29)$$

$$\Phi(1) = 0. \quad (11.5.30)$$

Here the filter $\Phi = \Phi(x, \xi)$ is parametrized by $\xi \in [0, 1]$ and $\delta(x - \xi)$ is a delta function. The reason for this parametrization is the presence of the functional parameter $\theta(x)$ in the domain. Therefore, loosely speaking we need an infinite “array” of filters, one for each $x \in [0, 1]$ (since the swapping design normally requires one filter per unknown parameter).

We also introduce the input filter

$$\psi_t = \psi_{xx} \quad (11.5.31)$$

$$\psi_x(0) = 0 \quad (11.5.32)$$

$$\psi(1) = u(1). \quad (11.5.33)$$

It is straightforward to show now that the error

$$\bar{e}(x) = v(x) - \psi(x) - \theta_1 \phi(x) - \int_0^1 \theta(\xi) \Phi(x, \xi) d\xi \quad (11.5.34)$$

satisfies the exponentially stable PDE

$$\bar{e}_t = \bar{e}_{xx} \quad (11.5.35)$$

$$\bar{e}_x(0) = 0 \quad (11.5.36)$$

$$\bar{e}(1) = 0. \quad (11.5.37)$$

The filters ϕ and Φ both have $u(0)$ as input. Therefore the following idea comes to mind: what if we try to represent the state $\Phi(x, \xi)$ algebraically through $\phi(x)$ at each moment in time? The following lemma establishes this connection.

Lemma 11.2. *The signal*

$$e(x) = v(x) - \psi(x) - \theta_1 \phi(x) - \int_0^1 \theta(\xi) F(x, \xi) d\xi \quad (11.5.38)$$

where $F(x, \xi)$ is given by

$$F_{xx}(x, \xi) = F_{\xi\xi}(x, \xi) \quad (11.5.39)$$

$$F(0, \xi) = -\phi(\xi) \quad (11.5.40)$$

$$F_x(0, \xi) = 0 \quad (11.5.41)$$

$$F_\xi(x, 0) = F(x, 1) = 0 \quad (11.5.42)$$

is governed by the exponentially stable heat equation:

$$e_t = e_{xx} \quad (11.5.43)$$

$$e_x(0) = 0 \quad (11.5.44)$$

$$e(1) = 0 \quad (11.5.45)$$

□

Proof. The initial conditions for the filters ϕ and Φ are the design choice so let us assume that they are continuous functions in x and ξ . We now write down the explicit solutions to the filters (see, e.g., [49]). The solution for the ϕ -system is

$$\begin{aligned} \phi(x, t) = & 2 \sum_{n=0}^{\infty} \cos(\sigma_n x) e^{-\sigma_n^2 t} \int_0^1 \phi_0(s) \cos(\sigma_n s) ds \\ & - 2 \sum_{n=0}^{\infty} \cos(\sigma_n x) \int_0^t u(0, \tau) e^{-\sigma_n^2(t-\tau)} d\tau, \end{aligned} \quad (11.5.46)$$

where $\sigma_n = \pi(n + 1/2)$.

The solution for the Φ -system is

$$\begin{aligned} \Phi(x, \xi, t) = & 2 \sum_{n=0}^{\infty} \cos(\sigma_n x) \int_0^1 \delta(s - \xi) \cos(\sigma_n s) ds \int_0^t u(0, \tau) e^{-\sigma_n^2(t-\tau)} d\tau \\ & + 2 \sum_{n=0}^{\infty} \cos(\sigma_n x) e^{-\sigma_n^2 t} \int_0^1 \Phi_0(s, \xi) \cos(\sigma_n s) ds \\ = & 2 \sum_{n=0}^{\infty} \cos(\sigma_n x) \cos(\sigma_n \xi) \int_0^t u(0, \tau) e^{-\sigma_n^2(t-\tau)} d\tau \\ & + 2 \sum_{n=0}^{\infty} \cos(\sigma_n x) e^{-\sigma_n^2 t} \int_0^1 \Phi_0(s, \xi) \cos(\sigma_n s) ds \end{aligned} \quad (11.5.47)$$

Multiplying (11.5.46) with $\cos(\sigma_n x)$ and using the orthogonality of these functions on $[0,1]$ we can rewrite the Φ -filter in the form

$$\begin{aligned} \Phi(x, \xi, t) = & -2 \sum_{n=0}^{\infty} \cos(\sigma_n x) \cos(\sigma_n \xi) \int_0^1 \cos(\sigma_n s) \phi(s, t) ds \\ & + 2 \sum_{n=0}^{\infty} \cos(\sigma_n x) e^{-\sigma_n^2 t} \int_0^1 \cos(\sigma_n s) \\ & \times (\phi_0(s) \cos(\sigma_n \xi) + \Phi_0(s, \xi)) ds. \end{aligned} \quad (11.5.48)$$

Here the first term represents the explicit solution of the system (11.5.39)–(11.5.42) and the second term is the effect of filters' initial conditions. Therefore we can represent Φ as

$$\Phi(x, \xi, t) = F(x, \xi, t) + \Delta F(x, \xi, t), \quad (11.5.49)$$

where ΔF satisfies

$$\Delta F_t = \Delta F_{xx} \quad (11.5.50)$$

$$\Delta F_x(0, \xi, t) = 0 \quad (11.5.51)$$

$$\Delta F(1, \xi, t) = 0, \quad (11.5.52)$$

and using (11.5.35)–(11.5.37) we get (11.5.43)–(11.5.45). \square

Lemma 11.2 allows us to avoid solving an infinite “array” of parabolic equations (11.5.28)–(11.5.30) by computing the solution of the standard wave equation (11.5.39)–(11.5.42) at each time step. Therefore we only have two dynamic equations to solve (filters ϕ and ψ).

11.6 Update laws

We take the following equation as a parametric model

$$\begin{aligned} e(0) &= v(0) - \psi(0) - \theta_1 \phi(0) - \int_0^1 \theta(\xi) F(0, \xi) d\xi \\ &= v(0) - \psi(0) - \theta_1 \phi(0) + \int_0^1 \theta(\xi) \phi(\xi) d\xi. \end{aligned} \quad (11.6.53)$$

The estimation error is

$$\hat{e}(0) = v(0) - \psi(0) - \hat{\theta}_1 \phi(0) + \int_0^1 \hat{\theta}(\xi) \phi(\xi) d\xi. \quad (11.6.54)$$

11.6.1 Gradient

We employ the gradient update laws with normalization

$$\hat{\theta}_t(x, t) = -\gamma(x) \frac{\hat{e}(0) \phi(x)}{1 + \|\phi\|^2 + \phi^2(0)} \quad (11.6.55)$$

$$\dot{\hat{\theta}}_1 = \gamma_1 \frac{\hat{e}(0) \phi(0)}{1 + \|\phi\|^2 + \phi^2(0)}, \quad (11.6.56)$$

where $\gamma(x)$ and γ_1 are positive adaptation gains.

Lemma 11.3. *The adaptive laws (11.6.55)–(11.6.56) guarantee the following properties:*

$$\frac{\hat{e}(0)}{\sqrt{1 + \|\phi\|^2 + \phi^2(0)}} \in \mathcal{L}_2 \cap \mathcal{L}_\infty \quad (11.6.57)$$

$$\|\tilde{\theta}\|, \tilde{\theta}_1 \in \mathcal{L}_\infty, \quad \|\hat{\theta}_t\|, \dot{\hat{\theta}}_1 \in \mathcal{L}_2 \cap \mathcal{L}_\infty. \quad (11.6.58)$$

□

Proof. Using a Lyapunov function

$$V = \frac{1}{2} \|e\|^2 + \frac{1}{2\gamma_1} \tilde{\theta}_1^2 + \int_0^1 \frac{\tilde{\theta}^2(x)}{2\gamma(x)} dx \quad (11.6.59)$$

we get

$$\begin{aligned} \dot{V} &= - \int_0^1 e_x^2 dx + \frac{\int_0^1 \tilde{\theta}(x) \phi(x) dx - \tilde{\theta}_1 \phi(0)}{1 + \|\phi\|^2 + \phi^2(0)} \hat{e}(0) \\ &\leq -\|e_x\|^2 + \frac{e(0) \hat{e}(0) - \hat{e}^2(0)}{1 + \|\phi\|^2 + \phi^2(0)} \\ &\leq -\|e_x\|^2 + \frac{\|e_x\| |\hat{e}(0)|}{\sqrt{1 + \|\phi\|^2 + \phi^2(0)}} \\ &\quad - \frac{\hat{e}^2(0)}{1 + \|\phi\|^2 + \phi^2(0)} \\ &\leq -\frac{1}{2} \|e_x\|^2 - \frac{1}{2} \frac{\hat{e}^2(0)}{1 + \|\phi\|^2 + \phi^2(0)}. \end{aligned} \quad (11.6.60)$$

This gives

$$\frac{\hat{e}(0)}{\sqrt{1 + \|\phi\|^2 + \phi^2(0)}} \in \mathcal{L}_2, \quad \|\tilde{\theta}\|, \tilde{\theta}_1 \in \mathcal{L}_\infty. \quad (11.6.61)$$

The rest of the properties (11.6.57)–(11.6.58) follows from the relation $\hat{e}(0) = e(0) + \tilde{\theta}_1\phi(0) - \int_0^1 \tilde{\theta}(x)\phi(x)dx$ and the update laws. \square

11.7 Main result

Theorem 11.4. *Consider the system (11.2.1)–(11.2.2) with the controller*

$$u(1) = \int_0^1 \left(\psi(y) + \hat{\theta}_1\phi(y) + \int_0^1 F(y, \xi)\hat{\theta}(\xi) d\xi \right) \hat{k}(1, y) dy \quad (11.7.62)$$

where $\hat{k}(x, y) = \hat{\kappa}(x - y)$ with $\hat{\kappa}(x)$ determined from

$$\hat{\kappa}'(x) = -\hat{\theta}_1\hat{\kappa}(x) - \hat{\theta}(x) + \int_0^x \hat{\kappa}(x - y)\hat{\theta}(y) dy \quad (11.7.63)$$

$$\hat{\kappa}(0) = \hat{\theta}_1, \quad (11.7.64)$$

the filters ϕ and ψ are given by (11.5.25)–(11.5.27), (11.5.31)–(11.5.33) and the update laws for $\hat{\theta}(x)$ and $\hat{\theta}_1$ are given by (11.6.55)–(11.6.56). If the closed loop system has a classical solution $(u, \phi, \psi, \hat{\theta}, \hat{\theta}_1)$ then for any $\hat{\theta}(x, 0)$, $\hat{\theta}_1(0)$ and any initial conditions $u_0, \phi_0, \psi_0 \in H_1(0, 1)$ the signals $\hat{\theta}(x, t)$, $\hat{\theta}_1$, $u(x, t)$, $\phi(x, t)$, $\psi(x, t)$ are bounded uniformly in x and $u(x, t)$ is regulated to zero:

$$\lim_{t \rightarrow \infty} \max_{x \in [0, 1]} |u(x, t)| = 0. \quad (11.7.65)$$

\square

The proof consists of several steps.

11.7.1 Target System

Denote

$$h(x) = \psi(x) + \hat{\theta}_1\phi(x) + \int_0^1 F(x, \xi)\hat{\theta}(\xi) d\xi \quad (11.7.66)$$

and use the following backstepping transformation

$$w(x) = h(x) - \int_0^x \hat{k}(x, y) h(y) dy := T[h](x). \quad (11.7.67)$$

Since we use certainty equivalence approach, the kernel $\hat{k}(x, y)$ is obtained from (11.4.14)–(11.4.16) simply by substituting parameter estimates instead of the unknown parameters. Therefore it is given by $\hat{k}(x, y) = \hat{\kappa}(x - y)$ with $\hat{\kappa}(x)$ defined by (11.7.63)–(11.7.64).

One can show that the inverse transformation to (11.7.67) is

$$h(x) = w(x) + \int_0^x \hat{l}(x, y) w(y) dy \quad (11.7.68)$$

where

$$\hat{l}(x, y) = \hat{\theta}_1 - \int_0^{x-y} \hat{\theta}(\xi) d\xi. \quad (11.7.69)$$

Using Lemma 11.2, the equations for the plant, filters ϕ and ψ , and the Volterra relationship between \hat{l} and \hat{k}

$$\hat{l}(x, y) = \hat{k}(x, y) + \int_y^x \hat{l}(x, \xi) \hat{k}(\xi, y) d\xi, \quad (11.7.70)$$

one can derive the following target system

$$\begin{aligned} w_t = & w_{xx} + \hat{e}(0) \hat{k}_y(x, 0) \\ & - \int_0^x w(y) \left(\hat{l}_t(x, y) - \int_y^x \hat{k}(x, \xi) \hat{l}_t(\xi, y) d\xi \right) dy \\ & + \dot{\hat{\theta}}_1 T[\phi] + T \left[\int_0^1 F(x, \xi) \hat{\theta}_t(\xi) d\xi \right] \end{aligned} \quad (11.7.71)$$

$$w_x(0) = \hat{\theta}_1 \hat{e}(0) \quad (11.7.72)$$

$$w(1) = 0. \quad (11.7.73)$$

Compared to the nominal target system (11.4.17)–(11.4.19), two types of additional terms appear. First, there are terms with $\hat{e}(0)$ both in the equation and in the boundary condition. Second, there are terms that are proportional to time derivatives of the parameter estimates.

Let us rewrite ϕ filter as follows:

$$\phi_t = \phi_{xx} \quad (11.7.74)$$

$$\phi_x(0) = w(0) + \hat{e}(0) \quad (11.7.75)$$

$$\phi(1) = 0 \quad (11.7.76)$$

We now have interconnection of two systems ϕ and w with forcing terms that have properties (11.6.57)–(11.6.58).

11.7.2 Boundedness in $L_2(0, 1)$

First, let us establish bounds on the gains $\hat{k}(x, y)$ and $\hat{l}(x, y)$. The boundedness of the parameter estimates $\hat{\theta}_1$ and $\|\hat{\theta}\|$ has been shown in Lemma 11.3. From (11.7.69) we get

$$|\hat{l}(x, y)| \leq \bar{\theta}_1 + \bar{\theta}, \quad (11.7.77)$$

where we denote $\bar{\theta}_1 = \max_{t \geq 0} |\hat{\theta}_1|$ and $\bar{\theta} = \max_{t \geq 0} \|\hat{\theta}\|$.

Using (11.7.70) and Gronwall inequality it is easy to get the following bound

$$|\hat{k}(x, y)| \leq (\bar{\theta}_1 + \bar{\theta})e^{\bar{\theta}_1 + \bar{\theta}} := K_1 \quad (11.7.78)$$

If we look at the right hand side of the w -system, we can see that the estimates for $\hat{k}_y(x, 0)$ and $\hat{l}_t(x, y)$ are also needed. They are readily obtained from (11.7.63) and (11.7.69):

$$|\hat{k}_y(x, 0)| \leq (\bar{\theta}_1 + \bar{\theta})K_1 + \bar{\theta} := K_2 \quad (11.7.79)$$

$$|\hat{l}_t(x, y)| \leq |\dot{\hat{\theta}}_1| + \|\dot{\hat{\theta}}\|. \quad (11.7.80)$$

We are now ready to start with stability analysis of (11.7.71)–(11.7.76). Consider a Lyapunov function

$$V_1 = \frac{1}{2} \int_0^1 \phi^2 dx. \quad (11.7.81)$$

Computing its derivative along the solutions of ϕ -system and using Young, Poincare, and Agmon inequalities, we get

$$\begin{aligned}
\dot{V}_1 &= \int_0^1 \phi \phi_t dx \\
&= -\phi(0)w(0) - \phi(0)\hat{e}(0) - \int_0^1 \phi_x^2 dx \\
&\leq \frac{1}{2}w^2(0) + \frac{1}{2}\phi^2(0) - \|\phi_x\|^2 \\
&\quad + \frac{|\phi(0)\hat{e}(0)|}{1 + \|\phi\|^2 + \phi^2(0)}(1 + \|\phi\|^2 + 2\|\phi\|\|\phi_x\|) \\
&\leq -\frac{1}{2}\|\phi_x\|^2 + \frac{1}{2}\|w_x\|^2 + c_1\|\phi_x\|^2 \\
&\quad + \frac{1}{4c_1} \frac{\hat{e}^2(0)}{1 + \|\phi\|^2 + \phi^2(0)} + \frac{c_1}{4}\|\phi\|^2 + c_1\|\phi_x\|^2 \\
&\quad + \frac{3}{c_1} \left(\frac{|\phi(0)\hat{e}(0)|}{1 + \|\phi\|^2 + \phi^2(0)} \right)^2 \|\phi\|^2 \\
&\leq -\left(\frac{1}{2} - 3c_1\right) \|\phi_x\|^2 + \frac{1}{2}\|w_x\|^2 + l_1\|\phi\|^2 + l_1. \tag{11.7.82}
\end{aligned}$$

Here c_1 is a positive constant that will be chosen later and l_1 denotes a generic bounded and square integrable function of time.

With a Lyapunov function

$$V_2 = \frac{1}{2} \int_0^1 w^2 dx \tag{11.7.83}$$

we get

$$\begin{aligned}
\dot{V}_2 &= \int_0^1 w w_t dx \\
&= -\hat{\theta}_1 w(0)\hat{e}(0) + \hat{e}(0) \int_0^1 \hat{k}_y(x, 0)w(x) dx \\
&\quad - \int_0^1 w_x^2 dx + \dot{\hat{\theta}}_1 \int_0^1 w(x)T[\phi](x) dx \\
&\quad + \int_0^1 w(x)T \left[\int_0^1 F(x, \xi)\hat{\theta}_t(\xi) d\xi \right] dx \\
&\quad + \int_0^1 w(x) \int_0^x w(y) \\
&\quad \times \left(\hat{l}_t(x, y) - \int_y^x \hat{k}(x, \xi)\hat{l}_t(\xi, y) d\xi \right) dy dx \tag{11.7.84}
\end{aligned}$$

We separately estimate each term on the right hand side of (11.7.84). Term 1:

$$\begin{aligned}
|\hat{\theta}_1 w(0) \hat{e}(0)| &\leq \frac{\bar{\theta}_1 |w(0)| |\hat{e}(0)|}{\sqrt{1 + \|\phi\|^2 + \phi^2(0)}} (1 + \|\phi\| + |\phi(0)|) \\
&\leq c_2 \|w_x\|^2 + \frac{\bar{\theta}_1^2}{c_2} \frac{\hat{e}^2(0)(1 + \|\phi\|^2)}{1 + \|\phi\|^2 + \phi^2(0)} \\
&\quad + \frac{\bar{\theta}_1 \hat{e}(0)(\|w\| \|w_x\| + \|\phi\| \|\phi_x\|)}{\sqrt{1 + \|\phi\|^2 + \phi^2(0)}} \\
&\leq c_2 \|w_x\|^2 + l_1 (1 + \|\phi\|^2) + c_3 \|w_x\|^2 \\
&\quad + \frac{\bar{\theta}_1^2 l_1}{4c_3} \|w\|^2 + c_4 \|\phi_x\|^2 + \frac{\bar{\theta}_1^2 l_1}{4c_4} \|\phi\|^2 \\
&\leq (c_2 + c_3) \|w_x\|^2 + c_4 \|\phi_x\|^2 \\
&\quad + l_1 \|w\|^2 + l_1 \|\phi\|^2 + l_1, \tag{11.7.85}
\end{aligned}$$

Term 2:

$$\begin{aligned}
&\hat{e}(0) \int_0^1 \hat{k}_y(x, 0) w(x) dx \\
&\leq K_2 \|w\| \frac{|\hat{e}(0)| (1 + \|\phi\| + |\phi(0)|)}{\sqrt{1 + \|\phi\|^2 + \phi^2(0)}} \\
&\leq c_5 \|w\|^2 + \frac{K_2 l_1}{c_5} (1 + \|\phi\|^2) + c_6 \|\phi_x\|^2 + \frac{K_2 l_1}{2c_6} \|w\|^2 \\
&\leq 4c_5 \|w_x\|^2 + c_6 \|\phi_x\|^2 + l_1 \|w\|^2 + l_1 \|\phi\|^2 + l_1, \tag{11.7.86}
\end{aligned}$$

Term 3:

$$\begin{aligned}
\dot{\theta}_1 \int_0^1 w(x) T[\phi](x) dx &\leq c_7 \|w\|^2 + \frac{(1 + K_1^2)}{2c_7} |\dot{\theta}_1|^2 \|\phi\|^2 \\
&\leq 4c_7 \|w_x\|^2 + l_1 \|\phi\|^2, \tag{11.7.87}
\end{aligned}$$

Term 4:

$$\begin{aligned}
& \int_0^1 w(x) T \left[\int_0^1 F(x, \xi) \hat{\theta}_t(\xi) d\xi \right] dx \\
& \leq (1 + K_1) \|w\| \|\hat{\theta}_t\| \left(\int_0^1 \max_{\xi} F^2(x, \xi) dx \right)^{1/2} \\
& \leq \frac{(1 + K_1)^2}{c_8} \|w\|^2 \|\hat{\theta}_t\|^2 \\
& \quad + c_8 \int_0^1 (F^2(x, 1) + 2\|F(x, \cdot)\| \|F_{\xi}(x, \cdot)\|) dx \\
& \leq l_1 \|w\|^2 + c_8 \int_0^1 \int_0^1 (F^2(x, \xi) + F_{\xi}^2(x, \xi)) d\xi dx \\
& \leq l_1 \|w\|^2 + c_8 \int_0^1 \phi^2(\xi) d\xi \\
& \quad + c_8 \int_0^1 \int_0^1 (F_x^2(x, \xi) + F_{\xi}^2(x, \xi)) d\xi dx \\
& \leq l_1 \|w\|^2 + c_8 (\|\phi\|^2 + \|\phi_x\|^2), \tag{11.7.88}
\end{aligned}$$

Term 5:

$$\begin{aligned}
& \int_0^1 w(x) \int_0^x w(y) \left(\hat{l}_t(x, y) - \int_y^x \hat{k}(x, \xi) \hat{l}_t(\xi, y) d\xi \right) dy dx \\
& \leq 2c_9 \|w\|^2 + \frac{1 + K_1^2}{2c_9} |\dot{\hat{\theta}}_1|^2 \|w\|^2 + \frac{1 + K_2^2}{2c_9} \|\hat{\theta}_t\|^2 \|w\|^2 \\
& \leq 8c_9 \|w_x\|^2 + l_1 \|w\|^2. \tag{11.7.89}
\end{aligned}$$

Finally, we obtain

$$\begin{aligned}
\dot{V}_2 & \leq (c_4 + c_6 + 5c_8) \|\phi_x\|^2 + l_1 \|w\|^2 + l_1 \|\phi\|^2 + l_1 \\
& \quad - (1 - c_2 - c_3 - 4c_5 - 4c_7 - 8c_9) \|w_x\|^2. \tag{11.7.90}
\end{aligned}$$

Using (11.7.82) and (11.7.90), for the Lyapunov function

$$V = V_1 + V_2 \tag{11.7.91}$$

we get

$$\begin{aligned}
\dot{V} & \leq - \left(\frac{1}{2} - c_2 - c_3 - 4c_5 - 4c_7 - 8c_9 \right) \|w_x\|^2 \\
& \quad - \left(\frac{1}{2} - 3c_1 - c_4 - c_6 - 5c_8 \right) \|\phi_x\|^2 \\
& \quad + l_1 \|w\|^2 + l_1 \|\phi\|^2 + l_1. \tag{11.7.92}
\end{aligned}$$

Choosing $c_2 = c_3 = 4c_5 = 4c_7 = 8c_9 = 1/20$, $3c_1 = c_4 = c_6 = 5c_8 = 1/16$, we get

$$\dot{V} \leq -\frac{1}{8}V + l_1V + l_1 \quad (11.7.93)$$

and by Lemma 7.2 we get $\|w\|, \|\phi\| \in \mathcal{L}_2 \cap \mathcal{L}_\infty$. From the transformation (11.7.68) we get $\|h\| \in \mathcal{L}_2 \cap \mathcal{L}_\infty$ and therefore $\|\psi\| \in \mathcal{L}_2 \cap \mathcal{L}_\infty$ follows from (11.7.66). From (11.5.38) and (11.3.4) we get $\|v\|, \|u\| \in \mathcal{L}_2 \cap \mathcal{L}_\infty$.

11.7.3 Pointwise Boundedness

In order to prove pointwise boundedness we need to show that $\|w_x\|$ and $\|\phi_x\|$ are bounded. Unfortunately, using the standard Lyapunov function of the form $V = \|w_x\|^2 + \|\phi_x\|^2$ does not lead anywhere in this case. The difficulty lies in the fact that systems (11.7.71)–(11.7.76) have the term $\hat{e}(0)$ in the boundary condition at $x = 0$. This term will produce the terms proportional to $\dot{\hat{e}}(0)$ in \dot{V} and the properties of this signal are not known to us. Therefore the following idea comes to mind: we can design the integral transformation (only for the purpose of proof) to convert (11.7.71)–(11.7.76) into a system with homogeneous boundary conditions. Let

$$\bar{w}(x) = w(x) - \hat{\theta}_1(1-x) \int_0^x \hat{e}(y) dy \quad (11.7.94)$$

$$\bar{\phi}(x) = \phi(x) - (1-x) \int_0^x (\hat{e}(y) + w(y)) dy. \quad (11.7.95)$$

Then \bar{w} and $\bar{\phi}$ satisfy

$$\begin{aligned} \bar{w}_t = & \bar{w}_{xx} - 2\hat{\theta}_1\hat{e}(x) + \hat{\theta}_1\tilde{\theta}_1(1-x)(\bar{w}(0) + \hat{e}(0)) \\ & - \dot{\hat{\theta}}_1(1-x) \int_0^x \hat{e}(y) dy + A(x) - \hat{\theta}_1(1-x) \int_0^x B(y) dy \end{aligned} \quad (11.7.96)$$

$$\bar{w}_x(0) = 0 \quad (11.7.97)$$

$$\bar{w}(1) = 0. \quad (11.7.98)$$

$$\begin{aligned}\bar{\phi}_t &= \bar{\phi}_{xx} - 2\hat{e}(x) - 2w(x) + (1-x)\theta_1\hat{e}(0) + (1-x)\tilde{\theta}_1\bar{w}(0) \\ &\quad - (1-x) \int_0^x (A(y) + B(y)) dy\end{aligned}\quad (11.7.99)$$

$$\bar{\phi}_x(0) = 0 \quad (11.7.100)$$

$$\bar{\phi}(1) = 0. \quad (11.7.101)$$

Here $A(x)$ is the right hand side of (11.7.71) without w_{xx} , i.e., $A(x) = A[w, \phi](x) = w_t - w_{xx}$ and

$$B(x) = \hat{e}_t - \hat{e}_{xx} = \tilde{\theta}(x)(\bar{w}(0) + \hat{e}(0)) - \dot{\hat{\theta}}_1\phi(x) - \int_0^1 \hat{\theta}_t(y)F(x, y) dy \quad (11.7.102)$$

With

$$V = \frac{1}{2}\|\bar{w}\|^2 + \frac{1}{2}\|\bar{\phi}\|^2 \quad (11.7.103)$$

one can show in the same way as in previous section that

$$\dot{V} \leq -\frac{1}{8}V + l_1V + l_1 \quad (11.7.104)$$

and therefore by Lemma 7.2 $\|\bar{w}_x\|, \|\bar{\phi}_x\| \in \mathcal{L}_2 \cap \mathcal{L}_\infty$. Using the fact that $\|\hat{e}\| \in \mathcal{L}_2 \cap \mathcal{L}_\infty$, from (11.7.94)–(11.7.95) we get $\|w_x\|, \|\phi_x\| \in \mathcal{L}_2 \cap \mathcal{L}_\infty$. By Agmon inequality, $w(x, t)$ and $\phi(x, t)$ are bounded for all $x \in [0, 1]$.

11.7.4 Regulation

It is easy to see from (11.7.93) that \dot{V} is bounded from above. Using Lemma 7.1 we get $V \rightarrow 0$, that is $\|\hat{w}\| \rightarrow 0, \|\phi\| \rightarrow 0$. From the transformation (11.7.68) we get $\|h\| \rightarrow 0$ and from (11.7.66) $\|\psi\| \rightarrow 0$ follows. From (11.5.38) and (11.3.4) we get $\|v\| \rightarrow 0$ and $\|u\| \rightarrow 0$. By Agmon inequality we get $\max_{x \in [0, 1]} |u(x, t)| \rightarrow 0$. The proof of Theorem 11.4 is completed.

11.8 Output Tracking

Consider the plant (11.2.1)–(11.2.2) and suppose we want the output $u(0, t)$ to follow a prescribed trajectory $r(t)$ (we assume that it is analytic and

bounded). Transforming the plant into observer canonical form (11.3.8)–(11.3.10) we reformulate the objective as $v(0, t) \rightarrow r(t)$. If the parameters $\theta(x)$ and θ_1 were known, the design would consist of two steps. First, the trajectory $v^r(x, t)$ should be generated such that $v^r(0, t) = r(t)$ and v^r satisfies (11.3.8)–(11.3.9). The second step is to stabilize the plant around this trajectory. However, in the case of unknown parameters the trajectory v^r cannot be generated. Therefore, our approach is to generate the trajectory $w^r(x, t)$ for the nominal *target* system. We have three conditions:

$$w_t^r = w_{xx}^r \quad (11.8.105)$$

$$w_x^r(0) = 0 \quad (11.8.106)$$

$$w^r(0) = r(t). \quad (11.8.107)$$

The well known solution to (11.8.105)–(11.8.107) is (see, e.g. [39])

$$w^r(x, t) = \sum_{n=0}^{\infty} \frac{r^{(n)}(t)x^{2n}}{(2n)!}, \quad (11.8.108)$$

which can be easily verified by direct substitution.

Note that the series (11.8.108) can be computed in closed form if $r(t)$ is a combination of exponentials, polynomials, and sinusoids, which covers all practically relevant trajectories. For example, for $r(t) = A \sin(\omega t)$ the reference trajectory is

$$\begin{aligned} w^r(x, t) &= \frac{A}{2} e^{\sqrt{\frac{\omega}{2}}x} \sin\left(\omega t + \sqrt{\frac{\omega}{2}}x\right) \\ &\quad + \frac{A}{2} e^{-\sqrt{\frac{\omega}{2}}x} \sin\left(\omega t - \sqrt{\frac{\omega}{2}}x\right). \end{aligned} \quad (11.8.109)$$

Theorem 11.5. *Consider the system (11.2.1)–(11.2.2) with the controller*

$$\begin{aligned} u(1) &= \sum_{n=0}^{\infty} \frac{r^{(n)}(t)}{(2n)!} + \int_0^1 \left(\psi(y) + \hat{\theta}_1 \phi(y) \right. \\ &\quad \left. + \int_0^1 \hat{\theta}(\xi) F(y, \xi) d\xi \right) \hat{\kappa}(1-y) dy \end{aligned} \quad (11.8.110)$$

where $r(t)$ is bounded analytic function for $t \geq 0$ and let the conditions of Theorem 11.4 be satisfied. Then for any $\hat{\theta}(x, 0)$, $\hat{\theta}_1(0)$ and any initial conditions $u_0, \phi_0, \psi_0 \in L^2(0, 1)$ the signals $\|\hat{\theta}\|$, $\hat{\theta}_1$, $\|u\|$, $\|\phi\|$, $\|\psi\|$ are bounded and

$$\lim_{t \rightarrow \infty} u(0, t) = r(t). \quad (11.8.111)$$

□

Proof. We only outline the proof. First we introduce the error variable $\tilde{w} = \hat{w} - w^r$. The adaptive target system (11.7.71)–(11.7.73) is then rewritten in the new variables and after the analysis similar to the one given in the proof of Theorem 11.4 we get $\max_{x \in [0, 1]} |\tilde{w}(x, t)| \rightarrow 0$ so that $\hat{w}(0, t) \rightarrow r(t)$. Then using the relationship $u(0) = \hat{w}(0) + \hat{e}(0)$ we get $u(0) \rightarrow r(t)$. □

11.9 Reaction-Advection-Diffusion Systems

The approach presented in the paper can also be applied to general reaction–advection–diffusion system

$$\begin{aligned} u_t &= \varepsilon(x)u_{xx} + b(x)u_x + \lambda(x)u \\ &\quad + g(x)u(0) + \int_0^x f(x, y)u(y) dy \end{aligned} \quad (11.9.112)$$

$$u_x(0) = -qu(0), \quad (11.9.113)$$

where $\varepsilon(x)$, $b(x)$, $\lambda(x)$, $g(x)$, $f(x, y)$, q are unknown parameters.

The parameters $g(x)$, $f(x, y)$, and q can be easily handled because the observer canonical form (11.3.8)–(11.3.10) is not changed in this case, only the PDE (11.3.5)–(11.3.7) and expressions (11.3.11) and (11.3.12) for the new unknown parameters are modified. Since we are not concerned with identification, the adaptive scheme stays exactly the same.

With unknown parameters $b(x)$ and $\varepsilon(x)$, however, additional difficulties

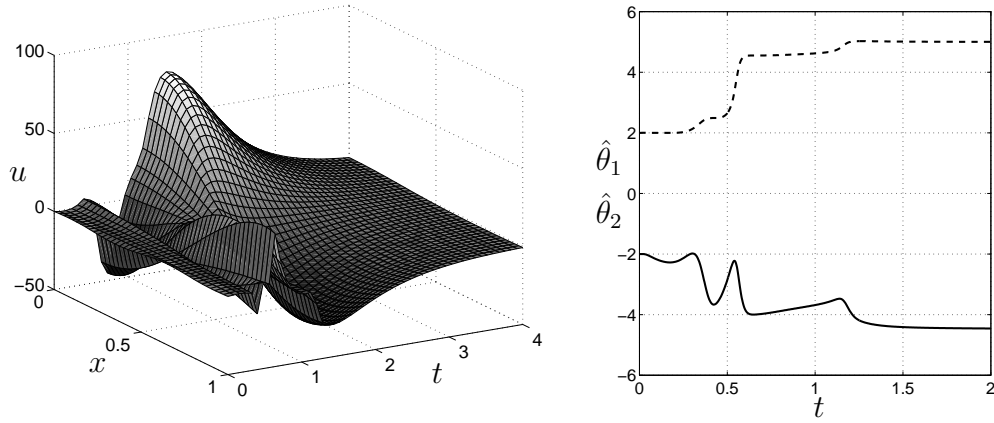


Figure 11.1: Left: The closed loop state $u(x, t)$. Right: The parameter estimates $\hat{\theta}_1(t)$ (solid) and $\hat{\theta}_2(t)$ (dashed).

arise. The observer canonical form is changed to

$$v_t = \theta_0 v_{xx} + \theta(x)v(0) \quad (11.9.114)$$

$$v_x(0) = \theta_1 v(0) \quad (11.9.115)$$

$$v(1) = \theta_2 u(1) \quad (11.9.116)$$

where the new constant parameters θ_0 and θ_2 appear due to $\varepsilon(x)$ and $b(x)$ respectively. We can see that one of the issues is the need of projection to keep the estimate of θ_2 positive since the filters should be stable and the controller is given as $u(1) = \hat{\theta}_2^{-1}v(1)$. This issue, although making the closed loop stability proof more challenging, does not pose a conceptual problem. The real difficulty comes from the fact that the parameter θ_0 , which comes from the unknown $\varepsilon(x)$, multiplies the second derivative of the state which is not measured. Therefore, while an unknown $b(x)$ is allowed, $\varepsilon(x)$ should be known.

11.10 Simulations

We now present the results of numerical simulations of the designed adaptive scheme. The parameters of the plant (11.9.112)–(11.9.113) are taken to be

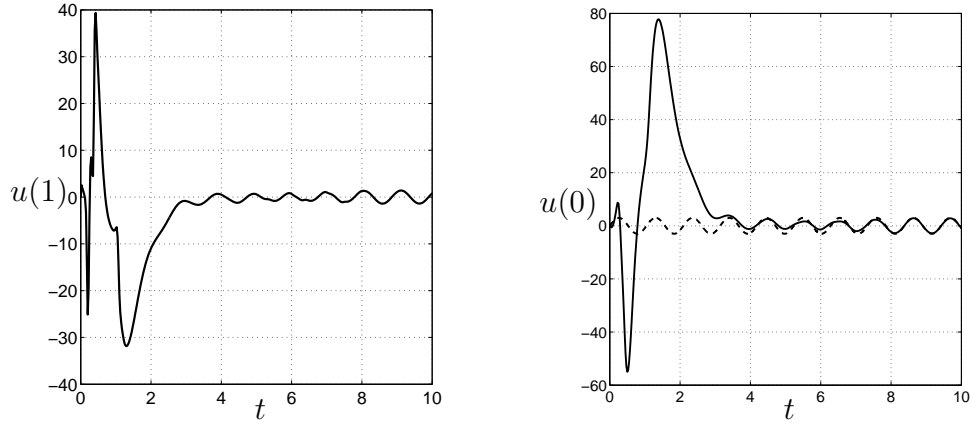


Figure 11.2: Left: The control effort for the adaptive tracking. Right: Reference signal at the boundary (dashed) and actual evolution of the output (solid).

$b(x) = 3 - 2x^2$ and $\lambda(x) = 16 + 3 \sin(2\pi x)$, $\varepsilon \equiv 1$, $g(x) = q = 0$, so that the plant is unstable. The evolution of the closed loop state is shown in Fig. 11.1. We can see that the regulation is achieved. The parameter estimates, shown in Fig. 11.1, converge to some stabilizing values.

For the second simulation, we set an objective to track the reference trajectory $u^r(0, t) = 3 \sin(6t)$. The control effort and output evolution are shown in Fig. 11.2. We can see that after the initial transient the output follows the desired trajectory.

This chapter is in part a reprint of the material as it appears in A. Smyshlyaev and M. Krstic, “Output-Feedback Adaptive Control for Parabolic PDEs with Spatially Varying Coefficients,” *2006 Conference on Decision and Control*.

The dissertation author was the primary author and the coauthor listed in this publication directed the research which forms the basis for this chapter.

Chapter 12

Future Work

The results presented in this dissertation provide the backbone for the further application of the backstepping method to the endless new problems in the control of the distributed parameter systems.

We present several possible directions of future research that extend the methodology in a natural way.

1. While the backstepping method has been applied to 1D hyperbolic PDEs (strings and beams), the development of the controllers for higher dimensional hyperbolic systems is still an open problem. For example, one would like to extend the approach to plates and shells, which has important applications (for instance, noise attenuation and aeroelasticity).
2. The backstepping approach was successful in handling 2D and 3D distributed systems with constant parameters. However, the more realistic case, when the physical parameters of the problem vary throughout the domain (for example, due to inhomogeneous media) is still an open problem.
3. So far, our efforts were mostly concentrated on second order (in space) PDEs (heat and wave equations). The Korteweg-de-Vries and Kuramoto-Sivashinsky equations are the standard representatives of 3rd and 4th order problems and are the next frontier for boundary control design. They arise

in models of shallow water waves, flamefront, and thin film instabilities and will be approached using tools that we recently developed for control of elastic beam models (fourth order in space), which have potential applications in atomic force microscopy.

4. The stabilization of nonlinear PDEs (of which the most challenging are Navier-Stokes equations) is a formidable problem for any control method. The backstepping approach allows state-dependent gain scheduling and, on the more theoretical side, the construction of feedback laws in the form of spatial Volterra series operators. The problem of nonlinear observer design is amenable to the same treatment and presents some pioneering opportunities in state estimation for nonlinear PDEs.
5. Classical results for finite-dimensional systems with actuator delays can be extended to PDEs with actuator, sensor, and distributed delays.
6. Some very challenging problems such as control of interconnected systems of PDEs (and ODEs) become tractable with the approach presented in this dissertation. One can imagine a graph of beams or irrigation canals connected through their ends. Such problems will be approached by generalization of the backstepping procedure to systems of several PDEs of a special, "strict-feedback" structure.
7. So far the adaptive boundary controllers have been developed only for reaction-advection-diffusion PDEs. The next natural step is to design the adaptive controllers for structural/acoustic systems.
8. Possible applications include such problems as channel flow turbulence, atomic force microscopy, noise attenuation, aeroelasticity, and plasma stabilization in fusion reactors.

Bibliography

- [1] M.J. Ablowitz, M.D. Kruskal, J.F. Ladik, "Solitary wave collisions," *SIAM J. Appl. Math.*, vol. 36, no. 3, pp. 428-37, June 1979.
- [2] H. Amann, "Feedback stabilization of linear and semilinear parabolic systems," in *Semigroup theory and applications*, (Trieste, 1987), pp. 21-57, Lecture Notes in Pure and Appl. Math., 116, Dekker, New York, 1989.
- [3] A. Balogh and M. Krstic, "Infinite dimensional backstepping-style feedback transformations for a heat equation with an arbitrary level of instability," *European Journal of Control*, vol. 8, pp. 165-175, 2002.
- [4] A. Balogh and M. Krstic, "Stability of partial differential equations governing control gains in infinite dimensional backstepping," *Systems and Control Letters*, vol. 51, no. 2, pp. 151-164, 2004.
- [5] B. Bamieh, F. Paganini and M.A. Dahleh, "Distributed Control of Spatially-Invariant Systems," *IEEE Trans. Automatic Control*, vol. 47, pp. 1091-1107, 2002.
- [6] J. Baumeister, W. Scondo, M. A. Demetriou, and I. G. Rosen, "On-Line Parameter Estimation For Infinite-Dimensional Dynamical Systems," *SIAM J. Control Optim.*, Vol. 35, No. 2, pp. 678-713, 1997.
- [7] A. Bensoussan, G. Da Prato, M.C. Delfour and S.K. Mitter, *Representation and control of infinite-dimensional systems. Vol. II. Systems & Control: Foundations & Applications*. Birkhauser Boston, Inc., Boston, MA, 1993.
- [8] J. Bentsman and Y. Orlov, "Reduced spatial order model reference adaptive control of spatially varying distributed parameter systems of parabolic and hyperbolic types," *Int. J. Adapt. Control Signal Process.* vol. 15, pp. 679-696, 2001.
- [9] M. Bohm, M. A. Demetriou, S. Reich, and I. G. Rosen, "Model reference adaptive control of distributed parameter systems," *SIAM J. Control Optim.*, Vol. 36, No. 1, pp. 33-81, 1998.

- [10] D. M. Boskovic and M. Krstic, "Stabilization of a solid propellant rocket instability by state feedback," *Int.J. of Robust and Nonlinear Control*, vol. 13, No. 5, pp. 483-95, 2003.
- [11] D. M. Boskovic and M. Krstic, "Nonlinear stabilization of a thermal convection loop by state feedback," *Automatica*, 37, pp. 2033-2040, 2001.
- [12] D. M. Boskovic and M. Krstic, "Backstepping control of chemical tubular reactors," *Computers and Chemical Engineering*, 26, pp. 1077-1085, 2002.
- [13] D. M. Boskovic, M. Krstic, and W. J. Liu, "Boundary control of an unstable heat equation via measurement of domain-averaged temperature," *IEEE Transactions on Automatic Control*, vol. 46, No. 12, pp. 2022-8, Dec. 2001.
- [14] J.A. Burns and K.P. Hulsing, "Numerical methods for approximating functional gains in LQR boundary control problems," *Mathematical and Computer Modeling*, 33, pp. 89-100, 2001.
- [15] J. A. Burns and D. Rubio, "A distributed parameter control approach to sensor location for optimal feedback control of thermal processes," *Proc. 36th Conf. Decision and Control*, San Diego, CA, Dec. 1997, pp. 2243-2247.
- [16] H. S. Carslaw and J. C. Jaeger, *Conduction of Heat in Solids*, Oxford, Clarendon Press, 1959.
- [17] P. Christofides, *Nonlinear and Robust Control of Partial Differential Equation Systems: Methods and Applications to Transport-Reaction Processes*, Boston: Birkhäuser, 2001.
- [18] D. Colton, "The solution of initial-boundary value problems for parabolic equations by the method of integral operators," *Journal of Differential Equations*, vol. 26, pp. 181-190, 1977.
- [19] R.F. Curtain, "Robust stabilizability of normalized coprime factors: the infinite-dimensional case," *Int. J. Control*, Vol. 51, No. 6, pp. 1173-1190, 1990.
- [20] R. F. Curtain and H. J. Zwart, *An Introduction to Infinite Dimensional Linear Systems Theory*, Springer-Verlag, 1995.
- [21] L. Debnath, *Nonlinear Partial Differential Equations for Scientists and Engineers*, Birkhäuser, 1997.
- [22] M. A. Demetriou and I. G. Rosen, "On-line robust parameter identification for parabolic systems," *Int. J. Adapt. Control Signal Process.* vol. 15, pp. 615-631, 2001.

- [23] M. A. Demetriou and I. G. Rosen, "Variable Structure Model Reference Adaptive Control of Parabolic Distributed Parameter Systems," *Proceedings of the American Control Conference Anchorage, AK*, May 2002.
- [24] M. A. Demetriou and K. Ito, "Optimal on-line parameter estimation for a class of infinite dimensional systems using Kalman filters," *Proceedings of the American Control Conference*, 2003.
- [25] M. S. de Queiroz, D. M. Dawson, M. Agarwal, and F. Zhang, "Adaptive nonlinear boundary control of a flexible link robot arm," *IEEE Trans. Robotics and Automation*, vol. 15, pp. 779–787, 1999.
- [26] T. E. Duncan, B. Maslowski, and B. Pasik-Duncan, "Adaptive boundary and point control of linear stochastic distributed parameter systems," *SIAM J. Control Optim.*, vol. 32, no. 3, pp. 648–672, 1994.
- [27] H. O. Fattorini, "Boundary control systems," *SIAM J. Control*, Vol. 6, No. 3, pp. 349–385, 1968.
- [28] N. Fuji, "Feedback stabilization of distributed parameter systems by a functional observer," *SIAM J. Control Optim.*, 18, pp. 108–121, 1980.
- [29] K. S. Hong and J. Bentsman, "Direct adaptive control of parabolic systems: Algorithm synthesis, and convergence, and stability analysis," *IEEE Trans. Automatic Control*, vol. 39, pp. 2018–2033, 1994.
- [30] P. Ioannou and J. Sun, *Robust Adaptive Control*, Prentice Hall, 1996.
- [31] M. Jovanovic and B. Bamieh, "Lyapunov-based distributed control of systems on lattices," *IEEE Trans. Automatic Control*, 50, pp. 422–433, 2005.
- [32] T. Kobayashi, "Adaptive regulator design of a viscous Burgers' system by boundary control," *IMA Journal of Mathematical Control and Information*, vol. 18, pp. 427–437, 2001.
- [33] T. Kobayashi, "Adaptive stabilization of the Kuramoto-Sivashinsky equation," *Int. J. Systems Science*, vol. 33, pp. 175–180, 2002.
- [34] A. J. Krener and W. Kang, "Locally convergent nonlinear observers," *SIAM J. Control Optim.*, vol. 42, No. 1, pp. 155–177, 2003.
- [35] H. Khalil, *Nonlinear Systems*, 2nd ed., Prentice-Hall, 1996.
- [36] M. Krstic, I. Kanellakopoulos, and P. Kokotovic, *Nonlinear and Adaptive Control Design*, Wiley, New York, 1995.
- [37] M. Krstic and H. Deng, *Stabilization of Nonlinear Uncertain Systems*, Springer-Verlag, 1998.

- [38] M. Krstic, “Adaptive Boundary Control for Unstable Parabolic PDEs—Part I: Lyapunov Design,” submitted to *IEEE Transactions on Automatic Control*, 2005.
- [39] B. Laroche, P. Martin, and P. Rouchon, “Motion planning for the heat equation,” *Int. J. Robust Nonlinear Control*, vol. 10, pp. 629–643, 2000.
- [40] I. Lasiecka and R. Triggiani, “Stabilization and structural assignment of Dirichlet boundary feedback parabolic equations,” *SIAM J. Control Optim.*, Vol. 21, No. 5, pp. 766–803, 1983.
- [41] I. Lasiecka, R. Triggiani, *Control Theory for Partial Differential Equations: Continuous and Approximation Theories, vol. 1*, Cambridge Univ. Press, Cambridge, UK, 2000.
- [42] W. J. Liu, “Boundary feedback stabilization of an unstable heat equation,” *SIAM J. Control Optim.*, vol. 42, No. 3, pp. 1033–1043.
- [43] W. Liu and M. Krstic, “Adaptive control of Burgers’ equation with unknown viscosity,” *Int. J. Adapt. Contr. Sig. Proc.*, vol. 15, pp. 745–766, 2001.
- [44] H. Logemann and S. Townley, “Adaptive stabilization without identification for distributed parameter systems: An overview,” *IMA J. Math. Control and Information*, vol. 14, pp. 175–206, 1997.
- [45] H. Logemann, “Stabilization and regulation of infinite-dimensional systems using coprime factorizations,” in *Analysis and optimization of systems: state and frequency domain approaches for infinite-dimensional systems* (Sophia-Antipolis, 1992), pp. 102–139, Lecture Notes in Control and Inform. Sci., 185, Springer, Berlin, 1993.
- [46] T. Nambu, “On the stabilization of diffusion equations: boundary observation and feedback,” *Journal of Differential Equations*, Vol. 52, pp. 204–233, 1984.
- [47] A. W. Naylor, G. R. Sell, *Linear Operator Theory in Engineering and Science*, Springer-Verlag, New York, 1982.
- [48] Y. Orlov, “Sliding mode observer-based synthesis of state derivative-free model reference adaptive control of distributed parameter systems,” *J. of Dynamic Syst. Meas. Contr.*, vol. 122, pp. 726–731, 2000.
- [49] A. D. Polyanin, *Handbook of linear partial differential equations for engineers and scientists*, Boca Raton, Fla. : Chapman & Hall/CRC, 2002.
- [50] A.P. Prudnikov, Yu.A. Brychkov, O.I. Marichev, *Integrals and Series, vol. 2: Special Functions*, New York : Gordon and Breach Science Publishers, 1986.

- [51] D.L. Russell “Controllability and stabilizability theory for linear partial differential equations: recent progress and open questions,” *SIAM Review*, Vol. 20, No. 4, pp. 639–739, 1978.
- [52] D.L. Russell, “Differential–delay equations as canonical forms for controlled hyperbolic systems with applications to spectral assignment,” *Proc. Conf. Contr. Theory of Distr. Parameter Systems*, Naval Surface Weapons Center, White Oak, MD, June 1976, published as *Control theory of systems governed by partial differential equations*, A.K. Aziz, J.W. Wingate, M.J. Balas, eds., Academic Press, New York, 1977.
- [53] T. I. Seidman, “Two results on exact boundary control of parabolic equations,” *Applied Mathematics and Optimization*, vol. 11, pp. 145–152, 1984.
- [54] A.D. Polianin, *Handbook of Linear Partial Differential Equations for Engineers and Scientists*, Boca Raton, Fla, Chapman and Hall/CRC, 2002.
- [55] A. Smyshlyaev and M. Krstic, “Closed form boundary state feedbacks for a class of 1D partial integro-differential equations,” *IEEE Trans. on Automatic Control*, Vol. 49, No. 12, pp. 2185–2202, 2004.
- [56] A. Smyshlyaev and M. Krstic, “Backstepping observers for a class of parabolic PDEs,” *Systems and Control Letters*, vol.54, pp. 613–625, 2005.
- [57] A. Smyshlyaev and M. Krstic, “On control design for PDEs with space-dependent diffusivity or time-dependent reactivity,” *Automatica*, 41, pp. 1601–1608, 2005.
- [58] A. Smyshlyaev and M. Krstic, “Adaptive Boundary Control for Unstable Parabolic PDEs—Part II: Estimation-based designs,” accepted to *Automatica*, 2006.
- [59] A. Smyshlyaev and M. Krstic, “Adaptive Boundary Control for Unstable Parabolic PDEs—Part III: Output Feedback Examples with Swapping Identifiers,” accepted to *Automatica*, 2006.
- [60] A. Smyshlyaev and M. Krstic, “Lyapunov adaptive boundary control for parabolic PDEs with spatially varying coefficients,” *Proceedings of 2006 American Control Conference*, pp. 41–48.
- [61] A. Smyshlyaev and M. Krstic, “Output-Feedback Adaptive Control for Parabolic PDEs with Spatially Varying Coefficients,” *2006 Conference on Decision and Control*.
- [62] V. Solo and B. Bamieh, “Adaptive distributed control of a parabolic system with spatially varying parameters,” *Proc. 38th IEEE Conf. Decision and Control*, pp. 2892–2895, 1999.

- [63] R. Temam, *Infinite-Dimensional Dynamical Systems in Mechanics and Physics*, Springer, 1988.
- [64] A. N. Tikhonov, A. A. Samarskii, *Equations of Mathematical Physics*, E. Mellen Press, New York, 2000.
- [65] R. Triggiani, “Well-posedness and regularity of boundary feedback parabolic systems,” *Journal of Differential Equations*, Vol. 36, pp. 347–362, 1980.
- [66] R. Triggiani, “Boundary feedback stabilization of parabolic equations,” *Applied Mathematics and Optimization*, vol. 6, pp. 201–220, 1980.
- [67] J. T.-Y. Wen and M. J. Balas, “Robust adaptive control in Hilbert space,” *J. Math. Analysis and Appl.*, vol. 143, pp. 1–26, 1989.